DISSERTATION

POOLS, RIFFLES AND SURFACE ROUGHNESS IN A PARTICLE INTERACTIONS MODEL OF STEEP GRAVEL-TO-COBBLE STREAMS

Submitted by

Nancy E. Brown

Department of Geosciences

In partial fulfillment of the requirements

for the Degree of Doctor of Philosophy

Colorado State University

Fort Collins, Colorado

Summer, 2006

INFORMATION TO USERS

The quality of this reproduction is dependent upon the quality of the copy submitted. Broken or indistinct print, colored or poor quality illustrations and photographs, print bleed-through, substandard margins, and improper alignment can adversely affect reproduction.

In the unlikely event that the author did not send a complete manuscript and there are missing pages, these will be noted. Also, if unauthorized copyright material had to be removed, a note will indicate the deletion.

ProQuest Information and Learning Company
300 North Zeeb Road
P.O. Box 1346
Ann Arbor, MI 48106-1346

COLORADO STATE UNIVERSITY

February 28, 2006

WE HEREBY RECOMMEND THAT THE DISSERTATION PREPARED UNDER OUR SUPERVISION BY NANCY E. BROWN ENTITLED POOLS, RIFFLES AND SURFACE ROUGHNESS IN A PARTICLE INTERACTIONS MODEL OF STEEP GRAVEL-TO-COBBLE STREAMS BE ACCEPTED AS FULFILLING IN PART REQUIREMENTS FOR THE DEGREE OF DOCTOR OF PHILOSOPHY.

Committee on Graduate Work
(*Please print name* _____

_____

_____

S.A. Schumm

S.L. Rathburn

Ellen Wohl

Adviser

Jorge A. Ramírez

Co-Adviser

Sally J. Sutton

Department Head/Director

ABSTRACT OF DISSERATION

POOLS, RIFFLES, AND SURFACE ROUGHNESS IN A PARTICLE INTERACTIONS MODEL OF STEEP GRAVEL-TO-COBBLE STREAMS

Particle interactions in poorly-sorted sediments arise from the constraints on particle mobility imposed on each sediment particle by the particles surrounding it. Such interactions can be evaluated in terms of the size and position of the top of a given particle and the tops of the neighboring particles. Particle interactions are important in sediment transport in mountain channels, and previous studies in physics suggest that they are important in the development of spatial differentiation of particulate surfaces. Model simulation results from a new particle interactions cellular automata, presented here, suggest that particle interactions lead to non-random structuring of the quasi-steady-state sediment surface, and influence the size and spacing of pools in pool-riffle channels. Pool spacing in the model results ranges from one to fourteen bed widths, similar to the range in theoretical predictions and the values measured in pool-riffle channels. The model pools are shallow, generally have an irregular shape in plan view, and are small, typically 1 to 2 meters in nominal length. Trends in pool characteristics were evaluated in a series of model runs by varying one initial condition in the model, while all other variables were held constant. In these variation series, pool length is somewhat greater where the channel bed is wide, and where the sediment is less mobile. In the bed width variation runs, pool spacing increases linearly from one to seven bed widths as the bed width doubles (widths nominally 1.75 to 3 m). Pool spacing shows a non-linear decrease as the particle size distribution varies from a

uniformly coarse sediment to encompass a greater fraction of finer sediment, with spacing decreasing from 14 to 1.6 channel widths as the particle size distribution width increases. The spacing of the pools was essentially unvarying at about 3 channel widths as slope and the mobility threshold were varied.

Nearest-neighbor analyses of the spatial distribution of cell-scale highs and lows in the detrended channel bed surface were conducted on model surfaces. The analyses indicate that the spacing of high points on the bed is non-random with a tendency toward regularity of the high points, with the preferred spacing in the range of 4 to 12 cells. Although the model can be evaluated as non-dimensional, in this application I assume that each cell is 0.256 by 0.256 meters, so the pool spacing is nominally 1.25 to 3 m. In addition, a tendency to develop clusters that spanned up to 4 cells (nominally 1 m), indicating a tendency toward clustering on a small scale, developed in two runs with very low particle mobility. Formation of such non-random spatial patterns from an initially random surface indicates a process of self-organization, resulting from particle interactions alone, that appears to be an important factor in the formation of the rough, irregular pools and proto-pools that are found in steep, gravel-to-cobble mountain streams.

The model bed surface coarsens in all runs, and the degree of coarsening varies between the local deeps and the higher surfaces on the channel bed. The greatest variation in surface particle size occurs with variation in the threshold for motion used in the model. Coarse areas on the model bed overlap deep areas in part, but the degree of overlap is generally small, so that bed tends to differentiate into deep and coarse areas. Such differentiation of deep and coarse areas may be analogous to pools and the steeper, coarser channel units such as are found in pool-riffle and other steep mountain streams.

Surface roughness of the model channel bed was characterized using the root-mean-square of the height deviations of the steady-state surface. The roughness of the model bed increases as a power of time, then reaches a maximum value at a value that is stable, on average, during the

remainder of the model run. The maximum roughness of the bed surface varies as a power of the model reach length and width. The maximum roughness also varies with other boundary conditions, including the slope, particle size distribution. The roughness also varies with the degree of vertical particle exposure, which is used as the driving variable in the model.

Keywords: Pool-riffle; Channel form, Sediment mobility; Cellular automata

Nancy E. Brown
Department of Geosciences
Colorado State University
Fort Collins, CO 80523
Summer, 2006

TABLE OF CONTENTS

A PARTICLE INTERACTIONS MODEL FOR POOL-RIFFLE FORMS IN STEEP GRAVEL-TO-COBBLE STREAMS

CHAPTER 1

A PARTICLE INTERACTIONS MODEL FOR POOL-RIFFLE FORMS IN STEEP GRAVEL-TO-COBBLE STREAMS

CHAPTER 2

POOLS AND OTHER CHANNEL DEEPS IN A PARTICLE INTERACTIONS MODEL OF STEEP GRAVEL-TO-COBBLE STREAMS

CHAPTER 3

PARTICLE PATTERNS AND STRUCTURE IN A PARTICLE INTERACTIONS MODEL OF STEEP GRAVEL-TO-COBBLE STREAMS

CHAPTER 4

PARTICLE PATTERNS AND ROUGHNESS IN A PARTICLE INTERACTIONS MODEL OF STEEP GRAVEL-TO-COBBLE STREAMS

CHAPTER 5

PARTICLE PATTERNS AND THEIR RELATIONSHIP TO POOLS, RIFFLES AND ROUGHNESS IN A PARTICLE INTERACTIONS MODEL OF STEEP GRAVEL-TO-COBBLE STREAMS.

FIGURES

Chapter 1

Chapter 2

Chapter 3

Chapter 4

TABLES

Chapter 1

Chapter 2

Chapter 3

Chapter 4

CHAPTER 1

A PARTICLE INTERACTIONS MODEL FOR POOL-RIFFLE FORMS IN STEEP GRAVEL-TO-COBBLE STREAMS

1.1. Introduction

1.1.1. Pools, riffles and steps in mountain streams

Pool-riffle sequences in steep, mountain streams with gravel-to-boulder size sediment are characterized by spatial differentiation into pools which are localized channel deeps, with slow flow at low water; and interspersed riffles. Riffles are relatively steep channel units, with flow that is shallower and more rapid at low water. Channel bars often constitute a third distinctive in-channel form in pool-riffle channels. Associated channel types, such as step-pool sets, rapids and cascades may also be interspersed between the pool-riffle units (e.g., Grant and others, 1990)

Stream channel types are typically associated with a characteristic range of channel slope. Pool-riffle forms are considered typical at slopes near 0.01. Montgomery and Buffington (1993; 1997; Montgomery and others, 1995) define a pool-riffle-bar channel type, with reach slopes typically just below 0.01, whereas Robert (2003) characterizes pool-riffle slopes as just above 0.01. Pool-riffle reaches have been reported on slopes as steep as 0.05 (Lenzi, 2001). At slopes of about 0.01 to 0.03, Montgomery and Buffington (1993) define a plane bed channel type, 'characterized by long stretches of relatively planar channel that may be punctuated by occasional channel-spanning rapids.' They distinguished plane-bed channel segments from pool-riffle channels based on the absence of distinct channel bars in plane-bed channels (Montgomery and others, 1995). Field data collected using these definitions indicate that plane-bed reaches may

contain a number of pools, but the pools are fewer and more widely-spaced than in the pool-riffle-bar channel type (Montgomery and others, 1995).

Distinct channel bars may or may not be present in pool-riffle channels. Grant and others (1990) noted that channel bars have been reported in flume studies at slopes up to 0.09, but are generally absent or indistinct in field studies at slopes exceeding about 0.02 (Florsheim, 1985, referenced in Grant and others, 1990). Both pool-riffle-bar and plane-bed reaches will be referred to here as pool-riffle reaches unless it is known that they are pool-riffle-bar or plane-bed reaches. Observations of pool-riffle sets in a newly-established channel demonstrate that pools grow in size over a period of years (or longer) after they are initiated (Keller and Melhorn, 1973).

Step-pool sets are considered characteristic at higher slopes than pool-riffle and/or plane bed forms. Step-pool forms are characterized by an abrupt to nearly-vertical step separating individual pools. Values quoted for the lower slope limit for observed step-pool forms range from as low as 0.02 (Robert, 2003). The flume experiments of Whittaker and Jaeggi (1982), suggest step-pools can form at or above slopes of 0.025 (Whittaker, 1987). However, the lower limit of step-pool formation may be as high as about 0.05, the typical limit found for the Santa Monica Mountains in California (Chin, 1989). Whittaker and Jaeggi (1982) also noted that their lower slope flume runs, at slopes of 0.022 to 0.042, yielded classic antidunes, often considered the initiating form for step-pools, but subsequent flow modifications (a hydraulic jump formed in the trough) made the forms appear more like pool-riffle sets than typical step-pool sets. Grant and others (1990) indicated the presence of steps in channels with slopes well over 0.20, whereas Buffington and others (2002) indicate step-pool channels are found at slopes up to at least 0.20.

Inter-mingling of pools, riffles, steps and other channel types is also common (Grant and others, 1990; Buffington and Montgomery, 1993; Chin, 2002). Recent research has documented intermingling of step-pool and pool-riffle sets (Grant and others, 1990; Chin, 2002), suggesting a gradual zone between pool-riffle and step-pool channel types. Chin (2002) used a spectral

analysis to quantify the spacing of the pool forms, and found that the larger pools within cascade channel units (Grant classification) had a pool-to-pool spacing on the order of five to seven channel widths, a range considered characteristic of pool-riffle sets (e.g., Gregory and others, 1994; Chin, 2002, p. 163-4). A wider range may also occur; analytical predictions have suggested a range of three to twelve channel widths (Yalin, 1971a; Blondeaux and Seminara, 1985).

Grant and others (1990) documented the sequencing of channel units in two steep streams in the Oregon Cascade Mountains (slopes of 0.022 and 0.038, both at 18.1 m width). They classified channel units as pools, riffles, steps, cascades and rapids, and conducted a Markov chain analysis on observed pairs in the sequences. The results showed that rapids, cascades and steps all preferentially terminate in pools. Chin (2002) also noted that the definition of step-pool forms differs between studies, and features defined as step-pools, cascades and rapids in various studies may represent similar forms at least in part. These data show that pool-riffle and step-pool sets are intermingled with cascade-pool and rapid-pool sets in steep streams.

Pools in pool-riffle channels are often assumed to be streamlined by the flow, making them compact in shape and oval to nearly circular in plan view. Pool-riffle channels may also contain pools with a highly irregular outline (Keller and Melhorn, 1973; personal observation). Keller and Melhorn documented two populations of pools, one irregularly-shaped and shallow, the other streamlined and deeper. The irregular pools were smaller and more closely-spaced than the stream-lined pools in the same channel. Keller and Melhorn (1973) evaluated a relationship for the number of small pools between larger stream-lined pools. For the channel widths evaluated in this study, and for the generally expected spacing of five to seven channel widths between primary pools, the relationship they identified predicts an average of 0.5 to 2.7 small pools between larger, primary pools. Recalculating a primary pool spacing of five to seven widths to include both primary pools and irregular, secondary pools, results in an expected spacing of 1.8 to

3.9 pools per channel width, or 2.2 to 6.4 pools per bed width. Very small pools also occur, have been called 'pocket pools,' and are typically not documented.

The fundamental issue of defining what is a pool, and the definition of other channel and bedform types, determines in part what relationships are observed in stream channels. Geomorphologists typically recognize pool-riffle pools, distinguishing 'freely-formed' and 'forced pools,' and also step-pools. More detailed characterizations are used by stream biologists, who recognize as many at 11 distinct types of pools based on form and flow characteristics (Bisson and others, 1982; Hawkins and others, 1993, noted in Montgomery and others, 1995). In future, such detailed form characteristics will undoubtedly need to be evaluated to address the effects of channel form and sediment patterns on stream biota.

A minimum size criterion must also be adopted for identification of pools. There is 'no widely accepted' definition for the minimum size of pools (Montgomery and others, 1995; Buffington and others, 2002). A frequently used standard was given by Lisle and Hilton (1992), who recommended defining pools as closed basins at least one-half the channel width in length. A study of forced pools (Montgomery and others, 1995) used the criterion that pools are deeps with residual depths at least 35 percent of the bankfull depth, and with length or width of the pool at least 10 percent of the channel width. These short length and width cutoffs were chosen because of the typically small size of forced pools (Montgomery and others, 1995). No absolute standard for a minimum pool size can be selected, as the issues being studied must dictate the size of features considered, but the half-channel-width criterion is a useful, although arbitrary, standard criterion.

Recent research has often focused on forced pools generated by flow disturbances around local obstacles such as boulders or large woody debris, and on the associated hypothesis that pools observed in pool-riffle and step-pool sets and sequences are initiated at randomly-distributed obstacles (Clifford, 1993; Madej, 1999; Thompson, 2002; Curran and Wohl, 2003).

However, a field-classification study of multiple pool-riffle systems identified some 20 percent of pools as freely-formed, even in pool-riffle channels where pool forms are often forced by flow variations at large obstacles (Buffington and others, 2002). The presence of a significant number of freely-formed pools in streams, and the observation that the controls on freely-formed pools can still be identified as significant influences on forced pools (Buffington and others, 2002), means that understanding these controls is important for understanding the formation of all pools. A better understanding of factors that promote in-channel spatial variability into pool and riffle segments is important because such spatial variability is an important influence on bed stability (Paola, 1996; Hassan and Church, 2000; Ferguson, 2002), and because pool habitats and their variability contribute to the diversity of aquatic species, including macroinvertebrates and fishes (Mermillod-Blondin and others, 2000; Rempel and others, 2000; Inoue and Nunokawa, 2002).

1.1.2. Particle interactions in steep mountain channels.

Steep channels, with their typically wide range of particle sizes, are also channels where particle interactions are expected to be significant (Bathurst 1987; Gomez, 1995). Particle interactions were early evaluated by Einstein (1950) under the term 'hiding effects', and have also been called shadowing effects (Egiazaroff, 1965; Barabási and Stanley, 1995). Particle interactions occur when individual particles constrain or enhance the mobility of nearby particles. Interactions are defined here to include the characteristics and degree of both sheltering from the flow (or hiding) and exposure to the flow (or protrusion) (Van Niekerk and others, 1992).

Particle interactions influence particle size selection for transport (Parker and Klingeman, 1982; Wilcock and McArdell, 1997); the distribution of vertical particle exposure (Parker and Klingeman, 1982; Iseya and Ikeda, 1987); spatial arrangements of particles (Iseya and Ikeda, 1987; Hassan and Church, 2000); sediment transport (Wilcock and McArdell, 1997; Hassan and Church, 2000) Particle interactions can result in characteristic scales of sediment surface roughness elements (Naden, 1987; deJong and Ergenzinger, 1998; Robert, 1991), and ultimately

influence channel form. Coarse-grained channels where particle interactions are important are also likely to be characterized by partial mobility and partial transport (*cf* Wilcock and McArdell, 1997), because some subfraction within each of the coarser particle size fractions may be effectively immobile under most flows in steep, gravel-to-cobble channels. Effects of particle interactions will be considered in more detail in Charter 2.

1.2. Existing hypotheses for the formation of pool-riffle and step-pool sequences

Although several hypotheses for the initiation of freely-formed pools were proposed in the late 1960s and the 1970s (Langbein and Leopold, 1968; Yalin, 1971b; Yang, 1971; Keller and Melhorn, 1973, 1978), none of the hypotheses has become fully established. Each highlights the influence of a single type of spatial differentiation observed in pool-riffle sequences, and how that spatial pattern may lead to localized scour and the development of pools and riffles. There is a single primary hypothesis for the formation of step-pool sets, as well as an extremal hypothesis that predicts form characteristics of step-pool sets. None of these hypotheses focus on the effects of particle interactions, and as such are incomplete in terms of predicting the surface characteristics in channels where particle interactions strongly influence particle mobility.

Riffles are relatively steep and pool segments are less steep, and this variation in slope may be explained by Yang's (1971) hypothesis of minimum energy dissipation, supported by his evaluation that alternating steeper and less steep channel segments minimize energy dissipation. Langbein and Leopold (1968) investigated particle interactions in rivers and flumes, and concluded that there is a natural tendency for moving sediment to differentiate into zones with greater and lesser concentrations of coarse sediment particles. They suggested that such differentiation would promote the formation of the alternately finer pool and coarser riffle channel segments described from pool-riffle channels. Iseya and Ikeda (1987) documented the development of alternately fine and coarse segments in flume runs using strongly-bimodal sediment, and related the origin of the fine and coarse segments to particle interactions. Keller

and Melhorn (1973, 1978) highlighted the effects of channel width and depth variations, and suggested that pools initiate in response to flow effects as the channel boundary alternates from wide to narrow, and from shallow to deep. Clifford (1993) evaluated a fourth hypothesis, that macroturbulent structures initiate pools as suggested by Yalin (1971a,b). Clifford documented the size of turbulent structures in low gradient pool-riffle channels, and found that they appeared to be too small to generate pools of the expected spacing. Clifford noted, alternatively, that the observed turbulent structures were about three times the channel width, approximately the size needed to generate pools corresponding to the modal value of pool spacing in Keller and Melhorn's data set. Based on this observation, Clifford suggested it would be worthwhile to re-evaluate the issue of pool spacing.

The above, single-control hypotheses appear to be fundamentally too limited, and a number of researchers have noted multiple, interacting controls on pool-riffle forms. One set of studies emphasizes a relationship between the bar-pool form and the development of longitudinally-differentiation of the channel into highs and lows associated with bars and pools. Although such analysis now provides a clear framework for understanding pool formation, neither field nor analytical studies yet allow a detailed explanation of transitions in channel width, depth, slope and particle size, particularly in the absence of channel bars. Keller and Melhorn (1973) described the formation of the pool-riffle form as depending on "... interaction between channel morphology, discharge, slope, bottom velocity and bed roughness, but the relative significance of each is not completely understood." Grant and others (1990) summarized the influences on channel form and sediment sorting as 'interactions among flow, bedload, channel boundary, and bed.' Clifford (1993) suggested that elements of all of the above four hypotheses, relating to slope, width and depth, particle sorting and macroturbulence, may play a role in the origin of pool-riffle sets. Montgomery and others (1995) reference Dietrich and Whiting (1989) and Nelson and Smith (1989) in specifying the influences of shear stress, sediment transport, and bed

and bank topography as important influences on freely-formed pools. In spite of such recognition of multiple, interacting influences on the pool-riffle form, only rare subsequent work has evaluated interactions among those influences for steep, gravel-to-cobble or boulder channels.

The most commonly-cited theory for the formation of step-pool bedforms is that they initiate as antidunes (Lenzi, 2001; Chin, 2002). Antidunes bedforms develop where flow is supercritical, such that the bed and water surface undulations are in phase (Yalin, 1971a, p. 205). Based on examples of conditions where step-pools have been observed in streams, Wohl and Grodek (1994) as well as Abrahams and others (1994) argued against any necessary association with antidunes (Lenzi, 2001). Chin (1989, 1999, and 2002) characterized step-pool channels and described important influences on step-pool forms. In addition to flow characteristics, maximum particle size appears to be significant in promoting the formation of step-pool rather than pool-riffle forms (Chin, 1989).

1.2.1. Observed pool spacing in pool-riffle and other steep channels

Pool spacing is typically evaluated in units of channel width, based on field observations, and on theoretical arguments that pool spacing and channel size should be proportional (Yalin, 1971a,b). Keller and Melhorn (1973, p. 265-266) described two distinct populations of pools in a channel with a slope of 0.0025, consisting of a group of large, streamlined, primary pools at a spacing approaching 9 channel widths (the maximum spacing observed) and a second group of smaller, shallower, irregularly-shaped pools at a spacing of 3 to 5 channel widths. Keller and Melhorn also noted these pool types were interspersed, and suggested the two populations originated under different controls. Grant and others (1990) also documented bimodal pool spacing. They conducted a detailed evaluation of two steep streams in the Cascade Mountains in Oregon (slopes of 0.022 and 0.038) and found one had a unimodal, and the other a bimodal distribution of pool spacing (Grant and others, 1990). The bimodal spacing, at the steeper stream, had a primary peak at three widths and a secondary peak at five to seven widths. At the less steep

stream, spacing was two to four channel widths, with a mean near four. This study also reported that pool spacing was inversely related to the number of large boulders in the channel, suggesting a population of forced pools.

Bimodal spacing was attributed to a mix of freely-formed and forced pools in a study by Montgomery and others (1995), who defined both plane bed and pool-riffle channel units. They found that these channel types occurred at similar low woody debris loading, yet had different typical pool spacings, averaging nine and two to four widths, respectively. They also distinguished forced pools, which had a closer spacing, typically less than two channel widths (Fig. 1.1). These forced pools occurred at slopes that overlapped the slope ranges where freely-formed pool-riffle and plane-bed channel types were observed. Similarly, Clifford (1993) noted bimodal distributions of pool spacing, and suggested that some of the pools he observed might have originated by flow disturbance around boulders; i.e. he hypothesized that they originated as forced pools.

Clifford, as well as Keller and Melhorn, emphasized that the pools documented by Keller and Melhorn (1978) had a modal value of pool spacing near three channel widths, although the average was about five to seven channel widths. Keller and Melhorn (1978) also appear to have used bed width rather than channel width to normalize the distance between pools, therefore, the spacing they reported may be inferred to be longer than would be found in a study that normalized using channel width.

Step-pools are generally smaller and more closely spaced than pool-riffle pools. Step-pool spacing with values of one to two channel widths was reported by many studies beginning in the late 1970s (Chin, 2002). The predominant pool spacing in small streams and boulder torrents was reported as two to 3.5 widths by Grant and others (1990). Such close spacing is similar to the spacings reported for forced pool-riffle pools, and to the extent that step-pool pools are forced by

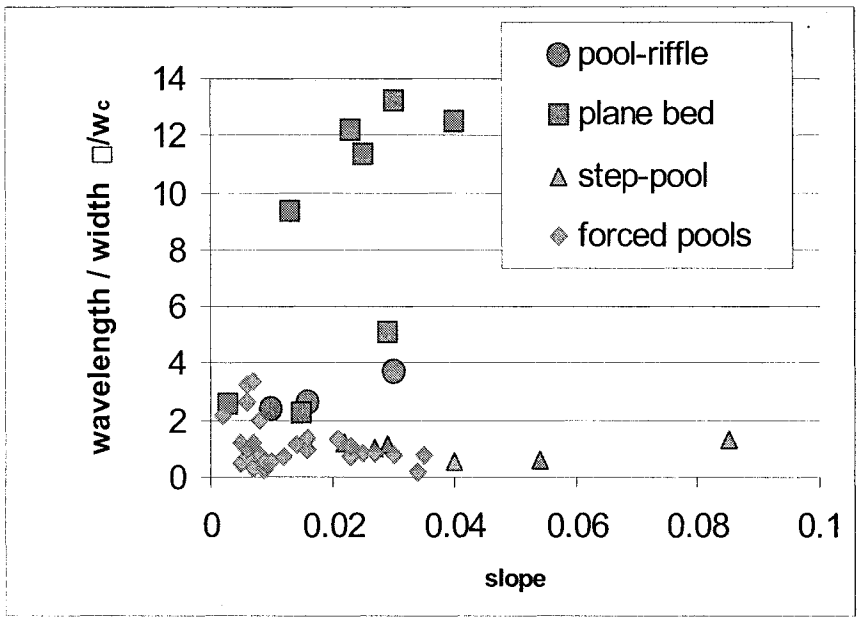

Fig. 1.1. Relationship between pool spacing and slope for pool-riffle, plane bed, step pool and forced pools in a data set presented by Montgomery and others (1995). The channels are located in western Washington and southeast Alaska, often with a large amount of large woody debris, and associated forced pools. Note distinctly larger spacing, averaging 9 channel widths, for the plane bed type, i.e., a channel with relatively few pools and without distinct channel bars.

the presence of individual coarse particles or groups of coarse particles, they may originate by similar mechanisms.

The spacing of both step-pools and pool-riffle pools is right-skewed, so that the mean tends to be larger than the mode (data in Keller and Melhorn, 1973; Chin, 2002, p. 153). Lenzi (2001) documented an increase in step spacing in the years after a major flood.

1.2.2. Relationship between pool spacing and slope.

Diverse relationships between pool spacing and slope have been reported. Wohl and others (1993) evaluated 122 pools in reaches at slopes between 0.002 and 0.172 and found wider pool spacing at the flatter slopes. Note that, with this wide range of slopes, a wide range of particle size distributions is also typical.

Montgomery and others (1995) obtained a spacing of about two to four channel widths in pool-riffle-bar channels, which increased to nine for the plane bed channels, which occurred at steeper slopes (Montgomery and Buffington, 1997). Based on flume studies, it has been suggested that slope is a significant control on spacing of forced pools (e.g., Thompson, 2002). Although Montgomery and Buffington (1997) found no trend with slope for forced pool reaches, Buffington and others (2002) documented larger pools at lower slopes in forced pool reaches, for slopes in the range of 0.01 to 0.05. They also documented decreased width-to-depth at the steeper slopes.

Based on a linear stability analysis (perturbation analysis), Furbish (1993) noted that, in general, increased slope is expected to suppress the growth of bedforms. However, he also noted that a stabilizing effect of streamwise sediment transport associated with the gravitational influence of bed slope is significant in the gravel and coarser channels he considered. This stabilizing effect tends to limit the range of wavelengths that may grow for some channel conditions. However, with increased lateral transport, a wider range of bedform spacing may be expected for a given channel width-to-depth.

1.2.3. Pool spacing and channel width

The distance between pools is generally assumed to vary in proportion to variations in channel width, such that pool spacing takes on a constant value when the distance between pools is normalized by channel width. A characteristic spacing of five to seven channel widths between pools is often quoted, but the field observational data summarized above indicate that pool spacing actually spans a much wider range, from about 2 to 12 widths, and is close to three channel widths for forced pools and possibly other pool types. It is not clear to what extent the relationship between width and spacing may vary as other factors, e.g., slope and the roughness of bed and banks, vary.

In general, streams tend to be narrower as drainage area decreases. Under some conditions, flume studies indicate that streams tend to become wider, and are also wider relative to their depth, as the slope increases (e.g., Schumm and others, 1987, p. 169 and 175, Fig 5.3.5). In contrast, Buffington and others (2002) documented decreased width-to-depth at steeper slopes in pool-riffle, plane-bed, step-pool and cascade channels. Effects that may cause these contrasting results from one channel system to another may include variations in channel roughness, the low erodibility of the channel boundary in steep streams with cobbles and boulders, as well as roughness contributed by bank vegetation and large woody debris. These sources of variablity have not been thoroughly explored in the field, or in flume and model experiments, but existing field evidence suggests that different combinations of roughness and slope allow a variety of combinations of channel width, pool spacing, and pool form, rather than generating a single trend as slope and particle size characteristics co-vary.

A large data set representing a pool-riffle reaches in mountain streams in a wide variety of climatic regimes was recently published (Wohl and Merritt, 2005). The data available for these reaches includes of channel width, depth, slope, D_{50}, D_{84}, shear stress, pool spacing and other characteristics of pool-riffle streams in a wide variety of climatic settings. These data indicate wider pool spacing at steeper slopes for these small, steep pool-riffle channels (Fig. 1.2b).

Step-pool form has also been related to slope. The ratio of the fall distance from the crest to the basin of the pool, H, relative to the length of the pool, L_p, is expected to be similar to the channel slope, S. The ratio of these two slopes, S and S_f ($= H/L_p$), has been evaluated as generally ranging from one to two based on theoretical arguments and flume results (e.g. Abrahams and others, 1994). Spacing of step-pool forms was evaluated by Grant and others (1990), who reported spacing of about 0.4 to 0.8 channel widths, Chin (1989) and Whittaker (1987) reported averages of 1.9 and 2.7 widths, respectively. Regardless of the source of these variations, it is clear that, given standard measurement methods, step-pool forms are more closely

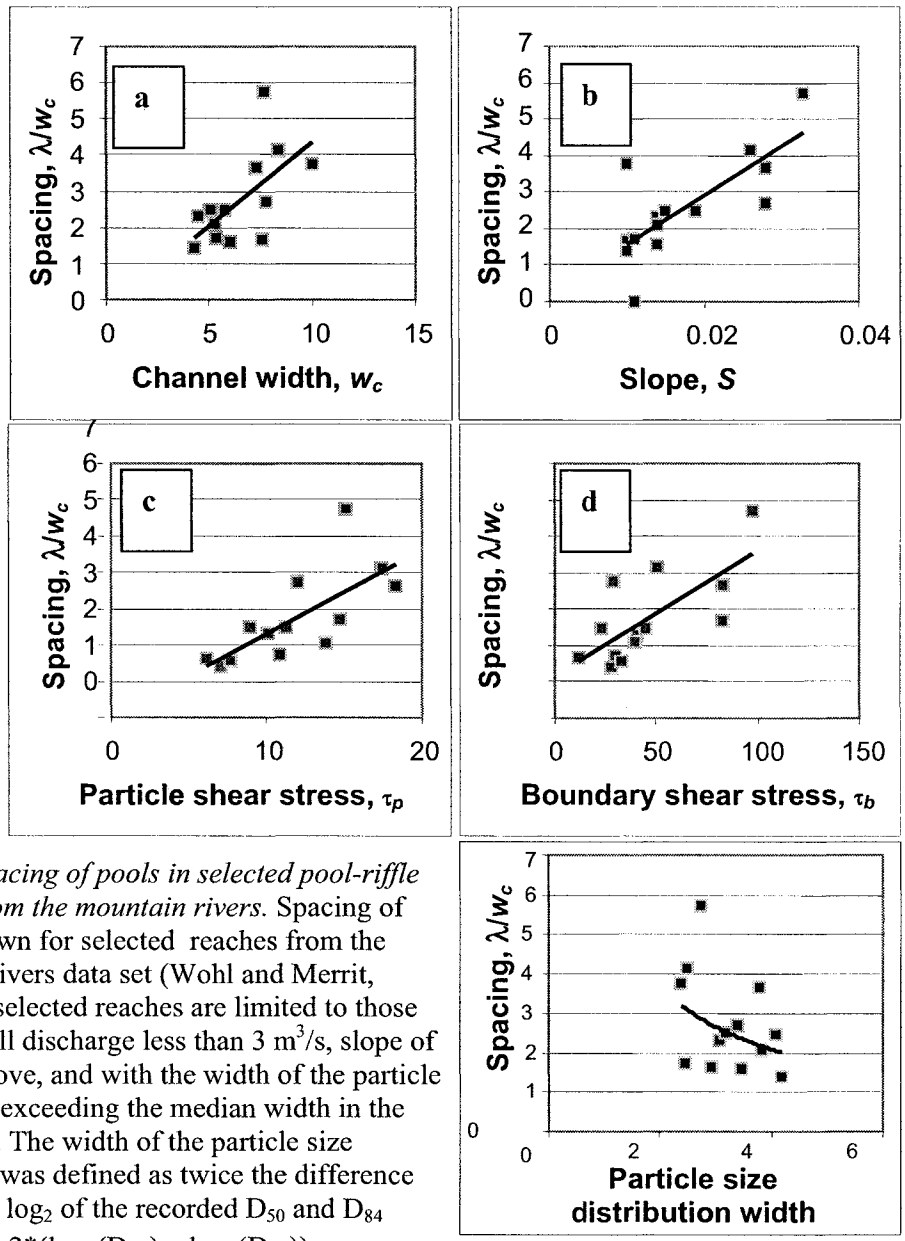

Fig. 1.2. Spacing of pools in selected pool-riffle channels from the mountain rivers. Spacing of pools is shown for selected reaches from the Mountain Rivers data set (Wohl and Merrit, 2005). The selected reaches are limited to those with bankfull discharge less than 3 m^3/s, slope of 0.01 and above, and with the width of the particle distribution exceeding the median width in the full data set. The width of the particle size distribution was defined as twice the difference between the $\log_2$ of the recorded D_{50} and D_{84} values, $w_p = 2*(\log_2(D_{84}) - \log_2(D_{50}))$.

spaced than pool-riffle forms. Step-pool spacing is, however, similar to the spacing of forced pool-riffle channels, at least in forested areas measurement methods, step-pool forms are more closely spaced than pool-riffle forms. Step-pool spacing is, however, similar to the spacing of forced pool-riffle channels, at least in forested areas measurement methods, step-pool forms are more closely spaced than pool-riffle forms. Step-pool spacing is, however, similar to the spacing of forced pool-riffle channels, at least in forested areas measurement methods, step-pool forms are more closely spaced than pool-riffle forms. Step-pool spacing is, however, similar to the spacing of forced pool-riffle channels, at least in forested areas based on correlations between spacing and wood frequency presented by Montgomery and others (1995).

1.2.4. Controls on pool size

Data on the relationship between pool size and other variables are limited. The most commonly noted controls on pool size include discharge, as well as slope and the particle size distribution. Thompson (2002) suggested that discharge had the primary effect on pool length, and that slope was secondary. The data from Thompson's flume studies show that pool length and depth are positively correlated with discharge (with r^2 values of 0.918 and 0.615, respectively, in a simple linear regression of the data). Multiple-regression results presented by Thompson indicate that both the channel-bed and energy slopes are significantly related to pool length in flume runs with in-flume constrictions. Thompson (2002) also reviewed five existing field studies that document a relationship between pool size and other channel variables. Drainage area, a surrogate for discharge, and pool length were evaluated in two of the five studies, with both reporting pool length positively correlated with drainage area. Two studies evaluated the relationship of drainage area and pool depth. The studies reported opposing relationships; one found a positive correlation, the other a negative correlation. Slope and pool length were evaluated in two of the four studies, and both reported negative correlations between the two variables. Slope and pool depth were evaluated in two of the studies, and also reported opposing

relationships. The positive relationship was found in a study that used local slope, rather than reach slope. For the other study, using reach-averaged conditions, pool depth decreased as slope increased. In summary, these studies report pool length positively correlated with drainage area and negatively correlated with slope. The studies report pool depth negatively correlated with slope, and possibly a variable relationship between pool depth and drainage area. It has been suggested that the inconsistency in the sense of the empirical correlations between pool size and the variables discharge or slope can be explained by variations in substrate resistance to erosion (Wohl and others, 1993; Thompson, 2002; Thompson and Hoffman, 2001). Results for step-pool systems also suggest there is no clear relationship between slope and pool size. For step-pools, Whittaker and Jaeggi (1982) reported no clear trends with slope in either flow width or step height (Lenzi, 2001).

The Mountain River data set (Wohl and Merritt, 2005) suggest that pool spacing increases with bed width and slope, and that spacing increases as local ('grain') and total shear stress increase (Figs. 1.2c, 1.2d). The data also suggest that pool spacing decreases nonlinearly as the width of the particle size distribution increases (Fig. 1.2e). Because the variability of spacing as the particle size distribution varied was high ($r^2 = 0.147$, n = 17), the spacing versus particle size distribution width data for the full data set were plotted for comparison (Fig. 1.3). The data were divided into four groups with differing discharge ranges. The highest and lowest discharge classes had power law correlations with decreasing spacing as the width of the distribution increased (Fig. 1.3a, 1.3b), whereas the other two classes had power law correlations with increasing spacing as the distribution width increases (Fig. 1.3a). r^2 values for the empirical data sets range from 0.11 to 0.42. The diverse relationships between slope and pool depth suggest a need to evaluate the effect of particle mobility/resistance to motion to understand the relationship between pool size and the particle size distribution.

An additional relationship between pool size and its status as either an aggrading or degrading reach was suggested by Lisle (1986). Lisle indicated that longer pools tend to be observed in streams undergoing degradation, and pools tend to partially fill and become shorter under aggradation.

1.3 A particle interactions hypothesis for organization of bed surface sediment in steep mountain rivers

Field observations from pool-riffle and steeper gravel-to-cobble-bedded streams clearly show the presence of several distinct form types in these streams: pools, riffles, steps, cascades. However, previous studies of the steep channels also show that there is an intermingling of the form types (e.g., Grant and others, 1990); Chin, 2002). The data also show that the fundamental sequence of forms can most simply be characterized as longitudinal differentiation into steep, coarse-bedded sections, alternating with pools (e.g., Grant and others, 1990). Longitudinal differentiation has also been observed to develop in a flume study, in which alternately steep, poorly-sorted and less steep well-sorted

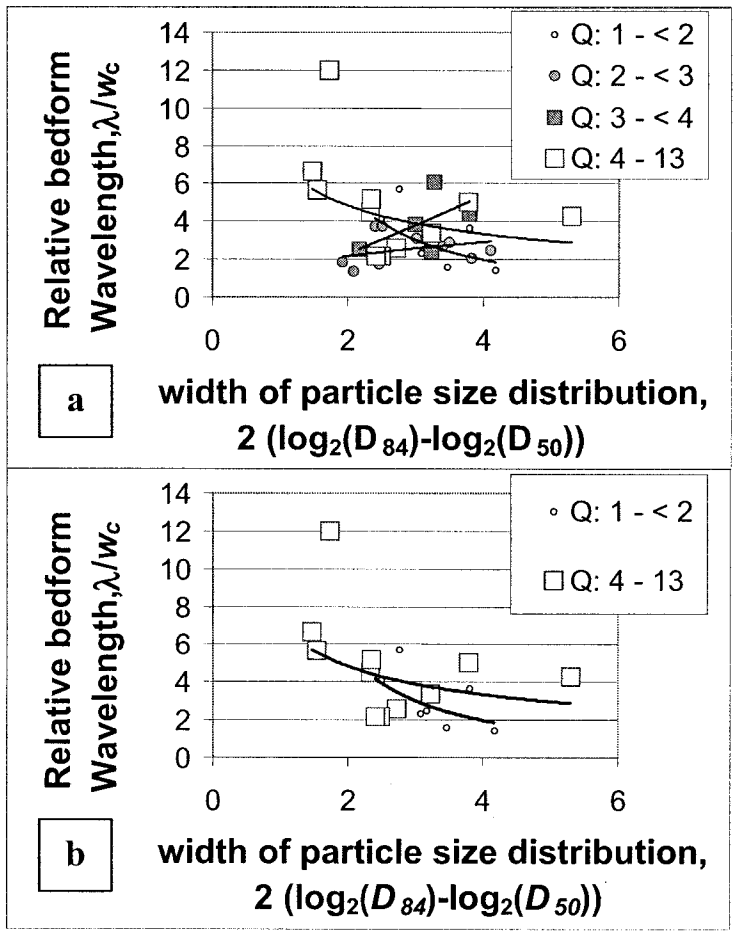

Fig. 1.3. Relationship between pool spacing and the width of the particle size distribution. The width of the particle size distribution was defined using D_{50} and D_{84}, in part because these are often the only data available to characterize the size distribution.

sediment developed as a result of particle interactions (Iseya and Ikeda, 1987). In that study, coarse particles were observed to roll rapidly on smooth, finer-grained surfaces, however, the coarse particle transport was reduced where many coarse particles were concentrated, resulting in mutual interference among the large particles. Taken together, these observations suggest that particle interactions may be an important factor in the development of longitudinal differentiation in stream channels, and that similar mechanisms may operate over a wide range of channel type from pool-riffle to cascade channels, and in many channels dominated by gravel-to-cobble sediment. Particle interactions may be defined as controls on transport and thus channel form that depend on local particle size, and the sizes and relative positions of the surrounding particles. This view of steep stream channels suggest that a better understanding of particle interactions, and how channel form and roughness is influenced by particle interactions, is crucial to understanding steep mountain streams form, at least in part, in gravel-to-cobble sediment. If particle interactions are shown to be important in controlling surface roughness under a wide range of conditions, it may be possible to predict channel boundary characteristics from an understanding of particle interactions and how they constrain transport over different bed surfaces. To test this idea, a simple model that transports sediment and thus evolves the channel form was constructed, and the model bed surface characteristics were compared to pool-riffle channel forms and sediment characteristics.

Thus, although pool-riffle, step-pool, and cascades interspersed with steps may be characterized as distinct channel forms, this study assumes that these forms have fundamental similarities and may be more simply viewed as a continuum of related forms, all characterized by pools alternating with coarse, rough channel segments. Assuming that there is such a continuum of forms, I hypothesized that the fundamental differences along the channel results from how particle interactions are influenced by other channel characteristics, most important of which I expected to be channel width, slope, particle size distribution and some measure of particle

mobility, such as discharge, boundary shear stress, or other measure of the forces that mobilized sediment particles.

1.4. Methods

1.4.1. Cellular automata

A cellular automata (CA) model was developed in this project to model movement of sediment in stream channels in which particle interactions control particle mobility and transport. The transport simulated in the model includes selection of the particles that are mobile and therefore transported, displacement of the particles to the lowest adjacent cell, and thus also simulation of the evolving channel form.

Several CA models of processes and forms in rivers and streams have been developed in the past two decades, including a model of fluid dynamics and movement of individual particles (Wolfram and Salem, 1985); models of channel form response in braided rivers (Murray and Paola, 1997; Crave and Davy, 2001); a model of channel adjustment coupled with hillslope environmental change (Coulthard and others, 2000); and a model of bank instability (Fonstad and Marcus, 2001). Other models have evaluated particle interactions based on simplified representations of individual particles (Naden, 1987; Tribe and Church, 1999; Malmaeus and Hassan, 2002). Finally, cellular automata have been used in physics as a means to evaluate the effects of particle interactions and their control on surface roughness (e.g., Family and Viscek, 1985; Barabási and Stanley, 1995).

The cellular automata approach was designed for a system with many, essentially similar, model elements that interact with each other. In the particle interactions model presented here, relatively small volumes of sediment are viewed as individual model elements, and the motion of these elements is used to model movement of sediment particles and groups of particles in a stream channel.

A strategy used in the design of cellular automata is to deliberately use a coarse-scale characterization of a minimal number of processes expected to be essential controls on the system (Bak, 1996; Hergarten, 2002). Although the individual model elements are numerous, the number of types of interactions can be significantly reduced by selecting only one or a few key processes, and by defining the processes simply and based only on local conditions (Bak, 1996; Chopard and Droz, 1998). Interactions that appear different on a wider scale, may sometimes be simplified to a single process in terms of local interactions.

Interactions are assumed to occur only between a central focal cell and the cells that surround it. In a CA, the focal cell, together with the surrounding cells that interacts with, are termed the neighborhood. This simple view of interactions allows minimizing assumptions about what type of motions occur and how frequently, yet still allows for the occurrence of all classes of events. In a CA model, the process is described as a designated set of responses that a given model element can make, and the criterion for choosing the response in each model time step is defined only in terms of the current state of the cells in the local neighborhood. These choices thus depend on the spatial configuration of states in the neighborhood of each model cell. In this model, the single class of events in the model is a cell-to-cell sediment motion, with packets of sediment that move from one cell to an adjacent cell. The particles that were determined to be mobile are then moved to the lowest adjacent cell in the neighborhood.

The rules determining motion do not differ for different particle sizes. However, the relative height of the particles and of their surroundings does determine whether particles move, so that local concentrations of fine or coarse particles, and local highs and lows do influence whether particles in a given cell move.

The relative simplicity of a CA model makes it feasible to explore a wide range of initial conditions, or to consider how the processes and boundaries of the model space influence the resulting spatial or temporal patterns. The use of local controls also facilitates simulation of the

spatial patterns that form in the system, which might otherwise not be observed in modeling (Hergarten, 2002; Chopard and Droz, 1998). Cellular automata also model nonlinear systems as readily as linear systems, and may in some cases be formally related to continuum models of particulate systems (Barabási and Stanley, 1995).

1.4.2. Overview of the model

The model introduced here was constructed to evaluate the development of pool-riffle pools in response to constraints imposed by particle interactions. The model provides a simulation of the most basic consequences of the constraints that individual particles and groups of particles impose on the mobility of nearby particles, using a simplified representation of a hypothetical channel in which particle interactions are the dominant control on sediment transport. Pools formed under particle interaction controls are expected to develop in channels where sediment is coarse and poorly-sorted. Given that, the model results are expected to approximate small, newly initiated pools that may develop in channels where sediment is coarse and poorly-sorted, including pool-rifle pools, as well as other small pools (forced pools, step-pools). The results may also be expected to generate other forms of sediment structuring such as the formation of ribs, lines and networks of particles, such as those described by Church and others (1998) and Hassan and Church (2001) from field and flume studies, respectively.

Given the model construction, I expect the model results to approximate the effect of particle interactions in real streams, and to provide a valid aid in understanding the origin and adjustment of pool-riffle channels to step-pool channels. However, the model does not incorporate all processes in such streams, and processes not included in the model may enhance or suppress adjustments that occur in the model. In particular, the model does not include effects of spatial patterns in flow intensity, or effects of macroturbulence.

1.4.3. Mobility threshold criterion

Particulate surfaces formed of gravel through cobbles (2 through 256 mm) are geometrically complex, but much of the geometry of individual particles or small groups of particles, as well as the mutual interactions among the particles, can be simply described in terms of particle size and of the height of the tops of individual particles or groups of particles. Vertical particle exposure is one variable that can be evaluated from data on the height of the tops of the particles at the surface of each cell, and the average exposure provides a simple approximation of the effects of hiding and protrusion.

Particle size, D, and the average vertical particle exposure, e, are the fundamental particle characteristics used to evolve the model. These variables are combined in a threshold variable, $R_{p,c}$, defined as the vertical particle exposure, e, divided by the particle diameter, D.

$$R_{p,c} = e / D \qquad (1)$$

Entrainment occurs at a threshold, or critical, value of the relative particle exposure, $R_{p,c}$. The definition of relative particle exposure, $R_{p,c}$, for a critical value, $Rp,c = 1/8$ is shown in Fig. 1.4. Actual sediment particles are typically not spherical, and, D is typically defined as the intermediate, or b-axis, diameter, but in some cases is defined as the nominal diameter. The nominal diameter is the diameter of a volume-equivalent spherical particle. The threshold criterion for particle motion used here is based on empirical observations of the relative particle exposure defined using the nominal particle diameter (Fenton and Abbot, 1977), and spherical particles are assumed in the model.

Relative particle exposure, $R_{p,c}$ is necessarily related to both the horizontal and vertical exposed cross-sectional area of a particle that protrudes into the flow, and to the particle friction angle. Both of the latter parameters often used to characterize controls on particle mobility (e.g., Wiberg and Smith, 1987).

Relationships between particle exposure and the critical shear stress at entrainment for individual particles have been modeled (Wiberg and Smith, 1987; Kirchner and others, 1990), observed and documented in a flume study (Fenton and Abbot, 1977), on sediment surfaces developed in a flume (Kirchner and others, 1990), and estimated in laboratory studies on natural sediment surfaces (Buffington and others, 1992). These studies have used a variety of approaches to identify the range of critical shear stress at which particles of a given size, and in a given geometric configuration, will move. These studies do not account for spatial variations in flow, or other factors that may modify the relationships between shear stress and particle size, e.g. the diversity of particle shape, density, orientation, and packing.

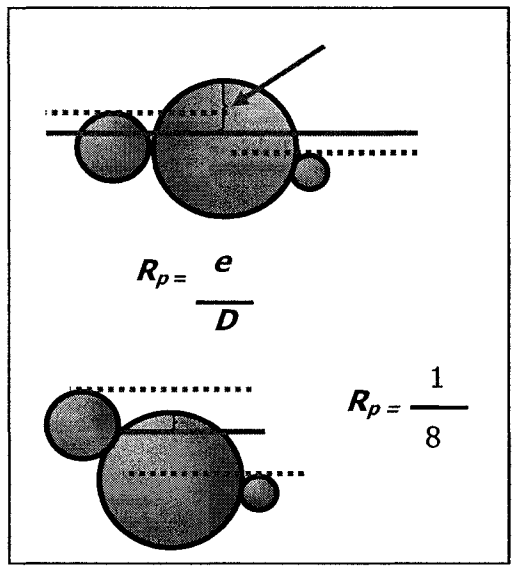

Fig.1.4. Definition sketch of relative particle exposure. The relative particle exposure, $R_{p,c}$, definition is illustrated with an example showing an $R_{p,c}$, of 1/8. The relative particle exposure, $R_{p,c}$ is defined as the ratio the particle exposure, e and the diameter of the particle, D. The exposure, e is defined as the average height that a particle rises above the four neighboring cells in the upstream, downstream, left and right directions.

Given information on the elevation and size of a particle, a force balance model might be used to evaluate forces at entrainment for a given local configuration of particles (Wiberg and Smith, 1987; Kirchner and others, 1990). Empirical data on the mobility of individual particles might also be used to define a relationship for determining critical values for particle motion, e.g., critical values of shear stress, friction angle, or vertical particle exposure. For example, Fenton and Abbot (1977) conducted flume studies and documented the critical vertical exposure at which individual particles were entrained. The Fenton and Abbot data span the range of particle sizes from 2.5 to

38 mm (very fine to coarse gravel). Their data include the shear stress at entrainment, τ_c, providing a relationship between vertical particle exposure and the critical shear stress, τ_c, at which motion began. This relationship is used as the basis for a critical relative particle exposure criterion for particle mobility in the model.

The dimensionless critical shear stress,

$$\theta_c = \tau_c / (\rho_s - \rho_w \; g \, D) \qquad (2)$$

is expected to be nearly constant for particle entrainment from rough surfaces. Fenton and Abbot (1977, Fig. 6, p. 535) showed that the variation in the dimensionless shear stress with relative particle exposure is significant, as it spans a wider range of dimensionless shear stress than the maximum variation with the shear-roughness Reynolds number, Re^*.

$$Re^* = u^* D / \nu \qquad (3)$$

where

$$u^* = \sqrt{\frac{\tau_b}{\rho}} \qquad (4) \qquad (4)$$

and τ_b is the boundary shear stress, and ν is the kinematic viscosity.

In the dimensionless critical shear stress, θ_c, the factors of water and sediment density, ρ_w and ρ_s, and the gravitational constant, g can be assumed to be essentially constant. This leaves the more strongly varying shear stress and particle size variables in the ratio, τ_c / D, as controls on the mobility of an individual particle. Here, I effectively substitute a value of particle exposure, e, for τ_c, divide it by the particle size and obtain a mobility criterion that should be constant for all particle sizes when surfaces are rough.

The Fenton and Abbot data plotted in Fig. 1.5 suggest that (a) relative particle exposure is strongly related to critical shear stress; (b) the relationship differs with particle size, but the difference is small, and not resolvable in the data scatter inherent in the experimental method, i.e., effectively the relative particle exposure corresponding to a given critical shear stress can, at present, best be treated as similar for all particle sizes; (c) the relationship has a nonlinear form, but can be can be considered as two quasi-linear segments, with differing slopes for particles that protrude above their surroundings versus particles that are hidden, i.e., do not rise above their surroundings; and (d) the variability of critical shear stress, τ_c and vertical particle exposure, e at entrainment appears to be higher for the hidden particles.

For use in the model, the data from Fenton and Abbot demonstrate that the critical shear stress for an individual particle can be associated with a corresponding critical particle exposure for entrainment of that particle. Those data suggest that the critical particle exposure will be constant for all particles of a given exposure, and will vary as the exposure varies.

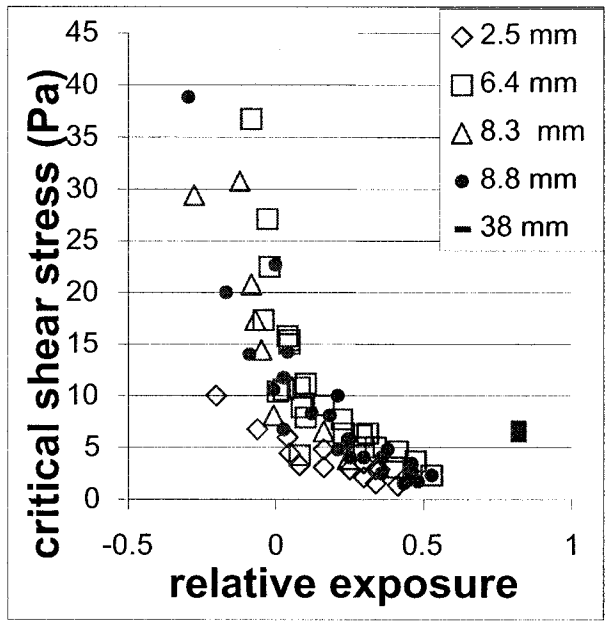

Fig. 1.5. Relationship between critical shear stress (Pa) and critical relative particle exposure. Empirical data relating relative particle exposure and critical shear stress for particles ranging from 2.5 to 38 mm is shown based on data from the flume experiments of Fenton and Abbot (1977). All particle sizes plot along a single trend, indicating the close relationship between τ_c and $R_{p,c}$

For convenience, in the model, the relative particle exposure is viewed as a substitute for the critical shear stress in parameterizing the initiation of motion for particles in the model cells. As an

approximation, in the absence of more detailed data, the relationship between τ_c and $R_{p,c}$ shown in the Fenton and Abbot data, for positive exposure, is assumed to be the same for all particle sizes. In the model runs, variations in the mobility threshold are limited to thresholds for which particles have positive exposure, i.e., must rise above their surroundings to be mobile.

The Fenton and Abbot data define the relationship between critical shear stress and particle exposure relatively well for the simplified experimental conditions, but the form of the relationship may vary with factors not included in the Fenton and Abbot study. Unrecognized variation in the critical value, $R_{p,c}$ for different particle sizes, possible differences in the form of the relationship between τ_c and $R_{p,c}$ for different particle sizes, and greater variability in $R_{p,c}$ for hidden versus protruding subfractions within a particle size class, may result in a different character of transport for different particle size classes. Different particle shapes, densities, and orientations may also modify the character of transport. These complications were not included in this particle interactions model.

In the model, relative particle exposure is obtained by averaging the heights of the tops of the particles that surround a central focal particle, then calculating the difference between the average height of the surrounding particles and the height of the focal particle. An example configuration of particles is shown in Fig. 1.4, where the tops of the adjacent particles are indicated by the dashed lines, and their average height by a solid line. The vertical exposed height of the focal particle is taken as the difference between the top of the focal particle and the average height of the surrounding particles in the directions upstream, downstream, left and right from the focal particle. A single value of $R_{p,c}$ is used for all particle sizes in a given model run, so that the mobility threshold is proportional to the particle's vertical exposure height, and inversely proportional to size of the particle. This means that mobility is controlled by the fraction of the particle height that is exposed above the surrounding particles. This criterion can be expected to

eliminate some secondary effects from the model results, while retaining the dominant effects of size selection and partial mobility within individual size classes. The model control is then a threshold criterion for particle mobility, defined as a value of the relative particle exposure, $R_{p,c} = e/D$ corresponding to the critical shear stress for mobility of a particle of that size and with that degree of exposure.

1.4.4. Structure of the cellular automata

The model space represents the channel and its boundaries, and is defined on a grid of cells, with a selected width and a length that is approximately 10 times the channel width, i.e., a length representative of a channel reach. Each model cell is assumed to be 0.256 meters in width and length, although there is no absolute spatial scale in the model, such that the channel may be viewed as larger or smaller limited only by the relationships between the size features incorporated in the model, such as, banks, floodplain, or sediment. The initial elevations assigned to each cell define a trapezoidal channel, inset within a larger valley.

To construct the model space, an initial slope is selected, then used to determine the mean elevation of the channel bed along the designated length of the channel reach. In each run, the channel also has a constant height and slope of the inner channel; a constant-width, floodplain that is level across its width, and a constant height and width of valley walls. The initial height of the water is also approximately constant, set to fill the initial inner channel to the top of the cell located closest to the point at 10 percent of the channel depth below the top of the channel.

In a model run, water in a given cell is partitioned among each of the three downstream cells, using the routing scheme defined by Coulthard (1999). Water is routed in the model only to determine which areas of the channel boundary are included in the wetted channel, defining the limits of the active bed. Particles are mobile only within the active channel. A standard or reference configuration of the modeled channel was selected (see Table 1.1).

Table 1.1. Channel form and particle characteristics for the reference channel

Variable	*cells*	*meters (nominal)*
Channel width	18	4.5
Bed width	8	2
Channel banks		
width	2	0.5
elevation drop per cell	0.5	0.125
Floodplain width	2	0.5
Valley wall		
width	2	0.5
elevation drop per cell	2	0.5
Reach length	80 to 90	20.5 to 23
Longitudinal slope	0.02 (dimensionless)	
Mobility threshold (particle exposure/D)	0.13 (dimensionless)	

A particle size distribution for the channel sediment was defined. First, the number of particle size classes was chosen. In the model runs described here, the median particle size in each class is 1 ϕ less than the previous, coarser size class, where $\phi = -\log_2(D)$. The standard particle size distribution includes particle size classes ranging from 2 to 256 mm. In some runs, the width of the particle size distribution was narrowed to a smaller number of size classes (each 1 ϕ in width), but the largest particle size was always 256 mm, identical to the nominal cell size. Next, each cell was randomly assigned a particle size. The particles occupying a cell at the channel surface can be visualized as a layer of spherical particles, one particle-diameter thick. The particles are 'placed' on the model grid, with the midline of the particles at the previously assigned mean elevation of the cell.

Particle sizes are similarly assigned to a set of subsurface layers. The depth of the subsurface sediment reservoir was assigned based on the size of the grid, and 54 subsurface layers

were maintained for the standard configuration. Each cell in the stack of cells underlying a given surface cell has a thickness equal to the assigned particle diameter for that cell. This substrate reservoir in the model space reduces the additional random element introduced in the mixing process of particle motion, in which a group of particles from one cell may move to another cell and bury the particles previously at the surface there. Each such particle motion, or motion of groups of particles, will bury some particles in the direction of motion, thus transferring them to the subsurface, and expose other previously buried particles at the surface.

A model run begins with an evaluation of whether the relative particle exposure criterion is met. The evaluation starts at one cell at the downstream end of the model space. For this cell, the elevation of the top of the particles in the cell are compared to the average height of all cells in the four surrounding neighbor cells. The difference between the height of the sediment in the cell being evaluated, and the average height of the neighbor cells gives the particle exposure, e. The relative particle exposure is then given by $R_p = e/D$ for the central, focal cell. Particles at the channel surface will move only if the local relative particle exposure exceeds the threshold value selected for the model run. When the particles in an individual cell are mobile, they move, all together as a group, in the direction of the lowest adjacent cell (with the constraint that moves are in one of the four cardinal directions). This rule, which directs moving particles to the lowest neighborhood cell, introduces a slope-dependent process into the model. The evaluation of whether the particles in each cell are mobile then proceeds to the next cell upstream.

Thus a packet of particles moves, if it is mobile, to the lowest adjacent downstream cell. If the group of particles is at the downstream edge of the model space, the particles are evaluated as if the upstream edge was connected to the downstream edge, in what is termed a cyclic boundary condition. Otherwise, the cells are evaluated from downstream to upstream, so that sediment vacates each downstream cell before the sediment in the upstream cell is evaluated to determine

whether it will move downstream. In rare cases, a single downstream cell may receive sediment from two or even three upstream cells, as long the receiving cell is still the lowest adjacent cell relative to those upstream cells.

Field observations of local particle patches with similar particle size provide a prototype for the cellular structure used in the model. When the particle size distribution is wide, particle patches are often about the size of the coarsest clasts, consisting of an accumulation of finer sediment surrounded or bordered by large clasts. Field observations of the phenomenon of group motions, in which many particles in a restricted area are mobilized more or less simultaneously (Nikora and others, 2002), also provides a prototype for the model process.

Although a single particle size is used to describe the sediment in a given cell, sizes on a prototype bed would not be exactly constant, and the boundaries of the model cells will not exactly correspond to the boundaries of small, local grain size patches on the bed. The model configuration is a simplification of the prototype.

Thus, this model develops spatial patterns in channel form and sediment size distributions only as a result of particle interactions. Local convergence and divergence of flow, and accompanying variations in flow velocity that may control the formation of pools and patches of coarse sediment are not included in the model. The only mechanism that generates pools and other form units in the model is interactions among particles beneath a flow that is otherwise homogenous in velocity and local shear stress.

1.4.5. Model runs and data analysis

The initial channel form and particle characteristics were varied in a series of model runs to provide data on the range of channel forms evolved from different initial configurations, and with different degrees of sediment mobility. The channels considered are intended to represent a set of reaches, from either a single channel or a set of many channels, in which the dominant variation between reaches is a change in a single variable. Such data can be obtained in field surveys.

Assuming such surveyed channels are in or near a stable state, the stable-state model results from a single variation series should reproduce the observed trends, at least if the channel processes are controlled by the constraints of particle interactions.

In the variation series described here, the two form variables of bed width and channel slope were evaluated, as well as the width of the particle size distribution. In an additional threshold variation series, the effect of flow magnitude was evaluated using particle mobility as a surrogate for variations in flow intensity.

One of the above four variables was incremented between each successive run in a given variation series, with all other initial conditions held constant. There are six runs in the bed width variation series, ten in the slope series, seven in the particle size distribution series, and seven in the threshold series, giving a total of thirty runs. The range of values of the variation variables are given in Table 1.2. The runs are primarily under conditions where pool-riffle sequences are expected, but the higher slope runs represent conditions where step-pools are expected. Alternatively, using different terminology, higher slope runs may correspond to plane-bed reaches with pools, as well as step-pool reaches at higher slopes.

Table 1.2. Range of variation variable values in model runs

Bed width	5 to 12 cells (nominally 1.25 to 3 m)
Channel slope	0.005 to 0.095
Particle size distribution width	3 to 9 phi size classes
Threshold relative particle exposure	0.18 to 0.48

The results presented in the following sections of this chapter are based on analyses of the model data for the final time step in the runs of the four variation series. Each simulation was continued for a duration initially found to be sufficient to reach a quasi-steady state, with a nearly

constant mean roughness of the channel (although with wide fluctuations about the mean). Two hundred and thirty time steps were standard.

Height deviations were extracted from the elevations of the channel and bed surfaces in the model grid for the final time step of a model run. Elevation data were converted to elevation deviations by subtracting the elevation of a sloping plane through the average elevation within the area of the channel to obtain channel roughness, and through the bed, to determine the bed elevation. The elevation deviations provide the same information as that used to define pools and riffles in the zero-crossing method described by Richards (1978). The width of the channel bed in the steady state channel was defined by identifying the cell in each cross-section with an elevation at or immediately above the level of the lowest 20 percent of the model channel.

Mean roughness of the channel or of the bed areas, defined as the root-mean-square of the height deviations, was used as the roughness parameter. Two different estimates of the steady state roughness of the model surface were used to check whether the channels had reached a steady state. The roughness of the surface was evaluated for all time steps. The extracted time series of roughness values can be viewed as two time periods; an early time with increasing roughness over time, and a later time with a stable mean value of roughness. The transition point between the time period when roughness adjusts and the time with steady-state roughness was evaluated by finding the intermediate time step that maximized the difference between the slope of the correlation lines through roughness values for later and earlier time. This method is a two-dimensional analogue to the zero-crossing method described by Richards (1978) for defining pools in pool-riffle channels.

Because the later time is expected to have constant roughness on average, the correlation line through the roughness values in the stable state time should be horizontal, and the intercept of this correlation should have the same value as the mean of all of the stable-state roughness values. The intercept of the correlation line through the sequence of roughness values during steady-state

time for the run is termed the 'intercept estimate' of roughness. The mean value of the roughness during the identified steady-state time is termed the 'averaging estimate' of roughness. If the roughness is stable through time, these two estimates will have the same value.

The difference between the intercept and averaging estimates of bed roughness was less than 1 percent in all except one of the runs. For the bed width variation Run 5, the two estimates differed by 6 percent. Similar estimates were made for the channel as a whole (bed and banks), and two runs differed by more than 1 percent for the channel roughness; for runs 8 and 10 of the slope variation series, the differences were 10 and 7 percent, respectively. These latter runs may not have reached a steady-state state in terms of roughness of the channel as a whole, but the similarity between the two roughness estimates indicates the bed surface has stabilized.

The final model surfaces represent a steady state in surface roughness, but quite slow adjustments may continue long after the surface roughness adjusts. This is apparent simply on the grounds that the volume of material that must be moved to effect an adjustment in surface roughness, particularly in a channel without distinct channel bars, will be tend to be small relative to the volume that must be moved to significantly adjust channel width, depth, or to the amount moved to modify slope.

1.4.6. Determining model pool size and spacing

Channel deeps were defined in each elevation grid as connected areas where the channel is locally deep. Channel deeps were identified by dividing the data into three classes, with class boundary values of 0, 0.375 (6/16), 0.625 (10/16), and all of the data. The length scale of a channel deep was defined as the square root of the area of the connected deep cells. Pools were defined as channel deeps with a length scale greater than half the channel width. This criterion is a two-dimensional analogue to the criterion commonly used to identify pools in the field based on their length. The model pools extracted in this way represent relatively extensive areas that are deep.

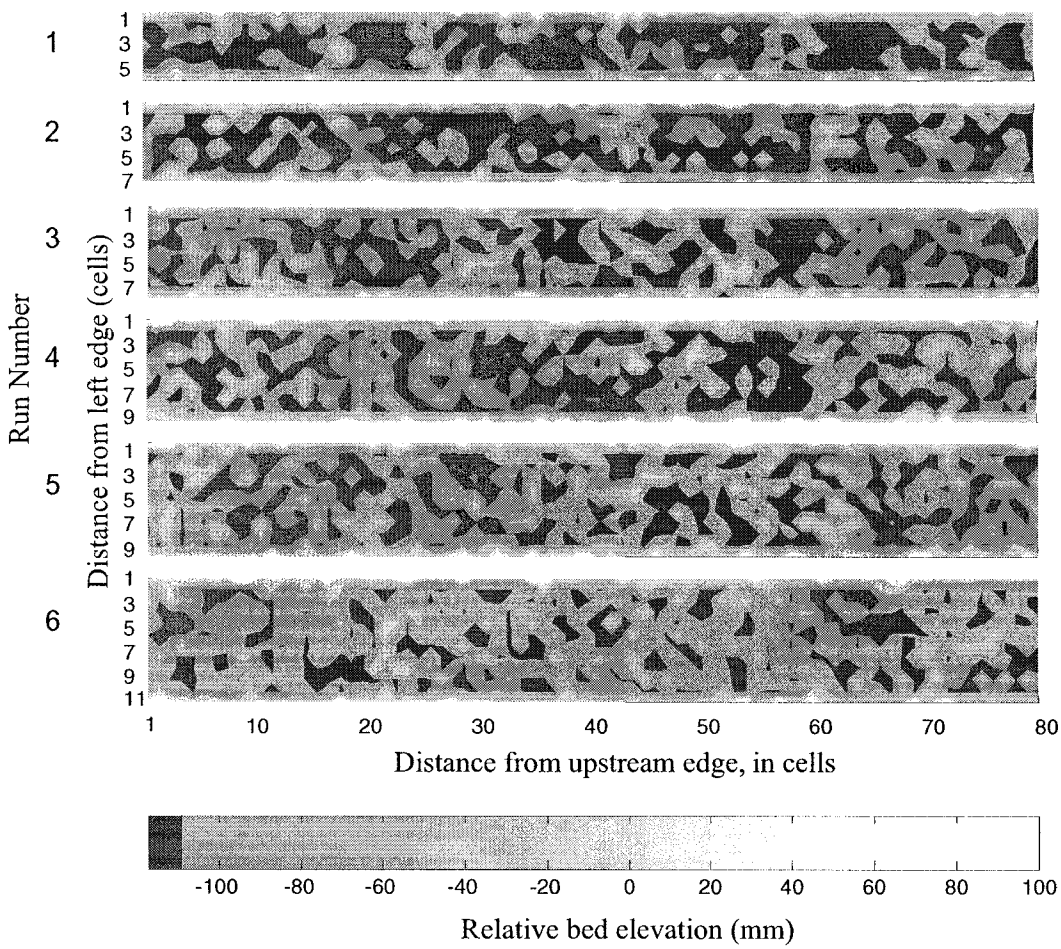

Fig. 1.6. Depth variation of the modeled channel bed surface in the bed width variation series. The spatial pattern of depth variation in the model bed surface as the width of the channel bed increases from 5 to 10 cells (nominally 1.25 to 2.5 m) is shown. The run number is shown to the left of each panel in the figure. The location and depth of channel deeps, dark areas in the plots, were defined as the height deviations, i.e., elevations were adjusted to remove the average slope of the channel bed. The black areas have a height deviation equal to or less than the 37.5 percentile value in the grid.

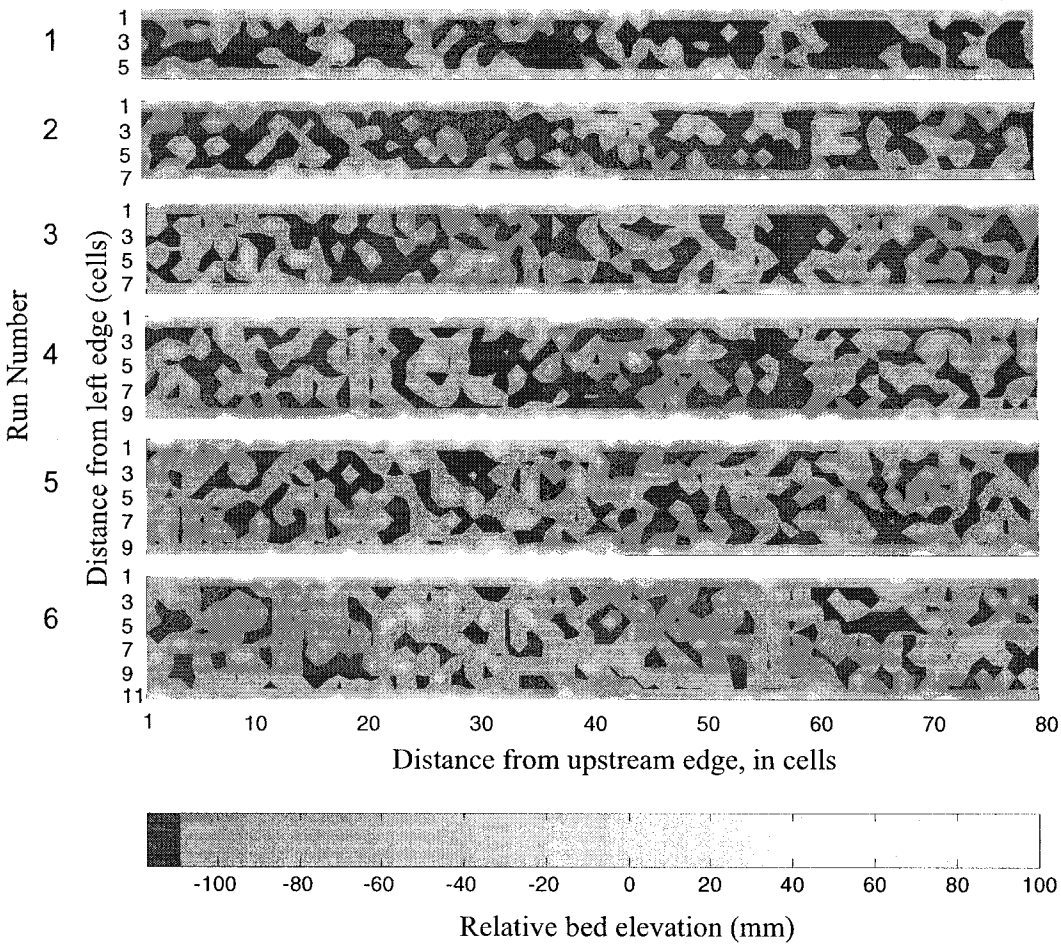

Fig. 1.6. Depth variation of the modeled channel bed surface in the bed width variation series. The spatial pattern of depth variation in the model bed surface as the width of the channel bed increases from 5 to 10 cells (nominally 1.25 to 2.5 m) is shown. The run number is shown to the left of each panel in the figure. The location and depth of channel deeps, dark areas in the plots, were defined as the height deviations, i.e., elevations were adjusted to remove the average slope of the channel bed. The black areas have a height deviation equal to or less than the 37.5 percentile value in the grid.

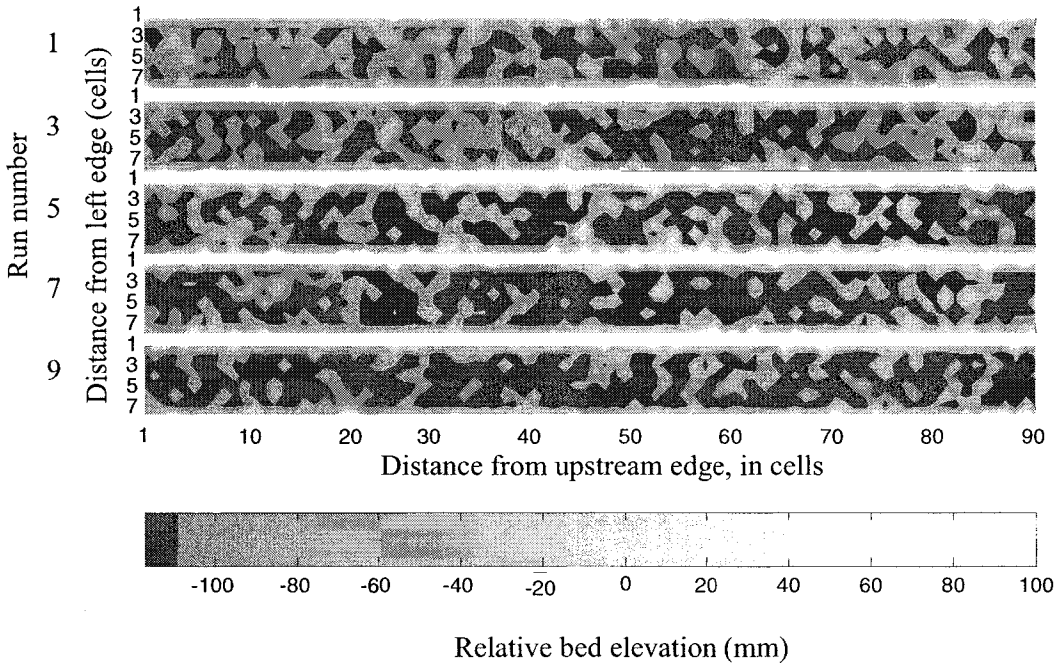

Fig. 1.7. Depth variation of the modeled channel bed surface in the slope variation series. The spatial pattern of depth variation in the model bed surface as the slope increases from 0.005 to 0.085 is shown. The location and depth of channel deeps, dark areas in the plots, were defined as height deviations, i.e., elevations adjusted to remove the average slope of the channel bed. The black areas have a height deviation equal to or less than the 37.5 percentile value in the grid.

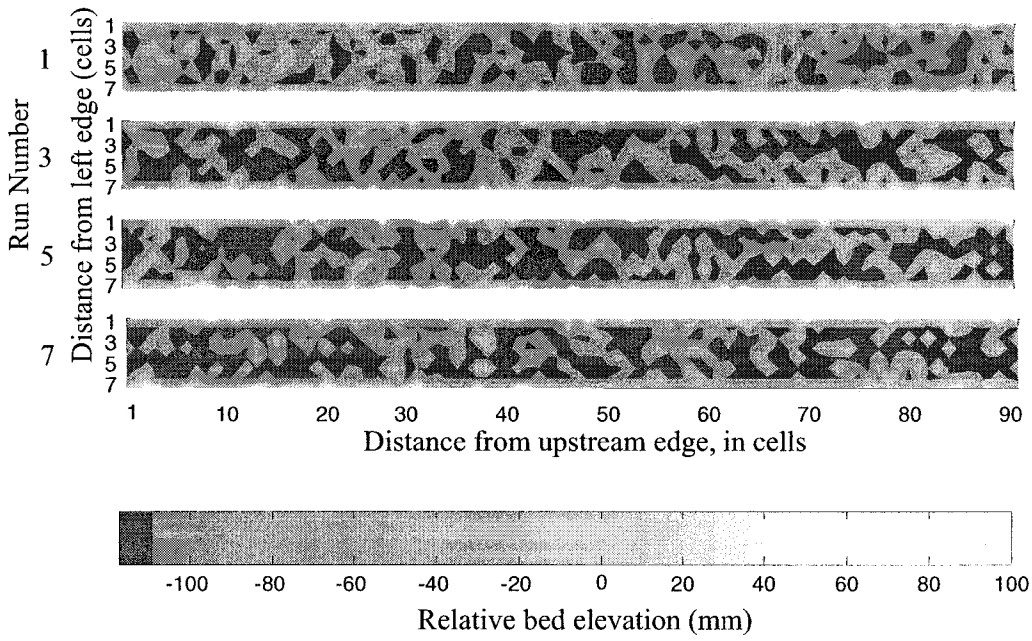

Fig.1. 8. Depth variation of the modeled channel bed in the particle size distribution series. The spatial pattern of depth variation in the model bed surface as the particle size distribution width increases from 3 to 9 size classes, each 1 ϕ in width is illustrated. The location and depth of channel deeps, dark areas in the plots, were defined as height deviations, i.e., elevations adjusted to remove the average slope of the channel bed. The black areas have a height deviation equal to or less than the 37.5 percentile value in the grid.

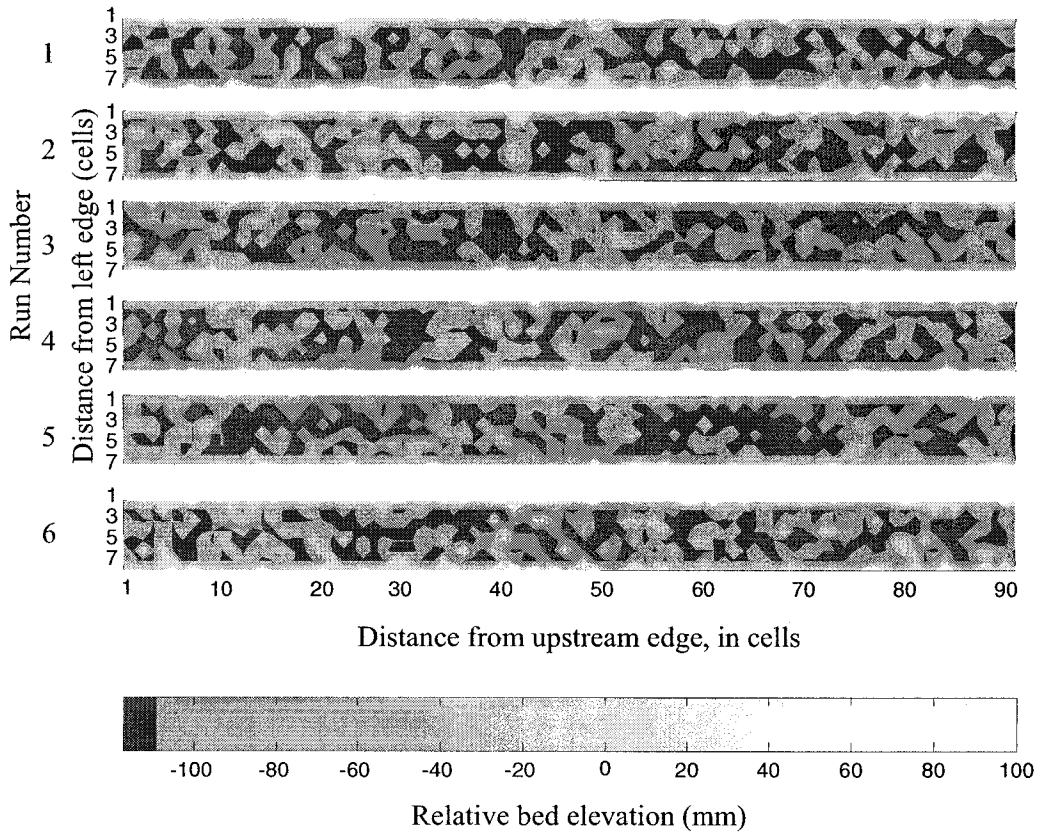

Fig. 1.9. Depth variation of the modeled channel bed surface in the threshold variation series. The spatial pattern of depth variation in the model bed surface as the mobility threshold increases from 0.13 to 0.48 is shown. The location and depth of channel deeps, dark areas in the plots, were defined as height deviations, i.e., elevations adjusted to remove the average slope of the channel bed. The black areas have a height deviation equal to or less than the 37.5 percentile value in the grid.

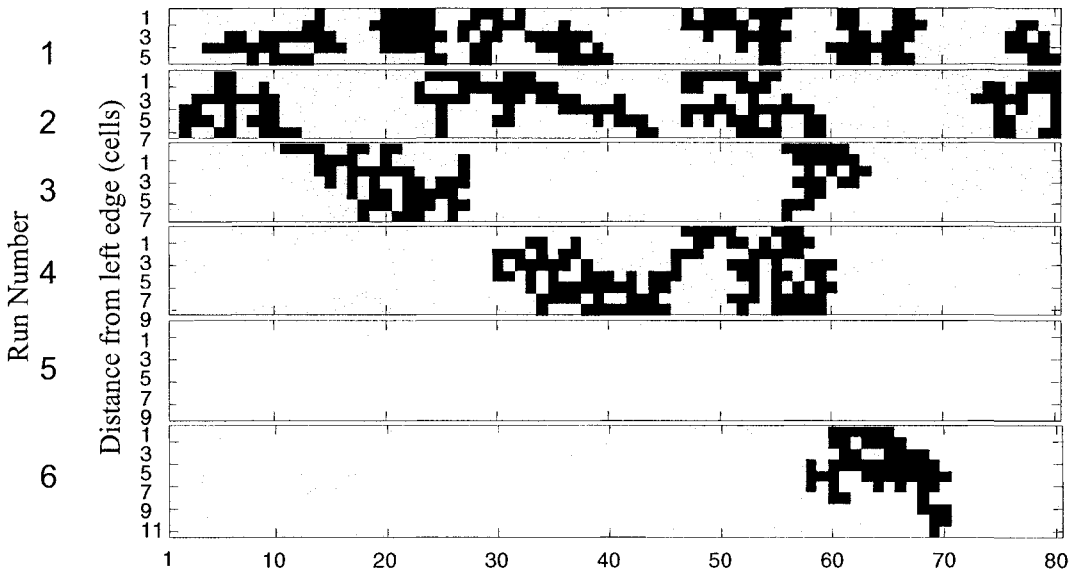

Fig. 1.10. Pools in the bed width variation series presented as a black and white grid. Pools in the bed width variation series are defined as all groups of connected deep cells with a length scale at least as long as one-half the bed width. This black and white presentation of the connected cells highlights the detailed, non-streamlined form of the pools.

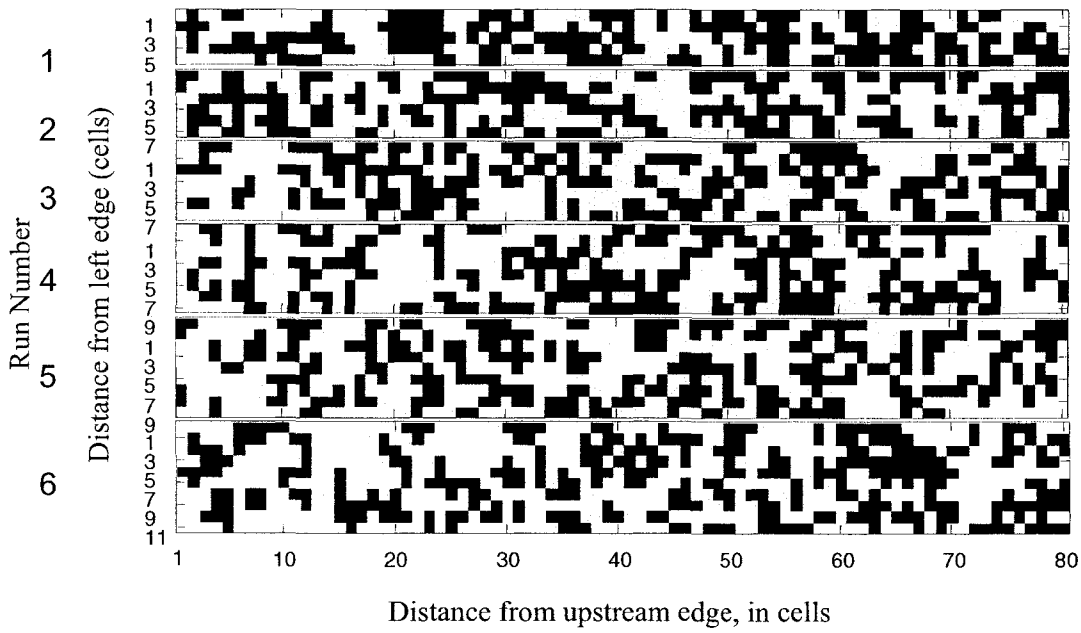

Fig. 1.11. Channel deeps in the bed width variation series presented as a black and white grid. Deeps in the bed width variation series, consisting of all groups of connected deep cells containing at least two cells. Isolated deep cells have been removed.

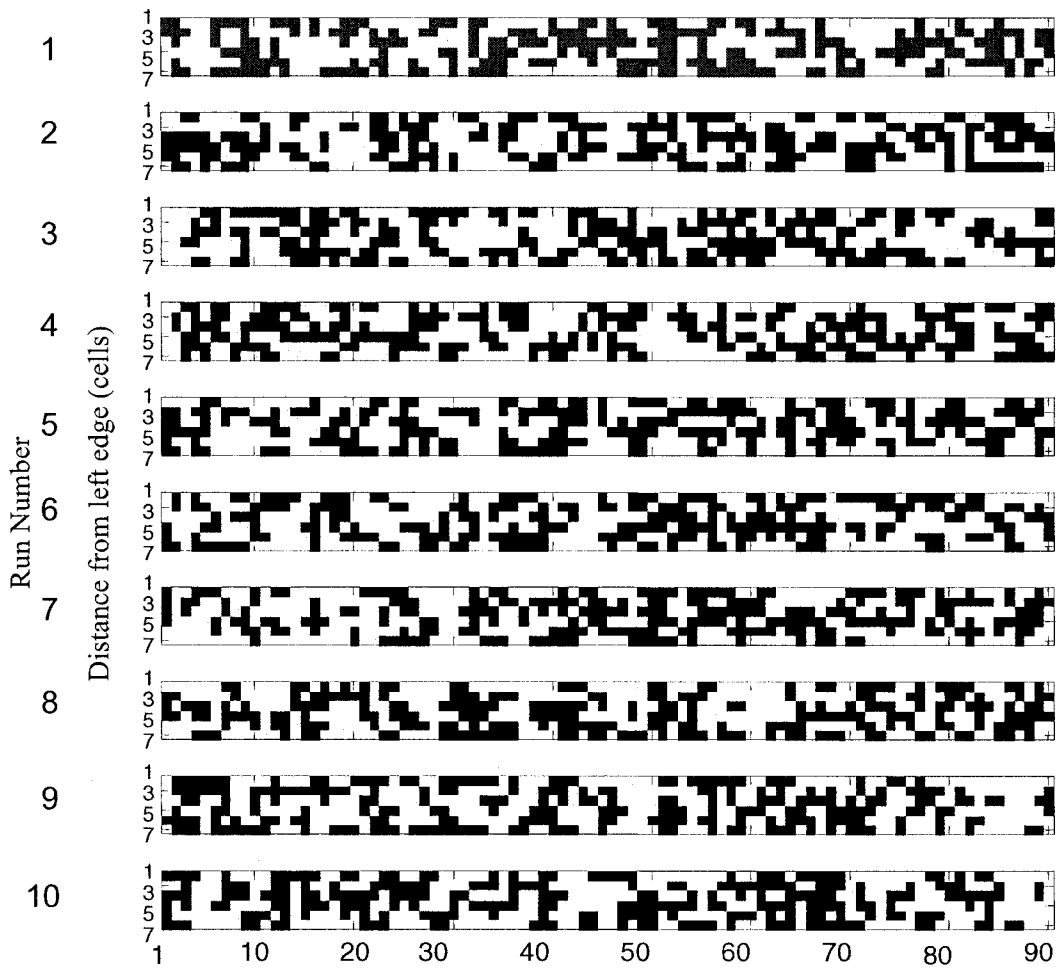

Fig..1.12. Deeps in the slope variation series presented as a black and white grid. Deeps in the slope variation series, consisting of all groups of connected deep cells containing at least two cells. Isolated deep cells have been removed.

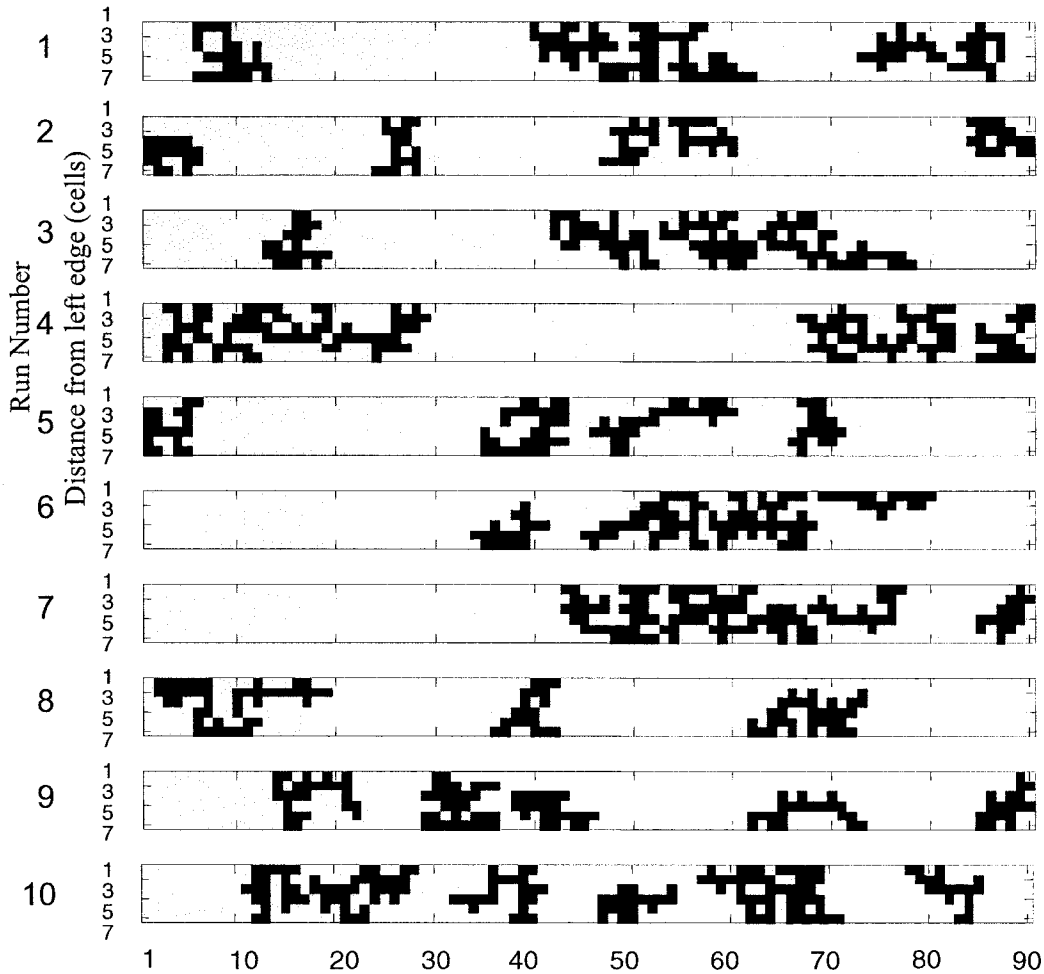

Fig. 1.13. Pools in the slope variation series presented as a black and white grid. Pools in the slope variation series This black and white presentation of the connected cells highlights the detailed, non-streamlined form of the pools.

Spatial patterns in the surface elevation deviations in the final grid in each model run are illustrated as a series of grayscale images in Figs 1.6, 1.7, 1.8 and 1.9. Pools and smaller channel deeps are plotted in black in these figures, and higher elevations are plotted in shades of gray. The range of the grayscale tones used to plot the threshold variation series differs from the grayscale range in the other plots, because this series included runs with a wider range of elevation deviations. Each image covers only the area of the channel bed, although a slight elevation increase toward the channel banks can be seen as white patches along the edges of the image.

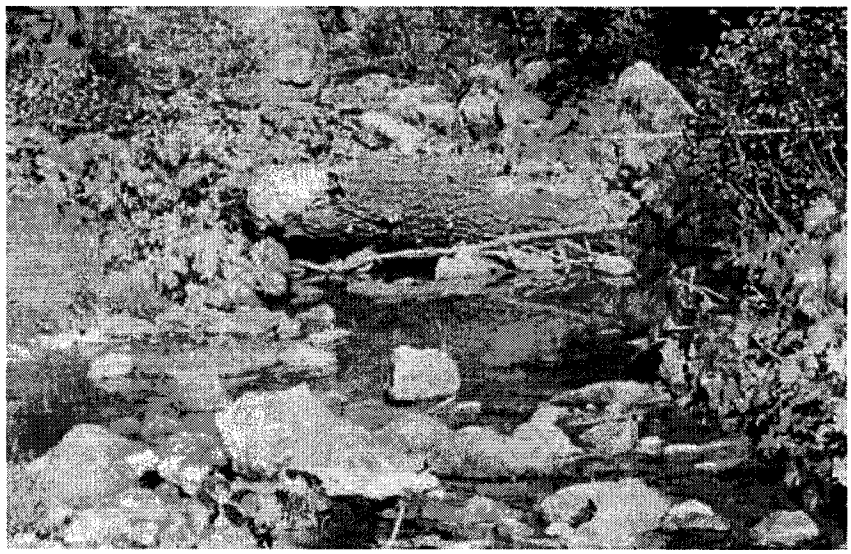

Fig. 1.14. View of a gravel-to-cobble dominated mountain river. View of a mountain river showing a patchy pattern of high elevation areas where particles rise above the low water level, and low elevation areas where particles are submerged. This view provides a visual analogue to the grid plots of the model data in Figs. 10 through 13.

Except for the bed width variation series, the panels are either six or seven cells in width (nominally 1.5 to 1.75 m in width). In the bed width series, initial bed width varies from seven to twelve cells in width (nominally 1.8 to 3.1 m), and the final average bed width varies from 1.6 to 2.8 meters. Black areas in the plots, characterized here as deeps, have a height deviation equal to or less than the 37.5 percentile value of the height deviation in the grid.

For comparison to the grayscale images (Figs. 1.6 through 1.9), black and white grids showing deeps (two or more connected deep cells), are plotted in Fig. 1.10 for the bed width series. These may be compared to the analogous black and white grids showing pools (large deeps) plotted in Fig. 1.11. Similarly, black and white grids showing deeps and pools in the slope variation series are presented in Fig. 1.12, and 1.13. These pools can also be identified in the bed width and slope grids showing channel deeps (Figs. 1.10 and 1.12).

This sort of sediment surface is illustrated in the photograph of a channel in Fig. 1.14. In very coarse channels, the channel surface tends to be highly irregular, so that local highs and individual large particle rise well above their surroundings. The model grids are analogous to the pattern one would see in such a channel at low water, as illustrated in Fig. 1.14, where the water surface aids visually dividing the sediment surface into local areas of high and low elevation. The resulting patchy pattern consists of large and/or elevated particles that rise above the water, analogous to the white areas in the grids, and areas where the particles are below water, analogous to the black areas in the model grids (Figs. 1.10 through 1.13).

1.3.7. Comparison to observed values

Published and unpublished data on pool spacing were obtained for comparison to the model results. The published data consist of data presented by Montgomery and others (1995) for spacing of pool-riffle, forced-pool, step-pools and plane bed channel reaches, and a set of data on pool-riffle spacing in mountain rivers (Wohl and Merritt, 2005). The latter data set is referred to here as the Mountain Rivers data. A subset of these data was selected, limited to channels with characteristics similar to the channels modeled, specifically, reaches with low bankfull discharge (< 3 m^3/s), slopes of 0.01 or above, and reaches where the difference between D_{50} and D_{84} was relatively large. This measure of sorting of the sediment is referred to here as the width of the particle size distribution. Given that the particle size distribution data in the data set consist of D_{50}

and D_{84}, the width of the size distribution is parameterized as twice the difference between the $\log_2$ of the recorded D_{50} and D_{84} values,

$$w_p = 2*(\log_2(D_{84}) - \log_2(D_{50}))$$

The data set was limited to channels where the size range between D_{50} and D_{84} exceeded the mean range for the data set.

CHAPTER 2

POOLS AND OTHER CHANNEL DEEPS IN A PARTICLE INTERACTIONS MODEL OF STEEP GRAVEL-TO-COBBLE STREAMS

2.1. An evaluation of the effect of particle interactions on pool length and spacing in steep gravel-to cobble streams

The particle interactions cellular automata, or *PICA,* model described in Chapter 1, was developed to move sediment and evolve the channel form. The model simulates the effects of particle interactions on sediment transport in steep, gravel-to-cobble streams. The model channels represent hypothetical streams in which only particle interactions control sediment transport, so that all effects of locally-varying flow, except particle-scale variations that are inherent in particle interactions, are omitted from the model. The model was designed to be relevant for conditions in pool-riffle and steeper channels, based on previous studies that indicate that particle interactions are important in the development of longitudinally-differentiated channels. This expectation may apply to both pool-riffle and steeper streams, but is evaluated here in terms of pool-riffle channels. Specifically, it was hypothesized in this study that the size and spacing of pool-like and riffle-like elements in the model channel bed surface will vary in the same direction as in steep, gravel-to-cobble, pool-riffle channels. It was also hypothesized that pool-riffle form variation

would be influenced by bed width, slope, particle size distribution and a measure of particle mobility, which is represented in the model by the critical relative particle exposure, $R_{p,c} = e/D$, and is related to the dimensionless critical shear stress, i.e. the Reynolds stress for motion of individual particles.

In this chapter, the model results are compared to the length and spacing of pools in pool-riffle channels. These sections include, first, an illustration, followed by analysis, of local deeps in the model bed surfaces. The larger local deeps are termed pools, defined as deeps with a length scale at least as great as half the bed width. The variation of final channel width as the four control variables, initial bed width, slope, particle size distribution and threshold for particle motion, $R_{p,c,}$ are varied is presented first. The following sections evaluate the size and spacing of the model pools, followed by a comparison of model and field examples of pool size and spacing, and how they vary as width, slope, particle size distribution and the sediment mobility threshold are varied. The final section describes the non-random character of particles arrangements on the model bed surface at steady state.

2.2. Overview and description of the model pools

Pool-like channel deeps in the model runs can be informally characterized as three types. The first two types are large compact pools, and large irregularly-shaped pools that are somewhat compact (Figs. 1.6, 1.7, 1.8, and 1.9). Similarly-described pool types have been reported from observations of streams (e.g., Keller and Melhorn, 1973, 1978). Large pool-size deeps observed in the model results also include forms that are not pool-like, including linear forms (very narrow relative to their width), and forms that are short in the downstream direction. Examples occur in various runs, including runs at a moderate slope of 0.005 (slope variation, Fig. 1.7, Run 1); runs with intermediate widths of the particle size distribution (distribution widths of 4, 5 and 6 ϕ-size classes; Fig.1.8, Runs 3 and 5); and a run at a low threshold, $R_{p,c} = 0.13$. (Fig.1.9, Run 1). Such

forms are included in the pools evaluated in the model data. There are also smaller deep areas, many with irregular shape, observable in the model results. These small deeps are too small to meet the size criterion, i.e., a length scale equal to or greater than one-half the channel width, for designating pools in this study. The pools identified in the model runs and described below are similar to pools in streams in a number of respects, but also differ in some ways. In general, the origin of these pools in the model is entirely controlled by particle interactions, and as such, the pools may be expected to be most similar to those found in streams where particles are only weakly mobile, but fundamentally dissimilar to large streamlined pools that are extensively sculpted under locally varying flow.

Relatively few compact pools were generated in the modeled sediment surfaces. An example of a completely compact pool, with no internal non-deep areas and mostly without embayments in its outer boundary, can be seen in Run 1 of the bed width variation series (Fig. 1.6). The channel bed in the figure is five cells wide (nominally 1.25 m) with the other model settings at their standard values. More model pools are similar to the compact but irregularly-shaped pools found in steep, gravel-to-cobble streams (e.g., Keller and Melhorn, 1973; personal observation). Such pools are found in most model runs.

2.3. Bed width adjustment from initial to final width

As the model channel evolves to a steady-state roughness, minor adjustment of the width of the channel bed occurs. Such adjustments are potentially important because bed width is a boundary condition that may influence channel form and roughness throughout the bed, via movement of sediment particles from banks to bed, and lateral transport across the bed. In addition, pool spacing is often described as proportional to channel width. Width variations that are independent of this established prediction, i.e., width variation out of proportion to variations in distance between pools, will influence the reported spacing. Because particle interactions are the sole control in the model, the theoretical argument that predicts pool spacing and channel

width as directly proportional cannot apply to the model pools, and independent variation of the distances between pools and bed width needs to be considered.

In the bed width variation runs, the final bed width, $w_{b,f}$, is strongly correlated with initial bed width, $w_{b,i}$ (Fig. 2.1a, Table 2.1). The bed width variation series shows a final width between 88 and 89 percent of the initial width as channel, as the initial width varies. A plot of final width against initial width shows a tendency for a slight decrease in the width of the final bed relative to

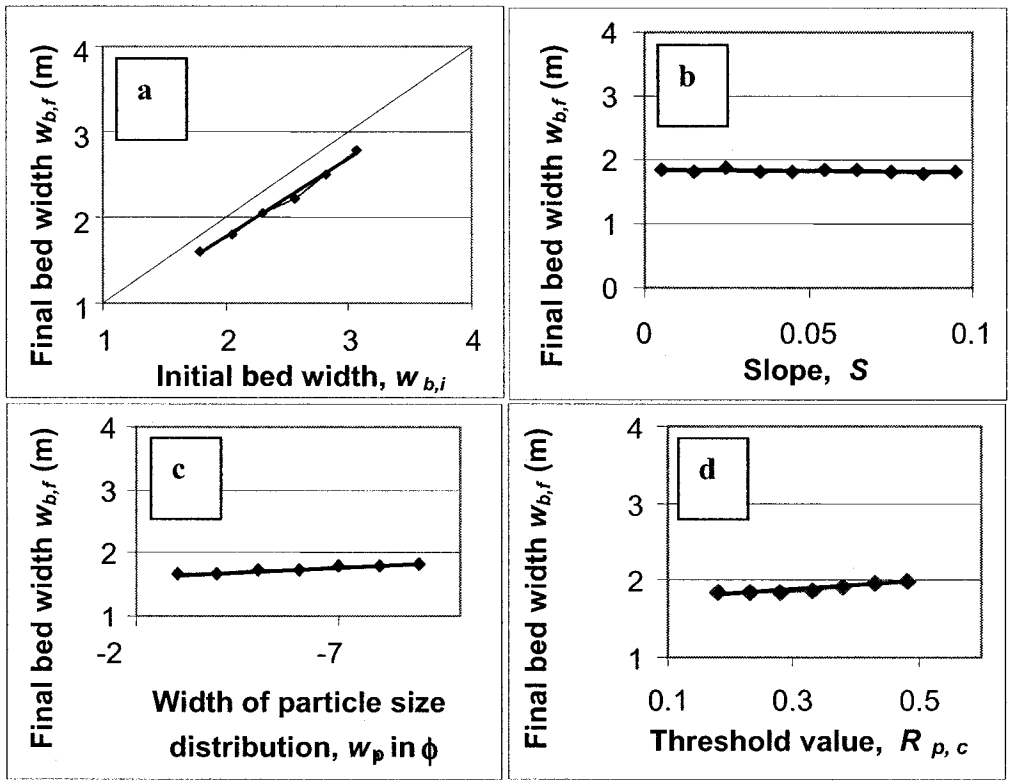

Fig. 2.1. Bed width adjustment. The bed width adjusts during the model runs. There are relatively minor adjustments in bed width in the variation series, but the trends are clear due to the lack of variability about the trends. In the bed width variation series, the bed narrows slightly and narrows more in wider beds. The bed width increases slightly as the width of the particle size distribution increases and as the threshold for motion increases (decreasing mobility). There is no trend in the adjustment as slope varies.

the initial width, for the widths used in this analysis. The decrease in width during a model run is somewhat greater for wider beds than for narrower ones; the adjustment is a decrease of 0.2 to 0.3 m as the initial width ranges from 1.6 to 2.8 m (Table 2.1). The trend in the adjustment is

Table 2.1: Width adjustment in the model variation series

Variation series	Linear correlation with final bed width (m)	r^2	n
Initial bed width	$w_{b,f} = 0.908\ w_{b,i} - 0.046$;	$r^2 = 0.995$	6
	$w_{b,f} - w_{b,i} = 0.0952\ w_{bi} + 0.0635$	$r^2 = 0.584$	6
Slope	$w_{b,f} = -0.366\ S + 1.84$	$r^2 = 0.136$	10
Particle size distribution width			
	$w_{b,f} = 0.0312\ w_p + 1.56$	$r^2 = 0.952$	7
Threshold relative particle exposure			
	$w_{b,f} = 0.581\ R_{p,c} + 1.70$	$r^2 = 0.902$	7

note: all widths in meters

visually apparent in the plots (Fig. 2.1a). A linear correlation between the change in width, ($w_{b,f}$ - w_{bi}), and the final width, $w_{b,f}$ has a moderate r^2 of 0.584 (Table 2.1). The comparison of initial and final width is, also, complicated by changes in channel form between the initial and final times in the model run. The initial form has an abrupt break in slope at the base of the banks, whereas the final form has a smooth transition between banks and bed. This means there is no absolute standard for defining a point with respect to the final form's transition section that is equivalent to the slope break in the initial form. The linear correlation noted above includes the effects of both form and width adjustment, resulting in a final bed width that ranges from 88 to 89 percent of the initial bed width. The relationship between initial and final width would differ if a

different initial form had been used. In the slope, particle size and threshold variation series, initial bed width is constant within each series. The bed width does not adjust in the slope series, and the reason for this is not clear. In the slope variation series, the initial bed width is 6 cells (nominally 1.5 m), and the final widths are 7.3 to 6.9 cells (nominally 1.8 to 2.0 m) through the series, which is 0.82 to 0.87 times the initial width. In the slope variation series, the correlation of final bed width with slope is weak ($r^2 = 0.136$; $n = 10$; Table 2.1).

The bed width does adjust in the particle size and threshold series, and the magnitude of the adjustment varies linearly through each of these series. In the particle size distribution series, the final bed width increases as the width of the particle size distribution (number of particle size classes in the model's truncated size distribution) increases (Fig. 2.1c; Table 2.1). The initial bed width is 5 cells (nominally 1.3 m). Final widths range from 6.5 to 7.1 cells (nominally 1.7 to 1.8 m), or 130 to 143 percent of the initial width. In the threshold series the initial width is 6 cells, and the final widths are 7.2 to 7.8 cells (nominally 1.8 to 2.1 meters), or 1.2 to 1.3 times the initial width, as the threshold increases (i.e. as sediment mobility decreases) (Fig. 2.1d; Table 2.1).

2.4. Pool size and form

2.4.1. Distribution of the length scale of channel deeps

The channel deeps extracted from the model grid range in size from a two adjacent cells, not directly connected to other deep cells, up to the largest pool observed in each model reach. The size distribution of the channel deeps is summarized here as a base two logarithmic transform of the length of the deeps. The maximum length of a deep in a given size class is twice as long as the maximum length of the deeps in the previous class. As an illustration, the distribution of the number of deeps in each size class is shown for the threshold variation series (Fig. 2.2). The distribution of the length of deeps is dominated by small deeps, i.e., the distribution of the size of the deeps is right-skewed, as are those for pools in stream channels.

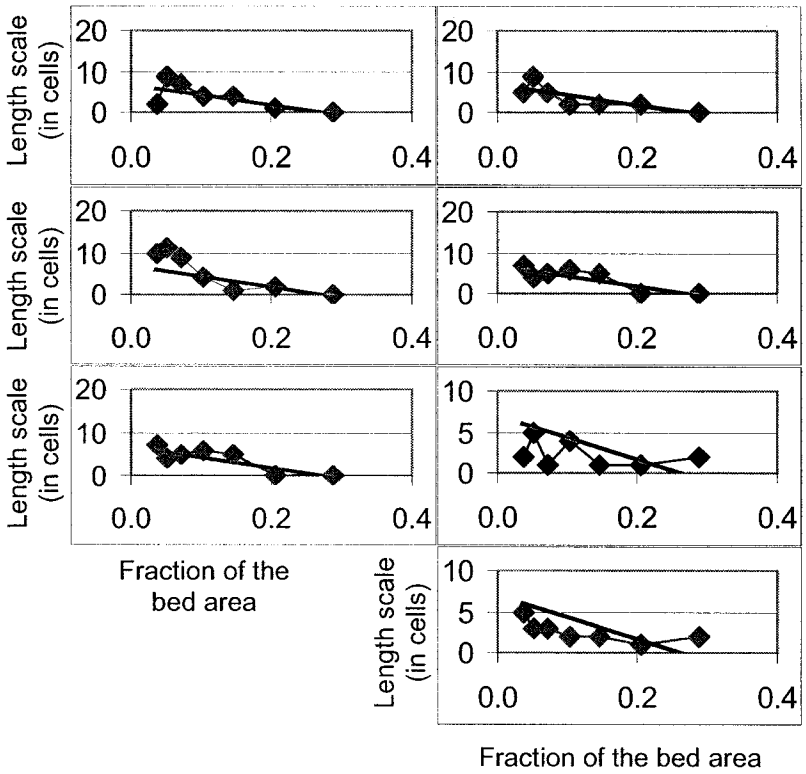

Fig. 2.2. Pool length distribution in the mobility threshold series. The distributions of the number of pools in successive length scale classes are right-skewed and generally unimodal, as are pool-riffle channels in streams.

2.4.2. Distribution of the depths of channel deeps

The maximum depth of pools and other deeps can be defined as the difference between the highest and lowest elevation deviations, relative to the planar sloping surface fitted through the modeled channel bed. There is a trend in the maximum depth of the pools and other channel deeps in two of the four variation series (Table 2.2). The range of the height deviations observed in the model results does not change as the width of the bed increases, or as slope increases. However, there is an increase in the range of the height deviations for both the particle size distribution and threshold series (Table 2.2). For the particle size distribution series, the range of the height deviations increases by a factor of about 2.6 as the number of size classes, 1-ϕ in width, increases from 3 to 9. The range of the height deviations increases by a factor of 1.6 as the threshold increases from 0.18 to 0.48.

Table 2.2. Elevation distributions relative to the bed surface: minimum and maximum elevation deviations in the variation series runs

Bed width		*1.5 m*	*2.8 m*
	Correlation of h_{med} with w_b	h_r (m)	h_r (m)
Deviations, *h*:	$h_r = -0.643\ w_b + 264$; $r^2 = 0.312$; n=6	258	257
Slope:		*0.005*	*0.095*
	Correlation of h_{med} with S	h_r (m)	h_r (m)
Deviations, *h*:	$h_r = -0.712\ S + 260$; $r^2 = 4E\text{-}05$; n=10	263	264
Particle size distribution width:		*2*	*9*
	Correlation of h_{med} with w_p	h_r (m)	h_r (m)
Deviations, *h*:	$h_r = 26.9\ w_p + 54.4$; $r^2 = 0.673$; n=5	99	261
Critical relative particle exposure:		*0.13*	*.73*
	Correlation of h_{med} with $R_{p,c}$	h_r (m)	h_r (m)
Deviations, *h*:	$h_r = 491\ Rp,c + 138$; $r^2 = 0.6394$; n=7	263	409

Note: h_r is the range of the height deviations

Variations of the maximum depth of the model pools and other deeps are also characterized by an increase in the maximum local depth. The negative height deviations become more negative through the slope, particle size and particle mobility variation series, but becomes less negative in the bed width variation series. The relationship between particle transport, structuring of particles and characteristics of the channel bed surface will be considered further in Chapter 3, represents deeps defined by a minimum depth criterion. The full range represented by

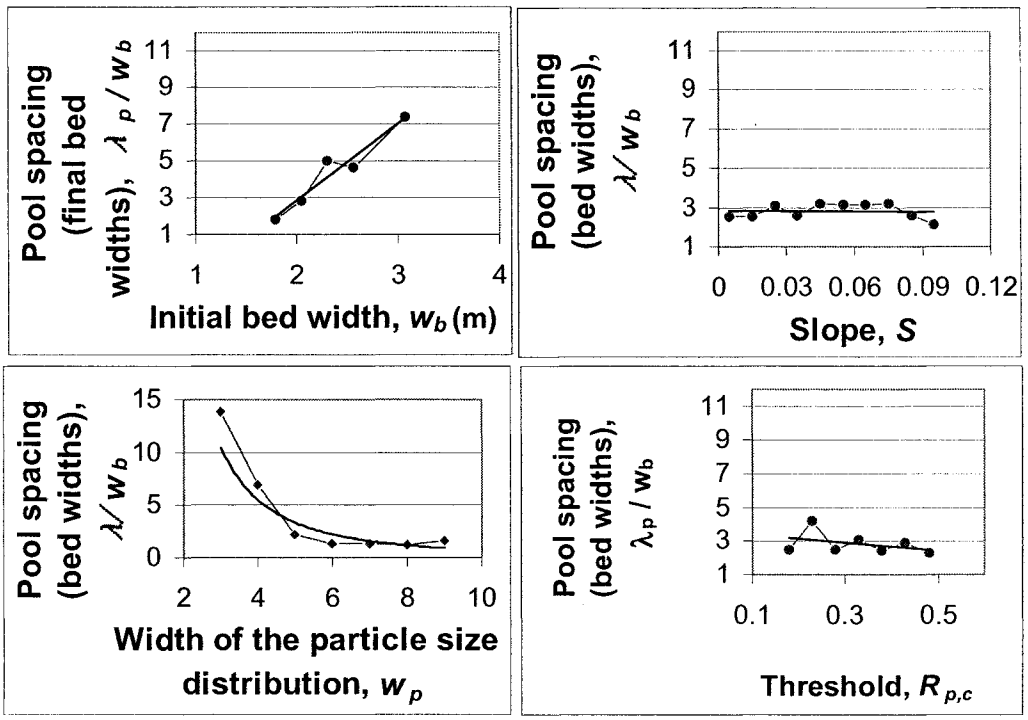

Fig. 2.3. Pool spacing in the bed width, slope, particle size and threshold variation series. Spacing of model pools increases with bed width, and shows a strong non-linear decrease with width of the particle size distribution. The spacing has no trend with slope and no significant trend with the $R_{p,c}$ threshold for motion.

the color scheme used in the threshold series is wider than for the other series. The gray-scale figures were constructed using a designated range of black to gray shades, and equal proportions the range of height deviations are designated by each shade. The area shown in the black shade depends on the fraction of the area that falls below a specified value. The pattern of depth variation is such that the fraction of the bed area below the cutoff for the black shade varies relatively little through the threshold variation series run, somewhat more strongly through the particle size distribution series, and varies most for the bed width and slope series. The black shade thus reflects the fraction of the model area that falls below an arbitrary reference level of the height deviations.

2.4.3. Width variation series

The elevation deviations observed in the bed width series provide information on the expected degree of channel adjustment in a group of channels with a range of initial bed widths, with all other initial conditions held constant. The spatial patterns of highs and lows in the model channels of the bed width series are shown in Fig.1.6 as gray-scale images, in Fig. 1.10 as black and white grids of the height deviations (excluding 1-cell deeps), and in Fig. 1.13 as black and white grids showing only the identified pool areas.

In the bed width variation series, the initial width increases from 7 to 12 cells (nominally 1.8 to 3.1 m), and the width increase is accompanied by a decrease in the number of pools as the initial bed width increases. The gray-scale plots illustrate that the minimum value of the local height deviations rises as the bed widens, as shown by the decreasing area shaded in black (Fig. 1.6). The narrow channels appear to more readily develop channel-spanning areas of positive height deviations, thus generating pool-like forms centered within the channel between the high areas. There are relatively few pools in the wider runs. The wide Run 5 had no deeps large enough to be classified as pools, and Run 6 has only 1 pool. In the narrow width runs (Fig. 1.6, Run 1), pools are smaller and more closely spaced. They are also more compact, with fewer internal high points, as can be seen in both the gray-scale plots (Fig. 1.6) and the black and white grids (Figs. 1.10 and 1.11).

As the number of pools decreases through the series, the corresponding pool spacing increases (Table 2.3; Fig. 2.4a). Pool spacing in the bed width variation runs ranges from 1.8 to 7.4. The spacing data presented here are normalized by the bed width. The slope, m, of the regression line is 4.19 for the model data, using pool separation normalized by bed width. As a standard of comparison, an empirical correlation of pool spacing with channel width was generated using the MR data set (Wohl and Merritt, 2005). In these field data, pool spacing increases as channel width increases. The modeled spacing was also normalized by channel

Table 2.3: Pool size and spacing in the bed width variation series

Linear correlation with initial and final bed widths	r^2	n
Number: $N_p = -4.69\ w_b + 14.1$;	0.804	6
Length: $L_{p,mn} = 0.543\ w_b + 0.353$;	0.798	5
Area: $A_p = 26.3$ (cells) - 20.2;	0.816	5
Spacing, model in bed widths: $\lambda/w_b = 4.19\ w_b - 5.56$;	0.937	5
Spacing, model, in final channel widths:		
$\lambda/w_c = 0.620\ w_c - 3.25$;	0.976	5
Spacing, MR data set (Montana and Yellowstone only from Wohl and Merritt,2005)		
in channel widths: $\lambda/w_c = 0.458\ w_c - 0.250$	0.391	13
Spacing, Montgomery and others, 1995:		
pool-riffle-bar: $\lambda/w_c = -0.0248\ w_c + 3.28$	0.453	3
plane bed: $\lambda/w_c = -0.398\ w_c + 12.8$	0.478	8
forced pool: $\lambda/w_c = -0.0225\ w_c + 1.31$	0.0401	29
step-pool: $\lambda/w_c = -0.0479\ w_c + 1.43$	0.737	6

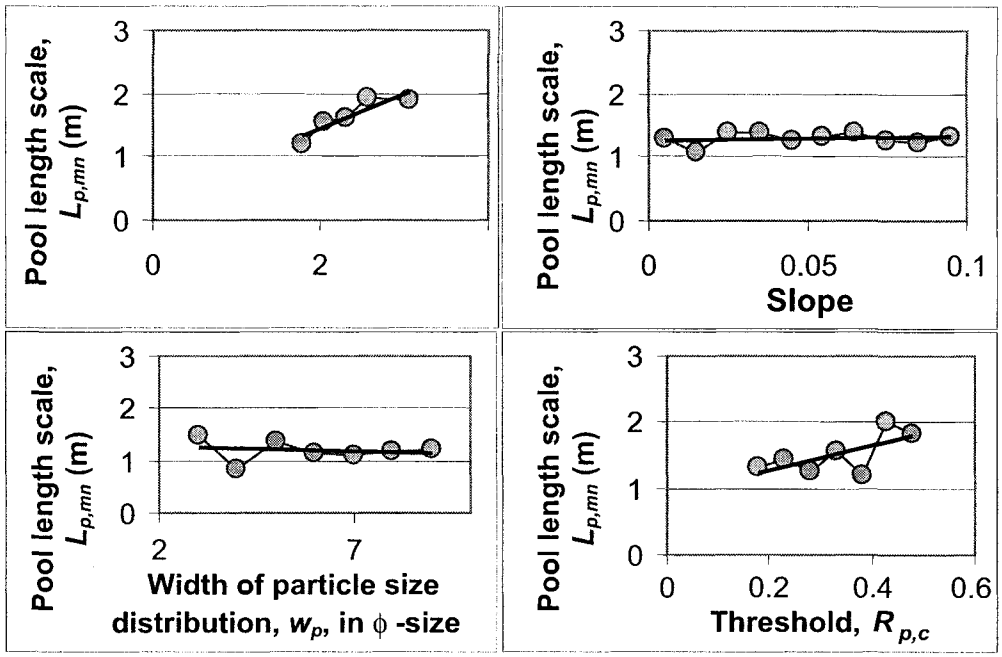

Figure 2.4. Length scale of the model pools in the bed width, slope, particle size and threshold variation series. The average length scale of the model pools increases as the bed width increases and The threshold increase (corresponding to a decrease in mobility). Pool length shows no trend with slope or with the width of the particle size distribution.

width, giving a range of spacing from 0.6 to 3.3 channel widths (Fig. 2.5). The rate that pool spacing varies with width is similar in the model data and the MR data set (Wohl and Merritt, 2005), as shown by the slope, *m*, of the regression lines (Fig. 1.1a). The regression slopes for the model and MR field data are 0.620 and 0.458, respectively, using pool separation normalized by channel width. In another comparison, the regression slopes are -0.0248 for a pool-riffle-bar channel, and -0.398 for a plane bed channel (Montgomery and others, 1995) (*see* Table 2.3; Fig 1.1). The reason for differences between the MR data (Wohl and Merritt, 2005) set and the Montgomery and others data sets is not clear, but I would suggest that the smaller number of pools in the Montgomery and Buffington data sets, combined with the potential error in identifying the different pool types, makes that data set less reliable.

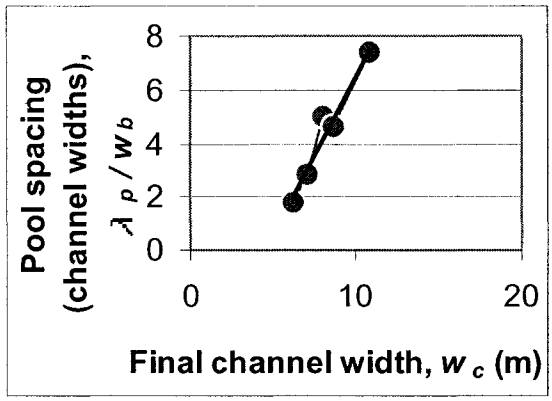

Figure 2.5. Normalized pool spacing in the bed width variation series. For comparison to field data normalized by channel width, the spacing normalized by final width of the channel ranges from 1.8 to 10.9.

2.4.4. Slope variation

Slope varies from 0.005 to 0.095 in the slope variation runs. The model channels do not have the well-developed alternating steeper and less steep channel segments considered characteristic of pool-riffle channels, although some runs show multi-cell slope variations along the length of the channel. This is a major, apparent difference from stream channel observations, and it is not clear why this is. One suggestion is that the model time scale is set allow the bed surface to reach a stable roughness of the particle surface, the criterion chosen for this project. But, that duration may be too short for distinct slope differentiation to develop in the model runs. This would

suggest that the stable roughness reached in the model is not an ultimate stable state, and that slow surface adjustments may continue. An additional possibility, which may be combined with the above, is that slope differentiation is suppressed in this model because the transport input is equal to output, so that the model reaches are neither aggrading nor degrading, but reflect a quite short-term balance between supply and transmission of sediment. This may limit the development of spatial variations in slope.

The spatial patterns of highs and lows in the channels are shown in Fig. 1.7 as gray-scale images, and in Fig. 1.12 and 1.13 as black and white grids of the height deviations for these runs. The gray-scale image shows a pattern of isolated small low areas at the lowest slopes, then greater numbers of small low areas, and some larger ones, as slope increases. This pattern in the images reflects that, as slope increases, the stable-state surface has a larger fraction of the bed area that falls below the plotting threshold represented by the black shade. This threshold is an arbitrary reference level, set equal for all runs in these plots.

Details that can be seen in the gray-scale plots include a form similar to a thalweg, seen as a narrow sinuous black area at the right in the lowest slope run. A feature that approximates a spatially-segregated deep, such as those found in pool-riffle channels, is seen in the second panel, at a slope of 0.015. As slope increases, by 0.01 between each pair of plots shown, the fraction of the channel area occupied by deeps increases. At even higher slopes, only narrow lines or ribs rise above this plotting threshold (Fig. 1.5). These features form reticulate to linear highs, similar to ribs (e.g,, Church and others, 1998; Hassan and Church, 2001) or to the channel-spanning steps in step-pool channels.

Deep areas and pools were identified in the model data. These deeps and pools were identified not on the basis of an absolute threshold value as seen in the gray-scale plots. Instead, deep areas were defined as those with a bed surface below the 36 percentile of bed elevations in a

given model run. Pools were then identified as deep areas with a length scale that exceeded one-half the channel width.

There is no clear trend in modeled pool spacing (Fig. 2.3) or pool length scale (Fig. 2.4) as slope varies. There is also no trend in the number of pools, or in the number of very small, two-cell deeps (*see* Table 2.4). Spatial variations in the maximum depth of the local deeps, illustrated in the sequence of gray-scale images in Figure 1.7, constitute the strongest pattern associated with varying initial slope in the model runs. These data indicate that although the area of the deeps does not vary with slope, the area that is occupied by pools (large deeps) may have a complex pattern of variation with slope. At model bed slopes of 0.005 to 0.025, the fraction of the bed area occupied by pools is variable; at slopes between 0.025 to 0.055, the fraction of the bed occupied by pools is constant; and at higher slope, the area occupied by pools increases linearly. This apparent complex pattern of variation in spacing as slope varies suggests three different ranges of slope that at least roughly correspond to the ranges expected for pool-riffle, plane-bed, and step-pool reaches. Although the number of model runs generated in this study is not sufficient evaluate trends in such an apparently complicated pattern of pool spacing variation, the model data can be compared to field data. Evaluation of the slope subselection of the MR data (Wohl and Merritt, 2005), indicates that pool spacing tends to increase with slope for these steep, gravel-to-cobble, relatively low discharge channels where particle interactions may be expected to be most important. A review of previous empirical studies, presented by Thompson (2002) suggests that there the direction of trend for variations of slope with pool spacing differs from stream to stream. Thus, these studies do not establish a clear relationship of spacing with slope. A hypothesis to explain the observed variation has also been proposed (e.g Wohl and others, 1993). It has been suggested that the observed relationships between slope and spacing differ because spacing depends on channel roughness and/or substrate resistance, as well as on slope. The model data

suggests instead that there may not be little or no direct relationship between pool spacing and slope where particle interactions are the primary control on sediment transport.

Some field data supports the idea that a lack of slope variation in pool spacing is associated with particle interactions. For channels in which at least 46 percent of the pools are forced pools, Montgomery and others (1995) found no slope dependence of the pool spacing. Based on this, a suggestion consistent with the available data is that the modeled lack of an influence of slope on pool spacing may reflect a process similar to the development of pools forced by large obstacles. That is, a reasonable hypothesis is that the coarse and partially mobile sediment characteristic of the model runs, for which individual particles alternately move and act as obstacles preventing motion of adjacent particles, influences the spacing of the relatively large, local deeps that form. As noted above, additional model runs would be needed to evaluate this possibility.

Table 2.4: Pool size and spacing in the slope variation series

Linear correlation with slope	r^2	n
Number: $N_p = 3.64\ S + 4.42$	0.0248	10
Length: $L_{p,mn} = 0.515 + 1.2751$	0.0235	10
Area: $A_p = 16.7\ S + 25.1$	0.0172	10
Spacing, model: $\lambda/w_b = -0.608\ S + 2.83$	0.0024	10
Spacing, MR data set: $\lambda/w_b = 118\ S + 0.645$	0.580	13
Spacing, > 46% forced pools, Buffington and Lisle, 2002: $\lambda/w_b = -14.7\ S + 1.33$	0.0101	57
Spacing in: pool-riffle AK, WA: $\lambda/w_b = 65.3\ S + 1.71$;	0.986	3
Spacing, plane bed: $\lambda/w_b = 262\ S + 2.75$	0.4412	8

2.4.5. Variation in the width of the particle size distribution.

The width of the particle size distribution in the model runs varies from 3 to 9 size classes, each class one ϕ in width. The elevation deviations observed in the particle size distribution variation series reflect the results of adding finer sediment to the channel sediment, thus reducing the area and volume fractions of the bed that are occupied by the coarser particles. All other initial conditions are held constant at the standard values in these runs. The spatial patterns of highs and lows in the model channels of the bed width series are shown in Chapter 1, Fig. 1.6 as gray-scale images. As the number of particle size classes increases, the channel bed transitions from a relatively featureless surface when the particle size distribution includes only three ϕ–size classes, to disconnected highs and lows, then connected areas of highs and lows when the size distribution spans 8 ϕ.

The number of pools increases, and there is a corresponding decrease in the spacing of pools, as the width of the particle size distribution increases (Fig. 2.4c). The number of pools increases approximately as the square of the number of particle size classes. The size of the pools, however, remains essentially constant.

The modeled decrease in spacing is also nonlinear, and a power law correlation indicates that spacing decreases approximately as the power –2 of the number of particle size classes (Fig. 2.3c). The analogous relationship in the MR data (Wohl and Merritt, 2005) has a power near –1 (Fig. 1.3, Table 2.5), and is thus not clearly different from a linear relationship. There is also enough scatter in the MR data (Wohl and Merritt, 2005), that a linear correlation on the field data has a low r^2 of 0.15. Power-law correlations for a wider set of the MR data were also examined. The data were divided into four sets, each of which contained channels with a limited range of discharge. Two of the four discharge classes fit a negative power-law trend, but two did not, so there is also too much variability in the relationships within the full data set to draw a conclusion

on the expected form of the relationship between pool spacing and the width of the particle size distribution (Fig. 2.3c, Table 2.5). The subselected mountain rivers data do generate a nonlinear trend somewhat similar to the modeled data, but there is wide scatter about the relationship. The diverse relationships observed, and the wide scatter, mean it is not possible to accept or reject the apparent non-linearity suggested by the model data.

The combined model and subselected field data do suggest that, for a set of stream channels that differ in particle size sorting but are otherwise similar, pools will be more widely-spaced

Table 2.5: Pool size and spacing in the particle size distribution width variation series

	Linear and power law correlations with particle size distribution width		r^2	n
Number:	Power law:	$N_p = 0.130\ w_p^{2.13}$	0.817	7
	Linear:	$N_p = 1.46\ w_p - 2.0714$	0.671	7
Length:		$L_{p,mn} = -0.015\ w_p + 1.28$	0.025	7
Area:		$A_{p,mn} = -0.834\ w_p + 27.3$	0.059	7
Spacing:		$\lambda/w_b = 120\ w_p^{-2.23}$	0.830	7
Spacing, MR* data, power law		$\lambda/w_b = 6.66\ w_p^{-0.840}$	0.147	12

**MR data from Wohl and Merritt, 2005*

where sediment is more well-sorted. A set of such channel reaches can be readily identified in stream data, but would generally not consist of a downstream sequence in any given stream. Instead, the modeled variation represents a diverse set of stream reaches in which coarse particles are present in all cases, while the subfraction that is finer sediment and the size range of that sediment, vary. It is the degree of sorting, which may also be viewed as the range of smaller sizes present in the sediment, which varies in successive model runs.

2.4.6. Mobility variation.

The critical value of the relative particle exposure, $R_{p,c,}$ ranges from 0.18 to 0.48 in the threshold variation runs. These values of the mobility threshold roughly correspond to local critical shear stresses from 5 to 2.5 Pa, based on the experimental data of Fenton and Abbot (1977; *see* Fig. 1.5).

The number of pools, and therefore the average spacing, λ_p/w_b, varies little between the threshold runs (Fig. 2.3). However, the fraction of the bed occupied by pools increases more strongly than the increase in area occupied by deeps (Fig. 1.12). The area occupied by pools initially increases slowly for thresholds from about 0.18 to 0.38, then rapidly in the last two runs in the series, with relative particle exposure thresholds of 0.38 to 0.48. In addition, the average length scale of the pools, $L_{p,av}$, increases linearly (Table 2.6), and nearly doubles over the range

Table 2.6: Correlation data for model results and mountain rivers relating width of the particle size distribution and pool spacing

	Power-law correlation with particle size distribution width		
		r2	***n***
	$\lambda/w_b = a\ w_b^{-x}$		
Model:	$139\ w_b^{-2.13}$	0.817	7
	$\lambda/w_b = a\ w_{bd}^{-x}$	***r2***	***n***
MR data:			
	Q1 - < 2 m3/s: $15.2\ w_{bd}^{-1.47}$	0.306	13
	Q2 - < 3 m3/s: $1.63\ w_{bd}^{0.420}$	0.107	13
	Q3 - < 4 m3/s: $0.986\ w_{bd}^{1.22}$	0.423	7
	Q4 - < 13 m3/s: $6.98\ w_{bd}^{-0.530}$	.156	9

(MR data from Wohl and Merritt, 2005)

of thresholds evaluated. The pool lengths in meters (nominal) range from 1.2 to 2 meters, with the average pool length about 1.3 m at the lowest threshold evaluated, and about 1.8 m at the highest threshold evaluated. For comparison to empirical data, discharge can be used as a surrogate for the exposure threshold for particle motion. Particles will be more mobile at a lower exposure threshold, or at higher flow. The increased length of pools as sediment becomes less mobile in the model is consistent with field and flume studies that indicate pool length tends to increase with decreasing discharge (reviewed and summarized by Thompson, 2002).

The MR data (Wohl and Merritt, 2005) were also used to construct a comparison between pool spacing and the particle mobility, using estimates of both the total shear stress and of the local stress on the particles ('grain' resistance). The local shear stress was estimated by partitioning the total shear stress between local particle resistance and form drag.

The total boundary shear stress is estimated as

$$\tau_b = \rho_w g R S \qquad (5)$$

where τ_b is the boundary shear stress, R is the hydraulic radius, and the other terms were defined above. A 'reduced' hydraulic radius, R', is then used to estimate the portion of the total shear stress that is attributable to fine-scale roughness of the sediment surface, rather than due to form roughness. R' is given by

$$R'^{2/3} = (u_{av} D_{50}^{1/6}) / (21.1 S^{1/2}) \qquad (6)$$

where u_{av} is the average downstream velocity. Equation 6 is taken from the method presented by Einstein and Barbarossa (1952) for rough beds. The local shear stress is then calculated by replacing the hydraulic radius, R, based on measurements, with the reduced hydraulic radius, R', representing the portion of the channel boundary that contributes only particle-scale roughness, as:

$$\tau_p = \tau_b - (\rho g R' S), \qquad (7)$$

where τ_p is the shear stress supported by the particles (e.g., Prestegaard, 1983). These data are summarized in Table 2.7, and each of the variation series is summarized in Table 2.8.

The field data suggests that pool spacing in streams increases as the threshold shear stress increases, with similar r^2 values obtained in correlations of spacing with either total shear stress or local, particulate shear stress. Critical shear stress and critical exposure are inversely related, so the model data suggest the same type of trend as the field data in that spacing decreases as the relative particle exposure threshold increases. This can also be described as a decrease in spacing as boundary shear stress increases.

Table 2.7: Pool size and spacing in the threshold variation series

	Linear correlation with the value of the relative particle exposure	r^2	n
Number:	$N_{p,mn} = 1.43\ R_{p,c} + 3.96$	0.0385	7
Length:	$L_{p,mn} = 1.90\ R_{p,c} + 0.887$	0.455	7
Area:	$A_{p,mn} = 95.6\ R_{p,c} + 4.82$	0.477	7
Spacing:	$\lambda/w_b = -2.30\ R_{p,c} + 3.61$	0.143	7
Spacing, MR subselection:	$\lambda/w_b = 0.234\ \tau_g - 0.0162$	0.523	13
Spacing, MR subselection:	$\lambda/w_b = 0.0348\ \tau_b + 1.1551$	0.515	13

MR data from Wohl and Merritt, 2005

Given the similar response of transport to increased particle exposure and decreased discharge, the model results are in accordance with flume results indicating that, of discharge and slope, the primary control on pool length is discharge (Thompson, 2002). Field evidence on pool length adjustment as slope increases is equivocal. Model results suggest that there is either no correlation between slope and pool length or spacing, or there is a complex pattern of variation between slope and the pool length and spacing.

Table 2.8: Recapitulation of model correlations with length and spacing

correlation with the variation variables	r^2	n
Bed width		
Length: $L_{p,mn} = 0.543\ w_b + 0.353$;	0.798	5
Spacing: $\lambda/w_b = 4.19\ w_b - 5.56$;	0.937	5
Slope		
Length: $L_{p,mn} = 0.515\ S + 1.275$	0.0235	10
Spacing, model: $\lambda/w_b = -0.608\ S + 2.83$	0.0024	10
Particle size distribution		
Length: $L_{p,mn} = -0.015\ w_p + 1.28$	0.025	7
Spacing: $\lambda/w_b = 120\ w_p^{-2.23}$	0.830	7
Threshold		
Length: $L_{p,mn} = 1.90\ R_{p,c} + 0.887$	0.455	7
Spacing: $\lambda/w_b = -2.30\ R_{p,c} + 3.61$	0.143	7

The primary control on pool length appears to be particle mobility. The primary control on pool spacing appears to be bed width. The mobility threshold and the bed width are indicated to have a subequal control on pool length. These model results indicate that bed width influences both pool size and spacing, and that larger pools are observed at larger bed widths and lower particle mobility, whereas widely-spaced pools may be expected in wide channels and with more well-sorted sediment. These associations are summarized in Table 2.9.

2.5. Character of the modeled process: random or non-random?

A brief review of the model process is needed as an aid to characterizing the influence of the process on the resulting sediment surface. The model moves sediment particles when the particles are exposed by more than a designated critical fraction of their height. This particle interactions control is approximately linearly related to shear stress in the range of thresholds modeled. The initial channel has a uniform slope, width and cross-sectional form. The particles that constitute the initial channel bed are selected by randomly assigning the particle size, drawn from one of the

Table 2.9: Matrix of modeled associations of pool size and spacing in coarse sediment with mobility controlled by particle interactions

Small pools narrow bed poorly-exposed particles (relatively stable sediment)	Large pools wide bed well-exposed particles (relatively mobile sediment)
Closely-spaced narrow bed poorly-sorted sediment	Widely-spaced wide bed well-sorted sediment

ϕ-size classes included in the particle size distribution, to each cell on the model surface. Particles of the selected size are then assigned to fill the cell one particle diameter deep. These particles all assigned a vertical placement that is centered at the elevation assigned to that cell, thus combining a regular vertical placement with a spatially random distribution of sizes across the surface. The initial pattern of highs and lows about the sloping plane is thus a random areal distribution of discrete elevations above a planar surface.

An analysis was conducted to evaluate whether the steady-state state surface at the end of the model runs has a random or non-random spatial distribution. Data on characteristics of the model surface, including the height deviations, particle size, relative particle exposure, and shelter margin, were classified as high, medium and low values of each of the variables. The variables of channel deeps and coarse sediment were also classified into two classes, i.e., deep vs. non-deep, and coarse vs. non-coarse sediment. Distributions of nearest neighbor distances, relative to Monte Carlo simulations of the range of values obtained in 99 randomly-rearranged surfaces, were generated using the *S-plus* statistics program. The analysis code was written by Dr. Robin Reich, Department of Forest, Rangeland and Watershed Stewardship, Colorado State University, Colorado.

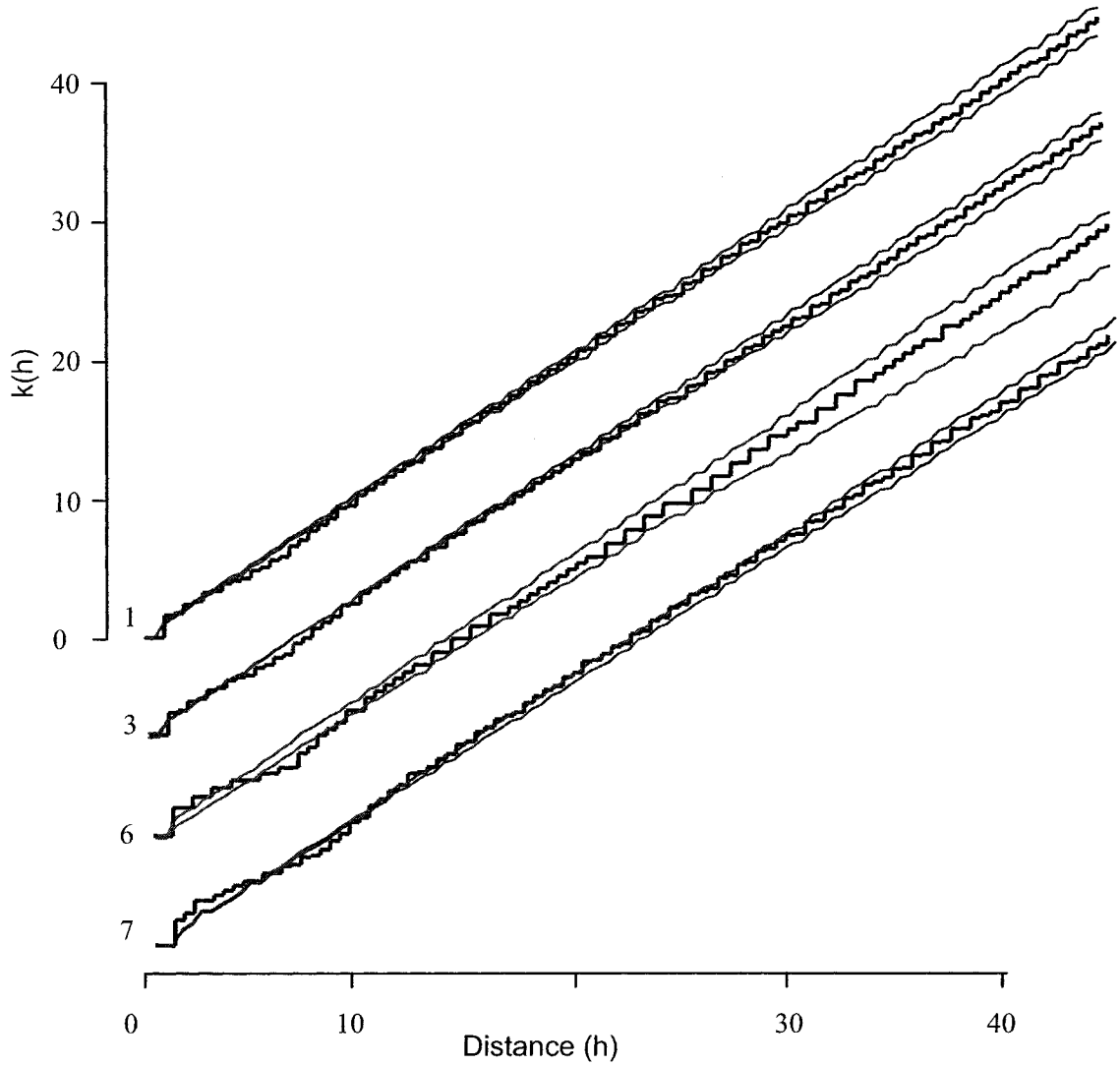

Fig. 2.6. Spatial analysis of threshold variation series, showing distances between high points in the modeled bed surface. The slanting, thick black line in the center of each plot represents the observed distribution of the distances between pairs of points. The two thiner lines indicate the range of values expected for the observed number of high elevation cells, at a 99% confidence level, obtained by Monte Carlo simulations. Essentially all runs in the variation series show a lack of high points with a spacing that averages about 10 cells apart. An additional feature is shown in the last two runs of the threshold variation series, also shown here. In these two runs, in addition to the lack of high points spaced about 10 cells apart, there is an excess of high points spaced about 5 cells apart. The lack of high points at a spacing of about 10 cells can be described as a signficant tendency for particles to exhibit some regularity in their spatial distribution. The excess of high points at shorter distances, present in a configuration with lower particle mobility than in the standard configuration evaluated, can be described as a tendency for clustering of particles over short distances.

Of the variables considered, only the height deviations consistently showed a significant departure from a random distribution of nearest neighbor distances (Fig. 2.6). Specifically, only the locations of points with an elevation relatively high above the planar sloping bed surface showed a non-random pattern (i.e., deviations outside the 99 percent probability envelope estimated by Monte Carlo simulations). A deviation of the data outside the 99 percent envelope was obtained for the class of points that are at high elevations in all but one of the runs evaluated.

The non-random nearest neighbor distances appear as a deficiency of high points spaced at relatively short separation distances, indicating that the distribution of high points has a degree of regularity in spacing that is statistically unlikely to occur in a surface formed by a random process. The separation distance at which the reduction occurred in the runs is within the range of 4 to 12 cell widths (nominally 1 to 3 m) (Fig. 2.6). This can be visualized as high points on the bed that are scattered, but tend to be spaced about as far apart as 4 to 12 times the size of largest particles in the grid. In addition, two runs of the threshold variation series, with the lowest particle mobility, showed a tendency for clustering. The spacing of clusters averages about 2.5 cell distances.

A mechanism that explains the tendency to regular arrangements in the location of high points, at least in part, is as follows. High points are often large particles which rise relatively high above their surroundings. Given such high points, particles of all sizes will tend to move laterally around the high point, because particles in the model move to the lowest adjacent site. This means that it will be common to find a zone directly downstream of large particles where there is a deficiency of other large particles. It seems likely that this observed characteristic separation distance should correspond to a characteristic transport distance, and thus have a significant relationship to the frequency of particle moves in a given run. Because each of the runs has a constant duration, the frequency of particle moves is directly and linearly related to the ratio of the total number of moves to the area of the bed in each run. For example, in the bed

width variation series, the total number of moves ranges from 13,800 to 26,900, which reduces to an averages of 21 to 37 moves at each cell (Table 2.10). The average number of particle moves from a given cell is smaller in the threshold series, ranging from 1 to 16, depending on mobility (Table 2.11).

Table 2.10: Number of particle moves in each run of the bed width variation series

Total number of particle moves in the bed width variation runs					
13,823	14,974	18,301	18,824	25,504	26,866
Width of active bed in final time step (m):					
6.3	7.1	8.0	8.7	9.8	10.9
Number of moves from the cells of the active bed					
27	26	28	27	33	31

Table 2.11: Number of particle moves in each run of the threshold variation series

Length 90: cells						
Total number of particle moves in the threshold variation runs						
9,527	10,116	8,432	4,557	3,988	1,409	748
Width of active bed in final time step (m):						
7.17	7.14	7.23	7.30	7.43	7.70	7.79
Number of moves from the cells of the active bed						
15	16	13	7	6	2	1

In summary, the spatial analysis of the distance between high points in the model bed surface suggests that the surface is close to random, but with a non-random bias such that high points on the bed surface tend to be spaced between 4 to 12 cells apart. This corresponds to 4 to 12 particle diameters for the coarsest particles in the sediment, or 1 to 3 m. The strongest deviation from a random pattern occurs at a spacing of 7 to 8 cells, corresponding to 1.75 to 2 m. As a statistically significant non-random pattern in the bed surface characteristics is rare except for this spatial pattern in elevation, it appears likely that this pattern is important in establishing

the trends in the size and spacing of pools with bed width, particle size distribution and mobility threshold described in the previous sections. The lack of clear trends in runs of the slope variation series and the corresponding lack of a non-random spatial pattern in elevations in the slope variation series are consistent with this interpretation. The observation that there is a characteristic spacing of high points on the bed is also consistent with documented development of particulate structures formed of coarse, protruding cobbles and boulders, such as those described by Hassan and Church (2000) in flume runs and by Robert (1987), Church and others (1998), and LaMarre and Roy (2001) in streams.

2.6. Discussion and conclusions on the formation of pools

A cellular automata model was constructed to simulate the stable-state roughness characteristics of a hypothetical channel in which particle interactions are the dominant control on particle transport, and consequently on channel form evolution. The fundamental process replicated in the model is the selection of the particles that are unstable enough to move, combined with motion of those particles to the lowest adjacent neighboring cell. Unstable particles are defined in the model as those that have a relative particle exposure that exceeds a threshold value. The relative particle exposure criterion approximates a dimensionless critical

Table 2.12: Spacing of non-random features in the runs of the threshold variation series

Maximum deviation indicating regularity at an average spacing, in cells, of						
none	na	7.5	7	7	7.5	8
Maximum deviation indicating clustering at an average spacing, in cells, of						
none	na	none	none	none	2.5	2.5

shear stress (Shields criterion) that varies with particle size. The selection and direction of motion of the particles is determined by particle interactions.

The basic process in the model, described above, was defined to reflect the characteristics of small, mountain streams with a channel bed about 3 meters in width, a slope of about 0.02, coarse sediment, including large cobbles and a variable fraction of finer particles down to granule size (granules are included with fine gravel in some particle size classifications). The channel surfaces that result from a model run are similar to mountain stream channels in many respects, and may be expected to be distinctly different in some respects. The model was used to generate a set of results showing how the channel characteristics change as a single initial condition is varied over the range of values expected in mountain rivers, with all other initial conditions held constant.

Because the model process was limited to particle interactions, the model results do not include effects associated with spatially-varying patterns of flow. In particular, the model results indicate features that may develop solely as a result of particle interactions, without spatial variations in flow or turbulence characteristics. As such, the model pools may be interpreted as reflecting recently initiated pools, before they grow large enough that the pool form significantly modifies flow.

The model runs demonstrate how spatial patterns in the sediment surface, including local depth variations, differ as a single initial characteristic of the channel is varied, holding all other initial characteristics constant. The characteristics varied are width, slope, particle size or the mobility threshold. These runs are comparable to field data from a group of reaches selected to be similar in most respects, yet the model data reflect less variability than is likely to be achieved in selecting and comparing stream reaches. The modeling approach provides information on the influence of a single channel characteristic on the subsequent adjustment of that channel, without addressing complications introduced by interactions among variables when multiple variables are modified. In the model results, there was no clear pattern of adjustment in pool size or spacing

when the initial slope was varied in model runs. Each of the other variables shows a trend in either or both pool size and spacing as the variation variable changes.

A distinction is usually made between freely-formed pools and forced pools. However, this distinction is not applicable where a continuous distribution of coarse particle sizes are present, so that several large particles may locally modify the channel flow and promote scour, yet the particles may move in a slightly larger flow. The particles here may range from highly mobile, through 'semi-mobile' to nearly immobile. Pools then also have a continuously varying degree of forcing, and few to none may be freely-formed.

The model pools have a right-skewed length distribution, as reported for both pool-riffle and step pool forms. The distributions are also generally unimodal. Both unimodal and bimodal distributions have been documented in streams (Keller and Melhorn, 1973; Grant and others, 1990). Bimodal distributions may occur because there are multiple populations of pools in streams with multiple types of obstructions (Montgomery and others, 1995), or when pools initiate at different times in response to intermittent high flows (e.g., Keller and Melhorn). Such effects are not included in the model. Bimodal distributions in the model results are relatively rare (e.g., Fig. 2.2), but appear to result from random variations in the initial sediment surface forming the channel.

The model results indicate that localized deeps, constituting typically shallow and irregularly-shaped pools, can develop as a result of particle interactions alone. The model results also indicate that the area and spacing of pools developed under particle interactions control is strongly influenced by bed width and the particle size distribution; is influenced by the degree of particle mobility; and is little influenced by slope.

Bed width adjusts during model runs. The bed width series shows that the prismatic initial channel form evolves to a channel width that is 88 to 89 percent of the initial width. That difference is likely due to both a changing definition of width necessitated as the channel form

changes, as well as some narrowing of the bed as a result of particle motion. In the other variation series, the bed width tends to increase as the sediment becomes less mobile, and as finer sediment fractions are added to the particle size distribution. The maximum difference in channel width within a variation series is in the particle size distribution variation series. There the channels with the widest particle distributions have a final width that is 90 percent of the width of the channel with the narrowest particle size distribution.

The range of pool spacing in all variation series spans from about one to fourteen bed widths, similar to the range in theoretical predictions (Yalin, 1971a), and observed in pool-riffle channels including both forced and freely-formed pools (e.g., Montgomery and Buffington, 1995). In two of the variation series, for slope and particle mobility, pool spacing is essentially constant at about three channel widths. Pools formed under particle interactions control may be viewed as an intermediate class, that are 'semi-forced'; i.e., freely formed in part and in part forced, and the range of values simulated in the model runs varies from strong limits to minor limits on particle motion as a result of particle interactions.

Results from the bed width variation series show that bed width strongly influences both pool size and spacing. Pool spacing varies from about 1.4 to 6.7 bed widths, in a linear relationship, as the initial width of the channel bed nearly doubles (nominally from 1.75 to 3 m). The length scale of the observed pools also nearly doubles, from 1.2 to 1.9 m nominal, while pool spacing increases by a factor of four (from 1.4 to 6.7 m nominal). These adjustments correspond to increasing bed width when the forces driving sediment transport increase, and when the resisting forces decrease.

It is also striking that the spacing of the model pools varies strongly, and non-linearly, with the number of particle size classes, 1 ϕ in width. As the particle size distribution becomes more poorly sorted (although always containing at least some sediment of the coarsest particle size considered), model pool spacing decreases rapidly, and can be approximated as a power law

decay with a power of –2. The spacing decreases by a factor of 8.5 as the width of the particle size distribution increases from 3 to 9 ϕ-size classes (1 ϕ in width). Empirical data are not inconsistent with a power-law decrease in pool spacing, but have too much scatter to confirm a power-law form. Pool length did not adjust as the particle size varied.

Neither model pool size nor spacing varies with slope, as slope ranges from 0.005 to 0.095. However, more of the deep areas on the bed reach lower elevations relative to the mean surface as slope increases (Fig 1.7.). The total area of the bed occupied by deeps has a weak correlation with slope ($r^2 = 0.2169$), but inspection of the plotted data suggests that the correlation may be weak because the pattern of variation is segmented into three ranges with different patterns of variation. The range cutoffs are near the values expected for the transition from pool-riffle to plane-bed and from plane bed to step-pool. The suggestion of this pattern is intriguing, and additional modeling to evaluate interactions as slope varies across this range may produce useful insights into pool formation.

The model and field data suggest a decrease in pool spacing as the mobility threshold increases, which may be expected to correspond to a decrease in spacing as critical shear stress increases. The field data suggest that pool spacing increases as shear stress increases, with similar r^2 values obtained in correlating spacing with either total stress or local, particle stress. The pool length scale also doubled as the exposure threshold for motion roughly tripled.

Field work has suggested the hypothesis that variable relationships between particle roughness and slope may explain apparently inconsistent relationships between slope and either pool size or spacing (Wohl and others, 1993). In contrast, the runs here suggest that bed width and particle roughness strongly influence spacing, whereas bed width and the threshold of motion strongly affect pool size, but that slope has little effect. Continuum models also suggest that undulatory topography is largely uninfluenced by slope, although some influence may be exerted through the relative magnitudes of transverse and longitudinal transport which varies with slope

(Furbish, 1993). Differences in longitudinal and transverse transport rates occur in the particle interactions CA, but do not result in a control on pool size or spacing in the particle interactions model. The model data suggest instead that the primary change in pool characteristics as slope varies is a variation in pool depth and in the total area occupied by pools, but changes in pool size are minor and there is no trend in pool spacing as slope varies.

Many researchers have suggested that pool-riffle formation depends on multiple factors. For freely formed pools, 'shear stress, sediment transport, and bed and bank topography' have been emphasized (Dietrich and Whiting, 1989; Nelson and Smith, 1989; Montgomery and others, 1995). Hypotheses of pool initiation emphasize existing spatial variations in width and depth and patterns in particle size, in slope, and in turbulence. In a related conceptual model, width-to-depth is used as a threshold criterion for the formation or lack of formation of bar-pool topography. The importance of width is apparent in the model results, whereas depth does not appear as a factor in the model results because depth was not varied. The model results suggest that the most important in-stream factors are bed width and the transport threshold, which encompasses two of the three factors most often highlighted, but there is no influence of pre-existing, non-random spatial variations in the model runs.

There are distinct trends in the size and frequency of pools and other channel deeps generated in the particle interactions model as the channel form and particle characteristics are varied (Figs. 1.6 through 1.9). In general, larger pools develop in the model where the bed is wider and where particles are more mobile, whereas pools are more closely spaced where the bed is narrow, and where there is a wide range of particle sizes.

Narrow channels appear to more readily develop channel-spanning areas of positive height deviations, generating pool-like forms centered within the channel between the high points (Fig. 1.6). At high slope, the model bed surface can be described as low areas separated by higher

elevation ribs of sediment, which may correspond to step pools, or may be analogous to the particulate lines and reticulate structures described by Church and others (1998).

Based on nearest neighbor analyses of the data, the model process of particle motion controlled by particle interactions results in non-random spacing of high points on the bed sediment surface for all but one of the grids evaluated. The high points have a tendency toward a regular spacing. The dominant spacing is at a separation distance of 7 to 8 cells (nominally 1.75 to 2 m). The threshold variation series shows an additional feature. The stable-state channel surface from the threshold variation run with the greatest particle mobility did not have the regularity found in all other model runs, and the two runs with the lowest particle mobility had not only the characteristic regularity in spacing, but also a tendency for high points to cluster together on a somewhat smaller scale of about 0.6 m. Such regularity and clustering indicate that particle interaction control produces a process of self-organization into the process of sediment transport and consequent channel evolution. The results also suggest that a regularity, or periodicity in the sediment organization is common, and that clustering does not occur at high particle mobility.

2.7. References: Chapters 1 and 2

Abrahams, G. Li and J. Atkinson. 1994. Step-pool streams: an adjustment to maximum flow resistance. in George V. Cotroneo and Ralph R. Rumer, eds., *Hydraulic engineering '94.* Vol. 2. ASCE. New York. p. 815-816.

Bak, P., 1996. *how nature works: the science of self-organized criticality.* Copernicus, New York, NY, 212 pp.

Barabási, A.-L. and H.E. Stanley, 1995. *Fractal concepts in surface growth.* Cambridge University Press, Cambridge, England, 366 pp.

Bathurst, J.C. 1987. Critical conditions for bed material movement in steep, boulder-bed streams. *in* Beschta, R.L., T. Blinn, G.E. Grant, G.G. Ice and F.J. Swanson, *Erosion and sedimentation in the Pacific Rim (Proceedings of the Corvallis Symposium): IAHS Publication 165.*

Bisson, P. A., J.L. Nielson, R.A. Palmason, and L.E. Grove. 1982. A system of naming habitat types in small streams, with examples of habitat utilization by salmonids during the low streamflow, in *Acquisition and utilization of aquatic habitat inventory information*, edited by N.M. Armentrout, p. 62-73, American Fisheries Society, Portland OR.

Blondeaux, P. and G. Seminara. 1985. A unified bar-bend theory of river meanders. *Journal Fluid Mechanics* 157: 440-470.

Buffington, J.M., W.E. Dietrich and J.W. Kirchner, 1990. Friction angle measurements on a naturally formed gravel streambed: implications for critical boundary shear stress. *Water Resources Research* 28(2): 411-425.

Buffington, J.M., T.E. Lisle, R.D. Woodsmith, S. Hilton, 2002. Controls on the size and occurrence of pools in coarse-grained forest rivers. *River Research and Applications* 18(6):507-531.

Chin, A., 1989. Step pools in stream channels. *Progress in Physical Geography* 13(3): 391-407.

Chin, A. 1999. The morphologic structure of step-pools in mountain streams. *Geomorphology* 27(3-4):191-204.

Chin, A. 2002. The periodic nature of step pool mountain streams. *American Journal of Science* 302:155-167.

Chopard, B. and M. Droz, 1998. *Cellular automata modeling of physical systems.* Cambridge University Press. 341 pp.

Church, M., M.A. Hassan and J.F. Wolcott, 1998. Stabilizing self-organized structures in gravel-bed stream channels: field and experimental observations. *Water Resources Research* 34: 3169-3179.

Clifford, N.J., 1993. Formation of riffle pool sequences - field evidence for an autogenetic process. *Sedimentary Geology* 85(1-4):39-51.

Coulthard, T. J. 1999. *Modelling upland catchment response to Holocene environmental change*, University of Leeds.

Coulthard, T.J., M.J. Kirkby and M.G. Macklin. 2000. Modelling geomorphic response to environmental change in an upland catchment. *Hydrological Processes* 14: 2031-2045.

Crave, A. and P. Davy, 2001. A stochastic "precipiton" model for simulating erosion/sedimentation dynamics. *Computers and Geosciences* 27(7):815-827.

Curran, J.H. and E.E. Wohl, 2003. Large woody debris and flow resistance in step-pool channels, Cascade Range, Washington. *Geomorphology* 51(1-3):141-157.

Dietrich, W.E and P. Whiting, 1989. Boundary shear stress and sediment transport in river meanders of sand and gravels. In: *River Meandering*. S. Ikeda and G. Parker (eds.), Water Resources Monograph 12, American Geophysical Union, Washington, DC, p. 1-50.

deJong, C. and Ergenzinger, P, 1998. Dynamic roughness, sediment transport, and flow structures in a mountain stream. *Gravel-bed rivers in the environment*. In: Klingeman, P.C., R.L. Beschta, R.L, P.D. Komar, and J.B. Bradley, eds.. Water Resources Publications. Highlands Ranch CO. p. 39 – 59.

Dietrich, W. E. and P.J. Whiting. 1989. Boundary shear stress and sediment transport in river meanders of sand and gravel, in S. Ikeda and G. Parker (Eds.), *River Meandering*, American Geophysical Union Water Resources Monograph 12, p. 1-50.

Egiazaroff, L.V. 1965. Calculation of non-uniform sediment concentration. *Journal of the Hydraulics Division, ASCE* 91 (HY4): 225-247.

Einstein, H.A., 1950. *The bed-load function for sediment transportation in open channel flows*. U.S. Dept. of Agriculture, Soil Conservation Service, Technical Bulletin 1026, 71 pp.

Einstein, H.A. and N. L. Barbarossa. 1952. River channel roughness. *Transactions of the American Society of Civil Engineers* 117:1121-1132, New York, NY.

Family, F. and T. Vicsek, 1985. Scaling of the active zone in the Eden process on percolation networks and the ballistic deposition model. *Journal of Physics A: Mathematics and General* 18:L75-L81.

Fenton, J.D and J.E. Abbott, 1977. Initial movement of grains on a stream bed: the effects of relative protrusion. In: *Proceedings of the Royal Society of London A* 352: 523-537.

Florsheim, J. 1985. Channel geometries limiting gravel bar formation, northwestern California, *EOS Transactions* 66(46): 912, American Geophysical Union, November 12, 1985.

Fonstad, M.A. and W.A. Marcus, 2001. A general theory of riverbank instability, *GSA Program with Abstracts*, Geological Society of America.

Ferguson, R.I. 2003.The missing dimension: effects of lateral variation on 1-D calculations of fluvial bedload transport. *Geomorphology* 56: 1 –14.

Furbish, D.J. 1993. Flow structure in a bouldery mountain stream with complex bed topography. *Water Resources Research* 29:2249-2263.

Gomez, B., 1995. Bedload transport and changing grain size distributions. In: *Changing River Channels*. A. Gurnell and G. Petts (eds.), John Wiley and Sons, Chichester, p. 177-199.

Grant, G.E., F.J. Swanson, and M. G. Wolman, 1990. Pattern and origin of stepped-bed morphology in high-gradient streams, Western Cascades, Oregon. *Geological Society of America Bulletin* 102:340-352.

Gregory, K.J., A.M. Gurnell, C.T. Hill and S. Tooth. 1994. Stability of the pool-riffle sequence in changing river channels. *Regulated Rivers* 9: 35 – 44.

Hassan, M. A. and M. Church, 2000. Experiments on surface structure and particle sediment transport on a gravel bed. *Water Resources Research* 36(7):1885-1895.

Hassan, M. A. and M. Church. 2001. Sensitivity of bed load transport in Harris Creek seasonal and spatial variation over a cobble-gravel bar. *Water Resources Research* 37(3):813- 825.

Hawkins, C.P., J.L. Kersner, P.A. Bisson, M.D. Bryant, L.M. Deckere, S.V. Gregory, D.A. McCullough, K.K. Overton, G.H. Reeves, R.I. Steedman, K.K. Young. 1993. A hierarchical approach to classifying stream habitat features. *Fisheries* 18(6):3-12.

Hergarten, S. 2002. *Self-organized criticality in earth systems*. Springer-Verlag, New York, NY, 272 pp.

Inoue, M. and M. Nunokawa, 2002. Effects of longitudinal variations in stream habitat structure on fish abundance: an analysis based on subunit-scale habitat classification. *Freshwater Biology* 47 (9): 1594-1607.

Iseya, F. and H. Ikeda, 1987. Pulsations in bedload transport rates induced by a longitudinal sediment sorting: a flume study using sand and gravel mixtures. Geografiska Annaler 69A:15-27.

Keller, E.A. and W.N. Melhorn. 1973. Bedforms and fluvial processes in alluvial stream channels: selected observations. In Morisawa, M. (ed.), *Fluvial geomorphology*. Binghampton, NY: New York State University Publications I Geomorphology, 253-83.

Keller, E.A. and W.N. Melhorn, 1978. Rhythmic spacing and origin of pools and riffles. *Geological Society of America Bulletin* 89: 723-730.

Kirchner, J.W., W.E. Dietrich, F. Iseya, and H. Ikeda. 1990. The variability of critical shear-stress, friction angle and grain protrusion in water-worked sediments. *Sedimentology* 37(4): 647-672.

Langbein, W.B. and L. B. Leopold, 1968. *River channel bars and dunes - theory of kinematic waves*. U.S. Geological Survey Professional Paper 422L.

LaMarre, H. and A. Roy. 2001. Organisation morphologique des blocs et des amas de galets dans les cours d'eau à lit de graviers. *Géographie physique et Quaternaire* 55(3):275-287.

Lenzi, M. A. 2001. Step-pool evolution in the Rio Cordon, Northeastern Italy. *Earth Surface Processes and Landforms* 25: 991-1008.

Lisle, T.E. 1986. Stabilization of a gravel channel by large streamside obstructions and bedrock bends, Jacoby Creek, northwestern California. *Geological Society of America Bulletin* 97: 999-1011.

Lisle, T.E. and S. Hilton. 1992. The volume of fine sediment in pools: an index of sediment supply in gravel-bed streams. *Water Resources Research* 28:371-383.

Malmaeus, M. and M.A. Hassan, 2002. Simulation of individual particle movement in a gravel streambed. *Earth Surface Processes and Landforms* 27(2):81-97.

Madej, MA 1999. Temporal and spatial variability in thalweg profiles of a gravel-bed river. *Earth Surface Processes and Landforms* 24(12):1153 - 1169.

Mermillod-Blondin, F., M.C. Des Chatelliers, P. Marmonier, M.J. Dole-Olivier, 2000 Distribution of solutes, microbes and invertebrates in river sediments along a riffle-pool-riffle sequence. *Freshwater Biology* 44(2):255 – 269.

Montgomery, D.R. and J. M. Buffington. 1993. *Channel classification, prediction of channel response and assessment of channel condition*. Timber, Fish and Wildlife publication TFW-SHlO-93-002, prepared for the SHAMW Committee of the Washington State Timber/Fish/Wildlife Agreement. Washington State Department of Natural Resources. Olympia Washington.

Montgomery, D.R. and J.M. Buffington, 1997. Channel-reach morphology in mountain drainage basins. *Geological Society of America Bulletin* 109 (5):596-611.

Montgomery, D.R., J.M. Buffington, R.D. Smith, K.M. Schmidt, G. Pess. 1995. Pool spacing in forest channels. *Water Resources Research* 31:1097-1105.

Murray, A.B. and C. Paola. 1997. Properties of a cellular braided-stream model. *Earth Surface Processes and Landforms* 22:1001-1026.

Naden, P., 1987. Modeling gravel-bed topography from sediment transport. *Earth Surface Processes and Landforms* 12: 353-367.

Nelson, J.M. and J.D. Smith, 1989. Evolution and stability of erodible channel beds. In: River Meandering. S. Ikeda and G. Parker (eds.), *Water Resources Monograph* 12, American Geophysical Union, Washington, DC, p. 321-377.

Nikora, V., H. Habersack, T. Huber. 2002. On bed particle diffusion in gravel bed flows under weak bed load transport. *Water Resources Research* 38 (6): Art. No. 1081.

Parker, G. and P.C. Klingeman, 1982. On why gravel bed streams are paved. *Water Resources Research* 18(5):1409-1423.

Paola C., 1996, Incoherent structure: Turbulence as a metaphor for stream braiding, In: *Coherent Flow Structures in Open Channels* (eds. P.J. Ashworth, S.J. Bennett, J.L. Best and S.J. McLelland): John Willy & Sons, p. 706-723.

Prestegaard, K. L. 1983. Bar resistance in gravel bed streams at bankfull stage. *Water Resources Research* 19(2):472-476.

Rempel L.L. J.S. Richardson, M.C. Healey. 2000. Macroinvertebrate community structure along gradients of hydraulic and sedimentary conditions in a large gravel-bed river. *Freshwater Biology* 45 (1): 57-73.

Richards, K.S. 1978. Simulation of flow geometry in a riffle-pool stream. *Earth Surface Processes and Landforms* 3(4):345-354.

Robert, A. 1991. Fractal properties of simulated bed profiles in coarse-grained channels. *Mathematical Geology* 23(3): 367-382.

Robert, A. 2003. *River processes: an introduction to fluvial dynamics.* Arnold, New York, NY, 214 pp.

Schumm, S. A. M. P. Mosley, and W.E Weaver. 1987. *Experimental fluvial geomorphology.* John Wiley & Sons : New York, NY, 413 p.

Thompson, D.M. 2002. Geometric adjustment of pools to changes in slope and discharge: a flume experiment. *Geomorphology* 46(3-4):257-265.

Thompson, D.M. and K.S. Hoffman. 2001. Equilibrium pool dimensions and sediment-sorting patterns in coarse-grained, New England channels. *Geomorphology* 38:301-316.

Tribe, S., and Church, M, 1999. Simulations of cobble structure on a gravel streambed. *Water Resources Research* 35(1):311-318.

Van Niekerk, A., K.R. Vogel, R.L. Slingerland, J.S. Bridge. 1992. Routing of heterogeneous sediments over movable bed – model development, *Journal of Hydraulic Engineering-ASCE* 118(2):246-262

Whittaker, J.G., 1987. Sediment transport in step-pool streams. In: *Sediment Transport in Gravel-Bed Rivers*, C.R. Thorne, J.C. Bathurst and R.D. Hey (eds.), John Wiley and Sons, Chi Chester, p. 545-579.

Whittaker, J.G., and M.N.R. Jaeggi. 1982. Origin of step-pool systems in mountain streams, *Journal of the Hydraulics Division-ASCE* 108(6): 758- 773.

Wiberg, P.L. and J.D. Smith. 1987. Calculations of the critical shear stress for motion of uniform and heterogeneous sediments. *Water Resources Research* 23(8):1471-1480.

Wilcock, P.R. and B.W. McArdell, 1997. Partial transport of a sand/gravel sediment. *Water Resources Research* 33 (1): 235-245.

Wohl, E. and Grodek, T., 1994, Channel bed-steps along Nahal Yael, Negev desert, Israel, *Geomorphology* 9: 117-126

Wohl, E., and D. Merritt. 2005. Prediction of mountain stream morphology. *Water Resources Research* 41(Art No. W08419):1-10.

Wohl, E.E., K. R. Vincent and D. J. Meritt. 1993. Pool and riffle characteristics in relation to channel gradient. *Geomorphology* 6:99-110.

Wolfram, S. and J.B. Salem. 1985. *Thermodynamics and hydrodynamics with cellular automata.* Thinking Machines Corporation Technical Report.

Yalin, M.S. 1971a. *Mechanics of sediment transport.* Pergamon Press, NY, 290 pp.

Yalin, M.S. 1971b. *On the formation of dunes and meanders.* Proceedings of the 14th International Congress of the Association for Hydraulic Research 3, Paper C13, 1-8.

Yang, C.T. 1971. Formation of riffles and pools. *Water Resources Research* 7(6): 1567-1574.

CHAPTER 3

PARTICLE PATTERNS AND STRUCTURE IN A PARTICLE INTERACTIONS MODEL OF STEEP GRAVEL TO COBBLE STREAMS

Abstract

Particle interactions in poorly-sorted sediment can be a significant control on particle motions and therefore on channel evolution. The term 'particle interactions' refers to constraints on particle mobility imposed on one sediment particle by surrounding particles. To investigate the fundamental consequences of particle interactions for channel response, a particle interactions cellular automata model was used to simulate a hypothetical channel in which particle interactions are the primary control on channel adjustment. Model results indicate that particle interactions, in the absence of local flow variation, can generate spatial segregation of particles by size, forming textural patches on the channel bed. Patches formed, but in most runs, statistical tests indicated that particle arrangements were not distinguishable from a random distribution of particle sizes. Nonetheless, the pattern of surface particle size varies enough as model controls are varied, such that adjustment of channel width and slope results in significant trends in the length and spacing of coarse textural patches. Characteristics of the coarse patches were compared to patterns in the size and spacing of riffles and of textural patches in streams. For comparison, field data on riffle length was evaluated from available data for 5 stream systems. The results indicate that (i) riffle spacing ranges from about 1 to 11 in the streams evaluated; (ii) average riffle lengths range from shorter than to much longer than the associated pool lengths; (iii) within a geographic

region, riffles tend to become shorter as pool lengths increase, with both lengths normalized by channel width, but the opposite relationship is found for the average of data from multiple regions. The origin of this difference in the trends within and between stream systems is not known. The field data from streams also indicate that the normalized riffle length, given by the ratio of riffle length to channel width, is essentially constant as slope varies within a study area, but the constant value differs between study areas. The relationships of riffle length to particle size distributions and particle mobility are less certain as fewer data were found for these variables. The available data suggest that riffle length increases with the width of the particle size distribution ($r^2 = 0.987$, n = 3), and is directly proportional to discharge ($r^2 = 0.805$, n = 7). Characteristics of the model bed surface were extracted from the data for comparison to riffle and textural patch characteristics identified in streams. Connected areas of coarse particles were identified, and such may be analogous to either riffles or smaller textural patches. The model sediment developed coarse patches with an average spacing of approximately 2 to 7 bed widths, and the size of the modeled patches tends to decrease as bed width and slope increase, and as particle mobility decreases. As the particle size distribution spans more ϕ sizes, and includes increasingly fine particles, patch length is nearly constant, but spacing shows a mild increase. A comparison of the lengths of coarse patches in the model to the lengths of riffles and patches in streams suggests that patch lengths in the model, which decrease with bed width, vary in the sense opposite that of riffles, but in the same sense as patches in streams. Riffle and patch lengths in streams, as well as coarse patches in the model, all decrease with slope. Riffles and patches in streams have diverse trends with varying width of the particle size distribution (increasing, decreasing, and constant in three field studies), and are approximately constant in the model. Riffle and patch lengths increase with discharge in both field and flume data, and patch lengths decrease with shear stress in the field data summarized here. The proportionality with discharge

suggests that the length of riffles may vary with energy dissipation requirements of the channels, as suggested by Yang (1971). Coarse patches in the model increase slightly in length as mobility of the sediment increases (as the relative particle exposure threshold decreases). Thus the model data suggest that particle interactions generate patterns of variation with slope, particle size distribution and sediment mobility that vary in the same direction as variations in stream data, although opposing trends in different field studies weaken the similarity. The data also suggest that riffle lengths vary more widely than previously suggested. Because the variation of riffle length with bed width and particle mobility in the model differs from the relationships identified in streams, it is suggested that factors other than particle interactions are important in determining riffle length. Two factors suggested in this study are energy dissipation as modified by local constraints on channel adjustment, channel adjustments driven high flows which were not modeled, and mechanisms that result in local oversteepening of the channel, neither of which is accounted for in the particle interactions model.

Keywords: Pool-riffle; Channel form, Sediment; Cellular automata

3.1. Introduction

3.1.1. Riffles and pools in steep, gravel-to-cobble streams

Spatial differentiation into riffles and interspersed pools is the primary characteristic of pool-riffle channels. Riffles are steeper than pool units, with flow that is shallower and more rapid at low water. A number of researchers distinguish a third basic bedform unit, termed runs. Jowett (1993) documented differences between pools, riffles and runs by visually identifying these form units in several stream reaches, then used discriminant functions to evaluate differences among the units. In his initial designation of the units, Jowett distinguished pools as areas with slower flow, and riffles as areas with swift flow at low water, such that a high proportion of the water surface was broken. Runs were identified as areas with a wavy water surface at low flow. Data analysis indicated that pools were unlike riffles and runs in most characteristics. The pools were best discriminated from runs by Froude number and velocity-to-depth ratios, and riffles could be discriminated from runs primarily by local slope. Jowett also found significant differences between pool and run pairs, and pool and riffle pairs for all other variables. In contrast, riffle and run units were more similar. Jowett found no significant difference in substrate size and relative submergence (h/D_{84}), whereas Froude number, velocity-to-depth ratio, slope, and depth could be used to distinguish riffles from runs (Jowett, 1993). For the purposes of this study, I will assume that runs are a part of the riffle units. Another term, glides, is also used, and this study assumes that glides in pool-riffle channels are also a part of the riffle unit.

Riffle units are sometimes described as formed in sediment deposited at bars. However, riffles have characteristics distinct from bars, including, at minimum, differences in particle size distribution (e.g., Milne, 1980). In addition, riffles units may or may not be spatially associated with conspicuous channel bars. Florsheim (Grant and others, 1990, citing Florsheim, 1985) found that channel bars were absent or inconspicuous at channel slopes above about 0.02, and

theoretical analyses similarly suggest that bars are unlikely to form at slopes above about 0.025 (Buffington and others, 2002). Field data in two large data compilations suggest the slope cutoff between pool-riffle and plane bed channels is close to 0.03 (Buffington and others, 2002; Wohl and Merritt, 2005).

These slopes are steep to very steep, using the descriptive classification system documented by Rundquist (1975, Table, 2.3, pp. 38-40). The classification system characterizes slopes between 0.001 and 0.01 as steep, and slopes above 0.01 as very steep, placing the dividing line within the slope range where pool-riffle channels are common. I will approximately follow this classification, but will refer to the whole range of slopes above 0.001 as steep, and the two sub-ranges, above and below 0.01, as relatively steep and very steep.

Montgomery and Buffington (1993, 1997) defined pool-riffle forms as those that are associated with prominent bars, and similar forms where bars were inconspicuous or absent and pools were less frequent, as plane bed channels. However, it is not clear that pool-riffle and plane bed units are distinct. The data compilation of Wohl and Merritt (2005, Fig. 2) indicates that plane bed channels are characterized by slopes within the range that characterizes pool-riffle channels, although limited to the steeper portion of that range. The data also indicate that pool-riffle and plane bed channel types do not have distinct ranges of D_{84} or of channel width. The field data include reaches in western United States, Panama, and New Zealand (Wohl and Merritt, 2005). Data presented by Buffington and others (2002) similarly indicate that pool-riffle and plane bed channels have similar slope (Figure 3.1). These data represent 142 reaches (plus 1 additional reach in the relative submergence data) in western North America and Europe (Buffington and others, 2002).

In the following descriptions of stream characteristics, I will refer to reaches that contain bars as bar-pool-riffle reaches, and reaches described as lacking bars as plane bed reaches. Many

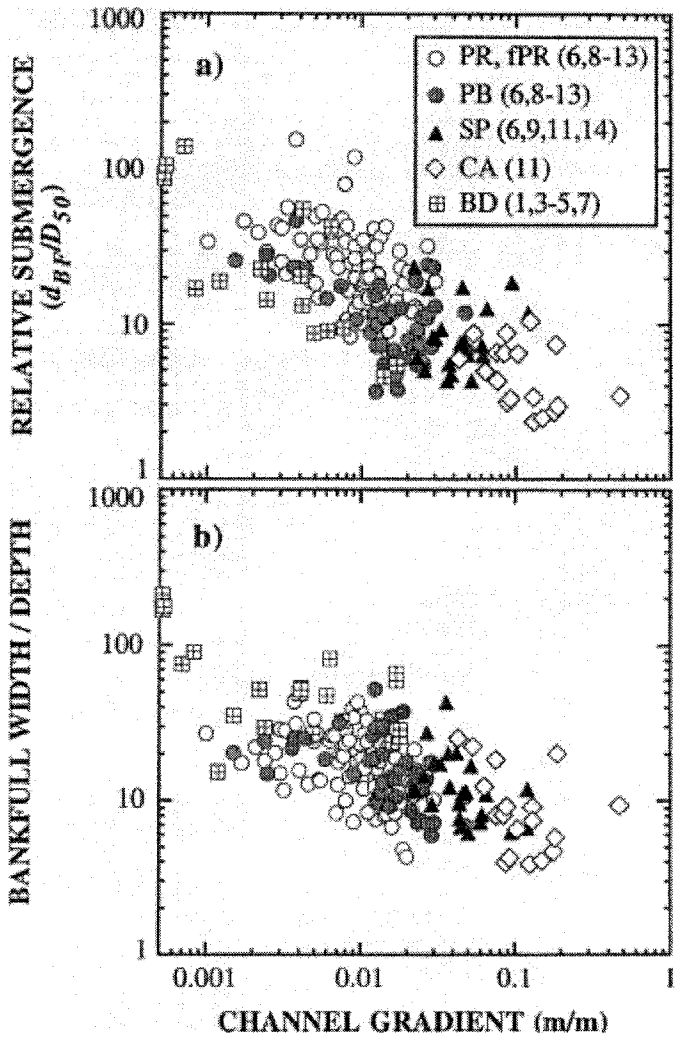

Figure 3.1. Relative submergence and bankfull width-to-depth at varying slope. Relative submergence and bankfull width-to-depth tend to differ for pool-riffle-bar (PR), forced pool-riffle (fPR), plane-bed (PB), step-pool (SP), cascade (CA) and braided (BD) channel morphologies (data from Lisle and others, 2000). Numbers in parentheses indicate data sources: 1, Leopold and Wolman, 1957 (mean annual discharge); 2, Fahnestock, 1963; 3, Emmett (1972); 4, Burrows and others, 1981); 5, Prestegaard, 1983; 6, Florsheim, 1985; 7, Ashworth and Ferguson, 1989; 8, Buffington and Montgomery (unpublished data); 9, Montgomery and others (1995); 10, Montgomery and others (1996b); 11, Montgomery and Buffington (1997); 12, Buffington and Montgomery (1999a); 13, Montgomery and others(1999); and 14, Traylor and Wohl (2000).

sources do not indicate whether bars are present, in which case I will simply characterize the reaches as pool-riffle reaches.

A width-to-depth criterion is typically used to predict the stability of bar-pool forms (Blondeaux and Seminara, 1985). To the extent that pool-riffle forms are analogous to bar-pool forms, width-to-depth should also be an important factor for predicting transitions between pool-riffle channels and channels with other bedform unit types.

roughly power-law relationship (i.e., a log-log linear relationship) between slope and width-to-depth can be identified from the data of Buffington and others (2002), as shown in Figure 3.1b. The variability in width-to-depth at a given slope is large, but average width-to-depth clearly increases as slope increases, for all unit types evaluated, including pool-riffle, plane-bed, step-pool cascade and braided channel types. The pool-riffle, plane bed, and braided types generally plot in the same range of slope. That range, and the slope ranges that characterize cascade and step-pool types, all differ (Figure 3.1b, see also Table 3.1). The data also indicate that pool-riffle and plane bed channel types have similar ranges of D_{84} and channel width.

Using the plots in Figure 3.2 (Buffington and others, 2002), it is possible to identify the approximate slope range, width-to-depth and relative submergence at which the different bedform types have been identified. The visually estimated central value of each range for the log-transformed data is listed in Table 3.1. The data show that the central value of relative submergence is somewhat different for bar-pool-riffle and plane bed channels; 7 versus 10, respectively, but that the central value of width-to-depth is similar for plane bed and pool-riffle channels, at about 13. Thus, this large data set suggests that plane bed channels are characterized by slopes in the same range as the pool-riffle channels, are not distinct in width, D_{84} or width-to-depth, but are distinct in relative submergence (defined in terms of D_{50}). This suggests that

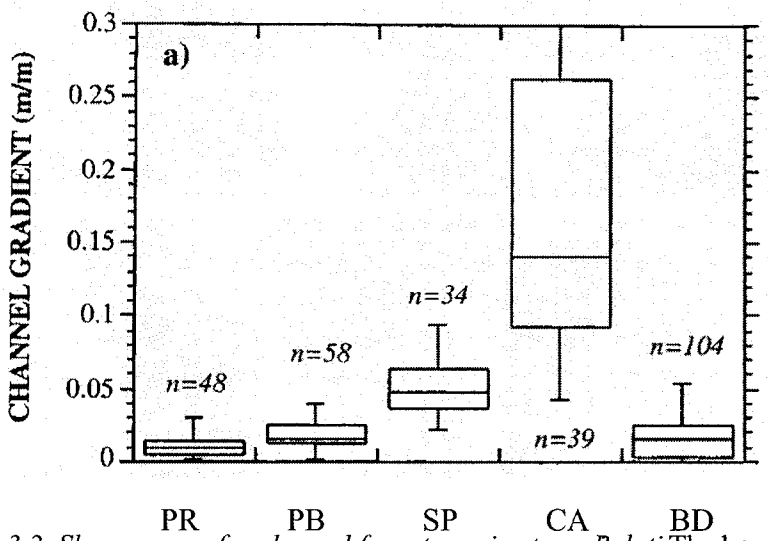

Figure 3.2. Slope ranges for channel form types in steep mixed alluvial. Relative The box and whiskers plots show distinct medians and quartiles, as well as overlapping ranges of slope (i.e., gradient) in reaches characterized as pool-riffle (PR), plane bed (PB), step-pool (SP), cascade (CA) and braided (BD) form types. Plots from Buffington and others, 2002. Median slope for the five channel types are 0.01, 0.02, 0.05, 0.14 and 0.02, respectively

Table 3.1. Relative length and slope of steep form units

	Length in active channel widths	*Slope*	*Ratio to average long profile slope*	*Ratio to mean of slope in preceding unit in classification*
Steps	0.3	0.122	0.2	--
Cascades	1.1	0.052	0.2	2.2
Rapids	1.6	0.024	1.1	2.3
Riffles	1.4	0.010	0.5	2.8

data from Grant and others, 1990

Table 3.2: Slope, width-to-depth and relative submergence of steep form units

	Slope	*Width-to-depth*	*submergence*
Cascade	*0.1*	*30*	*40*
Step-pool	*0.05*	*20*	*40*
Plane bed	*0.01*	*13*	*10*
Pool-riffle	*0.01*	*13*	*7*
Braided	*0.003*	*10*	*5*

bar-pool-riffle and plane bed channels are distinguished by either (a) depth, (b) D_{50}, (c) the degree of particle size sorting (here termed the width of the particle size distribution), or (d) some combination of those variables.

Grant and others (1990) documented the form unit length, sequence and other characteristics in reaches of two steep streams with differing slope, in the Cascade Mountains, Oregon. They identified pool, step, rapid and cascade form units, and noted that the steep step, rapid and cascade units each tended to be paired with pools. Thus, these steep form units tend to form step-pool sets, as well as rapid-pool and cascade-pool sets. Such steep bedform sets have also been found to be interspersed with pool-riffle units (Grant and others, 1990; Montgomery and Buffington, 1993; Chin, 2002). Very steep channel units, paired with pools, have been documented on slopes at least as steep as 0.17 (Wohl and others, 1993). In this study, I will consider the development of channel forms at slopes well above the slope range of pool-riffle channels, as these very steep streams may also be characterized by steeper channel units paired with less steep units.

Data from Grant and others (1990) indicates that the slope of each of the steep form units termed riffles, rapids, cascades and steps is two to three times as steep as the preceding unit listed (Table 3.1). The data of Buffington and others (2002) similarly show that the median slope for pool-riffle, cascade and step-pool form units is 2 to 3 times as steep as the preceding unit type (Figure 3.2, Table 3.2). Available data also indicate that cascade and rapid channel units are shorter when slopes are steeper, based on a detailed comparison of units in two streams with differing slope (Grant and others, 1990). Carling and Orr (2002) observed that both pools and riffles tended to become shorter, less asymmetric, and deeper as slope increased.

3.1.2. Overview of particle interactions and spatial patterns in sediment

Particle interactions were early evaluated by Einstein (1950) under the term hiding effects. Particle interactions have also been called shadowing effects (Egiazaroff, 1965; Barabási and Stanley, 1995), and have been parameterized under the terms protrusion, projection and exposure (Wiberg and Smith, 1987; Kirchner and others, 1990).

Particle interactions necessarily include the degree of both sheltering from the flow (i.e., hiding) and exposure to the flow (e.g., protrusion) (Van Niekerk and others, 1992). Particle interactions influence particle size selection for transport (Parker and Klingeman, 1982; Wilcock and McArdell, 1997; Hassan and Church, 2000); the distribution of vertical particle exposure (Parker and Klingeman, 1982; Iseya and Ikeda, 1987); and spatial arrangements of particles (Iseya and Ikeda, 1987; Hassan and Church, 2000). Such interactions appear to result in characteristic scales of sediment surface roughness elements (Naden, 1987; deJong and Ergenzinger, 1998, Robert, 1988, 1991, 2003).

Steep streams, with their typically wide range of particle sizes, are streams where particle interactions are expected to be most significant (Bathurst 1987; Gomez, 1995; *see* Chapter 1). Previous studies in physics suggest that particle interactions are important in the development of

Table 3.2. Slope, width-to-depth and relative submergence of steep form units

	Slope	*Width-to-depth*	*Relative submergence*
Cascade	*0.1*	*30*	*40*
Step-pool	*0.05*	*20*	*40*
Plane bed	*0.01*	*13*	*10*
Pool-riffle	*0.01*	*13*	*7*
Braided	*0.003*	*10*	*5*

Visually estimated from plots in Buffington and others (2002), see Figure 3.2.

spatial differentiation of surfaces formed by deposition and subsequent motion of particles (e.g. Barabasi and others, 1997). These observations suggest the hypothesis that riffles originate as a consequence of particle interactions.

Coarse-grained channels where particle interactions are important are also likely to be characterized by partial mobility and partial transport (Wilcock and McArdell, 1997), in which some subfraction within each of the coarser particle size fractions may be effectively immobile under most flows in steep, gravel-to-cobble channels. Pender and others (2001) suggested that most of the flume studies that provide detailed documentation of particle characteristics were conducted at marginal transport conditions. Talbot and LaPointe (2002, p. 10-10, citing Dietrich and others, 1989) noted that lower-energy systems are likely to be more strongly paved, may be farther from equal mobility, have more profile convexity, and more downstream fining. They also evaluated channel response to oversteepening. The oversteepened reach they evaluated developed a steep zone that translated downstream, and left a coarsened particle surface in its wake. Based on modeling, the channel adjustments included four main responses, (a) vertical changes in the

longitudinal profile, which they termed reprofiling, (b) meander regrowth, (c) bed surface coarsening, and (d) increased bank sediment inputs resulting from channel widening.

Under marginal transport conditions, mobility of the sediment is related to both shear stress and local particle characteristics. Particle characteristics that influence mobility include patchy particle texture and armoring, as well as vertical exposure of particles (Fenton and Abbot, 1977), structural arrangements that may stabilize particles (e.g., Sear, 1995), and spatial patterns that may modify resistance to flow (Ahmed, 1987; Gessler, 1989). Particle mobility will also vary as local roughness of the channel boundary varies, i.e. at bedform and bank undulations (Booker and others, 2001). Roughness will be considered in more detail in Chapter 4. This chapter focuses on characteristics of particle size distributions, particle arrangements, and spatial patterns at the scale of textural patches and channel units such as riffles.

Particle interactions in poorly-sorted sediments arise from constraints on particle mobility that are imposed on an individual sediment particle by surrounding particles. Such interactions can be evaluated in terms of the size and position of the top of a given particle and the tops of the neighboring particles. Large particles may buttress other large particles, and shelter smaller particles. Large particles have been described as tending to have a significant fraction of their height exposed (e.g Wiberg and Smith, 1987) and, depending on the size and degree of exposure of the surrounding particles, large particles may be preferentially entrained and transported (e.g., Iseya and Ikeda, 1987). Smaller particles are instead expected to form locally smooth surfaces that minimize collisions between moving and static particles. Smaller particles also may temporarily bury larger particles.

3.1.3. Early studies of particle interactions and the origin of particle arrangements.

Langbein and Leopold (1968) surveyed a number of phenomena in which spatial differentiation of sediment occurred during sediment transport, including spatial differentiation

into alternating gravelly and sandy zones in a plane bed river. As a result, they suggested that a fundamental tendency to spatial differentiation of sediment in transport might be the origin of contrasting particle size distributions between pools and riffles.

Subsequently, Ikeda and Iseya (1986) and Iseya and Ikeda (1987) conducted flume runs that documented spatial differentiation of the sediment surface into zones with differing texture. Their results provide a detailed, integrated evaluation of sediment transport and channel response controlled by particle interactions. As a baseline, Iseya and Ikeda documented a set of flume runs using gravel sediment, with an increase in gravel feed rate for each successive run, and observed that the equilibrium slope increased as the gravel supply increased. Next, Iseya and Ikeda conducted a set of runs with a bimodal sand and gravel sediment, with an increase in sand content for each successive run. With a sand content that was reasonably large, but still less than about 50 percent, the sediment surface differentiated into three zones, described as gravelly, transitional and a sand-gravel mix (Iseya and Ikeda characterized these zones as congested, transitional and smooth). The gravel zone exhibited a bed surface of closely-packed gravels. The transitional zone was characterized by a downstream transition from a predominantly gravel surface to intermittent patches or short segments of gravel. The mixed sand-gravel zone was characterized by a gravel framework with sand-filled interstices, such that sand largely buried the coarse particles, thus forming a smooth surface. The zones repeated along the channel, and migrated downstream with time. The longitudinal sequence of zones was also characterized by an aggrading-degrading sequence and by temporal fluctuations in transport.

These observations showed that mobility increased with sand content, and the greater the mobility of the sediment, the smaller the equilibrium slope (Iseya and Ikeda, 1987, p. 17). Thus, less energy was used to move a given volume of the sand-gravel mix than of the unimodal gravel. Iseya and Ikeda identified three particle interaction effects that contributed to the spatial variation

in surface roughness and transport: enhanced exposure of newly-deposited coarse particles, smoothing of the sediment surface by sand, and coarse particle impacts mobilizing sand.

The steep gravel zones were longer than the mixed sand-gravel zones, and the length of the zones increased in proportion to the sand content. Slope also varied among the zones, with the ratio of unit slopes a factor of 1.5 to 1.8 between the steeper gravel and the less steep mixed and transitional zones (the sand-gravel mix, gravel and transition zones had slopes of 0.031, 0.046 and 0.025, respectively, Iseya and Ikeda, 1987, Fig. 7).

Iseya and Ikeda's data demonstrated that less energy was needed to move a given volume of gravelly sediment when the sediment developed spatially-differentiated surfaces, providing a new mechanism consistent with the extremal hypothesis suggested by Yang (1971), that a stream system evolves toward minimization of energy dissipation by the development of alternating steeper and less steep segments. The Iseya and Ikeda study also suggests that the segments will be longer where the sediment contains a greater sand content.

3.1.4. Particle organization on a range of scales.

Riffles are typically viewed as channel-spanning features that are also long relative to the channel width. Spatial variations in particle size also develop on the finer scale of textural patches. Even finer scale features have also been described, including clusters, lines and reticulate networks of coarse particles. Textural patches and finer scale features are summarized here. More detailed information on the lengths of riffle and patches was needed for comparison to the particle interactions cellular automata model (*PICA* model) results, and these characteristics are reviewed in the following section (Section 3.3).

Several studies have documented textural patches, including the textural description of patches in pool-riffle and plane-bed channels (Buffington and others, 1999a; (Lisle and others, 2000), evaluations that relate textural patches to channel resistance (Buffington and Montgomery,

1999b; Lisle and others, 2000), documentation of spatial patterns in local sediment texture (Lisle and others, 2000), description of the spatial extent of mobile sediment under varying flows (Haschenburger and Wilcock, 2003), and description of variation between the center and the margins of the channel bed (Nikora and Goring, 2000).

Other studies have documented variations in particle mobility for particles in different local particle arrangements (Barta and others, 1994; Chase, 1994). Related patterns, described in terms of the placement of individual coarse particles, include particles arranged into connected clusters (Brayshaw, 1985), lines and networks (DeJong and Ergenzinger, 1998; Church and others, 1998; Hassan and Church, 2001, LaMarre and Roy, 2001), and more diffuse alignments of coarse particle patterns (Ahmed, 1987; Robert, 1988). Based on several studies, Robert (2003) suggested that spacing of particle clusters in streams tends to be about 10 D_{50} (Robert, 2003, p. 113). A wide range of other factors may influence spatial differentiation, including variable source areas, transient flows, dynamic/adjusting channels (Beschta, 1987), and large, weakly-mobile obstructions such as woody debris and boulders (e.g., Buffington and others, 2002).

Particle arrangements documented by Sear (1995) include classification of the local particle arrangements at pools and riffles, and as the structural strength of the riffle surface based on cone penetrometer tests. Sear found that riffles had greater structural strength, and noted that this suggests that a greater critical shear stress would be required to entrain riffle sediments.

At the finest scale, several researchers have collected field or flume data at a fine resolution that allows a more detailed description of the bed surface in streams (e.g., Furbish, 1987; Robert, 1987; Nikora and others, 1998; Goring and others, 1999; Nikora and Goring, 2000; Pender and others, 2001).

A wide range of other factors may influence spatial differentiation, including variable source areas, transient flows, dynamic/adjusting channels (Beschta, 1987), and large, weakly-mobile

obstructions such as woody debris and boulders (e.g., Buffington and others, 2002). Additional interactions among channel variables may also influence spatial differentiation. Carling (1983b) found the efficiency of entrainment of bedload sediments is related to channel geometry and distribution of roughness types across the channel bed, and varies as the proportion of submerged roughness elements changes with changing discharge (Beschta, 1987). The presence of more roughness elements may result in greater form drag so that the shear stress on the smaller particles is reduced. The small-scale influences described above, particularly those that reflect variations in vertical particle exposure are included in the model discussed below. Mechanisms that involve a larger scale flow response, and variation in shear stress are not in the model.

3.1.5. Are streambed particle arrangements random?

Several studies of particle arrangements are particularly relevant to this study and are described here in more detail. Furbish (1987) measured surface elevation across a stream channel, at a spacing smaller than the size of the coarse particles, and found that autocorrelation sequences of the elevation data indicated primarily an exponential decay in the correlation between the elevation of a given particle and the nearby particles as the separation distance increased. He noted that this exponential decay in the correlations is consistent with a random arrangement of the particles. Similarly, Kirchner and others (1990) evaluated a sediment surface formed in flume runs and concluded the particles were randomly arranged.

However, preferential arrangements of coarse particles have been documented in flume runs. Hassan and Church (2000) documented reticulate structures, or cells, formed of coarse particles in flume runs. Ahmed (1989) conducted a statistical evaluation of the placement of coarse particles on a flume-generated surface, and concluded that the particles were non-randomly arranged. Ahmed (1989) found that the spatial patterns were generally more well-defined as boundary shear stress increased, but the pattern began to be less well-defined just below the

maximum stresses evaluated. Based on these data, Ahmed (1989) suggested that the strongest spatial patterns in coarse particles developed at shear stresses near the critical shear stress for the mixture (Ahmed, 1989, p. 76-77). The coarsest particles were found to cover about 7.3 percent of the bed area at the highest shear stress in the study (Ahmed, 1989). Other studies have documented the position of very coarse particles in streams (e.g., Church and others, 1987; LaMarre and Roy, 2001). The available studies that document non-random spatial patterns in the placement of individual particles are few, and it is unclear to what extent the spatial distribution of particle size by size (or any other particle characteristics) is spatially non-random in streams. However, the available data is consistent with the weakly non-random spatial pattern in the elevation of the tops of particles developed in the model, as described in Chapter 1. That is, the *PICA* model surfaces exhibit a lack of high points at a spacing averaging about 10 cells apart, corresponding to 10 particle diameters of the largest particles in the model, or nominally 2.5 meters. In addition, in the two highest mobility runs there there is an excess of high points spaced about 5 cells apart (corresponding to 1.25 coarse particle diameters), indicating that when the sediment is highly mobile, small-scale clustering becomes statistically significant, in addition to the weak regularity of spacing local high points on the bed. However, the spatial distribution of coasre particles does not show a statistically significant non-random arrangemet. Thus, particles of many sizes constribute to a relatively fine-scale pattern of highs and lows on the bed.

Theory suggests that variations in the distributions of particle protrusion may occur as transport in streams adjusts toward an equilibrium (or quasi-steady) state. The stable state has been described as one in which all particles are equally mobile, such that particles of all sizes are transmitted downstream, in proportion to their presence in the bulk sediment rather than the less readily mobilized particles sizes being preferentially stored (Parker and Klingeman, 1982). Thus, assuming streams are in equilibrium, mechanisms that equalize mobility are expected to ensure

that large particles tend to be more well-exposed than smaller particles, either by having a greater areal exposure as in armoring, or a greater vertical exposure so that larger particles tend to rise higher into the flow (Parker and Klingeman, 1982). Greater areal exposure of coarse particles, such that the particle size distribution on the channel surface coarsens or 'armors' is common in streams. The model results indicate no statistically significant patterns in particle protrusion. It is possible that additional analyses might identify spatial patterns in the joint distributions of some of these characteristics, e.g. cells that have both coarse particles and those particles are well-exposed, or cells that have coarse particles and are high points, but such analyses were not conducted for this study.

3.1.6. Textural variations in pool-riffle channels

Sediment surfaces in streams clearly have spatial patterns in particle texture on the larger scales of patches and cross-stream variations. Textural patches were documented by Buffington and others (1999b). They noted that particle interactions may play a role in the development of textural patches, including mechanisms and factors such as kinematics waves, intergranular friction angles, relative grain protrusion (Kirchner and others, 1990; referred to here as relative exposure), and wake effects (Buffington and Montgomery, 1999b, p. 1903, referencing Iseya and Ikeda, 1987; Naden and Brayshaw, 1987; Whiting and others, 1988). Buffington and Montgomery (1999a) also noted that patterns of textural patches were more predictable in channels with less chaotic arrangements of flow obstructions. Buffington and Montgomery (1999a, Table 3, p. 3513) found that woody debris influenced the spacing of both pools and textural patches, as well as the amplitude and wavelength of bank and bar topography. For patches, they found that the number of textural patches ranged from 1 to 8 patches in plane bed reaches, 13 to 24 in wood-poor pool-riffle reaches, and 17 to 55 in wood-rich pool-riffle reaches on the Olympic Peninsula, Washington, USA.

Cross-stream variations in sediment texture have been documented in another study, with a comparison of the median particle size near the bank and near the centerline, in the Balmoral Irrigation Canal, North Canterbury, New Zealand (Nikora and Goring, 2000). The data were obtained by Wolman counts along several 2-m-long longitudinal profiles along the banks and near the channel center, respectively. Graphic standard deviation values were calculated from the average of the reported data range for these two locations. The values obtained are 2.48 for the banks and 1.30 for the bed (these were calculated as $2*[D_{84}-D_{50}]$). The values are similar when calculating the standard deviation as $(D_{84}-D_{16})$. The data indicate that the sediment at the banks has a wider range of sizes, i.e., is more poorly sorted. Bed elevations were also measured, and the standard deviation of bed elevation and the longitudinal length scale (similar to the correlation length) were derived from structure functions (*see* Nikora and others, 1998). The standard deviation of the elevations was 6.9 mm, and the longitudinal length scale was 41 mm in the central zone. The corresponding near-bank values were significantly larger, i.e., 34 and 180 mm, respectively. No obvious bed forms were observed on the bed profiles. Thus, particle size and

Table 3.3. Particle size variations in a gravel channel

	D_{16} (mm)	D_{50} (mm)	D_{84} (mm)
Banks	23.1–29.8	48.4–67.5	112–161.5
Center	7.4– 8.2	12.5–16.2	20.4–24.6

	Elevation standard deviation (mm)	Longitudinal length scale (mm)	Graphic standard deviation[#]
Banks	34	180	2.48
Center	6.9	41	1.30

Data from Nikora and Goring, 2000

[#] *The graphic standard deviation was calculated as* $2*(D_{84}-D_{50})$

surface roughness were much greater at the banks than in a central, homogenous 3-m-wide portion of the channel (Table 3.3).

3.1.7. Particle size distributions in pool-riffle channels

In steep mountain rivers, gravel, cobbles, and sometimes boulders cover much of the channel bed surface. The character of the particle size distribution in such streams is not particularly clear, and may be variable. A long fine-grained tail in the particle size distribution has been described as common (Hassan and Church, 2000). Svidchenko and others (2001, p. 2274) suggested that widely-graded, weakly bimodal sediment is typical of natural gravel-bed rivers. Parker (1990) suggested that gravel rivers tend to be strongly bimodal, depleted in sizes between 1 and 6 mm.

Coarsening of the channel bed is characteristic of gravel bed and coarser rivers, and the coarsened surface layer is generally termed an armor layer. Hassan and Church (2000) conducted flume studies and noted that the armor layer developed and stabilized quickly, generally within hours. Buffington and Montgomery (1999a) characterized the armoring ratio (ratio of surface to subsurface D_{50}), as typically 1 to 3 based on four weakly-armored steep reaches in western Washington and southeast Alaska. Whiting and others (1999) documented armoring ratios, for headwater gravel-bed streams in snowmelt-dominated areas of Idaho, that averaged 3.3 for eight sites, and ranged from 1.8 to 5.0.

Particle interactions are expected to be most important in poorly-sorted sediment. Buffington (1999) suggested that particle size distributions are roughly scale-independent for a large set of coarse-grained streams, with median grain sizes from 8 to 256 mm (-3 to -8 phi) (based on 1266 grain-size distributions from 44 studies of rivers throughout North America and the United Kingdom). The data showed no strong variation in the standard deviation of surface particle size, and the standard deviation of logarithmic grain sizes varied from about 0.5 to 2 ϕ in streams The particle standard deviation was generally proportional to median grain size when particle

distributions were expressed in linear size classes (i.e., mm). These data suggest that the shape of the particle size distribution does not vary widely.

Particle size differences between pools and riffles are considered characteristic of pool-riffle channels. In general, riffles are described as coarser than pools. However, several researchers have criticized this characterization (e.g., Thompson and others, 1996). One issue is that pools tend to fill with fine sediment during lower flows, thus covering the sediments that would form the bed at a formative flow. Yet, such fine sediment is not expected to remain in pools during the relatively high flows that determine channel form. In addition, Thompson and others (1996) found that coarse tracer particles were predominantly deposited on the pool tails, and suggested that high flow deposition at pools may actually consist of coarser sediment than at riffles. Determination of particle size differences between pools and riffles is also likely complicated by the different methods used to identify pools and riffles. The most common identification methods are the zero-crossing method (e.g. Nordin, 1971) and the closed basin method (Lisle and Hilton, 1992), each of which will tend to place the transition from pool to riffle at a different point along the pool-riffle cycle.

The most detailed evidence on the particle size contrast between pools and riffles of which I am aware is provided by Milne (1980). Milne documented sediment characteristics for one stream reach, finding that riffles are slightly coarser and better sorted than pools (Milne, 1980). Bar sediment was consistently finer. Pools and riffles were delineated using the zero-crossing method.

3.1.8. Spatial differentiation into pools and riffles, and mechanisms for their development

The mechanisms that result in alternately steeper and less steep zones in pool-riffle channels are not yet known. As noted above, the pool-riffle form has been associated with the bar-pool form. Riffles clearly may develop at a site where bar fronts are built up and steepened at bankfull stage and higher flows, as described by Parker and Peterson, 1980 (p. 1650-1651). To the extent

that riffles are formed from channel bar sediment, this suggests that depositional episodes are necessary to maintain riffles, and subsequent erosion of the lower levels of the bar is necessary to modify the particle size distribution.

Other mechanisms may also be important, particularly in steep streams where bars are rare or inconspicuous. Yang proposed an extremal hypothesis that channels evolve in a direction that minimizes the time rate of potential energy expenditure per unit mass of water, within the limits determined by "the constraints applied to the stream by its environment" (Yang, 1971, p. 1570), i.e. due to boundary conditions. Yang's analysis indicates that the maximum energy expenditure occurs along a channel of uniform slope, and that spatial differentiation into segments with varying slope will reduce the energy dissipation. Thus, any configuration with alternating steep and less steep segments contributes to minimization of energy dissipation. A feature that minimizes energy may be expected to persist, but the constraints on the development of such slope variations, which require considerable erosion and/or deposition, may also influence the resulting lengths of pools and riffles.

Locally steeper zones may be relatively easy to generate in mountain streams, and they may tend to persist. Suggested mechanisms, in addition to local aggradation at bar, include (a) particle interactions (Iseya and Ikeda, 1987), in which steeper and coarser channel segments form during transport of bimodal sediment; (b) chute cutoff formation (Keller and Melhorn, 1981); (b) faulting in tectonically active areas, (c) failure of woody debris dams, and (d) landslide deposition. It is not known how the length of locally steep sections evolves over time. In one example, Lisle (1982) described a riffle adjusting by 'laying back', thus the riffle lengthened and decreased in slope. In general, locally oversteepened sections will tend to become locally coarsened. An example was documented by Talbot and LaPointe (2002) in which a steep and armored (i.e., coarsened) zone migrated downstream, in a process they termed reprofiling.

3.1.9. Effect of the width of the particle size distribution

Laboratory experiments demonstrate that scour at obstructions decreases as the width of the particle distribution increases, and with an increase in the median particle size (Buffington and others, 2000). Another data set (Lisle and others, 2000, Figure 3.1b) suggests that pool-riffle and plane bed channels have similar central values for slope and width-to-depth, but differ in relative submergence (Table 3.1). The plane bed channels, with more widely spaced pools, are associated with smaller relative submergence. This suggests that particle size alone may influence channel form, with plane bed channels having greater particle size, than pool-riffle channels.

3.1.10. Effects of bed width and increasing fines in the particle size distribution.

Toro-Escobar and others (2000) evaluated the influence of variation in sand content, in flume examples with 33 and 55 percent sand, and variations in channel width, with flume examples at 0.3 and 2.7 m. Increased channel width promoted formation of transverse topography, enhanced development of sediment patches, and an increased rate of gravel fining. Increasing sand content also resulted in a much more concave longitudinal bed profile, marked patch development, and increased rate of downstream fining for all gravel-size bed material. Patches increased with increased width and increased sandy fines.

3.2. Size of coarse patches and mobile patches in streams

3.2.1. Size of patches

Lisle and others (2000) presented data on the size of textural patches for three streams in California, USA and one in Colorado. The streams are described as pool-riffle channels with channel bars. The study included two reaches of Redwood Creek, and these reaches were more similar to each other than to the reaches at two additional creeks (Grouse Creek and Jacoby Creek). The Redwood Creek reaches had similar particle size and area occupied by each size class, but differed in the number of patches. Redwood 2 generally had fewer patches.

Textural patches in reaches of these four streams were classified as fine pebbles, coarse pebbles, cobbles, and bimodal sediment. The area occupied by coarse cobble patches ranged from 20 to 53 percent of the bed area in these streams. Coarse pebble patches from 31 to 57 percent, fine pebble patches covered from 8 to 27 percent, and bimodal textures from 9 to 18 percent of the bed. The data record about 3 patches per 100 meter in all of the streams except Grouse Creek, which had about 6.3 patches per 100 meters.

The nominal length of the coarse patches was calculated from the data of Lisle and others (2000) for comparison to model data, and is shown in Figure 3.3. The nominal length is defined for this analysis as the length of the reach divided by the total number of patches on the bed, representing an average for patches of all textures. Because many patches may not span the width of the bed, actual patch lengths may be expected to be longer than the nominal length in the downstream direction. This calculation indicates that the length scale of patches ranges from shorter than to longer than one channel width. The data are summarized in Table 3.4.

3.2.2. Variation in patch size with channel width, slope, D_{50} and discharge

Based on data presented by Lisle and others (2000), patch length increases as channel width increases, but the correlation is weak ($r^2 = 0.182$). Their data also indicates that patch length tends to be inversely proportional to slope ($r^2 = 0.567$). Median particle size, D_{50}, was the only particle size data available for this dataset. Because width of the particle size distribution is generally positively correlated with median particle size, D_{50} was used here as a surrogate for particle size distribution width. The length of patches in this data decreases with increasing median particle size, but the correlation is weak ($r^2 = 0.234$). Patch length increases with discharge ($r^2 = 0.364$), suggesting that patch length increases with increasing particle mobility, although the correlation is weak. The weak correlations in these data are in large part because the data set is small.

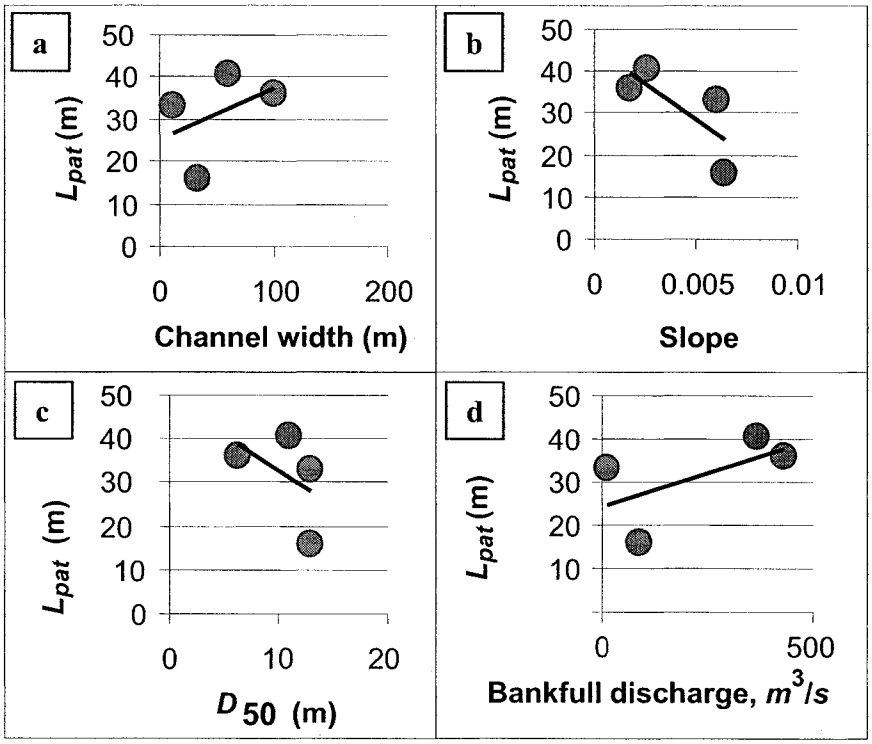

Figure 3.3. Variation in the size of textural patches versus width, slope, width of the particle size distribution and mobility threshold. The relative size of textural patches, L_{pat} is approximated here as the total number of patches in the study reaches, divided by reach length (data from Lisle and others, 2002). (a) the length of patches may increase as channel width varies, but the correlation is weak ($r^2 = 0.182$) for this small data set. (b) The length of patches tends to be inversely proportional to slope ($r^2 = 0.567$). (c) Median particle size, D_{50}, was the only particle size data available for this data set. The width of the particle size distribution is generally expected to have a positive correlation with median particle size, and here D_{50} was used as a surrogate for the width of the particle size distribution. The length of patches may decrease with increasing median particle size, but the correlation is weak for this small data set ($r^2 = 0.234$). (d) The length of patches is directly proportional to discharge ($r^2 = 0.364$), suggesting that patch length increases with increasing particle mobility, although the correlation is weak. The general lack of strong correlations is expected given the limited data. Additional data are needed to confirm these relationships.

Table 3.4: Selected Rivers in California and Colorado

Stream	Bankfull Width m	Slope *	D_{50} *1 mm	D_{s50} *1 mm	Drainage area km^2	Sediment yield Mg km^{-2} yr^{-1} *2	Bankfull discharge m^3 s^{-1}
Jacoby Ck.	12	0.006	26	13	36	180	14
Grouse Ck.	33	0.0064	39	13	140	1800	93
Redwood Ck. 2	60	0.0026	15	11	520	1400	370
Redwood Ck. 1	100	0.0018	11	6.3	600	1400	430

Stream	*Percent of area occupied by patch type*				*Number of patches by patch type*			
	Fine pebble	Coarse pebble	Cobble	Bimodal	Fine pebble	Coarse pebble	Cobble	Bimodal
Jacoby Creek	23.8	56.6	19.6	0	1	19	15	0
Williams Fork	27.5	43.4	19.8	9.3	6	13	8	5
Grouse Creek	16.7	31.1	34.1	18.1	5	5	5	5
Redwood Creek 2	8.5	38.9	52.7	0	2	2	2	0

*1, bar(D_{50}) and bar(D_{s50}) are median particle sizes of surface and subsurface sediment;
*2, mean annual basin yield for clastic sediments

Buffington and Montgomery (1999b) also presented data on the number of patches in a stream reach. I converted those data to a length scale of patches, assuming that only half of the channel area was channel bed, and that only the bed had patches. These lengths only approximate patch lengths, but the relative lengths scales should reflect the direction of variation of patch length with other channel variables (Figure 3.4). Data is available for pool-riffle, plane bed and forced pool-riffle channels. The direction of variation of these patch lengths with other channel

variables differs in most cases from the lengths derived from the data given by Lisle and others (2002). It is thus not clear how patch lengths vary with other channel variables.

3.2.3. Data from streams on partial mobility of sediment

Particle mobility in streams varies with the threshold for particle motion. Thus mobility may vary with spatial variation in particle size, or with variations in exposure of particles and variation in local flow intensity. Data on the degree of particle mobility as discharge varies were presented by Haschenburger and Wilcock (2003) for Carnation Creek, British Columbia, Canada (Figure 3.5). They found that approximately 25 to 50% of the bed was in a state of partial mobility during a flood with a two-year return period. Surface grain entrainment was nearly complete in a 7-year return period flow, corresponding to a bankfull discharge with an estimated flow velocity of 35 $m^3 s^{-1}$. Booker and others (2001) found a lower level of particle mobility at bankfull. They found that mobile particles occupied as little as 50% of the channel width at near-bankfull stage (Booker and others, 2001, p. 570). These data indicate that sediment in steep pool-riffle channels may be far from fully mobile at bankfull stage.

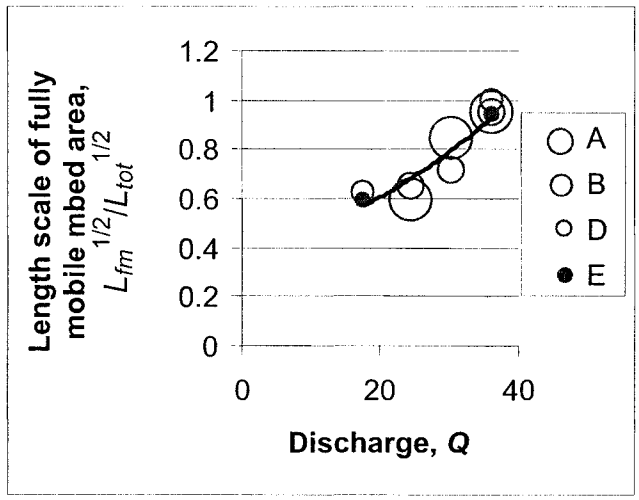

Figure 3.5. Areal frequency of mobile sediment at varying discharge. The relative length scale derived from the area of fully mobile sediment on the channel bed is $(A_{fm}/A_{tot})^{1/2}$, where A_{fm} is the fully mobile bed area and A_{tot} is the total bed area in the reach. The data are for Carnation Creek, Canada (data from Wilcock and Haschenburger, 2003). The relative length scale of textural patches shows a nearly linear to weakly exponential increase as water discharge varies in four floods (see correlations in the text). Different symbols indicate different segments of the channel.

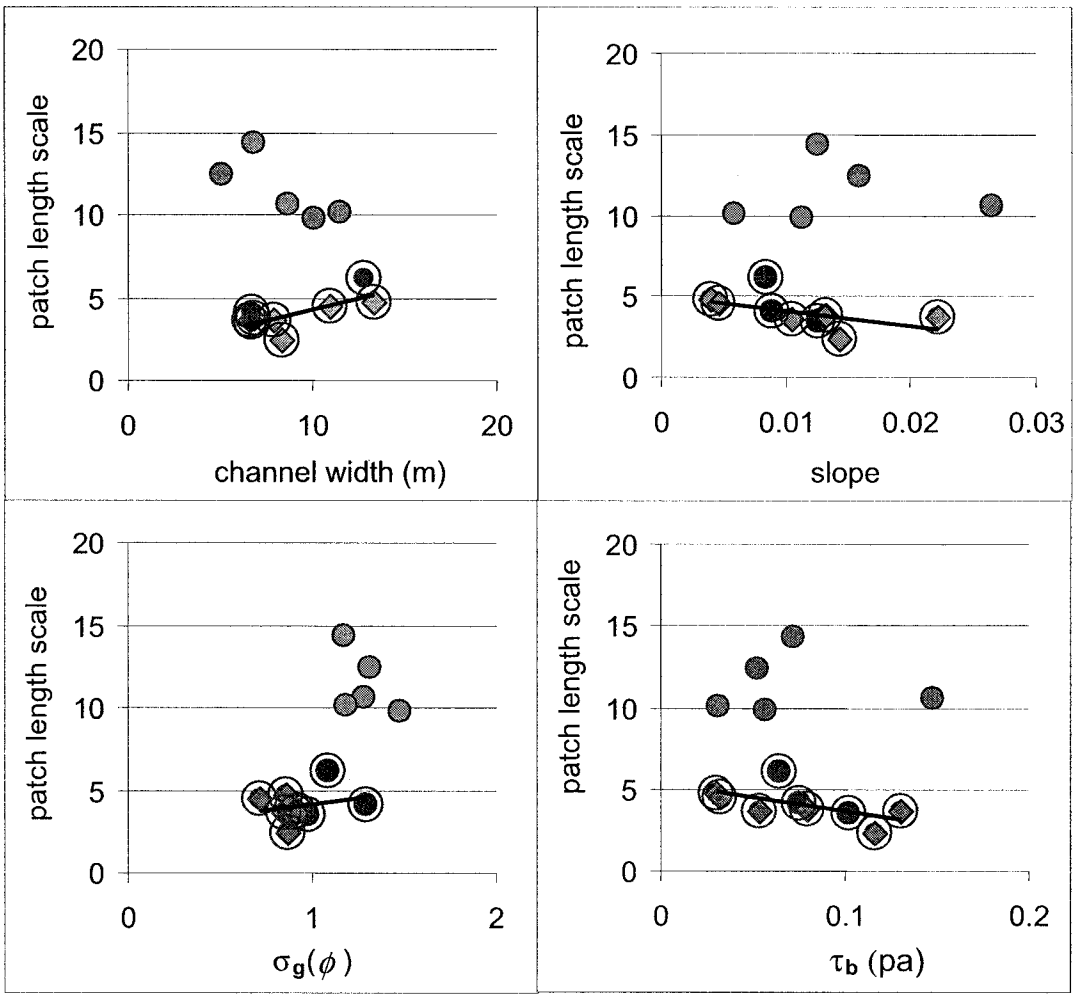

Figure 3.4. Patch length scale in the data from Buffington and Montgomery (1999b). The plots show the relationship of patch length scale to channel width, slope particle size and mobility threshold. The correlation lines shown are for the data excluding the forced pool reaches.

3.3. Analysis of the length of riffles in pool-riffle channels

3.3.1. Observed spacing of riffles

Information on the the development of spatial patterns in particle size and their association with particle interactions, summarized above, is suggestive of riffle origins, but it is not known which, if any, of these observations constitutes a key control on the development of riffles. Before these can be understood, more information on the length of riffles relative to pools and other channel features is needed.

When bedforms consist of pool and riffle sets, the average spacing of riffles is necessarily similar to the average spacing of pools. Typically, the separation distance between the head of one pool and the head of the next pool (or between one riffle crest and the next) is measured, and pool-riffle spacing is evaluated as the average of these separation distances. Studies of pool-riffle forms that document the individual lengths of pools and riffles generally do not also report pool-riffle spacing. When only pools and riffles are defined elements of the stream channel, pool-riffle spacing may be approximated as the average length of pools plus the average length of riffles.

Average spacing of pools and riffles is often described as approximately proportional to channel width, typically from 5 to 7 channel widths (Leopold and others, 1964; Keller and Melhorn, 1981; Gregory and others, 1994). As a result, pool-riffle spacing is usually characterized relative to channel width.

Although average spacing may be well-constrained in larger rivers, recent field studies have documented a wide range in such spacing in many channels (*see* Chapter 1). For example, a compilation of data from pool-riffle mountain rivers, representing widths less than 10 m, slopes greater than 0.01 and low flow less than 3 $m^3 s^{-1}$ (Wohl and Merritt, 2005), includes reaches with average pool-riffle spacing from 1.4 to 13.9 channel widths. This is, however, consistent with, theoretical analyses of bar-pool spacing which suggest a range of about three to 12 channel

widths (Yalin, 1971a; Blondeaux and Seminara, 1985). Step-pool forms and forced pool spacing varies from about 0.5 to 3 channel widths (Chin 2002).

3.3.2. Standard conceptual model of pool and riffle forms

Conceptual models of the pool-riffle form typically present pool and riffle segments as subequal in length, forming symmetrical undulations of the surface. This conceptual model was presented by Yalin (1971a, 1971b) in his hypothesis for the origin of pool-riffle channels. Yalin also related pool spacing to channel depth, although most subsequent analyses present pool spacing as proportional to channel width. Buffington and others (2002) suggested that pool length and depth may also scale in proportion to channel dimensions, at least approximately. Taken together, these standard conceptual models suggest that pools and riffles are subequal in length, and that pool and riffle lengths are proportional to channel width, depth, or both. However, documented hydraulic geometry exponents for channel width and depth suggest distinct differences in their rate of change in downstream sequences (e.g., Singh and others, 2003). Varying hydraulic exponents suggest that pool-riffle spacing varies at different rates relative to channel width in different channels, and that channel width and depth vary independently from each other. Given that width and depth do not scale in proportion to each other, it is worth considering whether the lengths of riffles and pools may also vary at different rates.

3.3.3. Evaluation of riffle length variations as width, slope, particle size distributions and particle mobility vary

Patterns of variation in riffle length were extracted from five existing studies that provide data on riffle length, as well as at least some of the reach characteristics of width, slope, particle size and sorting, and shear stress or related measures of particle mobility (e.g., discharge). The studies include published data and unpublished data available on the internet.

The five studies summarized below include studies by Lere, 1984 (Montana); Grant and others, 1990 (Oregon); Wohl and others, 1993 (coastal California); Carling and Orr, 2002 (UK), Ebell and others, 2004 (British Columbia, Canada). One of the studies defines pool, riffle and run form units (Wohl and others, 1993); one defines riffle and glide units (Ebell and others, 2004); the other three studies define pools and riffles, and not runs or glides (Carling and Orr, 2002; Grant and others, 1990, Lere, 1984).

Lere (1984) documented the lengths of pools and riffles in two mountain valley reaches of the West Fork of the Bitterroot River, Montana, USA. Lere described the streambed as typified by large gravel bar deposits, and a network of side channels. Pool and riffle lengths were determined at 10 pool-riffle pairs.

Grant and others (1990) determined the lengths of pools and riffles in the Cascade Mountains of western Oregon, USA. Because the data of Grant and others (1990) include all pool types in a single category, the reported pool lengths may be systematically shorter than typical of pool-riffle reaches because the study did not distinguish between riffles in pool-riffle sequences and other, typically smaller pools such as step-pools. However, the reported lengths do not appear unusually short.

Wohl and others (1993) measured unit lengths for riffles, pools and runs in coastal streams of California, USA. They also measured streams at a range of slope within the study area, including a very steep stream with a slope of 0.17 m. The latter stream was not assigned a form designation.

Carling and Orr (2002) documented pool and riffle forms in three steep stream reaches in the Severn River, UK, based on a detailed longitudinal profile which they segmented into pools and riffles using the zero-crossing method. In the zero-crossing method, a riffle segment will generally rise from its upstream end to some intermediate point, termed the riffle crest, then

descend from the crest to the end of the riffle, thus placing the transition at the high point between one pool deep and the next. Thus Carling and Orr's results may have systematic differences from pools and riffles identified using the closed basin definition. However, I believe the results appear similar enough to be combined here.

Ebell and others, (2004) defined glides (as well as pools and riffles) in a pool-riffle segment of the Elk River in British Columbia, Canada. They note that over the past 70 years the river has changed from a comparatively narrow, single thread channel to a multi-thread, laterally unstable, aggraded channel as a result of increased flow and sediment availability and decreased bank resistance associated with decreased vegetation, resulting in a four to seven times increase in the unvegetated channel width (Ebell and others, 2004; Redden and Cuthbert, 2004).

As noted above, I will assume that the sum of the length of riffles and runs (or riffles and glides) represents the length of riffles that would have been measured if only riffles and pools were documented. For clarity, in the following, I refer to lengths that are the sum of riffle and run lengths as riffle-run lengths. Pool-riffle spacing when riffles and runs are both present will then be defined as the sum of pool, riffle and run lengths. Equating the pool-riffle spacing with the sum of all unit lengths assumes that a single run unit, where defined, occurs within each pool-riffle cycle. The following review of the available data presents both riffle and riffle-run lengths, and both are shown in each plot (gray diamond and gray triangle points, respectively).

Each data set in this compilation represents reaches in one or a few nearby streams in the same region, with generally similar climatic, lithologic, tectonic, topographic, and land use characteristics. Three of the five data sets represent reaches in an individual stream. Reaches in the Lere (1984) study are more dissimilar, including both well-watered, single thread and periodically dewatered, multi-thread channels.

3.3.4. Variation of riffle length with pool length.

There is a general expectation that the spacing of pool-riffle forms scales with channel width. To the extent that the channel width and pool-riffle spacing scale together, it is reasonable to consider whether other channel and bedform dimensions scale together, as suggested by Lisle and others (2000). In addition, flume studies by Thompson (2002) indicate that pool depth and length scale with discharge, although the variability is high for pool length. It is reasonable to suggest that the length scales for riffles and riffle-runs might similarly scale with channel width.

Figure 3.6 shows three different parameterizations of the relationships between pool, riffle (or riffle-run), and channel length scales. The plots show the relationship between (a) the lengths in meters of pools, L_p in relation to the lengths in meters of riffles and riffle-runs, L_{riru} and L_{rif} (Figure 3.6a), (b) pool length in meters, L_p, in relation to riffle and riffle-run lengths scaled by pool length, L_{rif}/L_p and L_{riru}/L_p, (Figure 3.6b), and (c) pool length scaled by channel width, L_p / w_c relative to riffle and riffle-run lengths scaled by channel width, L_{rif} / w_c and L_{riru} / w_c (Figure 3.6c).

In the data from the five studies described above, riffle lengths, L_{rif} and riffle-run lengths, L_{riru}, range from 7.4 to 155 meters (Figure 3.6a). The relationship between the lengths of riffles and pools in Figure 3.6a is not linear. Instead it is a double-valued relationship, with a given riffle or riffle-run length occurring in most reaches with very short pools, but in a few reaches with very long pools. There is a v-shaped pattern, slightly skewed, in the data points, and the data on each limb of the 'v' show a positive relationship between riffle and pool length. The heavy black and gray lines in the plot are the correlation lines for all riffle lengths, and all riffle-run lengths, respectively. The thinner dashed lines show correlations for individual study areas.

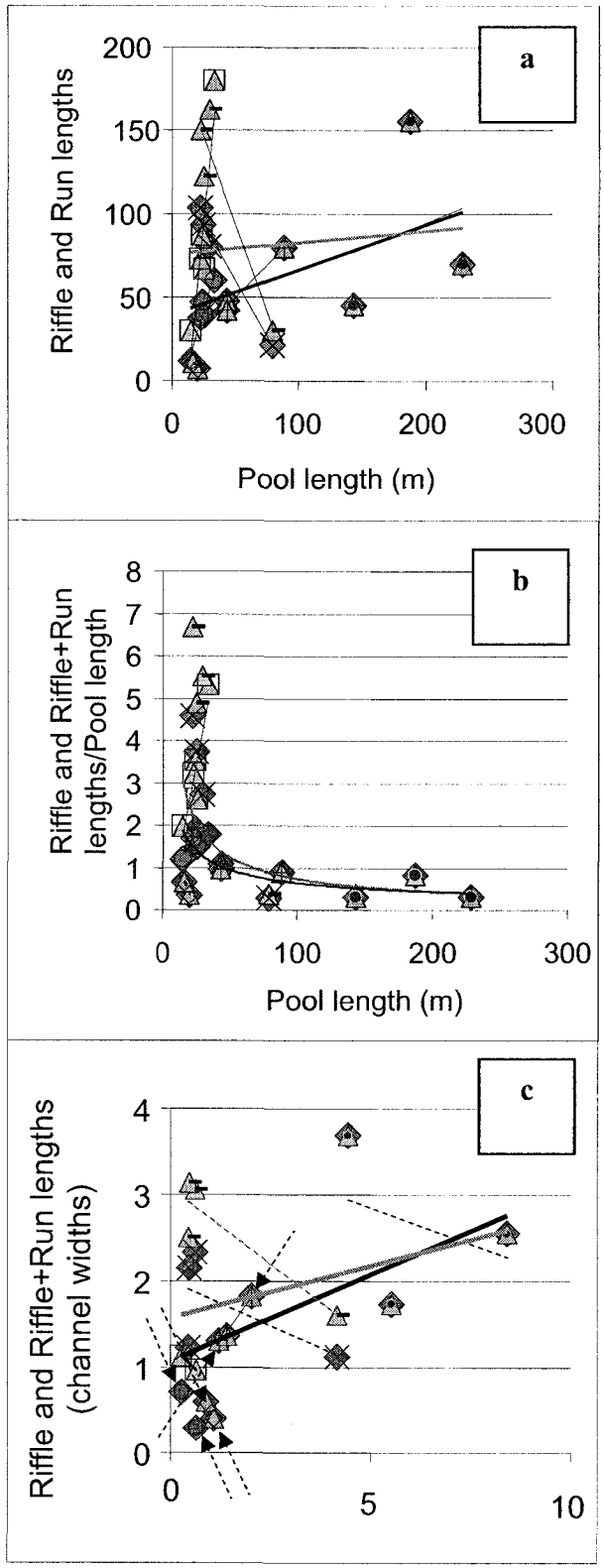

Figure 3.6. Lengths of riffles and pools. The length of riffles and pools are shown based on data from five field data sets (Lere, 1984; Grant and others, 1990; Wohl and others, 1993; Carling and Orr, 2002; Redden and Cuthbert, 2004). The heavy black line in each figure is the correlation lines for all riffle lengths, the heavy gray line is the correlation for all riffle-run lengths; dashed lines are correlation lines for individual studies. See the text for the correlation equations. (a) The v-shaped pattern of data points shows that riffle lengths are a double-valued function of pool length. (b) Riffle length is normalized by pool length (L_{rif}/L_p and L_{riru}/L_p), where L_p is pool length, L_{ri} is riffle length, and L_{riru} is riffle+run length. A power law correlation approximately describes the relationship, but does not reflect the nearly vertical to slightly positive trend for small pools in the data. (c) The relationship between pool and riffle lengths normalized by channel width is shown. The correlation lines for all data shows a trend of increasing relative riffle length as pool length increases, for all riffle+run lengths. However, the subparallel correlations for data from four of the five individual study sites show a decrease in relative riffle and riffle-run length as relative pool length increases. This suggests that riffle length does not scale with channel width, but varies under the influence of other channel characteristics.

Data symbols are as follows: Lere, 1984, ( ); Grant and others, 1990,( ); Wohl and others, 1993, riffle ( ), riffle+run ( ); Carling and Orr, 2002,( ); Ebell and others, 2004, riffle ( ), riffle+run ( ).

A large proportion of the data points in Figure 3.6a represent reaches with relatively short pools, up to about 40 meters in length, and plot in the near vertical limb of the v-shaped pattern. A smaller number of reaches, with longer pools, plot in the right-hand limb of the v-shaped pattern. Five reaches are clearly part of the latter group, including the three reaches in Wyoming (Lere, 1984), one of the British Columbia reaches (Ebell and others, 2004), and one of the reaches evaluated by Carling and Orr (2002). (The Ebell and others data include points for both riffle and for riffle-run lengths.) Thus, the more sparsely populated limb of the v-shape pattern includes data from several different study areas, making it less likely that a bias or variation in definitions is the origin of the double-valued relationship. Note, however, that two of the studies with points in the right-hand limb (from British Columbia and Wyoming), were described as disturbed, with bifurcated channels. Also note that because of the wide scatter in the data points for these five reaches, the maximum length of pools associated with short riffles is near 180 meters, approaching the maximum length of pools associated with long riffles, about 250 meters.

The riffle and riffle-run lengths scaled by pool length, L_{rif} / L_p and L_{riru} / L_p, range from 0.27 to 6.7 (Figure 3.6b). Riffles evidently may be either longer than or shorter than pools. The pattern of data points in this plot is largely similar to the previous plot, except that here the two limbs of the data pattern consist of a nearly vertical limb with a strongly positive correlation for the relationship between riffle (and riffle-run) lengths, scaled by pool length, versus pool length (in meters), and a nearly horizontal limb with a slightly negative correlation of riffle (and riffle-run) lengths, scaled by pool length, to the pool lengths. The transition between these two trends, pool length, L_{rif}/L_p and L_{riru}/L_p, (Figure 3.6b), and (c) pool length scaled by channel width, L_p / w_c relative to riffle and riffle-run lengths scaled by channel width, L_{rif} / w_c and L_{riru} / w_c (Figure 3.6c).

In the data from the five studies described above, riffle lengths, L_{rif} and riffle-run lengths, L_{riru}, range from 7.4 to 155 meters (Figure 3.6a). The relationship between the lengths of riffles and pools in Figure 3.6a is not linear. Instead it is a double-valued relationship, with a given riffle or riffle-run length occurring in most reaches with very short pools, but in a few reaches with very long pools. There is a v-shaped pattern, slightly skewed, in the data points, and the data on each limb of the 'v' show a positive relationship between riffle and pool length. The heavy black and gray lines in the plot are the correlation lines for all riffle lengths, and all riffle-run lengths, respectively. The thinner dashed lines show correlations for individual study areas.

A large proportion of the data points in Figure 3.6 represent reaches with relatively short pools, up to about 40 meters in length, and plot in the near vertical limb of the v-shaped pattern. A smaller number of reaches, with longer pools, plot in the right-hand limb of the v-shaped pattern. Five reaches are clearly part of the latter group, including the three reaches in Wyoming (Lere, 1984), one of the British Columbia reaches (Ebell and others, 2004), and one of the reaches evaluated by Carling and Orr (2002). (The Ebell and others data include points for both riffle and for riffle-run lengths.) Thus, the more sparsely populated limb of the v-shape pattern includes data from several different study areas, making it less likely that a bias or variation in definitions is the origin of the double-valued relationship. Note, however, that two of the studies with points in the right-hand limb (from British Columbia and Wyoming), were described as disturbed, with bifurcated channels. Also note that because of the wide scatter in the data points for these five reaches, the maximum length of pools associated with short riffles is near 180 meters, approaching the maximum length of pools associated with long riffles, about 250 meters.

The riffle and riffle-run lengths scaled by pool length, L_{rif} / L_p and L_{riru} / L_p, range from 0.27 to 6.7 (Figure 3.6b). Riffles evidently may be either longer than or shorter than pools. The

pattern of data points in this plot is largely similar to the previous plot, except that here the two limbs of the data pattern consist of a nearly vertical limb with a strongly positive correlation for the relationship between riffle (and riffle-run) lengths, scaled by pool length, versus pool length (in meters), and a nearly horizontal limb with a slightly negative correlation of riffle (and riffle-run) lengths, scaled by pool length, to the pool lengths. The transition between these two trends, pool length, L_{rif}/L_p and L_{riru}/L_p, (Figure 3.6b), and (c) pool length scaled by channel width, L_p / w_c relative to riffle and riffle-run lengths scaled by channel width, L_{rif} / w_c and L_{riru} / w_c (Figure 3.6c).

In the data from the five studies described above, riffle lengths, L_{rif} and riffle-run lengths, L_{riru}, range from 7.4 to 155 meters (Figure 3.6a). The relationship between the lengths of riffles and pools in Figure 3.6a is not linear. Instead it is a double-valued relationship, with a given riffle or riffle-run length occurring in most reaches with very short pools, but in a few reaches with very long pools. There is a v-shaped pattern, slightly skewed, in the data points, and the data on each limb of the 'v' show a positive relationship between riffle and pool length. The heavy black and gray lines in the plot are the correlation lines for all riffle lengths, and all riffle-run lengths, respectively. The thinner dashed lines show correlations for individual study areas.

A large proportion of the data points in Figure 3.6a represent reaches with relatively short pools, up to about 40 meters in length, and plot in the near vertical limb of the v-shaped pattern. A smaller number of reaches, with longer pools, plot in the right-hand limb of the v-shaped pattern. Five reaches are clearly part of the latter group, including the three reaches in Wyoming (Lere, 1984), one of the British Columbia reaches (Ebell and others, 2004), and one of the reaches evaluated by Carling and Orr (2002). (The Ebell and others data include points for both riffle and for riffle-run lengths.) Thus, the more sparsely populated limb of the v-shape pattern includes

data from several different study areas, making it less likely that a bias or variation in definitions is the origin of the double-valued relationship. Note, however, that two of the studies with points in the right-hand limb (from British Columbia and Wyoming), were described as disturbed, with bifurcated channels. Also note that because of the wide scatter in the data points for these five reaches, the maximum length of pools associated with short riffles is near 180 meters, approaching the maximum length of pools associated with long riffles, or about 250 meters.

The riffle and riffle-run lengths scaled by pool length, L_{rif} / L_p and L_{riru} / L_p, range from 0.27 to 6.7 (Figure 3.6b). Riffles evidently may be either longer than or shorter than pools. The pattern of data points in this plot is largely similar to the previous plot, except that here the two limbs of the data pattern consist of a nearly vertical limb with a strongly positive correlation for the relationship between riffle (and riffle-run) lengths, scaled by pool length, versus pool length (in meters), and a nearly horizontal limb with a slightly negative correlation of riffle (and riffle-run) lengths, scaled by pool length, to the pool lengths. The transition between these two trends, one positive and one negative, is near a pool-scaled riffle or riffle-run length, L_{rif} / L_p and L_{riru} / L_p, of 1.5. Most reaches in the sub-horizontal limb have riffle lengths shorter than pool lengths. This relationship, in which riffle lengths are scaled by pool length, also shows less scatter than the relationship in Figure 3.6a, where riffle length is not scaled by pool length.

Because the relationship between riffle length, scaled by pool length and as pool length in meters, plots as a nearly vertical line, I did not construct a correlation for predicting pool-scaled riffle length from pool length. Instead, I used the length of riffles to develop a predictive relationship for the length of pools. The pool-scaled riffle length (L_{rif} / L_p), including only reaches with L_{rif} / L_p <=1.5, was used to predict the length of short pools, as:

riffle	$L_p = -0.537$	$L_{rif} / L_p + 27.8$	$r^2 = 0.0052, n = 12$
riffle-run	$L_p = -0.180$	$L_{riru} / L_p + 27.3$	$r^2 = 0.0017, n = 12$

The correlations are weak because the variation in average pool length is small. The corresponding correlations for longer pools, with $L_{rif} / L_p >= 1.5$, are:

riffle: $L_p = -84.74\ L_{rif} / L_p + 145.8$ $r^2 = 0.2234$, n = 11
riffle and run: $L_p = -47.95\ L_{riru} / L_p + 126.5$ $r^2 = 0.2249$, n = 11

A single power law relationship also fits the whole data set, although it does not reflect the positive relationship between short pools and the pool-scaled length of riffles (and riffle-runs) relative to pools.

riffle: $L_{rif} / L_p = 8.5259\ L_p - 0.5617$ $r^2 = 0.3134$, n = 14
riffle and run $L_{riru} / L_p = 22.224\ L_p - 0.7384$ $r^2 = 0.3408$, n = 14

In summary, the relationship between pool-scaled riffle length versus pool length can be separated into two, nearly linear trends. In most reaches in most geographic areas, riffles are longer than pools, often much longer. However, in a few reaches in several of the geographic regions, riffles tend to be close to the length of pools, slightly longer to somewhat shorter than the pools. In this second group, riffles are generally less than about 1.5 times the length of pools.

A third comparison of the bedform dimensions is to compare the lengths of riffles (or riffle-runs) to the length of pools, when both are scaled by channel width. Supposing that the pool-riffle forms maintain the same proportions for both smaller and larger channels, as channel width increases, dimensionless ratios of all pairs of the following variables would be approximately constant: spacing of pool-riffle bedforms, channel width, pool depth, pool length, riffle length (or riffle-run length), and riffle depth. The relationship between the length of pools and riffles can be presented as in Figure 3.6c, which shows the relationship between the length of riffles and riffle-runs, scaled by channel width, versus pool length, also scaled by channel width. If all these dimensions scale in proportion together, these scaled riffle lengths would then plot along a single line, and the line would be horizontal.

The scaled riffle lengths derived from field data are shown in Figure 3.6c. In the figure, the

riffle (and riffle-run) lengths, scaled by channel width, range from about 0.29 to 3.6. The correlation lines for all riffles and all riffle-runs, scaled by channel width, at least approach horizontal lines. The correlation trends indicate that the riffle and riffle-run lengths, scaled by channel width (L_{rif} / w_c and L_{riru} / w_c), tend to fall between 1.5 to 2.5. In spite of the mild slope of the correlation line, the correlations might be interpreted as suggesting that on the average, channel-scaled riffles and riffle-runs are about 1.5 to 2.5 times the length of pools, although channel-scaled riffle (riffle-run) lengths increase somewhat faster than channel-scaled pool lengths.

However, the detail in the figure suggests otherwise. The actual plot also suggests a revised interpretation of the anomalous double-valued pattern in the relationship shown in the previous figures. The correlation lines for individual studies (shown as thin, dashed lines) in the plot (Figure 3.6c) show a series of sub-parallel, negative correlations rather than a positive correlation between pool and riffle lengths, both scaled by channel width. Each of the individual studies generally represents reaches with similar climatic, lithologic, tectonic, topographic, and land use conditions. These data indicate that riffle lengths scaled by channel width become shorter for reaches within a given region, as pool lengths scaled by channel width become longer. The plot can then be interpreted as riffle lengths, scaled by channel width, that tend to decrease as pool lengths, scaled by channel width, increase. Thus, for reaches in an individual study area, increasing elongation of pools tends to be accommodated by reducing riffle extent.

Thus, riffle length has a positive relationship with pool length (both scaled by width) between areas and the opposite relationship within an area, suggesting that the controlling factors within and between study areas are different. The controlling factor within an area does not appear to be discharge, as the riffle lengths within a study area do not clearly vary in order of downstream distance, although the interpretation is complicated by the study area descriptions

that note within study variations in some stream characteristics, including discharge.

The data also indicate that the range of variation in riffle spacing within a study area, i.e., within a region, is less than the range of variation between study areas. For all study areas, the trend line for channel-scaled riffle length ranges from about 1 to 3. Within a region, the average values differ, but the range of values is relatively constant with riffle (riffle-run) length, spanning about 1 to 2 channel widths about the trend of the correlation line for all data (e.g. from 1 to 3 channels widths, or from about 2 to 4 channel widths).

Clearly pool and riffle length may vary somewhat independently. Another plot was constructed to clarify these relationships. The riffle lengths, scaled by channel width, are plotted relative to the spacing of pools in Figure 3.7. The channel-scaled spacing ranges from 1.1 to 11, with an average of 4.1.

The riffle lengths, scaled by channel width, range from 0.29 to 3.7, with an average of 1.5. The riffle-run lengths, scaled by channel width, range from 0.40 to 3.7, with an average of 1.8. The relationship between the channel-scaled variables of riffle length and pool-riffle spacing tends to collapse into a somewhat better constrained trend when comparing the channel-scaled spacing and riffle lengths to each other. However, the difference in trends for the between-study-area, and within-study data remains. The double-valued (v-shaped) relationship is also still apparent.

Again, the correlation line (thick black line for riffles, thick gray line for riffles-runs) shows a positive relationship between the channel-scaled bedform and riffle (riffle-run) lengths. The thick, dashed, black line shows the trend that would be observed if pools and riffle-run lengths scale in proportion, in which case the riffle (riffle-run) length increases at half the rate that the spacing increases. The data points are fairly close to this 2:1 slope (spacing increasing at twice the riffle length normalized by channel width), although the correlation line, which falls below

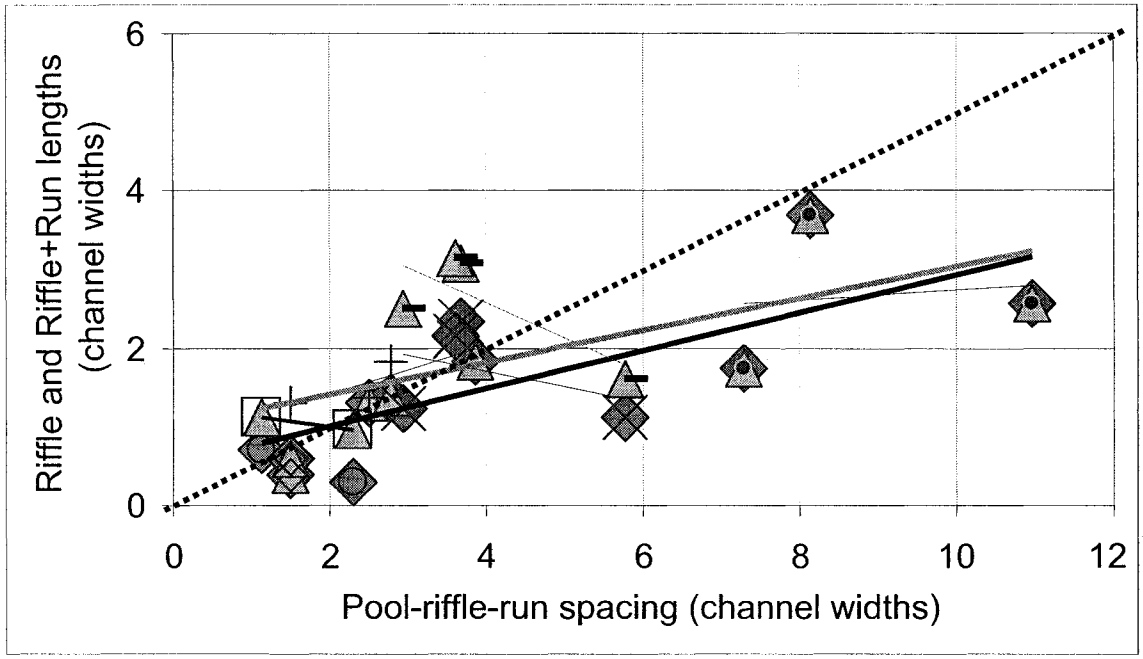

Figure 3.7. Relationships among channel width and the length of pools, riffles, riffles plus runs, and the pool-riffle cycle. For these data, the spacing of pools and riffles is defined as the sum of the lengths of riffles or riffle-runs and pool length, normalized by channel width. The spacing of pools and riffles is plotted here against the length of riffles and riffle-runs, also normalized by channel width. The data represent study areas in Montana, Oregon, coastal California, UK and British Columbia. As expected, the normalized riffle lengths and pool-riffle cycle lengths increase together. The heavy dashed line shows the trend that would be observed if pool and riffle (or riffle-run) lengths increased at equal rates, in which case the spacing would increase at twice the rate of the increase in riffle-run length. The correlation lines for all data (heavy gray line for riffles+runs, heavy black line for riffles) fall below this 2:1 line, showing a somewhat greater increase in pool than in riffle length (both normalized by channel width). However, within study areas, representing a relatively homogenous environment, the relationship tends to have the opposite sense (thin, dotted lines show correlations for individual study areas). The correlations for most individual study areas show that the riffle and riffle-run lengths decrease as the length of the pool-riffle cycle increases. Because the pool-riffle cycle is approximated here as the sum of average pool, riffle and run lengths, this indicates that riffles occupy a smaller fraction of the pool-riffle cycle as the cycle length increases.

Data symbols are:

Lere, 1984, ( ): Grant and others, 1990, ( ); Wohl and others, 1993, riffle ( ), riffle+run( ); Carling and Orr, 2002,( ); Redden and Cuthbert, 2004, riffle ( ), riffle+run ( ).

the line 2:1, indicates a proportionally larger increase in pool length, at the expense of riffle length, as bedform spacing increases. Additional data would better constrain the relationship. The correlation equations, for riffles and riffle-runs respectively, are:

$$L_{rif}/w_c = 0.240\ (L_{riru}+L_p)/w_c + 0.528 \qquad r^2 = 0.541,\ n = 14$$

$$L_{riru}/w_c = 0.202\ (L_{riru}+L_p)/w_c + 1.01 \qquad r^2 = 0.342,\ n = 14$$

The differing sense of the relationships of the between-study and within-study trends is still apparent (within-study-area correlations are shown by the thin, dashed lines). Within most of the local study areas, when the bedform is long relative to the channel width, the pools occupy more of the bedform. This preference for increasing pool length at the expense of riffle length is in accordance with the pool-riffle hypothesis suggested by Yang (1971) that minimum energy dissipation will be promoted by slope variations in the channel in which less steep, pool segments are longer than the steeper, riffle segments, resulting in reduced energy dissipation. The pattern here also suggests that the longer bedforms (relative to channel width) have a greater proportion of the channel length in pools, and less in riffles. The data reflect pool-riffle cycles in the range of about 1 to 11 channel widths. Based on a review of the data, the plotted sequence of decreasing riffle lengths within individual study areas does not represent a downstream sequence. In contrast, across diverse regions, there is a wider overall range in pool-riffle spacing, and in environments where spacing is greater, both pool and riffle lengths are greater.

In summary, it appears that pool-riffle bedform length (i.e., spacing) in a local region varies from about 1 to 11 channel widths. Pools occupy a larger fraction of the bedform, and riffles less, as the bedform length increases, for the channels evaluated here. Opposing trends are observed for individual study areas than for the set of all data. There are not enough data in the present data set to evaluate what causes such the within-study-area variations. Flume studies have demonstrated that pool length correlates with discharge (Thompson, 2002), but the observed data

trend in individual studies does not appear to represent a downstream variation in discharge. In this data compilation, the issue may be confused by temporal and spatial variations in discharge in the two studies with bifurcated rivers.

3.3.5. Effect of sediment supply on pool volume

Supply effects may also modify the relationship between pool and riffle lengths. Kirchner and others (1990) argue that supply effects are the dominant control on sediment transport, rather than adjustments in particle arrangements and textural patches. Greater sediment supply may reduce net scour and therefore decrease the size of pools. The conditions under which coarse inputs affect pool volume and frequency are poorly understood (Buffington and others 2002), but Buffington and others argue that coarse inputs may either increase or decrease pool size, by changing the entrainment threshold, or by modifying the balance between pool scour and fill as the flood wanes (Buffington and others 2002). Large sediment inputs may lead to channel widening or braiding and aggradation, substantially reducing pool volume and frequency (Buffington and others, 2002).

3.3.6. Discussion of width-to-depth relationships

Variation in channel bedform type is often related to channel slope. There is also a relationship between slope and width-to-depth (e.g., Figure 3.1b) suggesting that channel types could alternatively be related to width-to-depth. This may be a more direct relationship, based on the use of width-to-depth as a criterion for whether or not bar-pool undulations will form (e.g., Blondeaux and Seminara, 1985). The plotted data (Figure 3.1) also suggests that relative submergence correlates equally well with slope and similarly reflects bedform type.

Only two of the stream studies in the summary compiled here (Lere, 1984 and Carling and Orr, 2002) reported the channel depth data needed to determine width-to-depth ratios. Width-to-depth in the two studies ranges from 5.5 to 78. The channel widths range from 26 to 44 meters,

and widths in the two studies just overlap. In contrast, the reaches in one study were quite deep, 3.4 to 6.6 meters, and in the other depths were quite shallow, 0.44 to 0.54 meters. The plotted relationship between riffle length and width-to-depth (Figure 3.8) is clear, although the restricted data set means the results must not be considered to be reliable for prediction. The data indicate that both riffle length and channel-scaled riffle length increase with width-to-depth. The pool-scaled riffle length also decreases with channel width-to-depth, indicating that the relative dimensions of riffles and pools change as width-to-depth changes. In this data, the channel-scaled riffle length decreases as pool-scaled riffle length increases, so that both approach one channel width as width-to-depth becomes small. If pool and riffle length converge at small width-to-depth, and each becomes equal to about one channel width, this suggests that the characteristic spacing is about two channel widths for small width-to-depth. The large dataset presented by Lisle and others (2000) suggests such small width-to-depths correspond to very steep streams.

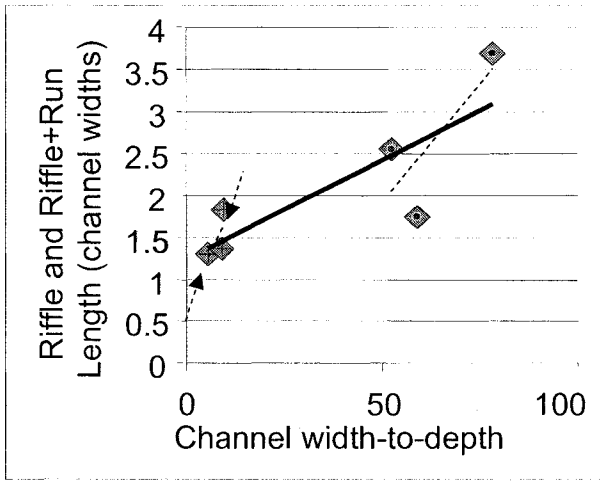

Figure 3.8. Variation of the length of riffles and pools with varying width-to-depth. An alternative possibility is that riffle length scales with channel width-to-depth. Only two of the available studies include both width and depth information. Although the data are minimal, these studies, plotted here, also suggest that the riffle length to channel width ratio is not constant as channel width varies. Data symbols are as follows:
Lere (◆); Carling and Orr (◆).

3.3.7. Variation of riffle length with channel width, slope, particle size and shear stress.

In addition to the above evaluation of riffle and pool length, the five data sets presented at the beginning of this section (Section 3.3) were used to plot relationships between riffle length and other reach characteristics, including

channel width, slope, particle size distribution, and shear stress. In spite of the relatively clear relationship between riffle length normalized by channel width and other channel dimensions, for the following, I have chosen to compare riffle lengths in meters to other channel characteristics. The variables other than riffle length were available in only some of the studies, so each of the plots has a different number of data points. Width of the particle size distribution was calculated as the graphic standard deviation, $(\phi_{84} - \phi_{16})/2$. The shear stress was calculated as $\tau = \rho g h S$ (pascals). Correlation coefficients are given in bold if they are equal to or greater than 0.3, and are listed in Table 3.5.

3.3.8. Riffle length variation with channel width

Riffle length (in meters) tends to increase as channel width increases (Figure 3.9a). A plot of the compiled data shows a dense line of points for reaches about 18 and 20 meters in width, and these data points indicate a rapid rate of increase in riffle length as the channel width increases. In wider channels, the riffle and riffle-run lengths increase more slowly with increasing channel width. In addition, the rate of increase is quite variable for the different data sets. The individual studies in the wider channels tend to show different rates of change in riffle length as channel width increases. The slope of the correlation lines for individual studies ranges from near zero to about three, thus riffle-run length increased up to about three times as fast as the channel width. The r^2 is 0.406 for the correlation of riffle-run lengths with channel width (n = 11).

3.3.9. Riffle length variation with channel slope.

Spacing is typically normalized by channel width, suggesting there may be a simple relationship between riffle length, normalized by channel width, and the channel width. That relationship is plotted in Figure 3.10.

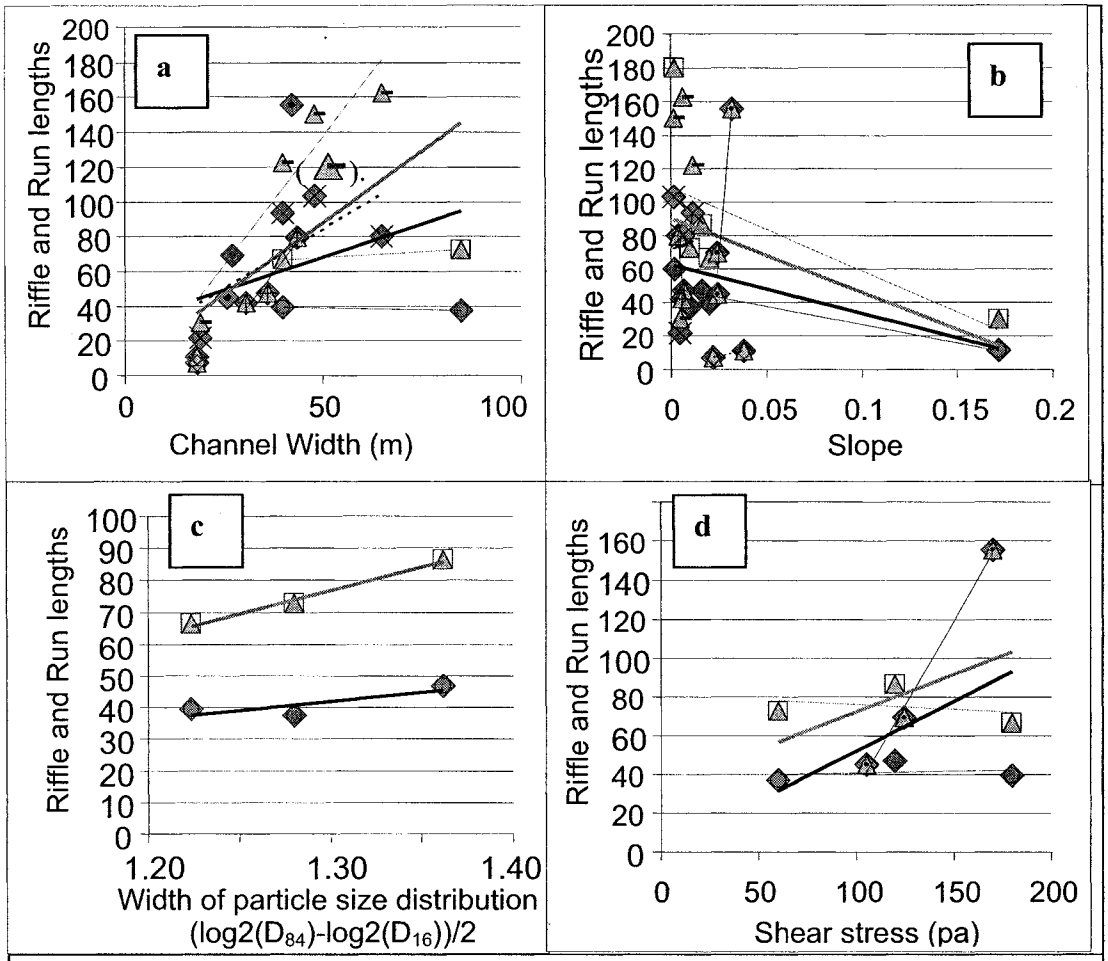

Data sources:

Lere, 1984,(◆): Grant and others, 1990 (◇); Wohl and others, 1993, riffle (◆); riffle+run (△); Carling and Orr, 2002,(◇); Redden and Cuthbert, 2004, riffle (✕), riffle+run (▲).

Figure 3.9. Variation of riffle length with varying channel width, slope, particle size distribution and mobility. (a) Riffle length increases with channel width. Riffle length appears to increase slowly in channels 18 to 19 meters in width, although this may be due to the limited range of width in these channels. Riffle length increases more rapidly for larger channels, and is more variable, showing a different degree of response in studies from different regions. (b) Riffle length shows relatively little dependence on slope at low slope. The single very steep reach shows shorter riffle-like features (possibly cascades) than other reaches. (c) Riffle length increases as sediment becomes more poorly sorted. (d) Riffle length shows a variable response as bankfull shear stress increases, indicating that riffle length is constant or increasing with shear stress and increasing sediment mobility.

*Table 3.5: Correlation of riffle length vs. width, slope, particle size distribution, and mobility**

Variables/Correlation	r^2
Channel width	
$L_{rif} = 0.7536\ w_b + 30$	$r^2 = 0.122$
$L_{riru} = 1.64\ w_b + 5.71$	**$r^2 = 0.406$**
Slope	
$L_{rif} = -291\ S + 62.8$	$r^2 = 0.091$
$L_{riru} = -441\ S + 90.3$	$r^2 = 0.102$
Width of particle size distribution	
$L_{riru} = 145\ w_p - 112$	**$r^2 = 0.987$**
$L_{rif} = 57.9\ w_p - 33.4$	**$r^2 = 0.660$**
Mobility threshold: shear stress	
$L_{rif} = 0.510\ \tau + 1.00$	$r^2 = 0.243$
$L_{riru} = 0.390\ \tau + 33.2$	$r^2 = 0.203$
Mobility threshold: discharge	
$L_{rif} = 0.0463\ Q + 10.15$	**$r^2 = 0.809$**
$L_{riru} = 0.0463\ Q + 11.60$	**$r^2 = 0.805$**

**bold typeface indicates data for correlations with r^2 values of 0.3 or more*

The relationship of riffle length to channel slope is shown in Figure 3.9b. The trend of the correlation line for riffle and riffle-run length are determined by the very steep bedforms documented in the steepest channel, which is much steeper than any of the other channels in the data set. Without that reach, there is considerable scatter, but the trend for the data on riffles is essentially constant, whereas the trend for riffle-runs is slightly decreasing:

riffle $L_{rif} = -202\ S + 61.6$, $r^2 = 0.0037$

riffle-run: $L_{riru} = -1701\ S + 107$ $r^2 = 0.121$

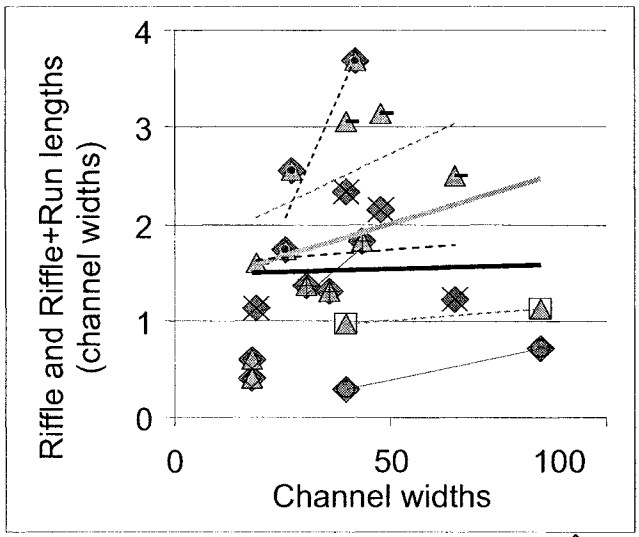

Figure 3.10. Variation of riffle and riffle-run lengths scaled by channel width, as channel width varies. The riffle data as a whole, and some of the individual data sets, have nearly constant values of riffle length scaled by particle size. However, riffle-run lengths do not scale with channel width, and several of the individual study areas have riffle lengths, scaled by channel width, that increase rapidly as channel width increases. Data symbols are as follows: Lere, 1984, ( ); Grant and others, 1990,( ); Wohl and others, 1993, riffle ( ), riffle+run ( ); Carling and Orr, 2002, ( ); Ebell and others, 2004, riffle ( ), riffle+run ( ).

The trends are not significant. Except for the Lere (1984) study, the individual data sets show a correlation trend in which riffle (riffle-run) length as slope increases is close to constant (Grant and others, 1990; Ebell and others, 2004) or somewhat decreasing (Table 3.6). The nearly constant riffle length as slope varies in several of the individual studies suggests that an additional control, or controls, determine the scale of riffles within a given study area. Which variable or variables provide this control is not known. Because riffle length and riffle spacing are related, a relationship with channel width may be important. The relationship between slope and riffle length normalized by channel width is presented in Figure 3.10. The data do not indicate any effect of slope on riffle length within study areas. Thus, these within-region variations do not reflect the indirect relationship between pool-spacing and slope that derives from the reduced

Table 3.6. Correlations of riffle length with slope for five data sets

Data set					*Correlation equation*
Riffle excluding run/glide					
Wohl and others: riffle:	L_{rif} =	-948	S	+ 57.3	$r^2 = 0.517$
Ebell and others: riffle:	L_{rif} =	449	S	+ 71.8	$r^2 = 0.0025$
Riffle or riffle-run					
Wohl and others :riffle-run:	L_{riru} =	-579	S	+ 170	$r^2 = 0.733$
Carling and Orr 2002:	L_{rif} =	-14,633	S	+ 136	$r^2 = 0.876$
Lere:	L_{rif} =	12,753	S	- 254	$r^2 = 0.956$
Ebell and others: riffle-glide:	L_{riru} =	-734	S	+ 121	$r^2 = 0.0025$
Grant and others:	L_{rif} =	226	S	+ 2.26	$r^2 = 1$

Data from: Lere, 1984 (Montana); Grant and others, 1990 (Oregon); Wohl and others, 1993 (coastal California); Carling and Orr, 2002 (UK), Ebell and others, 2004 (British Columbia, Canada).

lateral motion of particles when slopes are steep that was noted by Furbish (1998). Cross-correlations between slope and particle size as suggested by Wohl and others (1993) and Thompson (2002), or between slope and relative submergence, or width-to-depth, may still be important.

3.3.10. Riffle length variation with width of the particle size distribution.

Particle size data sufficient to determine the width of the particle size distribution are reported in only one of the studies presented here, by Wohl and others (1993). The necessary data consist of, at minimum, D_{50} and D_{84} for the channel reaches. Here D_{16} is also available. The plotted width of the particle size distribution is the graphic standard deviation, calculated here as

(ϕ_{84} - ϕ_{16})/2. The data consist of values for three reaches in one study area in coastal California, and are insufficient to determine general trends. The data indicate that riffle length increases as the width of the particle size distribution increases, both for length in meters (Figure 3.4.c) and length in channel widths (not shown). Riffle length relative to pool length (L_{rif} / L_p and L_{riru} / L_p) decreases as the sediment becomes more poorly sorted (increasing w_p, represented by the graphic standard deviation). For the three data points, the correlation between riffle length and width of

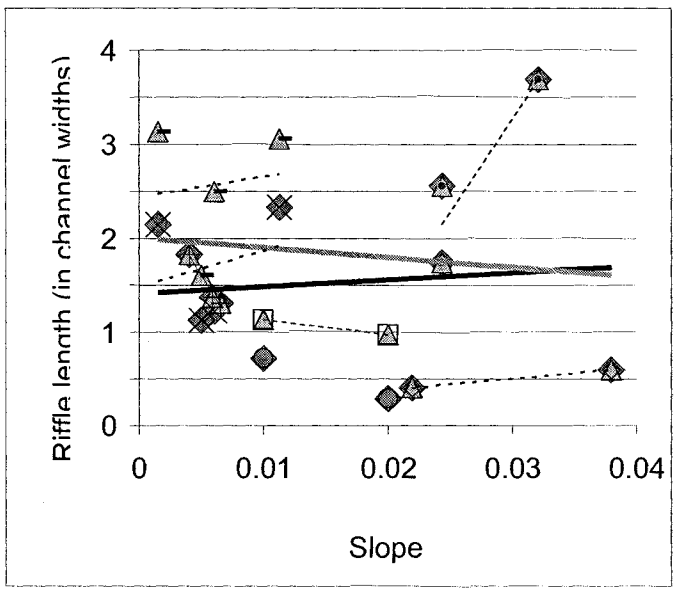

Figure 3.11 Variation in riffle and riffle-run lengths, scaled by channel width, as slope varies. Correlations of riffle (and riffle-run) lengths versus slope (thin, dashed lines) for individual data sets are nearly constant, with the exception of the Carling and Orr (2002) study.

the particle size distribution had a correlation coefficient of 0.809.

3.3.11. Riffle length variation with bankfull shear stress.

Two data sets provide data sufficient to determine of bankfull shear stress, Wohl and others (1993) and Lere (1984). Bankfull discharge estimates might be used in lieu of bankfull shear stress, and discharge data for five reaches, in the Wohl and others (1993) data set, are available. Riffle length versus bankfull shear stress is shown in Figure 3.8d. The relationship between shear stress and riffle length is variable, with one data set showing that riffle length is nearly constant with shear stress, and the other that length increases with shear stress (Figure 3.8d).

The relationship between discharge and both riffle and riffle-run length is, however, clear (Figure 3.11). Riffle and riffle-run lengths increase linearly as discharge increases. The relationship is strong, with r^2 values of 0.809 and 0.805, for five data points, for riffle and riffle-run correlations respectively. Both the length of riffles in meters, and the length of riffles in units of channel width (not shown), tend to increase with increasing discharge. The data in Figure 3.8d and 3.11 suggest that riffle length increases with shear stress and with discharge, but the data sets are too small to show how much these relationships may vary.

3.3.12. Summary of variations in riffle length.

In summary, the analysis of riffle length data in pool-riffle channels suggests that riffle length is a double value function of the length of pools. Riffles associated with small pools increase rapidly in length as pool length increases, and observed riffles are up to nearly seven times the length of pools. Riffles associated with large pools are shorter than about 1.5 times the length of the associated pools, and decrease in relative length as pool length increases. The origin of the two limbs in the pattern of the data is not known, but might be related to channel disturbance. Limited data on the width of the particle size distribution indicates that riffle length increases with width of the particle size distribution, and does so whether or not it is normalized by channel width. Insufficient data on shear stress prevent a useful correlation between shear stress and riffle length, but there is a strong correlation indicating that riffle length increases as discharge

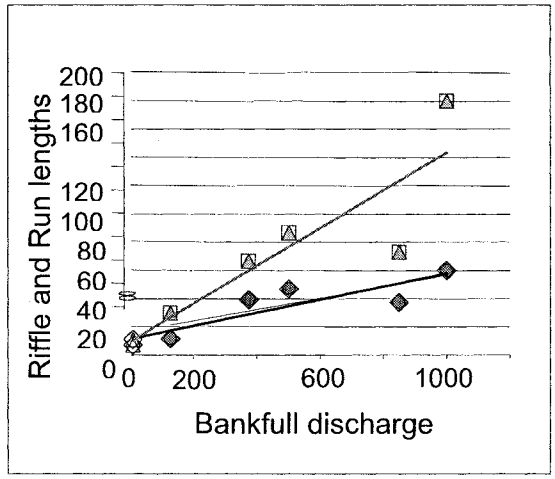

Figure 3.12. Riffle length variation with discharge. Riffle lengths clearly increase as bankfull discharge increases, and the pattern of data points shows relatively little variability.

increases. The data also indicate that when both pool and riffle lengths are normalized by channel width, riffles in a given stream system range from shorter than to longer than pools, and the pool length increases at about 3 to 5 times as fast as the riffle lengths.

The data on riffle length tend to collapse to a single relationship when the channel-scaled riffle length is plotted against pool spacing. Spacing here is defined as the sum of the average pool and riffle lengths. The channel-scaled pool-riffle spacing ranges from 1.1 to 11 with an average of 4.1 in these streams, and for the data as a whole, channel-scaled riffle length increases as channel-scaled spacing increases. However, there are contrasting trends between the full data set and the data from individual study areas. Within most individual studies, if the bedforms are long relative to the channel width, pools occupy a greater fraction of the bedform than when bedforms are short relative to the channel width.

The pattern of variation here suggests that the longer bedforms (relative to channel width) tend to have a greater proportion of the channel length in pools, and less in riffles. The r^2 is 0.406 for the correlation of riffle-run lengths with channel width ($n = 11$). Although the relationship of channel slope with riffle length (Figure 3.8b) showed no clear pattern, when riffle length is scaled by channel width, the scaled riffle lengths are essentially constant with slope within individual study areas, indicating a strong relationship among riffle length, slope and channel width (Figure 3.11). Several other factors may contribute to this relationship, because other characteristics of pool-rifle channels have been shown to correlate with slope, including particle size, width of the particle size distribution, relative submergence, and width-to-depth.

Yang hypothesized that minimum energy dissipation will be promoted by slope variations in the channel, including any longitudinal pattern of variation that differs from the straight line slope, within the constraints imposed on the channel. This observed relationship of pool and riffle lengths, with pool lengths increasing faster than riffle lengths within a given stream system,

suggests that this relationship reflects the ability of a channel to minimize energy dissipation per unit volume of water, in accordance with the pool-riffle hypothesis suggested by Yang (1971). The reverse trend when comparing different stream systems, with riffle length increasing faster than pool length, suggests some factor(s) that vary between regions limit the length of pools, more than the length of riffles. The constraint on riffle length factor does not appear to be explained by discharge variations. Restraints that vary more strongly over regional scales will include precipitation excess, and particle size distributions, among other factors.

3.2.13. Comparison of pool-riffle spacing in studies that report riffle length and the data used to illustrate pool characteristics.

For comparison to the spacing of pools based on the reaches reported in Chapter 2, pool-riffle spacing in the five studies is shown in Figure 3.12. The stream data show longer riffles when channel width increases, including the riffle length in meters and length normalized by channel width. The data show that pool-riffle spacing normalized by width increased with width, slope, shear stress and discharge. Spacing decreased with width of the particle size distribution. This compilation shows the same relationships except for variations with width.

3.4. Modeling the effect of particle interactions on the development of riffles and textural patches.

The particle interactions cellular automata, or *PICA* model, described in Chapter 1, was used as a standard of comparison to evaluate whether coarse zones in the model surfaces have length and spacing characteristics consistent with the length and spacing of riffles. The model simulates the effects of particle interactions in sediment transport in steep, gravel-to-cobble streams. The model channels represent hypothetical streams in which only particle interactions control sediment transport, so that all effects of locally-varying flow, except particle-scale variations that are inherent in particle interactions, are omitted from the model. The model was expected to be

relevant for conditions in pool-riffle and steeper channels, based on the hypothesis that development of longitudinally-differentiated channels in both pool-riffle and steeper streams is strongly influenced by particle interactions. Specifically, it was hypothesized that the size and spacing of riffle-like elements in the model will vary in the same direction as in steep, gravel-to-cobble channels. Secondly, it was also hypothesized that form variation would also be influenced by bed width, slope, particle size distribution and a measure of particle mobility, which is represented here by the critical relative particle exposure, $R_{p,c} = e/D$. The comparisons presented in the remainder of this chapter suggest that the organization of particles into textural patches or zones, such as riffles, in streams is more complex than the patterns generated in the PICA model in which sediment transport, and thus channel form and bed sediment characteristics are controlled by particle interactions.

In remainder of this chapter, the field data on the length and spacing of riffles and textural patches are compared the model simulations. The characteristics of surface particle size coarsening ('armoring'), and the degree of differentiation into riffle-like and pool-like sections are compared to stream characteristics. The data indicate that surface particle patterns and other arrangements are either more complex than those in the model, or our knowledge of how they vary is quite incomplete, or both.

3.5. Methods for evaluating model results

3.5.1. Textural patches

Textural patches were identified on the channel bed surface at the final timestep of each model run after the run evolved to a steady-state roughness. Only the area of the channel bed was evaluated, and portions of the bed that curved upward toward the banks were omitted. However,

the geometry of the channel is not rectilinear, and portions of the curve upward toward the banks are included in the area evaluated.

3.5.2. Definition of large coarse patches

It is useful to define a minimum size criterion for features that will be evaluated as textural patches. The coarse patches were identified and classified in a method analogous to that for identifying local deeps and pools in the model results (*see* Chapter 1). The primary difference is that equally-spaced cutoffs were used to define patches.

In this method, each patch was delineated as a collection of connected cells for which the particle size in the cell exceeds the particle size in the coarsest one-third of the particle sizes in the area being evaluated. The area occupied by a given patch may surround other cells not characterized by coarse particles, but the non-cells are not considered part of the patch. The area of the patch is equal to the area of the coarse cells in the patch. Connected cells are arbitrarily defined as those that share a face, not just a corner. The patch length scale is calculated as the square root of the area of the patch. Patch length scales presented for each run are the average length scale for all large patches. The following discussion of particle size patches in the model results focuses on these coarse patches. Fine patches were extracted from some runs. They have patch size distributions visually similar to the size distributions of coarse patches, and were not otherwise evaluated.

A criterion analogous to the criterion used to delineate pools was adopted for large patches. There is no recognized size criterion for defining significant textural patches. The patches are distinguished from isolated areas where one or a few cells are coarse, by designating coarse patches only where the patch length scale is at least one-half the bed width.

The exception is that the runs in the series with varying width of the particle size distribution have between three and nine particle size classes, each class one ϕ in width. Most runs have particle size classes ranging from -8 to -1 ϕ. Runs in the series where the width of the particle size distribution is varied ranged from -9 to -1 ϕ (512 to 2 mm), to the narrowest range of -8 to -6 ϕ (256 to 64 mm classes). The full range of sizes considered in all runs spans from -9 to -1 ϕ.

In general, there are 8 particle size classes, one ϕ in width, in the model sediment, and the size of coarse particle patches includes all cells where the particles are as large or larger than the largest size in the coarsest one-third of the bed surface. With varying numbers of size classes, the sizes in the coarsest one-third of the distribution may be biased by the position of the size class boundary.

3.5.3. Comparisons of particle size at pools and large, coarse patches

In the model, local slope is quite variable, so it is difficult to identify locally steep segments that might correspond to riffles or incipient riffles. The simplest alternative for identifying areas analogous to riffles is to present particle size distributions for the identified pool areas, and contrast those with the particle size distribution in non-pool areas. That approach is taken here.

Particle size distributions for all deep areas are presented. These are contrasted to all non-deep areas, all pool areas, and all non-pool areas. Finally, the degree of overlap between areas of the bed that are pools, and large, coarse patches on the bed are presented. These are obtained by plotting the fraction of the bed area that is designated as a pool, the fraction that is designated as a large, coarse patch, and the fraction of the bed that is both a pool and a large coarse patch. For comparison, the area fractions of the bed that are deep are contrasted to areas that are coarse.

3.6. Results

3.6.1. Armoring of the bed surface

Coarsening of the bed surface, also termed armoring, occurs early during the model runs. The particle sizes adjust rapidly at first, and at a decreasing rate throughout a run. The coarsest several size classes adjust to the greatest degree, and the multiple intermediate to fine sizes each adjust to a lesser degree. The rapid initial adjustment is consistent with results from flume studies that documented particle patterns (Hassan and Church, 2000; Pender and others, 2001). Hassan and Church noted that coarsening occurred within hours during their flume study.

After the initial coarsening, a continuing slow increase in the coarse particle fractions, and a slow decrease in the finer particle fractions, is apparent in the model runs. This slow coarsening is slight, but appears to continue throughout the model run, even after the surface roughness stabilizes. In the model runs, which typically have eight particle size classes, surface coarsening is accompanied by size adjustments in all other particle size classes, i.e., by a decrease in the fraction of finest particle sizes, and an intermediate degree of adjustment, from decreasing to increasing particle size, in the intermediate size classes. This slow long-term adjustment has not been documented in streams or flume studies to my knowledge.

Wilcock and Detemple (2001) noted that armoring appears to be ubiquitous in recirculating flumes. In contrast, in sediment-feed flumes, armor layers tend to form at low transport rates and vanish at large transport rates (Wilcock and Detemple, 2001). The model is constructed with a cyclic boundary condition at the upstream and downstream ends of the model reach, thus having sediment supply characteristics comparable to feed in a recirculating flume. Based on the above, armoring is then expected to develop.

Although bed surface adjustment of the finer portion of the particle size distribution is rarely described in as much detail as coarsening, a decrease in the fraction of fines necessarily

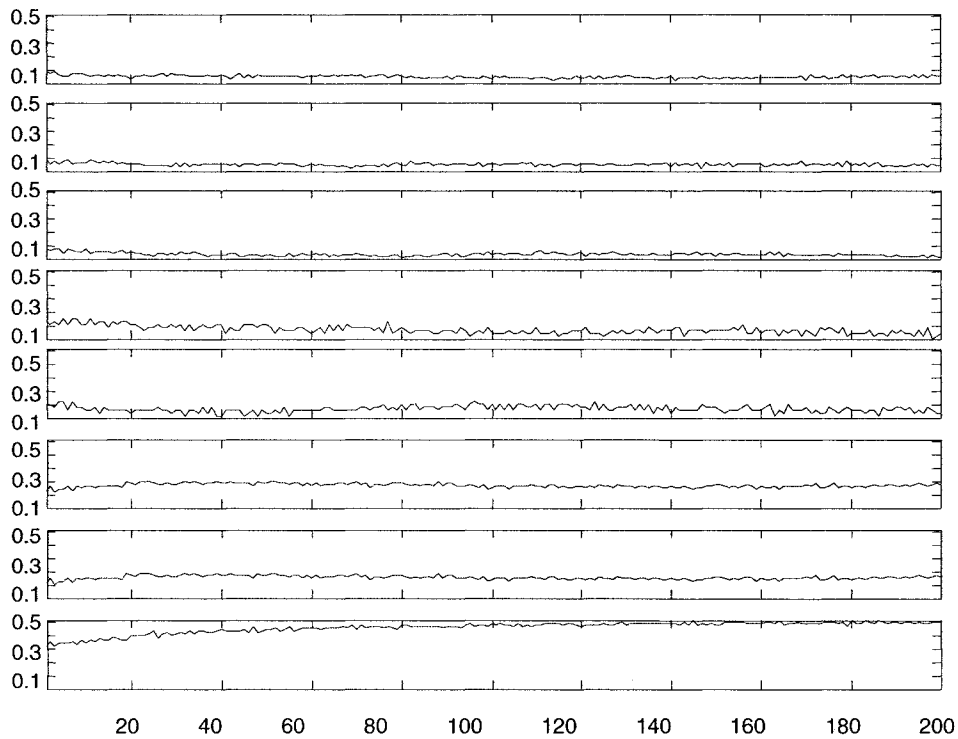

Figure 3.1.4.. Initial coarsening of the channel bed. The evolution of particle sizes at the bed is illustrated by these time series showing the fraction of the area of the bed occupied by particles of each particle size class. The particle size classes range from -8 to -1 phi (256 to 2 mm), and each size class is one phi in width. The finest size class is shown in the top panel, the smallest size class in the bottom panel. The coarsest particles occupy the largest fraction of the area of the bed. The coarsest sizes coarsen rapidly at first, but a slow adjustment is visible throughout most or all of the run. The fraction of the bed in the finer half of the sediment appears to stabilize sooner, after about 30 time steps.

accompanies an increase in the coarse fractions. In this model, the surficial particles include all particles that are exposed at the surface, and no subsurface particles. Thus, coarsening of the surficial particle size distribution necessarily results in a reduced fraction of fine particles at thesurface. In stream studies, adjustment of the finer fractions has been attributed, in part, to fines dropping downward between the interstices of larger particles (e.g., Wilcock and McArdell, 1993). That mechanism does not occur in the model. Instead, coarsening of the model surface occurs only by size-selective processes of transport, and may include a non-random mobilization of particles by size, as well as a bias toward burial of finer particles by coarser particles.

To better characterize the process, it necessary to describe the sequence of events in some detail. At the start of a run, the sediment that is transported contains more coarse particles than a random entrainment of particles would include, because coarse particles on the bed tend to shelter fines, reducing the mobility of fines (reducing the relative particle exposure). The initial high exposure of coarse particles is a consequence of the model initial conditions in which all particles were initially centered on the sloping plane used as the initial channel bed. This initial arrangement, however, seems a reasonable, although simplified, approximation of sediment structure in streams.

Next, coarsening of the bed begins as soon as transport begins, and continues throughout the adjustment phase, although it is more rapid initially, and quite slow during most of the adjustment phase. During this phase, the observed coarsening requires that the size fractions in transport are biased toward the coarser particles, so that the sediment size fractions on the bed are biased toward the finer particles. This means that, when coarser particles are deposited, there is a bias those particles being deposited covering finer particles. In other words, the frequency of occurrence of a coarse particle being deposited on finer particles is greater than would occur in a random arrangement of particles combined with random selection of particle sizes for transport,

combined with the particle size covered being randomly selected. The structuring of the particle surface, and the importance of particle exposure in transport of individual particles, suggests that spatial distribution of particle exposure for each of the particle sizes is not random. I am not aware of data on whether depositional sites are also non-random in streams.

Given the initial occurrence of well exposed particles in the model, and that entrainment depends on relative particle exposure, the probability of mobilization of the particle size fractions then evolves over time. In general, this process steadily increases the fraction of fine particles that are buried, and increases the surface fraction of coarse particles that are exposed. However, there are exceptions; in some runs either fine or intermediate size particles come to dominate some areas of the bed. The particle size distributions and these exceptions are described below.

The result in the model system is that finer sizes tend to become buried, coarser sizes become enhanced at the surface, and the degree of adjustment varies smoothly from one size class to the next, with one exception. There is usually an inflection point between the coarse and fine fractions of the sediment in the model runs. Although slipping of fines into the interstices between coarse particles undoubtedly occurs in streams, the above mixing process, driven by a bias in stability of coarse and fine particles under continuing motion of the particles, is sufficient to result in a reduction of surface fines in gravel-to-cobble streams, and modification of the entire particle size distribution.

Hassan and Church (2000) noted, in addition to the initial coarsening they documented, that resistance to flow, which reflects surface roughness, continued to adjust for many hours. They attributed the additional roughening to structuring of surface particle arrangements. Such additional roughening may result from at least two component effects, including the effect of enhanced vertical exposure of some particles sizes, and the enhanced areal exposure of the less mobile, larger particles (Parker and Klingeman, 1982).

The model results and the review of observations from streams suggest that coarsening in the model is characterized by (a) an increase in the frequency of stable structural arrangements, which may be described as groupings in which the central particles are stable because the surrounding particles prevent their motion by even an oblique downstream movement, and (b) increasing surface particle size in two phases: a rapid initial coarsening, followed by a slow increase in coarse particle size patches over the long-term. There may also be additional effects not identified here, that result from particle interactions. In streams, additional mechanisms that are not controlled by particle interactions may also be expected. The rapid initial coarsening has been reported by Hassan and others (2000). To my knowledge a phase of slow coarsening has not been documented.

3.6.2 Lateral variation in particle size

Particle size in the model results was averaged for points on two downstream sections near the centerline and for two pairs of lines near the transition from bed to banks, for several model runs. Particle size was distinctly larger near the banks. Similar coarsening at the outside margins of the bed was documented in the field by Nikora and Goring (2000) (*see* Section 3.1.4).

3.6.3. Modeled coarse patches as bed width varies

In the bed width variation series, the length scale of coarse patches (nominal, in meters) decreases as the bed width increases (Figure 3.14a), with an r^2 of 0.840 ($n = 6$). Patch lengths range from 1.1 to 1.8 meters. The number of cells at the threshold for defining a patch (a pool-sized patch) ranges from 12 to 36 as the bed width varies, corresponding to a range of minimum length scales from 0.9 to 1.5 nominal meters in runs of the series. The largest patch observed was 49 cells, in a wide run (Run 5). The first three runs had five, four and three pool-size patches, respectively. The last two runs each had one pool-sized patch. The spatial patterns in particle size formed in the bed width variation runs are illustrated in four-color, gray-scale images in Figure

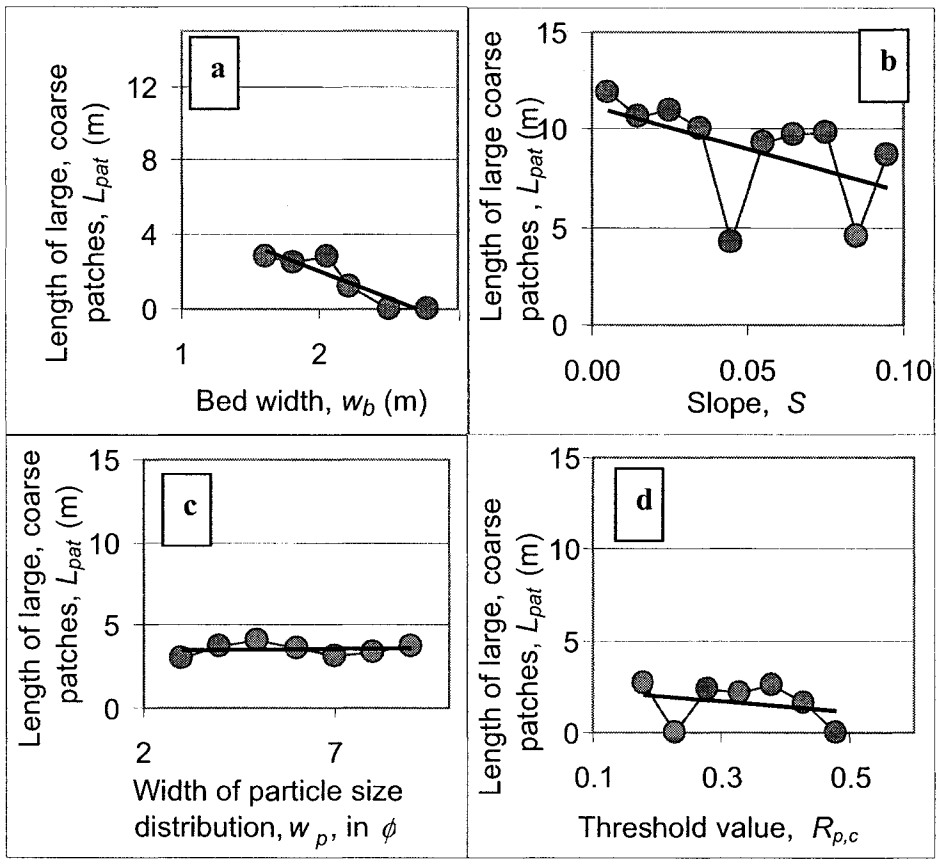

Figure 3.15. Variation in the length of large, coarse patches as width, slope, width of the particle size distribution and mobility threshold vary. (a) Large, coarse patches decrease in size as the width of the channel bed decreases. In the two widest channels the length of patches was always less than the channel width. (b) The length of large coarse patches decreases with slope. (c) The length of large coarse patches is constant as particle sorting varies. (d) The length of large coarse patches decreases as the mobility increases (a lower $R_{p,c}$ threshold for motion).

3.15. These images represent reaches in which the bed width varies from seven to twelve cells (nominally 1.8 to 3.1 meters). The images appear to show a reticulate pattern in particle size, not unlike the pattern described by Hassan and Church (2000) based on flume runs. However, particle size arrangements in the modeled bed surfaces are generally not statistically distinguishable from a spatially random distribution.

The distributions of coarse patch length for each run of the bed width variation series are presented in Figure 3.16. The size classes are logarithmic classes, obtained as the log (base 2) of the patch length in meters. The distribution of patch sizes for each run is shown, together with the correlation line for one of the runs, with an intermediate value of the variation variable. This correlation line, for a bed width of ten cells (2.5 m) (Run 4), provides a reference line for comparing the plots. The runs generally have a reduced number of patches of small size, a peak number in the second size class (with a length scale of one-half meter), and decreasing numbers at larger sizes. This can be related to the coarsening of the bed, or armoring. Coarsening acts to limit the number of small patches, because increasing the fraction of coarse particles increases the likelihood that a given coarse cell will be adjacent to another coarse cell. Runs 4 and 5 are exceptions, having a continuously decreasing number of patches in each size class. Characteristics of patches in the bed width variation series are presented in Table 3.7 and summarized in Table 3.8. The spacing of coarse patches varies in the opposite direction as patch length. Spacing tends to increase with bed width ($r^2 = 0.552$, n=6) (Table 3.8, Figure 3.17a). Thus, the correlation between patch spacing and bed width necessarily has the opposite sense from the correlation of patch length with bed width, but are otherwise similar, in this and all runs.

Bed width also adjusts during the runs. The correlation between initial and final bed width in the bed-width variation series is given by $w_{b,f} = 0.912\ w_{b,i} - 0.212$, $r^2 = 0.994$, where $w_{b,f}$, is the

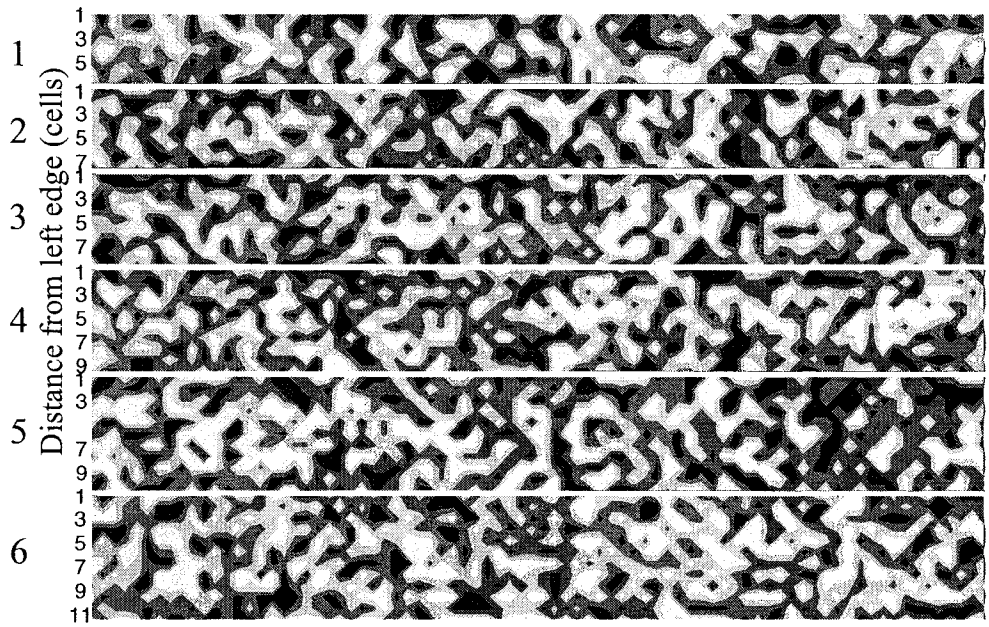

Figure 3.16. Spatial pattern of particle size in the bed width variation series. Particle sizes in the cells of the model grid are shown in this gray-scale plot (four shades). Particle size patterns appear to form a reticulate pattern, but spatial analysis indicates the pattern is random.

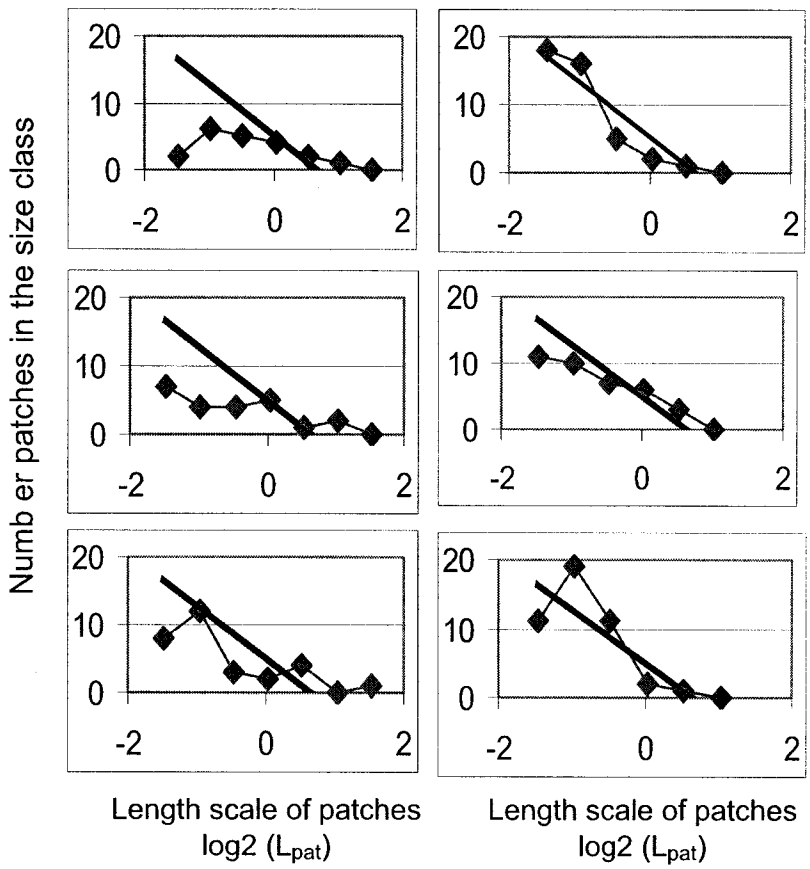

Figure 3.1,7. Number of coarse patches in runs of the bed width variation series. The bed widths in the runs ranged from 7 to 12 cells, nominally 1.8 to 3.1 meters. Classes are a log (base 2) scale based on patch length in meters.

Table 3.7. Textural patch characteristics in the bed-width variation series

Length scale cutoff for a pool (m): 0.9 m to 1.5
Area cutoff for a pool (cells): varies: 12 to 36 cells
Textural patches, maximum observed length scale: 1.8 m (7 cells)
Ratio of scales textural patches to pool criterion : 202%
Number of patches as large as pools: 1 to 5 in the runs
Reach length: 20.1 m (80 cells)
Bed width (initial and final): 1.8 to 3.1 m (7 to 12 cells)

Run	*Bed Width w_b (m)*	*Maximum coarse patch (cells)*	*(nominal area, m^2)*	*Length scale of largest patches (nominal length, m)*
1	0.68	37	2.4	1.6
2	0.72	38	2.5	1.6
3	0.77	49	3.2	1.8
4	0.81	23	1.5	1.2
5	0.85	21	1.4	1.2
6	0.89	18	1.2	1.1

final width and is $w_{b,i}$ is the initial width. The final width is slightly less than the initial width, and the reduction is greater for wider beds.

The absolute difference between the initial and final width is also be influenced by the initial conditions. The initial widths are constant along the length of the model, and are unambiguously defined for the initial trapezoidal channel form. As the channel evolves, the outside edges of the bed become scoured out, and the bed widens. As the bed form changes, the sediment removed from the banks covers the bed. If the sediment eroded were to be equally spread across the bed, it would slightly raise the average elevation of the bed. Because the banks are farther apart at higher elevation, this results in a small width increase. Thus, the width increase due to scouring will be slightly less in a wider channel, where a greater volume of sediment is needed to raise the bed elevation. Alternatively, if the sediment is not equally spread across the bed, it will in part form a slope that bridges between the original banks and bed. The width of channel will then also depend on how steeply this bridging sediment surface slopes. Because the width of the bed extracted from the model was based on finding the most abrupt change in slope near the bed, the extracted width will also depend on random variations in local height due to local variations in particle size. The final widths extracted from the model show that the width is narrower in the final configuration, attributable to formation of bridging slopes. This implies formation of a bridge between the former banks and bed, with the maximum change in curvature relatively low on the channel banks. Also, the observed width increase is slightly less in wider channels, which may be attributed to similar amounts of eroded sediment raising the bed to elevations where the width of between the banks is greater.

3.6.4. Textural patches as slope varies

Initial channel slope varied from 0.005 to 0.095 in the runs of the slope variation series. Characteristics of the stable channel in the slope variation series are summarized in Table 3.9.

Table 3.8: Correlations of channel width, slope, particle size and mobility with patch length and patch spacing (relative to final width) in the PICA model

variable	*Correlation*				r^2
Length					
Width	L_{pat} =	- 2.79	w_b	+ 7.57	$r^2 = 0.840$
Slope	L_{pat} =	- 44.3	S	+ 11.2	$r^2 = 0.270$
Slope, excluding outliers					
	L_{pat} =	-29.04	S	+ 11.5	$r^2 = 0.806$
Particle size distribution width					
	L_{pat} =	0.0184	w_p	+ 3.39	$r^2 = 0.012$ (*constant*)
Particle mobility:	L_{pat} =	- 3.22	R_{pc}	+ 2.68	$r^2 = 0.090$
Particle mobility: excluding zeros:					
	L_{pat} =	- 3.03	R_{pc}	+ 3.23	$r^2 = 0.456$
Spacing (relative to final channel width)					
Width	$\lambda/w_{b,f}$ =	5.12	w_p	- 5.47	$r^2 = 0.552$
Slope	$\lambda/w_{b,f}$ =	49.3	S	+ 2.72	$r^2 = 0.133$
Slope, excluding outliers					
	$\lambda/w_{b,f}$ =	16.9	S	+ 2.50	$r^2 = 0.613$
Particle size distribution width					
	$\lambda/w_{b,f}$ =	0.130	w_p	+ 0.9	$r^2 = 0.381$
Particle mobility	$\lambda/w_{b,f}$ =	23.4	R_{pc}	- 2.39	$r^2 = 0.360$

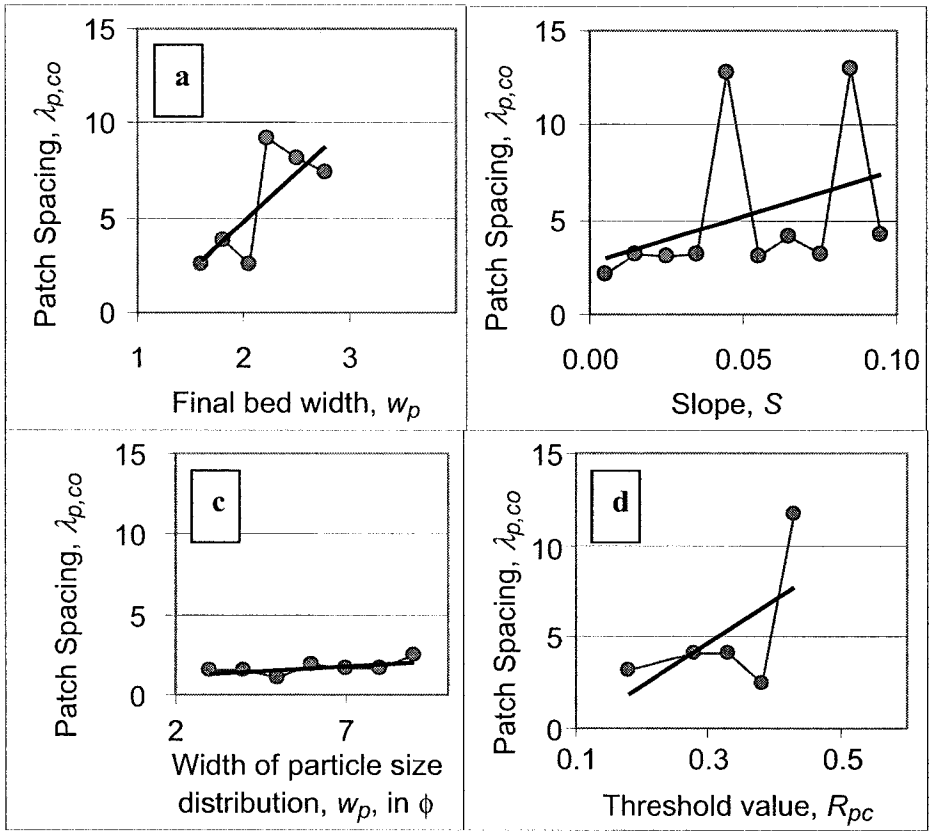

Figure 3.18. Variation in the spacing of large, coarse patches as bed width, slope, particle size distribution and mobility threshold vary. Large patches have a length scale equal to at least channel width. The spacing was determined as the number of large patches divided by the reach length. The relative spacing is the spacing divided by the final channel width. (a) Patch spacing tends to increase as the bed width increases. (b) Patch spacing increases with slope. (c) Patch spacing is nearly constant to slightly increasing as the width of the particle size distribution increases. (d) Patch spacing increases as the threshold for motion increases, and mobility decreases.

There is a weak tendency for an increase in the number of small, 2-cell deeps, and a decrease in the size of the largest pool as the bed slope increases, results from the different techniques used to measure the bed width in the initial trapezoidal and final, scoured channel form in the model. However, the tendencies are not significant. There is also a weak tendency for bed width to increase as slope increases. This tendency is stronger than those for the size characteristics of patches, but is not statistically significant.

The length scale of patches in the slope variation series decreases with increasing slope (Figure 3.14b). The range of patch lengths is 1.1 to 1.9 nominal meters. The minimum area to define a patch is 16 cells, or 1 meter. The largest patch in the run, 53 cells, has a nominal length of 3.7 meters. The number of patches in the ten runs was greatest in the first run, with 6 patches, otherwise typically 4 patches, and 3 patches in runs 7 and 10. Slope in these runs varied from 0.005 to 0.095. The correlation equation for patch length scale versus slope has a low r^2 value of 0.270. The correlation has a low r^2 because two of the ten runs deviate significantly from the otherwise clear trend indicated by other runs (Figure 3.14a). It is not clear why these two runs differ from the others in the series. Without the two outliers, the r^2 is 0.806 ($n = 8$). The trend of in patch spacing is opposite that of patch length, but the correlations are otherwise similar in detail.

The size of patches is much greater in the slope series than in any of the other series, with a nominal length scale of more than 10 meters, versus less than 5 meters in each of the other series. It is not clear why this occurs. The two anomalous runs in this series are also less than 5 meters in length scale, similar to patch length in the other runs. In these variation series, the spacing of patches is more variable than the length scale of the patches, making it difficult to

Table 3.9. Textural patch characteristics in the slope variation series

Length scale cutoff for a pool 4 cells, 1 (m)
Area cutoff for a pool (cells): varies: 16 cells
Textural patches, maximum observed length scale: 7.28 cells; 1.9 m
Ratio of scales textural patches to pool criterion : 202%
Number of patches as large as pools: 1 to 6 in the runs
Reach length: 23 m (90 cells)
Bed width, initial : 6 cells, 1.5 m
Bed width, final active: 6.9 to 7.3 cells; 1.8 to 1.9 m
Bed width, final, form 14.1 to 14.8 cells, 3.6 - 3.8 m
Bed width, evaluated: 8 cells, 2.0 m

Run	*Slope*	*Maximum coarse patch*		*Length scale of largest patches*
		(cells)	*(nominal area, m^2)*	*(nominal length, m)*
1	0.005	33	2.2	1.5
2	0.015	51	3.3	1.8
3	0.025	53	3.5	1.9
4	0.035	48	3.1	1.8
5	0.045	18	1.2	1.1
6	0.055	29	1.9	1.4
7	0.065	39	2.6	1.6
8	0.075	28	1.8	1.4
9	0.085	21	1.4	1.2
10	0.095	34	2.2	1.5

relate this greater patch size to patterns in spacing. The greater variability in patch length, relative to the variability in spacing appears to relate to differences in bed width among the runs.

3.6.5. Textural patches as the particle size distribution width varies

There is no trend in patch length scale in the runs with increasing content of fines, i.e., with increasing width of the particle size distribution ($r^2 = 0.012$, $n = 7$). Patch lengths in these runs range from to 1.9 to 0.85 m, with a minimum of 36 cells to define a coarse patch, nominally 0.63 meters. There are 13 patches in the third run, 10 in the second run, nine in the first and the last

two runs, seven in the fourth run, and eight in the fifth run. The number of ϕ-size classes, each one ϕ in width, was varied from 3 to 9 classes in the model runs. The maximum particle size was 256 mm in all runs. Patch characteristics in the particle size distribution variation series are summarized in Table 3.10. There is also minimal variation in the number of small, 2-cell patches and the size of the largest patch as width of the particle size distribution varies. Patch spacing shows a minor increase ($r^2 = 0.381$) as the width of the particle size distribution increases. There is very little variation about the trend. For comparison, the summary of stream data also indicates that riffle lengths increase, and one of two studies of textural patches indicate patch lengths increase with width of the particle size distribution. Flume studies that used bimodal sand and gravel sediment similarly found that increasing fines content resulted in longer patches (Iseya and Ikeda, 1987).

The final active bed width clearly depends on the width of the size distribution ($w_b = 0.122 w_p + 6.09$, $r^2 = 0.952$). Bed width increases linearly, from 6.5 to 7.1 nominal meters, with increase in the width of the size distribution.

3.6.6. Textural patches as sediment mobility varies

The average patch length scale in the threshold variation series decreases as the threshold increases (mobility decreases) with an $r^2 = 0.456$ excluding the zeros shown in the plot ($r^2 = 0.090$ including the zero values for runs with no large patches). The variation in the average length scale of patches in the threshold variation series is shown in Figure 3.14d. No patches as large as the pool-size criterion were found in the second run and in the last run. The patches ranged from 0.3 to 2.7 nominal meters. The size cutoff for defining a large patch was 16 cells for the first 5 runs, and 25 for the final 2 runs. The cutoff was higher for the last two runs because the bed was wider. The cutoff is equivalent to patches with length scales of 2.0 to 2.5 meters. The number of large patches was 4, 0, 3, 3, 5, 1, and 0.

Table 3.10. Textural patch characteristics as the number of particle size classes increases

Length scale cutoff for a pool: 3 cells (nominally 0.75 m)
Area cutoff for a pool: 9 cells
Textural patches, maximum observed length scale: 7.4 cells (nominally 2.0 m)
Ratio of scales: largest patch to pool criterion: 247%
Number of patches as large as pools: 5 to13 in the runs
Reach length: 90 cells (nominally 23 m)
Bed width, initial : 5 cells (nominally 1.3 m)
Bed width, final active: 6.5 to 7.1 cells; 1.7 to 1.8 m
Bed width, final, form 12 to 15 cells (nominally 3.1 - 3.8 m)
Bed width, evaluated: 8 cells (nominally 2.0 m)

Run	*Number of particle size classes*	*Maximum coarse patch (cells)*	*(nominal area, m^2)*	*Length scale of largest patches (nominal length, m)*
1	3	18	1.2	1.1
2	4	44	2.9	1.7
3	5	31	2.0	1.4
4	6	24	1.6	1.3
5	7	11	0.7	0.8
6	8	17	1.1	1.1
7	9	55	3.6	1.9

Spatial arrangement of in particle size in the threshold variation series are shown as gray-scale plots in Figure 3.18. This series has the greatest variation in patch length scale of the four series. A pattern of large patches, shown in the lightest tone, can be seen in the gray scale images in the first few runs of this series, in which the sediment is the most mobile. The threshold of relative particle exposure, $R_{p,c}$ for these runs was varied from 0.18 to 0.48 in the seven runs. Patterns of relative particle exposure for the threshold variation series are shown in Figure 3.19.

The patch size distributions of coarse textural patches for these runs are presented in Figure 3.20. Distributions of the number of coarse patches of all sizes, in $\log_2$ size classes, are shown in

individual plots for each run. A reference correlation line is shown on each of these plots, the correlation for the number of patches in the run at an intermediate threshold value of $R_{p,c} = 0.33$.

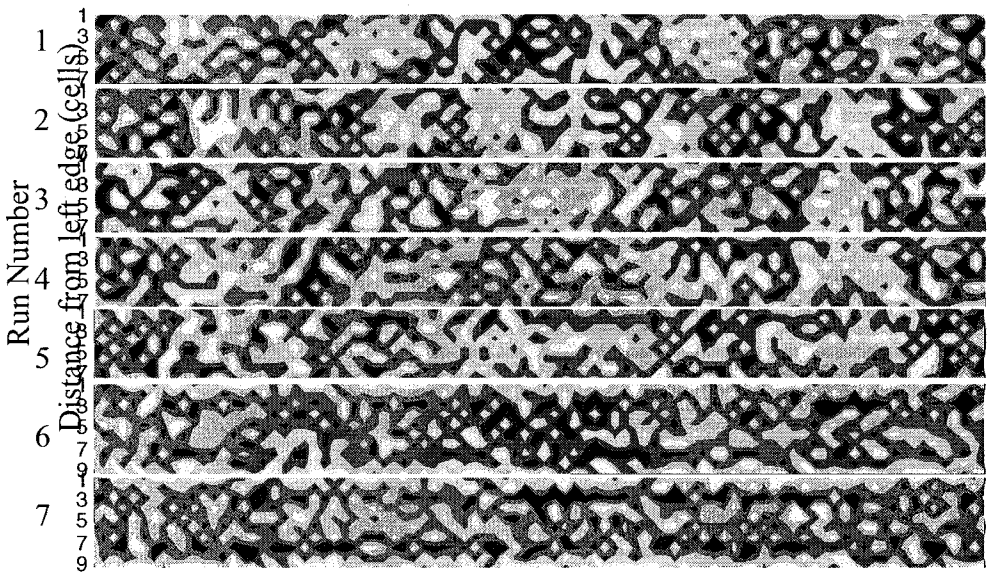

Figure 3.19. Pattern of relative particle exposure in the threshold variation series. The relative particle exposure in the threshold variation series shows a variation in the pattern from Run 1 through Run 7. Large connected areas with relatively small relative particle exposure are apparent in the early runs, with a lower threshold (greater particle mobility). There is also spatial differentiation within the channel bed. Areas with high relative particle exposure are more common toward the margins of the bed, and smaller relative particle exposure occurs toward the center of the bed. However, most of the surfaces did not constitute statistically significant spatial patterns. The bed width is eight cells in the upper five panels, and ten cells in the lower two panels, giving nominal bed widths of 2 to 2.5 meters.

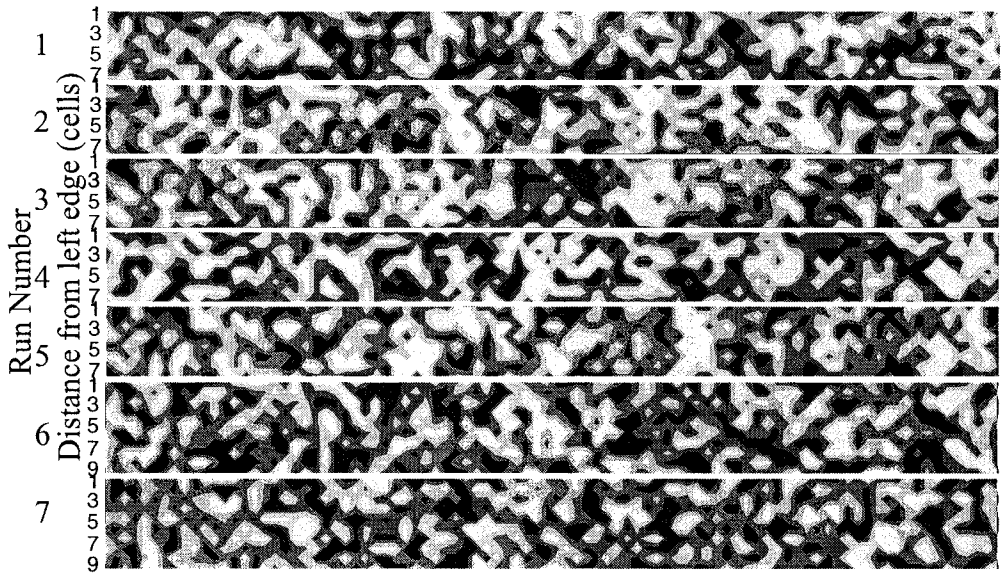

Figure 3.20. Particle size patterns on the bed surface in the threshold variation series. Runs 1 through 7 of the bed width variation series. Bed widths given are the evaluated bed width, and range from 8 to 12 cells (nominally 2.05 to 3.07 meters) The grid widths, from top to bottom, are 8, 10, 10, 10, and 12 cells. The gray-scale plots illustrate four particle size classes, each 2 ϕ in width, as four shades of gray.

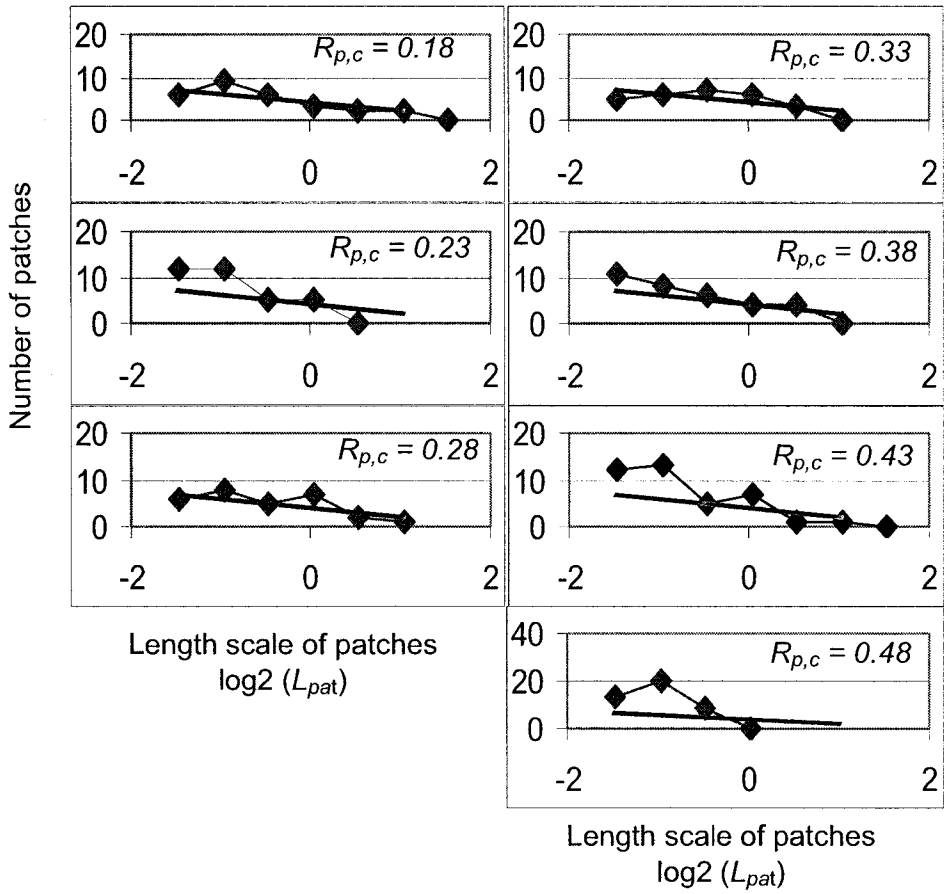

Figure 3.21. Distribution of patch sizes in the threshold variation series. The number of patches in $\log_2$ size classes for patch size classes for the seven runs of the threshold variation series. Note that the scale on the final run is twice the scale on the previous runs.

The correlation line provides a visual reference for the comparison of the plots. The plots are similar to the analogous plots presented for the bed width variation series, but the variation in most runs is subdued compared to that series. The last run in this series is shown with a different vertical scale in the figure. This run, with the lowest particle mobility, has many more relatively small coarse patches than any of the other runs. There are 20 patches in the second size class in this run, compared to a maximum of 12 in the other runs.

The average patch lengths in the series decrease as the threshold increases (mobility decreases). The second and last runs have no large coarse patches. A correlation that includes these zeros has a very low r^2 (0.090). Excluding these zeros, the correlation equation is:

$$L_{pat} = -3.027\, R_{p,c} + 3.23 \quad (r^2 = 456,\ n = 5).$$

Conversely, the number of fine textural patches increases with decreasing mobility. The length scale of fine patches also increases:

$$L_{pat,f} = -1.70\, R_{p,c} + 1.73 \ (r^2 = 0.724,\ n = 7).$$

In addition, the final width of the channel bed is closely related to mobility, and increases as the threshold increases. The correlation is $w_b = 0.581\, R_{p,c} + 1.70$, $r^2 = 0.90$. Additional run and patch characteristics are summarized in Table 3.12.

Where particle interactions are the dominant control on particle mobility, the number and size of the large patches, of both coarse and fine texture, are likely to decrease as the threshold increases (sediment mobility decreases). Variations in the length scale of fine and coarse patches have a similar relationship to mobility, and large patches of all textures tend to be more common when the threshold is low (mobility is high), within the range of mobility evaluated here. A pattern with a few large patches at a low threshold (high mobility), gives way to a pattern with more small patches, for the range of mobility modeled here. It also appears that the stable state bed width depends on mobility, and channels with more mobile sediment tend to be wider.

Table 3.11. Particle patterns with decreasing mobility as the threshold value increases

Summary data:
Length scale cutoff for a pool (m): 1.4 m
Area cutoff for a pool (cells): 32 cells
Textural patches, maximum observed length scale: 6 cells; 1.6 m
Ratio of scales of maximum textural patch to pool criterion: 113 %
Patches as large as pools: 0 to 5 in the runs
Reach length: 23 m
Bed width: 8 to 10 cells; 2 to 2.5 m

Run	*Mobility Threshold* $R_{p,c}$	*Maximum patch size (cells)*	*(nominal area, m^2)*	*Length scale of largest patches* (L_{co}, *nominal length, m)*
1	0.18	38	2.5	1.6
2	0.23	23	1.5	1.2
3	0.28	19	1.2	1.1
4	0.33	22	1.4	1.2
5	0.38	22	1.4	1.2
6	0.43	13	0.9	0.9
7	0.48	14	0.9	1.0

3.6.7. Discussion of model results on coarse patches

The linear correlations of patch length as the bed width, slope, width of the particle size distribution and relative particle exposure (inversely related to dimensionless critical shear stress), suggest that requirements for the development of large coarse patches include any of the following: (a) a high relative particle exposure threshold (moderate to high mobility) within the range evaluated here, (b) narrower beds, and (c) a lower, rather than higher, slope in the range from 0.005 to 0.105. The model results show a weak influence of the width of the particle size distribution on patch length.

These trends may be compared to the lengths of pools in the model. The length of model pools and patches vary inversely, i.e., pool length increases as the length of the large, coarse patches decreases. An opposing relationship also occurs as the threshold varies. As slope increases, the patch size decreases and pool size is nearly constant. The relationship as more fines are added to the particle size distribution, giving a greater width of the particle size distribution, s indicates that both pool and large coarse patch lengths vary relatively little with the particle size distribution increase. However, the variation in spacing as the distribution widens is significant.

These variations indicate that pool length and coarse patch length vary independently. The data show that both pool and coarse patch length vary with bed width and with the threshold, and coarse patch length varies with slope. The independence of the variation, although resulting from the same transport events, indicate that particle interactions, in which particle size, particle exposure, and bed surface structure combine to determine transport, suggests that the transport process involves the interaction of at least these three factors.

The analogous channel form elements that are associated with variation in the spacing of pools and coarse patches (or riffles) are somewhat different. These relationships differ in part because they are normalized by channel width. To the extent that pools and large, coarse patches tend to occupy different portions of the channel, these elements account for the size and frequency of pools and large, coarse patch elements, rather than just frequency. Spacing of both pools and large coarse patches increases with bed width. They extend over similar ranges, from about 1 to 10 channel widths. Spacing of pools is nearly constant with slope, but spacing of patches increases and has anomalous values with slope. Spacing of pools decreases strongly and non-linearly with width of the particle size distribution, and patch spacing increases only slightly. Patch spacing increases strongly and non-linearly as the threshold increases (mobility decreases) and the pools vary only slightly, showing a slight decrease.

3.6.8. Comparison of patch length, riffle length and length of coarse patches in the model.

In summary, there is a tendency for model patch size to decrease (r^2 of 0.840, $n = 6$), and spacing to increase ($r^2 = 0.552$), as bed width increases. Patch size and spacing do not correlate well with channel slope, because patch length in two of the runs had distinctly different values than the remaining runs. Omitting the two anomalous runs, patch length in the slope runs is longer than in the other runs, about 8 to 12 nominal meters, versus less than 5 in the other variation series. The origin of the anomalous features in the slope runs is unknown. In these runs, patch length decreases and spacing increases as slope increases. Patch length is nearly constant as the width of the particle size distribution varies, whereas spacing increases slightly ($r^2 = 0.381$). The length of patches decreases with the relative particle exposure threshold (increases with mobility) ($r^2 = 0.362$). Like riffles and textural patches in streams, the textural patches in the model span a range of sizes, and may include very small patches (compare Fig. 3.9, 3.3 and 3.4 to 3.17, see also model patch distributions in Fig. 3.16, 3.20).

Field studies of textural patches in streams also indicate a positive relationship of patch size with channel width in pool-riffle (and plane bed) channels, although pool-riffle channels reported in one Pacific Northwest study show the opposite relationship. The studies of riffle length also indicate increasing length of coarse zones, i.e. riffles, in pool-riffle and plane bed channels. In contrast to these pool-riffle and plane bed channels, the model patches are negatively correlated with bed width. The only field data that shows such a decreasing trend is the field data on forced pools. The differing behavior of forced pool-riffle channels is intriguing, as it suggests that at least trends in pool spacing (and therefore riffle or at least inter-pool spacing) responds to channel width in both forced pool and pool-riffle channels, but in opposing directions. In fact, the trends in riffle lengths in forced pool streams have the opposite trend to riffles in pool-riffle and plane

bed reaches in three of the variations evaluated here, in channel bed width, slope, and width of the particle size distribution. Only the data reflecting variations in shear stress vary in similar directions in the stream data analyzed.

The field data on textural patches shows a number of differences from the data on riffles. As slope varies, the two field studies of textural patches show a decrease in patch length with increasing slope in pool-riffle channels. Riffle length data show the same direction of the relationship as for textural patches, with decreasing riffle length as slope increases. Discounting the two anomalous runs (out of 10), the model data also show a decrease in length of coarse patches as slope increases. Thus patch and riffle features in all of these settings show a decrease in length as slope increases, with the exception of forced pools. Spacing between coarse patches shows the opposite response, increasing, at least slightly, in each of the model variation series.

For particle sorting variations, the Pacific Northwest study shows a weak positive relationship of increased patch length as the width of the particle size distribution increases in pool-riffle and plane bed channels. The width of the particle size distribution was not available in the California data. However, a correlation with D_{50}, which is likely to have the same trend as with width of the particle size distribution, shows a decrease in length of patches. Based on the compilation of riffle data, riffles tend to lengthen with width of the particle size distribution. In contrast, the model data indicate no trend, in these runs where the particle size distribution variation consists of an increase in the finer sizes. Thus, field data suggests that riffles may become longer and patches shorter as particle size distributions become wider (except for forced pool reaches), but the model data, specific to the case of varying amounts of intermediate to fine particles, shows essentially constant length of coarse patches, regardless of the quantity of finer sediment. For comparison, Iseya and Ikeda (1987) found that both coarse and fine channel segments lengthened with an increase in the sand content with the gravel in their flume runs.

As particle mobility varies (as relative particle exposure, or its obverse, dimensionless critical shear stress), the Pacific Northwest study shows decreasing patch length as shear stress increases in pool-riffle, plane bed channels and forced pool channels. Comparable data were not available in the California study, but the dataset does include discharge data which is also related to particle mobility. In these data, the length of patches increased with increasing bankfull discharge. The model patches decrease in length as the threshold increases, corresponding to an increase in length as mobility increases, analogous to the field data.

3.6.9. Summary: Length of textural patches and riffles in streams compared to length of model patches

In summary, most of the data on patches and on riffles, both in the field and in the model, suggest that patch and riffle length increase with channel width, but the trend corresponding to the trend with bed width in the model is shown in the field only for forced pools. Most coarse surface structures evaluated, including textural patches, riffles and the model patches, decrease in length as slope increases. Only patches in forced pool reaches differed, and reflect an increase in length as slope increases. In addition, in the spatial patterns described by Iseya and Ikeda (1987), the length of both coarse and fine zones increased as the bed decreased in slope (although this was also associated with increasing sand in the sediment mixture). Field studies of particle sorting variations include one patch study that shows a weak positive relationship of longer patches in pool-riffle and plane bed channels with increasing width of the particle size distribution. The other patch study suggests shorter patches would occur with wider sorting, although this is indirect, based on the expected wider distribution as D_{50} increases This data, as well as data on forced pool reaches, suggest a decrease in patch length as the particle size distribution widens. The model data instead indicate no trend in length, but a minor adjustment in slope, at least when the particle size distribution variation is entirely an increase in the finer sizes.

3.7. Particle size distributions

3.7.1. Particle size distribution in the model in channel deeps

The initial particle size distribution in the model runs consists of a random assignment of particle sizes in each cell, at the surface and below the surface, within the range of particle sizes chosen for the run. Each of the particle size classes in the distribution is equally likely to be assigned to a cell, so that the particle size distribution will have approximately equal area covered by particles in each of the eight size classes. The final particle size distribution at the surface results from the mixing process inherent in particle transport under particle interactions control in the model.

The final distributions of particle sizes in the deep areas of the channel are shown in Figure 3.21 for the bed width, slope, particle size, and threshold variation series. In the figure, an increase in fine particles can be seen as a decreased symbol size (for square symbols), or decreased darkness of fill (for circle symbols), as shown in the legend. The direction of variation in the fraction of a given particle size can be seen from the order in which the symbols fall along a vertical line representing a given ϕ-size class.

The particle size distributions for channel deeps in the bed-width variation series are shown in Figure 3.21a. The distributions for all runs in the series are only slightly modified from the straight line distribution that would be expected for the original model surface. Each of the runs shows a slight decrease in finer particle sizes and increase in coarser particles. Because the differences between particle size distributions are relatively small, the trend through the runs of the sequence is difficult to see. It is clearest in the threshold variation series, which shows increasing symbol sizes at a particle size of zero ϕ, and decreasing symbol sizes at the coarse end of the plot, at -7 ϕ. These trends indicate a sequence of increasing fraction of fines as the threshold increases (mobility decreases), accompanied by a successively decreasing fraction of

coarse particles as the threshold increases. The runs with varying width of the particle size distribution cannot be compared in this way because the number of size classes present varies. The runs with a greater curvature of the distribution, however, indicate greater coarsening and

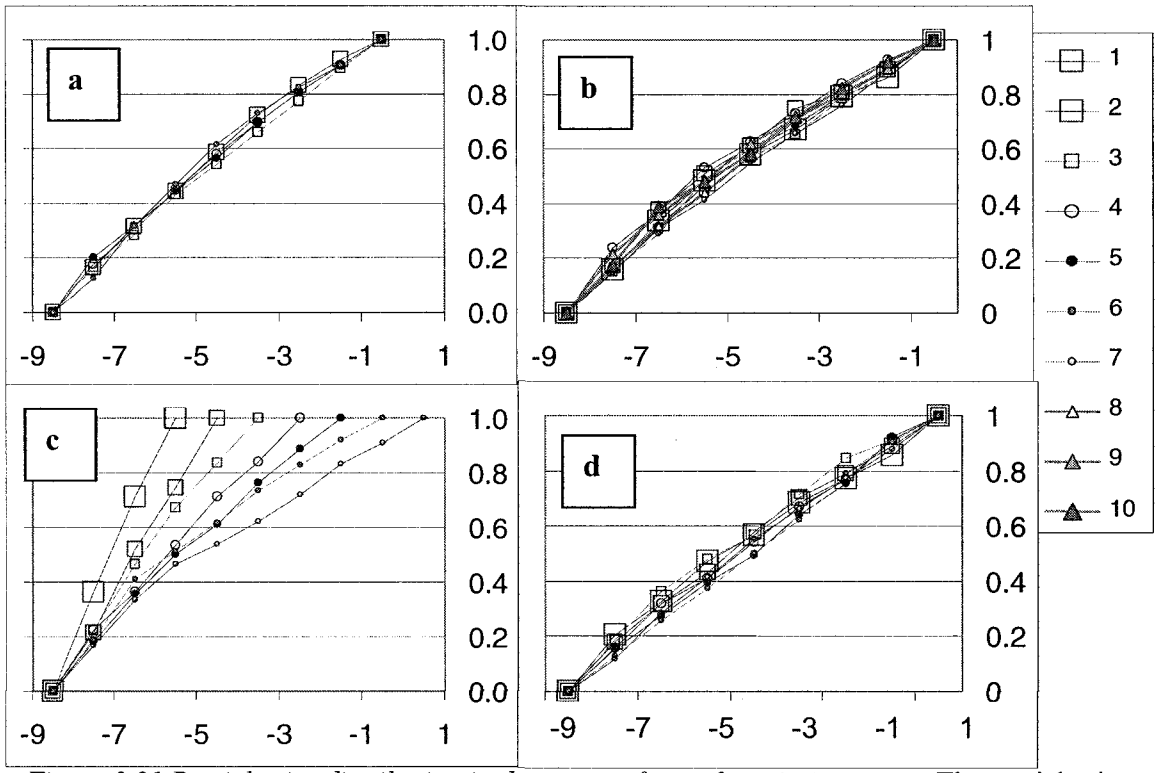

Figure 3.21 Particle size distribution in deep areas for each variation series. The particle size distributions for all runs are only slightly modified from the straight line distribution expected for the original, randomly-generated spatial distribution of particle sizes. In the plots, units on the x-axis are particle sizes in ϕ. An increase in the fine particle fraction can be seen as a decreased symbol size (for square symbols), or decreased darkness of fill (for circle symbols) on the right side of each plot. *a.* The runs of the bed width variation series tend to show a slight decrease in fines content in deeps as the bed width increases. *b.* There is a somewhat more pronounced increase in fines as slope increases. *c.* As the width of the particle size distribution increases, there is a greater reduction in fines content for runs with more fines initially, indicated by the increasing curvature of the distributions through the series. *d.* For the threshold variation series, there is a slight increase in the fines component of the sediment in deeps as the threshold increases (decreasing mobility).

loss of fines by the increasing curvature as the number of particle size classes increases.

In general, the particle size distributions for the deep areas show relatively little adjustment in particle size. The runs tend to show a slight decrease in fines content in deeps as the bed width

increases (Figure 3.21a). A transition between decreasing fines and increasing coarse occurs at sizes between -5 and -6 phi (32 to 64 mm). For the slope variation series (Figure 3.21b) there is a somewhat more pronounced change in fines in deeps, in this case an increase in fines, as slope increases. The transition between coarsening and fining in the slope series occurs for a size between -6 and -7 ϕ (64 to 128). In Figure 3.21c, in which the particle size distribution varies, there is a greater reduction in fines content for runs with more fines initially, indicated by the increasing curvature of the distributions. For the threshold variation series, there is a slight increase in the fines component of the sediment in deeps as the threshold increases (decreasing mobility). The transition from increasing to decreasing fines content occurs at a finer size than for the previous variation series. Here, the transition is between -3 and -4 ϕ (8 to 16 mm).

3.7.2. Particle size distribution in the model in non-deep areas

Particle size distributions in non-deep areas for the bed width, slope, particle size distribution and threshold variation series are shown in Figure 3.22. For three of the four series of particle size distributions, the adjustment is more extensive in the non-deep areas than in the deep areas.

The adjustment in the particle size distributions is small for the bed-width series. The slope series shows sediment sorting adjustments that are similar to, but more pronounced than for the associated deep areas. In contrast to the deep areas, the transition size between increased coarse and decreased finer particles occurs at a smaller size, between about -3 and -4 ϕ (8 to 15 mm) for the bed width and slope series.

For the series with varying width of the particle size distribution, the size distributions for the non-deep areas show a strong inflection near the coarse sizes for narrow size distributions, and a gradual transition for the wider distributions; i.e., there is an abrupt change in the frequency of fines in the distribution with only 3 particle size classes, and a less abrupt transition as the number of size classes increases. An abrupt transition between -4 and -5 ϕ (16 and 32

mm) is seen in the distributions for all runs of the threshold variation series. The non-deep areas are thus less modified than the deep areas for all the variation series.

3.7.3. Particle size distribution in the model in pool areas

Particle size distributions for pool areas in the bed width, slope, particle size distribution and threshold variation series are shown in Figure 3.22. The larger deep areas of the bed, identified as pools, show considerably more particle adjustment than the rest of the bed.

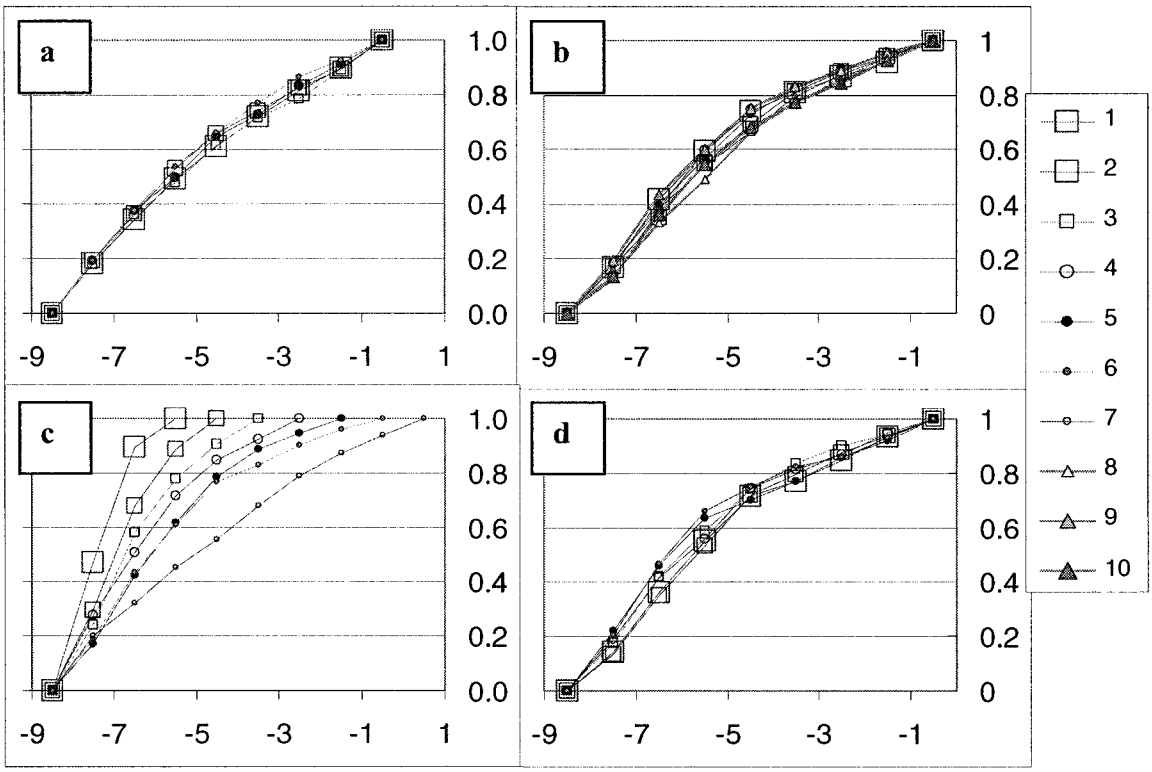

Figure 3.22. Particle size distributions in non-deep areas for each variation series. For three of the four series of distribution in non-deep areas, the adjustment is more extensive in the non-deep areas than in the deep areas. The particle size distributions for the deep areas generally show relatively little adjustment in particle size. a. There is a slight decrease in fines content in deeps as the bed width increases. b. There is a somewhat more pronounced increase in fines as slope increases. c. As the width of the particle size distribution increases, there is a greater reduction in fines content for runs with more fines initially. d. In the threshold variation series, there is a slight increase in the fines component of the sediment in deeps as the threshold increases (decreasing mobility). Particle sizes are in ϕ.

The particle size distributions for the sediment in pools show a greater depletion of fines as the bed width increases. The slope variation series shows a slight decrease in fines in the finest size class. The particle distribution variation series shows a pattern similar to the pattern in the deep areas as a whole, consisting of a slight depletion of the finer sizes in all runs. The threshold variation series is somewhat different than the other areas. The finer portion of the particle size distribution is nearly a straight line, indicating little adjustment in the sizes at the surface. Instead, there is a strong depletion of coarse sizes in the two runs with the highest threshold (lowest mobility), and a moderate coarsening in the lower threshold runs. These two runs also have anomalous clustering of high areas. Such clustering was described in Chapter 1.

3.7.4. Particle size distribution in the model in non-pool areas

Particle size distributions for non-pool areas for the bed width, slope, particle size distribution and threshold variation series are shown in Figure 3.23. The particle size distributions are similar to those for the non-deep areas. All runs show some curvature of the particle size distribution, with the sense of curvature reflecting surface coarsening and depletion of fines.

3.7.5. Summary of adjustments of the particle size distribution in pool, deep, non-pool and non-deep areas.

The bed width, slope, sorting and threshold variation series show some coarsening and associated depletion of fines relative to the initial particle size distribution, with the exception of the pool areas in the threshold variation series. All other areas and runs have a curvature of the distribution indicating that the coarser sediment covers an increased fraction of the bed area, and the finer sediment is depleted from the bed surface, with the transition between depletion and increase near the mean size of particles included in the model run. In the threshold variation runs, instead, there is no depletion of fines, but an increased fraction of sediment in the intermediate

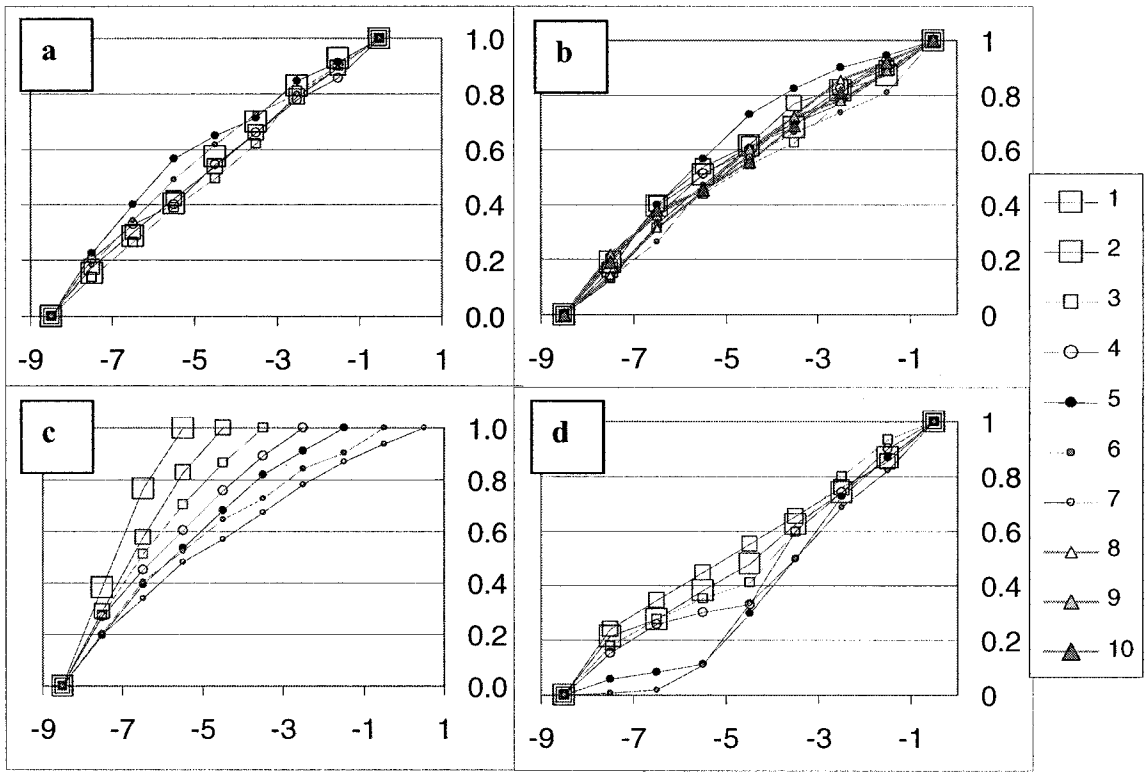

Figure 3.23. Particle size distributions for pool areas for each variation series. For three of the four series of particle size distributions, the adjustment is more extensive in the non-deep areas than it was in the deep areas. *a.* The adjustment in the particle size distributions is small for the bed-width series. *b.* Adjustments in particle size in the slope series are similar to, but more pronounced than for the associated deep areas. *c.* With variation in the width of the particle size distribution, the size distributions for the non-deep areas show a strong inflection, with an abrupt change in the frequency of fines in the distribution with only 3 particle size classes, and a less abrupt transition as the number of size classes increases. *d.* As sediment become less mobile at higher $R_{p,c}$, the bed surface changes from armored, to depleted in the intermediate particle sizes, to depleted in the finer particle sizes. Particle sizes are in ϕ.

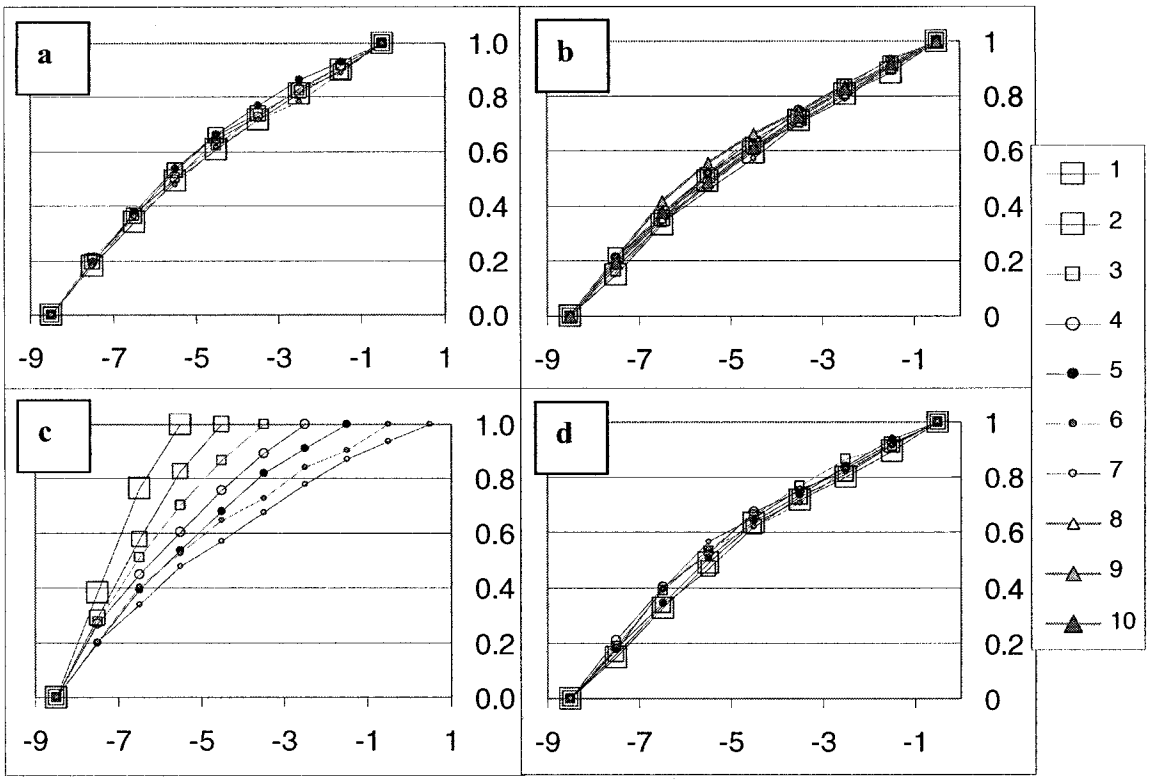

Figure 3.24. Particle size distributions for non-pool areas for each variation series. The particle size distributions are similar to those for the non-deep areas. All runs show some curvature of the particle size distribution, with the sense of curvature reflecting surface coarsening and depletion of fines, but the adjustments are mild.

size classes. In two of the three highest threshold (lowest mobility) runs, the particle size distribution in pools is also characterized by a near absence of the coarsest particle sizes. In comparison, sediment in the deeps and pools is less modified from the original particle size distribution than the non-deep and non-pool areas, again excepting the two runs of the threshold variations mentioned above.

Trends in the adjustment of fines within a variation series are more clearly visible in the plots than trends in coarsening, and the adjustments are described here in terms of depletion of fines. However, except where noted, the fraction of the bed occupied by the coarser size classes increases to an extent that is similar to the depletion of the fines. Sediment in the deep areas of the

model surface shows more depletion of fines for wider beds, flatter slopes, wider particle size distributions and lower thresholds (higher mobility). Sediment in pool areas has similar trends, with the exception of two anomalous runs in the threshold variation series, which are low mobility runs. In two of the three runs with the highest threshold (lowest mobility), the bed surface becomes strongly depleted in coarse particles of the three coarsest particle classes (-8 to -6 phi, 256 to 64 mm), whereas the other runs have an increased fraction of the coarsest particle sizes. Sediment in the non-deep areas shows similar trends as the sediment in the deep areas, greater overall adjustment from the initial distribution, and a distinct breakpoint between the rate of increase in the coarser sizes, and the lower rate of increase in the finer classes. In the slope and threshold runs, the non-deep areas also show coarsening by an increase in intermediate sizes, but without an increase in the representation of the coarsest size class. Particle size distributions in the non-deep and non-pool areas have an overall similarity.

3.7.6. Summary of particle size armoring in deeps, pools, non-deep and non-deep areas

Nearly all areas of the bed, including those classified as pool, non-pool and non-deep areas, clearly coarsened relative to the bulk particle size distribution in most of these runs. The deep areas showed the least coarsening.

The pool areas generally showed the greatest particle size adjustment in the model runs, relative to the non-pool, non-deep or deep areas. The area classified as pools also show the greatest variability in the degree of coarsening in some runs, although there was little variation in the runs with varying width of the particle size distribution. The greatest textural adjustment in the pool areas was in the threshold variation series. In the threshold series, the two runs with the highest threshold (in which even poorly-exposed particles are mobile) resulted in strong fining in pools. The next two runs resulted in a depletion of intermediate-size particles, resulting in a bimodal distribution in pools. The final two runs of the threshold series resulted in coarsening in

the pools. This indicates that, at higher dimensionless shear stress, for which particles of most sizes are in motion, fines on the model bed were less able to move out of pools than were larger particles which rise above their surroundings. These trends with variation in the mobility threshold indicate that fine sediment in the model is sequestered in pools at low $R_{p,c}$ (corresponding to high dimensionless critical shear stress, i.e., high Shields stress). At intermediate dimensionless shear stress, both fine and coarse particles are more commonly exposed at the bed surface in pools than are intermediate size particles. Finally, at low dimensionless shear stress, pool sediment becomes coarser than the bulk sediment. These patterns evolve in the model because particles of all sizes tend to move downslope if possible, and because fine particles mixed with coarse particles tend to low protrusion above their surroundings, and thus rarely move. These patterns differ from what is believed to occur in streams, which are described as having fines accumulated in pools when little sediment is in motion. In the model, fines instead accumulate in pools, rather than when sediment is only weakly mobile. However, lack of observations in streams at higher flow means that the conditions in pools at higher flows are poorly-understood. At present, it is not clear whether these modeled particle size trends develop in pools in streams.

No linear trends in the degree of coarsening of pool sediment were observed in the series with varying width of the particle size distribution. However, the median particle size in pools deviated the least from the initial size distribution for an intermediate width of the particle size distribution in these model runs.

Runs with a wide bed and a run with a very steep slope developed more coarsened surfaces in the pools than did the runs in the other variation series. Another run with very steep slope showed the least coarsening in pools. These trends in coarsening in the model pools modeled suggest that the particle size distribution in pools represents a mutual adjustment that is

influenced by bed width and the mobility threshold, and that the degree coarsening in pools may be highly variable. The trends suggest that the size distribution of surface sediment in pools will run from fine to coarse, depending on the magnitude and duration of recent floods.

Deeps differ from pools in including both large and small areas that lie well below the local mean channel elevation. The degree of adjustment and the strength of the trend with variation in the influencing variables were similar to, but less distinct than, the area occupied by pools.

The particle size distributions evolved in the non-deep areas contrast most strongly with the pool areas. In the non-deep areas, the particle size distributions of the $R_{p,c}$ series show a distinct break in slope in the plotted cumulative distribution, such that the plot of the cumulative particle size distribution approximates two line segments at different slopes. The sediment can then be described as having all particle size classes in the coarser end of the distribution occupying an equal area of the bed, and each of the particle size classes in the finer half of the particle size distribution occupying a equal area of the bed, but a smaller area than that occupied by the coarse particles. The coarse half occupies about 80 percent of the bed, and the finer half about 20 percent of the bed surface. In addition, in the non-deep areas of the $R_{p,c}$ series, each of the particle size classes in the coarser half of the distribution is found at a smaller percentile, and each of the particle sizes in the finer half of the distribution is found at a slightly larger percentile, as the $R_{p,c}$ increased, i.e., as Shields stress and mobility decreased.

Taken together, the particle size distributions of the variation series indicate that the degree of coarsening in the deeps is inherently variable, at least as bed width, slope and particle mobility ($R_{p,c}$). There is no linear trend as slope varies. There is some indication that the greatest coarsening occurs at an intermediate width of the particle size distribution (i.e., when particle sizes span about 5 to 6 phi, rather than 3 or 8 phi).

Bed armoring is less noticeable in the deeps than in pools, non-pool and non-deep areas. In the threshold run, there is no coarsening in run with the highest relative particle exposure, thus all particle sizes were equally mobile in this run. The maximum armoring in deeps reflected an increase in the percentile at which the median particle size is plotted of 17 percent above its initial plotting point at 50 percent. The bed width and slope series had a degree of intermediate coarsening of the surface sediment.

The above observations of the difference in armoring in deep and in pool areas are the inverse of the difference in armoring in the non-deep and non-pool areas. However, several additional points are worth noting. The surface particle sizes in the non-pool areas show a distinct break in the plotted cumulative particle size distribution between the -7 and -6 phi sizes in the slope variation series. The distributions for the threshold series show a break at about the -5 phi size. Secondly the degree of adjustment varies more widely between the series, with the increase in the plotting percentile intermediate particle size ranging from 3 percent for the bed width series to 14 percent for the threshold series. Thirdly, the non-pool areas for all runs of the threshold series, show a distinct break in slope at the intermediate particle size.

3.7.7. Differentiation of areas of the bed that are deeps, pools, non-deep and non-pool areas

Relationships between the area fractions of the bed that are deep, that are a pool, and that are coarse are shown in Figure 3.28. The area of overlap, i.e., the area of the bed that is both a pool and coarse tends to decreases as bed width increases, indicating increasing spatial differentiation between pools and riffle-like areas of the bed. The area that is deep decreases most noticeably, from just above 30 percent to just above 10 percent. As slope increases, the area of the bed that is coarse generally decreases, and the area that is deep or is a pool is constant or increasing. However, there is no observed increase in differentiation between deeps or pools and coarse areas. As the initial content of fines increases and the width of the distribution increases from 3 to

9 size classes, one ϕ unit in width, the area of the bed that is coarse is variable, but there is no distinct trend.

The influence of slope on channel form under particle interactions is unclear in the model runs evaluated here. As described in chapter 2, the model data suggests spatial variations in the maximum depth of the local deeps are observed as slope varies, but that there is no clear trend in spacing (Fig. 2.3), pool length scale, number of pools or number of deeps, or area occupied by deeps (see Chapter 2) as slope varies. There are variations in the area occupied by pools as slope varies, but the data collected in the model runs is not sufficient for analysis of the apparent, complicated pattern of variation. However, it appears reasonable that the lack of trends in the area of deeps as slope varies may be analogous to the lack of slope dependence in the spacing of forced pools, which was previously identified in field studies (Montgomery and others, 1995).

As the threshold increases (corresponding to decreasing mobility), the area of the bed that is both deep and coarse tends to decrease, as does the area that is both pools and coarse. This occurs in spite of an accompanying tendency for the total area of each type of areas: coarse sediment, deeps and pools, to increase. This suggests that low to moderate particle mobility is conducive to development of a spatial differentiation between pool deeps and the non-deep coarse areas that may be related to riffles, and possibly also to textural patches. Lower sediment mobility and a wider channel bed appear to have the greatest effect in reducing the overlap of deep and coarse areas, thus enhancing longitudinal differentiation of the channel. The effect of width of the particle size distribution is equivocal, but may indicate more spatial differentiation with a relatively coarse but narrowly-graded size distribution. These model runs thus suggest that the factors that are most important in developing spatial differentiation of channels into riffles and pools, or on development of other textural patches, are a relatively narrow channel bed, with relatively low mobility sediment. The role of the particle size distribution is unclear, but may

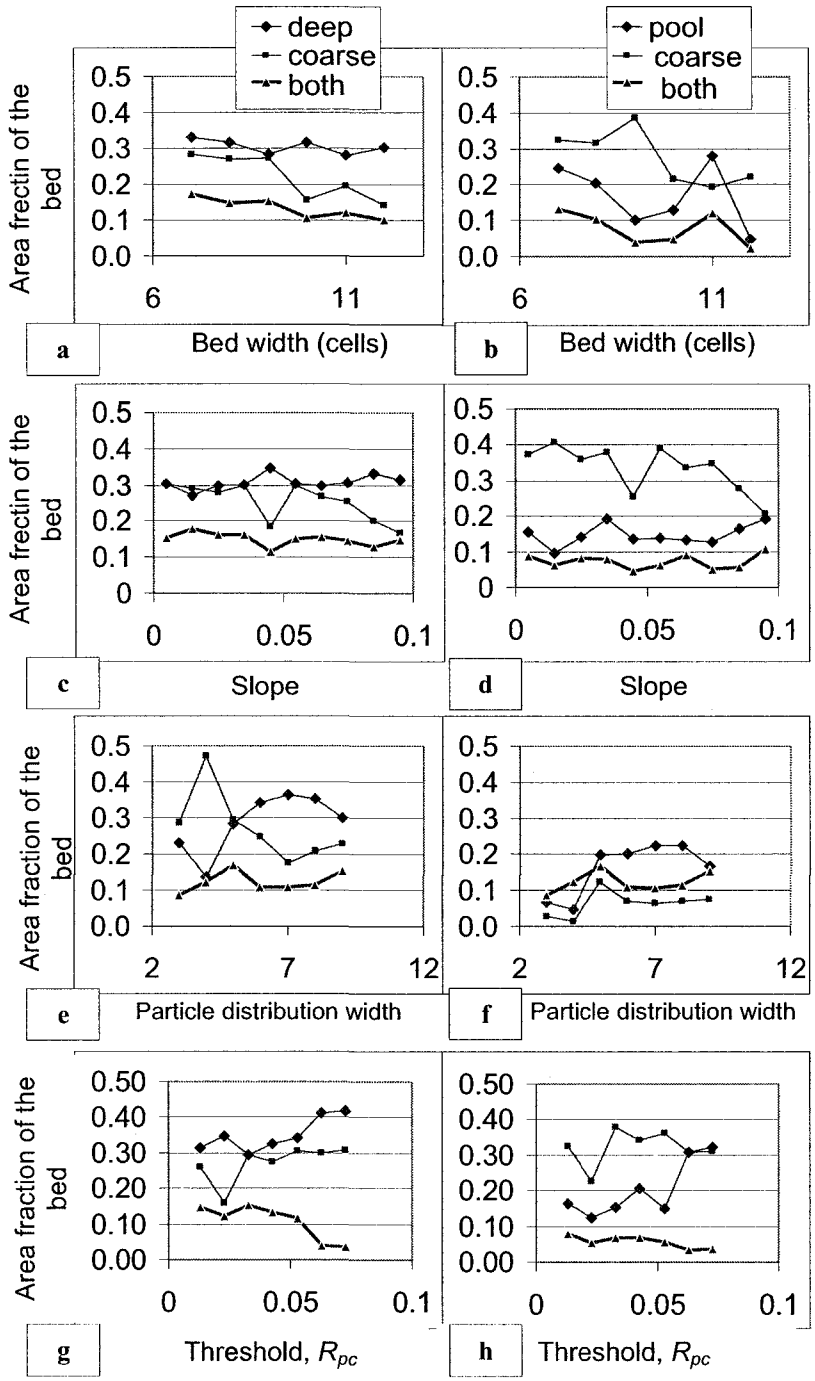

Figure 3.28. Differentiation between area of the bed that are coarse and areas that are deep or pools. Pool-riffle channel are characterized by a differentiation of pools or deeps and coarser grained riffles. Greater differentiation is shown here as a reduction in the area that is both coarse and deep, which occurs in the model results primarily for wide beds and weakly mobile sediment.

indicate that relatively fine (although weakly mobile) sediment is also conducive to spatial differentiation. Channel slope appears to be unimportant in development of spatial differentiation.

3.7.7. Longitudinal variation in particle size and particle exposure

Particle size patterns in the model data suggest that local particle size distributions are strongly related to local bed depth. Based on the threshold variation series, the particle size distribution for deep areas in the model runs are much more coarse-dominated than the particle size distributions of locally high areas. Differences in the particle size distribution between pools and non-pool areas are more subtle. Using the threshold variation series as an example, there is a trend in the relationship between the particle size distribution of pools and of non-pool areas as mobility decreases (Figure 5.1).

3.7.8. Particle size distribution summary.

The particle size distribution at the beginning of each run would plot as approximately a straight line, in which all particle sizes cover roughly equal fractions of the bed area. The observed adjustments in the form of the particle size distribution occur entirely as a result of the mixing process inherent in erosion and deposition of sediment, under the relative particle exposure threshold criterion in the model. The particle size distributions at the end of the model runs generally show a moderate coarsening, and accompanying depletion of fines, as shown by the curvature of the distributions. The exception is in the distributions for pool areas in the threshold variation series. The generally curved distributions change to an abrupt rather than a gradual change in slope for distributions from the non-deep areas. The abrupt change is most pronounced in the threshold variation series, next in the slope variation series, and least in the bed width variation series. The sharp transition indicates a distinct difference in mobility and transport resulting in distinctly different response of the coarse half and the finer half of the sediment in the non-deep areas. The particle size distributions obtained from the model runs show the greatest

modification from the initial distribution in the threshold variations, less in the slope variations, and even less in the particle size distribution and bed width variations. Similar but somewhat less distinct differences distinguish pool and non-pool areas in most runs, with greater adjustment in the non-pool areas. In particular, the transition is gradual rather than abrupt for the non-pool areas.

A few distinctly different distributions are found in pools at high values of the threshold variable (low mobility runs). The threshold variation as a whole shows an increased fraction of the coarsest particle size (256 mm) in the low threshold runs, and very strong reduction in the presence of coarse particles, for the coarsest three particle sizes, in the two highest threshold (low mobility) runs. This indicates that when particles must be well-exposed to be mobilized (high threshold runs), the bed surface in pools tends to coarsen at higher mobility, but to become finer rather than coarser at low mobility. This appears to reflect the model analogue of fines accumulating in pools at low flow.

The contrast between pool and non-pool areas is generally less distinct than between deep and non-deep areas. An important exception is in the threshold variation runs. In the threshold runs, most distributions are depleted in either the coarse or coarse-to-intermediate size sediment. For example, the fraction of the sediment on the surface that is coarser than -5 phi (32 mm), f_{32mm} decreases as the threshold , R_{pc} increases (mobility decreases): $f_{32mm} = -0.739\ R_{pc} + 0.642$. This decrease in the coarse fraction of the bed may occur from a combination of increased exposure of the coarsest sediment, decreased exposure of the finest sediment, and a transition between the two. The sharpness of the transition varies between deep and non-deep areas. The runs of the threshold variation further suggest that when mobility is particularly low, the exposed surface area in the pool deeps is dominated by fine sediment, based on the characteristics of the final two runs of the threshold variation series, in which very few cells with coarse particles are found in

the pool areas. These variations in the particle size distributions indicate an interesting variability in the sediment surface distribution as mobility varies. However, the details of this process are not central to the comparison of the model runs and how they relate to pool-riffle channels, which is the focus in this study.

Table 3.12. Correlations on area of the bed in deep, pool or coarse patch

Bed width variation series				
1	***Deep***	***y = - 0.0059x + 0.361***	***r^2= 0.321***	-
2	***Coarse***	***y = - 0.0302x + 0.506***	***r^2= 0.785***	-
3	***Deep and coarse***	***y = - 0.014x + 0.266***	***r^2= 0.825***	-
4	*Pool*	*y = - 0.0209x + 0.367*	*r^2= 0.189*	-
5	***Coarse***	***y = - 0.0305x + 0.566***	***r^2= 0.544***	-
6	***Pool and coarse***	***y = - 0.0137x + 0.207***	***r^2= 0.305***	-
Slope variation series				
1	*Deep*	*y = 0.3106x + 0.293*	*r^2= 0.217*	+
2	***Coarse***	***y = -1.1971x + 0.315***	***r^2= 0.493***	-
3	*Deep and coarse*	*y = -0.2699x + 0.164*	*r^2= 0.216*	-
4	*Pool*	*y = 0.3358x + 0.131*	*r^2= 0.118*	+
5	***Coarse***	***y = -1.4873x + 0.407***	***r^2= 0.476***	-
6	*Pool and coarse*	*y = 0.0205x + 0.0716*	*r^2= 0.001*	--
Width of particle size distribution				
1	***Deep***	***y = 0.0258x + 0.132***	***r^2= 0.473***	+
2	***Coarse***	***y = -0.0294x + 0.449***	***r^2= 0.426***	-
3	*Deep and coarse*	*y = 0.0045x + 0.096*	*r^2= 0.118*	+
4	***Pool***	***y = 0.0243x + 0.015***	***r^2= 0.510***	+
5	*Coarse*	*y = 0.0069x + 0.0214*	*r^2= 0.183*	+
6	*Pool and coarse*	*y = 0.0045x + 0.096*	*r^2= 0.118*	+
Threshold				
1	***Deep***	***y = 1.7461x + 0.275***	***r^2= 0.638***	+
2	***Coarse***	***y = 1.5632x + 0.204***	***r^2= 0.415***	+
3	***Deep and coarse***	***y = -1.8704x + 0.1867***	***r^2= 0.711***	-
4	***Pool***	***y = 3.0146x + 0.074***	***r^2= 0.66***	+
5	*Coarse*	*y = 0.3454x + 0.306*	*r^2= 0.023*	+
6	***Pool and coarse***	***y = -0.6514x + 0.084***	***r^2= 0.681***	-

**series with an r^2 greater than 0.3 are in bold type*

3.7.9. Comparison of trends in coarse areas, deep and pool areas as bed width, slope, particle size and the threshold for motion vary.

The trend in the fraction of the bed area that is designated as a pool within each variation series is summarized in the correlations in Table 3.12. Areas of the bed that are coarse may be considered to be analogous to riffles or the precursors to pools. The area of overlap between the total area of pools and the total area of riffles indicates the degree to which the model reaches are *not* characterized by distinct pool-like and riffle-like areas. To the extent that pools and coarse areas in the model are distinct, the overlap between deep areas and coarse areas should be small. The degree of overlap between deep and coarse areas is summarized by the following correlations.

In the bed width variations, the area that is deep decreases as bed width increases, although the correlation has a low r^2. The area that is coarse and the area of overlap decrease as the bed width increases. The area of overlap ranges from 13 down to 2 percent. Clearly the wide runs, with 2 percent of the bed in the area of overlap, have a distinct separation between pools and coarse areas (r^2= 0.825). It is not clear what degree of overlap is consistent with pool-riffle forms; to the best of my knowledge this has not been investigated in streams, and will depend on the definitions used to identify pools and riffles. Lacking a criterion, I will characterize the degree of overlap as small when it is less than or equal to 0.10.

The degree of overlap in the slope variation series is constant on average (low r^2 of 0.001). The fraction of the bed that is both coarse and deep is small, at 0.046 to 0.11. In the particle size distribution variation series, the fraction of the bed that is both coarse and pool ranges from 0.014 to 0.074, and is thus low. The runs with the wider particle size distributions have a greater degree of overlap. In the threshold variation, the fraction of the area of the bed that is both coarse and a pool ranges from 0.08 to 0.033, with less

overlap when the threshold is high (low mobility). The total fraction that is coarse is close to 30 percent and the fraction that is pool is between 10 and 20 percent (or more) except for the run with the widest bed, and for most of the particle size distribution variation series. If the fraction of the bed that is pools is characterized as about 0.15, the area that is both coarse and pool would generally be expected to be about half the combined area of 48 percent, i.e., near 24 percent. The combined fraction is generally less than 10 percent, except in the particle size distribution series. This suggests that particle interactions result in less overlap of large, deep pool-like areas and coarse areas than would be expected for a random spatial distribution

3.8. Discussion and conclusions.

The results of this analysis of spatial patterns in sediment that arise as a result of particle interactions in cellular automata model, *PICA*, suggest that the simple conceptual model typically used to introduce pool-riffle channels is too simple. An analysis of the relationship of riffle length to pool length and to channel width was developed using data previously documented in stream channels. Here riffles and runs are assumed to form a single coarse, steep unit in the channels. Although the analysis indicates that pools and riffles are often approximately similar in length, the studies also demonstrate that riffle (and riffle-run) lengths vary significantly, in their absolute length, in length relative to channel width, and in length relative to the associated pools. The data suggest that riffles may be either shorter or longer than pools. The data show that riffles in different geographic areas (characterized by different topographic, lithologic, tectonic, climatic and land use conditions) tend to occupy a greater fraction of the pool-riffle (pool-riffle-run) cycle as the length of the pool-riffle cycle increases relative channel width (Figure 3.6). However, within a geographic region, riffles tend to occupy a smaller fraction of the pool-riffle cycle as the

length of the pool-riffle cycle increases (Figure 3.6). There is not enough information to explain this pattern, although the available data suggest it is not in response to downstream variations in discharge.

The tendency for riffles and pools to differ in length is consistent with the minimization principle suggested by Yang (1971), in which pools and riffles, characterized by differing slope, develop and stabilize because they tend to minimize energy dissipation per unit channel mass of water. The relative lengths and slopes of pools and riffles may then be expected to minimize energy dissipation for given local and regional constraints on channel adjustment. Increases in the length of pools relative to the length of riffles will tend to accomplish this. Stream data suggest the characteristics of these variations. The stream data suggest that riffles may be either longer or shorter than pools, and that lengths may increase as the width of the particle size distribution increases. The data also suggest that, within a stream system, riffle lengths have a constant relationship to slope, and are either constant or increasing with bed width. The data also indicate that riffle lengths increase in proportion to discharge.

Large, coarse patches form in the model. Their characteristics were evaluated here in terms of the extent to which these large coarse patches may reflect the initiating form for riffles in stream systems. The characteristics of channel deeps, including all deeps, and large, deep areas characterized as pools, were evaluated previously (Chapter 2). Large, coarse patches in the model tend to be spatially segregated from the model pools, suggesting a segregation of the channel into areas that are coarse, analogous to riffles, and areas that are finer and deep, analogous to pools.

A comparison of trends in the size of pools and of large, coarse patches indicates that there are two types of relationships between pool and riffle lengths as different channel characteristics vary. First, the length of pools increases whereas the length of riffles decreases as bed width and the threshold for motion increase. These variations indicate a trade-off between the length of the

model bed surface that is coarse and the length of the model bed surface that is a local deep, which occurs as bed width and the threshold for motion increase (corresponding to a decrease in sediment mobility). Variation of channel slope in the model affects the patch lengths, but not the pool lengths; the length of pool in the model is essentially constant with slope, whereas the length of coarse patches decreases. Finally, the length of pools shows no trend with width of the particle size distribution.

Thus, like the variations within a given geographic region in the stream data, the model is a system in which increases in riffle length tend to be offset by decreases in pool length, and vice-versa, and the model indicates that these adjustments are a response to variations in bed width and in the threshold for transport. The stream data suggest that (a) riffle lengths vary from constant to increasing as channel width increases within a single geographic region, and increase at a wide range of rates in different geographic regions, (b) riffle lengths within a geographic region are constant with slope and decrease with slope among geographic regions, (c) riffle lengths increase with the width of the particle size distribution and (d) riffle lengths increase with shear stress and with discharge. There is insufficient information to consider whether there are differences in the direction of variation within and among geographic regions when the width of the particle size distribution or shear stress is considered. The data available to consider the variation in riffle length as discharge varies are also insufficient to generalize, but show a clear increase in riffle length as discharge increases in a single study area. The available data on patches and riffles indicate that both patch and riffle lengths increase with bed width, unless the system is a forced pool-riffle system. The two available studies indicate that patch lengths decrease with slope, again unless the system is a forced pool-riffle system. The two studies that are available give differing trends for patch lengths as particle size and discharge increase.

The model results suggest a non-random spatial distribution of coarse particles relative to pool areas, with a tendency toward separation between deep and coarse areas. This is considered characteristic of pool-riffle channels.

There is no clear correspondence between the length of coarse patches in the model runs and the variations in the available stream studies. Looking at data for patches and riffles, neither clearly follows the patterns followed by the variations in the model. Riffles, in particular, strongly violate the pattern of a general decrease in patch length as the length of deeps increases. Patch lengths in pool-riffle channels also do not clearly follow the pattern in the model.

As a result of this review, I would suggest that the constraints on pools, riffles and their relationship in coarse channels is in part approximated by the results in the PICA model, but differs in part. This is somewhat surprising considering that pools in the model follow trends that are generally similar to trends in streams. I would suggest two alternate possibilities for the differences. The first possibility I would suggest is that the results in the PICA model may be those that would occur relatively early in the adjustment of a stream after some major change which causes the channel to undergo a significant adjustment, and thus do not correspond to conditions generally observed in streams. Thus, the results may suggest what would be observed within a few years after a major flood, or other resetting event, and that subsequent, slower evolution of the pool and riffle forms modifies the relationships. A second possibility is that pools in the model and in streams develop by similar mechanisms, but the population of riffles in streams includes riffles initiated by local events that generate oversteepened segments in the channel. Such locally-oversteepened segments of the channel may form as a result of tectonic activity, channel switching, chute cutoffs or failure of debris dams. Initiation and evolution of riffles by mechanisms other than those inherent in bar-pool instability has not been studied to my knowledge. Riffles initiated by such mechanisms may have a frequency and length controlled by

factors other than particle interactions, giving a pattern of variation in riffle length that differs from the patterns initiated by particle interactions. In addition, as a steep channel with gravel-to-cobble sediment adjusts, particle interactions may contribute to the characteristics of pools, but energy dissipation mechanisms such as those proposed by Yang may control the formation of riffles.

In addition, the relationships between pool and riffle forms within and between study areas in streams appear to generally have opposing trends, and the reason is not obvious. This increases the uncertainty of comparisons between the model and stream systems. Are these patterns universal? May these patterns be related to channel disturbance?

The particle size distributions for the deep and non-deep areas of the channel provide information about the relationship between the distribution of mobility of sediment in the different particles size classes, and the development of pools and coarse patches on the bed. The slope of the particle size distribution develops an abrupt change, rather than a gradual transition, for sediment in the non-deep areas of the model channel bed. The abrupt change is most pronounced in the threshold variation series, next in the slope variation series, and least in the bed-width variation series. This sharp transition indicates a distinct difference in mobility and transport resulting in distinctly different response of the coarse half and the finer half of the sediment in the non-deep areas. This suggests that differentiation between pools and riffles tends to occur as a necessary consequence of transport of particles with varying size, when the mobility of particles is controlled by their relative particle exposure, without spatial variations in flow characteristics. The observed tendency toward spatial variation in flow then acts to enhance these features.

3.9. Chapter 3 References

Ahmed, M.M.E. 1989. *Rearrangement of coarse grains and patterns in armor coats*. PhD dissertation. Colorado State University, CO. 186 pp.

Barabási, A.-L. and H.E. Stanley. 1995. *Fractal concepts in surface growth*. Cambridge University Press, Cambridge, England, 366 pp.

Barabási, A.-L., M.A. Makeev, C.S. Lee, and R. Cuerno. 1997. Roughening of ion eroded surfaces. In Kim, D., H Park; and B Kahng, eds. *Dynamics of fluctuating interfaces and related phenomena* : proceedings of the Fourth CTP Workshop on Statistical Physics: Seoul National University, Seoul, Korea, 27-31 January 1997. Singapore; River Edge, N.J., World Scientific.

Barta, A. F., P.R. Wilcock, and C. Shea. 1994. The transport of gravels in boulder-bed streams. in George V. Cotroneo and Ralph R. Rumer, eds., *Hydraulic engineering '94*. Vol. 2. ASCE. New York. p. 780 - 784.

Bathurst, J.C., 1987. Distribution of boundary shear stress in rivers. In: *Adjustments of the Fluvial System*. D.D. Rhodes and G.P. Williams (eds.), George Allen & Unwin, London, p.95-116.

Beschta, R.L., 1987. Conceptual models of sediment transport in streams. In: *Sediment Transport in Gravel-Bed Rivers*. C.R. Thorne, J.C. Bathurst, and R.D. Hey (eds.), John Wiley, Chichester, p. 387-419.

Blondeaux, P. and G. Seminara. 1985. A unified bar-bend theory of river meanders. *Journal Fluid Mechanics* 157:440-470.

Booker, D.J., D.A. Sear and A.J. Payne. 2001. Modelling three-dimensional flow structures and patterns of boundary shear stress in a natural pool-riffle sequence. *Earth Surface Processes and Landforms* 26:553-576.

Brayshaw, A.C. 1985. Bed microtopography and entrainment thresholds in gravel-bed rivers. *Geological Society of America Bulletin* 96:218 – 223.

Buffington, J M, 1999. Variability of sediment sorting in coarse-grained Rivers: a case of self-similarity. AGU Fall Meeting.

Buffington, J.M., and D.R. Montgomery. 1999a: A procedure for classifying textural facies in gravel-bed rivers. *Water Resources Research* 35(6):1903-1914.

Buffington, J. M., and D.R. Montgomery. 1999b. Effects of hydraulic roughness on surface textures of gravel-bed rivers. *Water Resources Research* 33(11):3507-3521.

Buffington, J.M., T.E. Lisle, R.D. Woodsmith, S. Hilton, 2002. Controls on the size and occurrence of pools in coarse-grained forest rivers. *River Research and Applications* 18(6):507-531.

Carling, P. A. and H. G. Orr. 2000. Morphology of riffle-pool sequences in the River Severn,

England. *Earth Surface Processes and Landforms* 25(4)369-384.

Chase, K.J. 1994. Thresholds for gravel and cobble motion. in George V. Cotroneo and Ralph R. Rumer, eds., *Hydraulic engineering '94*. Vol. 2. ASCE. New York. p. 790-794.

Church, M., M.A. Hassan and J.F. Wolcott. 1998. Stabilizing self-organized structures in gravel-bed stream channels: field and experimental observations. *Water Resources Research* 34: 3169-3179.

DeJong, C. and P. Ergenzinger, 1998. Dynamic roughness, sediment transport and flow structures in a mountain stream. *Gravel-Bed Rivers in the Environment*. P.C. Klingeman, R.L. Beschta, P.D. Komar, and J.B. Bradley, eds., 39-60, Water Resources Publications LLC, Highlands Ranch, Colorado.

Dietrich, W.E., J.W. Kirchner, Hiroshi Ikeda, and Fujiko Iseya. 1989. Sediment supply and the development of the coarse surface layer in gravel-bedded rivers. *Nature*, 340:215-217.

Ebell, J.P., I.D. Redden. and I.D. Cuthbert. 2004. Quantitative assessment of fish habitat conditions in the lower Elk Rive. December 2, 2004, unpublished report, http://www.bchydro.com/bcrp/completed_projects/04CA01.pdf

Egiazaroff, L.V., 1965. Calculation of non-uniform sediment concentration. *Journal of the Hydraulics Division, ASCE*, 91 (HY4): 225-247.

Einstein, H.A., 1950. The bed-load function for sediment transportation in open channel flows. U.S. Dept. of Agriculture, Soil Conservation Service, Technical Bulletin 1026, 71 pp.

Fenton, J.D and J.E. Abbott, 1977. Initial movement of grains on a stream bed: the effects of relative protrusion. *Proceedings of the Royal Society of London* A 352:523-537.

Florsheim, J.L. 1985. *Fluvial requirements for gravel bar formation in northwestern California.* M.S. thesis. Arcata, California, Humboldt State University, 105 pp.

Furbish, D.J., 1987. Conditions for geometric similarity of coarse stream-bed roughness. *Mathematical Geology* 19 (4): 291-307.

Furbish, D.J. 1998. Irregular bed forms in steep, rough channels. I. Stability Analysis. *Water Resources Research* 34 (12): 3635-3648.

Gessler, J. 1989. Friction factor of armored river beds. *Journal of Hydraulic Engineering* 116 (4): 531- 543

Gomez, B., 1995. Bedload transport and changing grain size distributions. In: *Changing River Channels*. A. Gurnell and G. Petts (eds.), John Wiley and Sons, Chichester, p. 177-199.

Grant, G.E., F.J. Swanson and M.G. Wolman. 1990. Pattern and origin of stepped-bed morphology in high-gradient streams, Western Cascades, Oregon. *Geological Society of America Bulletin* 102:340-352.

Gregory, K.J., A.M. Gurnell, C.T. Hill and S. Tooth. 1994. Stability of the pool-riffle sequence in

changing river channels. *Regulated Rivers* 9: 5-44.

Haschenburger, J. and P. R. Wilcock. 2003. Partial transport in a natural gravel bed channel. *Water Resources Research* 39(1), ESG 4-1:4-9.

Hassan, M.A., and M. Church. 2000. Experiments on surface structure and particle sediment transport on a gravel bed. *Water Resources Research* 36(7):1885-1895.

Hassan, M. A. and M. Church. 2001. Sensitivity of bed load transport in Harris Creek seasonal and spatial variation over a cobble-gravel bar. *Water Resources Research* 37(3):813- 825.

Iseya, F. and H. Ikeda. 1987. Pulsations in bedload transport rates induced by a longitudinal sediment sorting: a flume study using sand and gravel mixtures. *Geografiska Annaler* 69A:15 – 27.

Jowett, 1993. A method for objectively identifying pool, run and riffle habitats from physical measurements. *New Zealand Journal of Marine and Freshwater Research* 27:241-248.

Keller, E.A. and W.N. Melhorn, 1981. Bedforms and fluvial processes in alluvial stream channels: selected observations. In: *Fluvial Geomorphology*. M. Morisawa (ed.), The "Binghamton" Symposia in Geomorphology International Series , No. 4., p. 253-283, George Allen & Unwin, London.

Kirchner, J.W., W.E. Dietrich, F. Iseya and H. Ikeda, 1990. The variability of critical shear stress, friction angle, and grain protrusion in water-worked sediments. *Sedimentology* 37: 647-672.

Konrad, C.P., D.B. Booth, S.J. Burges, D.R. Montgomery. 2002. Partial entrainment of gravel bars during floods. *Water Resources Research* 38(7):art 1104, 16 pp.

LaMarre, H. and A. Roy. 2001. Organisation morphologique des blocs et des amas de galets dans les cours d'eau à lit de graviers. *Géographie physique et Quaternaire* 55(3):275-287.

Langbein, W.B. and L.B. Leopold, 1968. River channel bars and dunes - A theory of kinematic waves. *U.S. Geological Survey Professional Paper 422-L.*

Leopold, L.B, M.G. Wolman and J. P. Miller, 1964. *Fluvial Processes in Geomorphology*. W.H. Freeman & Co., San Francisco, 522 pp.

Lere, M.E. 1984. Montana Department of Fish, Wildlife and Parks, Bonneville Power Administration, Division of Fish and wildlife, Contract No. DE-AI79-1983BP13076, Project No. 1983-463, 120 electronic pages (BPA Report DOE/BP-13076).

Lisle, T.E., 1982. Effects of aggradation and degradation on riffle-pool morphology in natural gravel channels, Northwestern California. *Water Resources Research* 18 (6): 1643-1651.

Lisle, T.E. and S. Hilton, 1992. The volume of fine sediment in pools: an index of sediment supply in gravel-bed streams. *Water Resources Bulletin* 28(2): 371-383.

Lisle, T.E., J.M Nelson, John Pitlick, M.A. Madej, Brent L. Barkett. 2000. Bed mobility

variability in natural gravel-bed channels and adjustments to sediment load at local and reach scale. *Water Resources Research* 36(12):3743-3755.

Milne, J. A. 1980. Bed forms and bend-arc spacing of some coarse-bedload channels in upland Britain. *Earth Surface Processes and Landforms*, 7:227-240.

Montgomery, D.R. and J.M. Buffington, 1993. *Channel classification, prediction of channel response, and assessment of channel condition.* Report TFW-SH10-93-002 prepared for the SHAMW committee of the Washington State Timber/Fish/Wildlife Agreement, 107 pp.

Montgomery, D.R. and J.M. Buffington, 1997. Channel-reach morphology in mountain drainage basins. *Geological Society of America Bulletin* 109 (5):596-611.

Naden, P.S., 1987. Modeling gravel-bed topography from sediment transport. *Earth Surface Processes and Landforms* 12: 353-367.

Naden, P. S. and Brayshaw, A.C. 1987. Small- and medium-sized bedforms in gravel rivers. *in River Channels: environment and process*. 249-271. ed. K.S. Richards. Blackwell, Cambridge, MA.

Nikora, V. and D. Goring. 2000. Flow turbulence over fixed and weakly mobile gravel beds. *Journal of Hydraulic Engineering*, 126(9):679-690.

Nikora, V.I.; D.G. Goring; B.J.F. Biggs. 1998. On gravel-bed roughness characterization. *Water Resources Research* 34(3): 517–527.

Nordin, C. F. 1971. Statistical properties of dune profiles. *US Geological Survey Professional Paper 56-F*, 41 pp.

Parker, G., 1990. Surface based bedload transport relation for gravel rivers. *Journal of Hydraulic Research* 28(4): 417-436.

Parker, G. and P.C. Klingeman, 1982. On why gravel bed streams are paved. *Water Resources Research* 18(5): 1409-1423.

Parker, G. and A.W. Peterson, 1980. Bar resistance of gravel-bed streams. *Journal of the Hydraulics Division, ASCE*, 106(HY10): 1559-1575.

Parker, G. and P. Wilcock. 1995. Sediment feed and recirculating flumes - fundamental difference. Journal of hydraulic engineering - ASCE 121(3)L293-294.

Pender, G., T. B. Hoey, C. Fuller, and I. McEwan. 2001. Selective bedload transport during the degradation of a well-sorted graded sediment bed. *Journal of Hydraulic Research* 39(3).

Prestegaard, K. L. 1983. Bar resistance in gravel bed streams at bankfull stage. *Water Resources Research* 19(2):472-476.

Redden, I.D. and I.D. Cuthbert. 2004. Elk River Channel Stabilization Project. Streamline Environmental Consulting, Ltd. Unpublished manuscript. http://www.bchydro.com/bcrp/completed_projects/04CA01a.pdf

Robert, A. 1988. Statistical properties of sediment bed profiles in alluvial channels. *Mathematical Geology*, 20(3), 205-225.

Robert, A. 1991. Fractal properties of simulated bed profiles in coarse-grained channels. *Mathematical Geology* 23(3): 367-382.

Robert, A. 1997. Characteristics of velocity profiles along riffle-pool sequences and estimates of bed shear stress. *Geomorphology* 19(1-2):89-98.

Robert, A. 2003. River Processes: An Introduction to Fluvial Dynamics. Arnold

Rundquist, L.A. 1975. *A classification and analysis of natural rivers*. PhD dissertation. Colorado State University.

Schumm, S.A., M.D. Mosley and W.E. Weaver. 1987. *Experimental fluvial geomorphology*. Wiley, NY, 413 pp.

Singh, V. P., C. T. Yang, and Z.Q. Deng. 2003. *Water Resources Research* 39(12):Article No.1337, 15 pp.

Solari, L. and G. Parker. 2000. The curious case of mobility reversal in sediment mixtures. *Journal of Hydraulic Engineering* 126(3):185 – 197.

Svidchenko, A.B., G. Pender, and T. B. Hoey. 2001. Critical shear stress for incipient motion of sand/gravel streambeds. *Water Resources Research* 37(8):2273-2283.

Talbot, T. and M. Lapointe. 2002. Modes of response of a gravel bed river to meander straightening: the case of the Sainte-Marguerite River, Saguenay Region, Quebec, Canada. *Water Resources Research* 38(6): 10-1 – 10-10

Thompson, D.M. 2002. Geometric adjustment of pools to changes in slope and discharge: a flume experiment. *Geomorphology* 46(3-4):257-265.

Thompson, D.M., E.E. Wohl, R.D. Jarrett. 1996. A revised velocity reversal and sediment-sorting model for a high-gradient, pool-riffle stream. *Physical Geography* 17: 142 – 156.

Toro-Escobar, C.M. C. Paola, G. Parker, P.R. Wilcock, J.B. Southard, JB. 2000. Experiments on downstream fining of gravel. II: Wide and sandy runs. *Journal of Hydraulic Engineering-ASCE*.

Van Niekerk, A., K.R. Vogel, R.L. Slingerland, J.S. Bridge. 1992. Routing of heterogeneous sediments over movable bed – model development. *Journal of Hydraulic Engineering-ASCE* 118(2):246-262.

Whiting, P.J., W. E.. Dietrich, L.B. Leopold, T. G. Drake, and R. L. Shreve. 1988. Bedload sheets in heterogeneous sediment. *Geology* 16(2)105-108.

Whiting, P. J., J. F. Stamm, D. B. Moog, and R. L. Orndorff. 1999. Sediment-transporting flows in headwater streams. *Geological Society of America Bulletin* 111(3): 450–466.

Wiberg, P.L. and J.D. Smith. 1987. Calculations of the critical shear stress for motion of uniform and heterogeneous sediments. *Water Resources Research* 23(8):1471-1480.

Wilcock, P.R. and Detemple, B. 2001. Armor layers in flumes and streams. *GSA Annual Meeting, Paper No. 67-0.*

Wilcock, P.R. and B.W. McArdell, 1997. Partial transport of a sand/gravel sediment. *Water Resources Research* 33 (1): 235-245.

Wohl, E.E. and D. Merritt. 2005. Prediction of mountain stream morphology. *Water Resources Research* 41(Article W08419):1-10.

Wohl, E. E., K. R. Vincent and D. J. Merritts. 1993. Pool and riffle characteristics in relation to channel gradient. *Geomorphology*, 6:99-110.

Yalin, M.S. 1971a. *Mechanics of sediment transport.* Pergamon Press, NY, 290 pp.

Yalin, M.S. 1971b. *On the formation of dunes and meanders.* Proceedings of the 14th Annual conference of the association for Hydraulic Research 3, paper C13:1-8.

Yang, C.T., 1971. Formation of riffles and pools. *Water Resources Research* 7(6): 1567-1574.

CHAPTER 4

PARTICLE PATTERNS AND ROUGHNESS IN A

PARTICLE INTERACTIONS MODER OF STEEP GRAVEL-TO-COBBLE STREAMS

Abstract

Particle interactions in poorly sorted sediment can be a significant control on particle motions and therefore on channel evolution. The term 'particle interactions' denotes constraints on particle mobility imposed on one sediment particle by the surrounding particles. These constraints have also been termed hiding, sheltering, protrusion and exposure effects. To investigate the fundamental consequences of particle interactions on channel response, a cellular automaton model was developed to simulate a hypothetical channel in which particle interactions are the sole control on channel evolution. Based on studies in physics on the roughening of surfaces, combined with stream studies that indicate the importance of particle interactions in steep, rough streams, I hypothesized that model surfaces in a cellular automata would develop a surface roughness that varied with the area of the model reach, both its length and width. Based on a review of studies of particle transport in streams I also hypothesized that particle interactions would vary with the particle size distributions. Finally, early model results also indicated that surface roughness also varied with bed width and with slope of the model domain. The relationship between surface roughness and roughening rates, as well as the effects of other channel characteristics on roughness, were evaluated, following methods developed in physics.

The results show that the model bed surface adjusts during an initial time period. The time for the system to adjust to a steady state depends on multiple factors, including constraints imposed by the size of the system as well as the particle size and threshold for motion of the sediment. The effect of the initial channel slope is more difficult to understand, as the results show variability but no clear trend in roughness as slope varies. The rate of adjustment of the model surface varies with the initial model conditions, decreasing as the channel length increases, as well as with slope and width of the particle size distribution. Conversely, the rate of roughening increases as the threshold for motion increases.

Keywords: Pool-riffle; Channel form, Sediment; Cellular automata

4.1. Roughness in streams

4.1.1. Description of the rough channel surface

Roughness of the channel boundary surface is a crucial characteristic for predicting flow and transport in stream channels. Channel roughness includes both particle-scale roughness and the larger roughness elements termed form roughness. The use of the term 'roughness' to denote resistance to flow highlights its importance in studies of stream flow a well as channel form.

Particle size generally increases in steeper channels, such that slope and particle size are viewed as closely related. Billi and others (1998) reported r^2 values for correlations between slope and particle size as 0.88 and 0.71, for D_{50} and D_{84}, respectively. Thus, steep streams are generally coarse-grained. The surface coarseness of such streams is enhanced by armoring, in which the coarser particles are preferentially exposed at the surface. Buffington and Montgomery (1999) described the armoring ratio (ratio of surface to subsurface D_{50}) as typically 1 to 3 based on four studies, and other studies documented armoring ratios from 1.8 to 5.0 (see Chapter 3).

Talbot and LaPointe (2002, p. 10-10) noted that a high-energy system is more likely to be weakly paved, and may also be closer to equal mobility and have less profile convexity and downstream fining. Buffington and Montgomery (1999a) obtained paired surface and subsurface samples of textural patches at sites with little armoring. These samples demonstrated a strong correlation between surface and subsurface median grain sizes, with coarser textural patches having coarser subsurface sizes. Buffington and Montgomery (1999) also evaluated textural response by comparing reach-averaged median gravel size (D_{50}) to that predicted using total bankfull boundary shear stress (τ_b), representing a hypothetical reference condition of low hydraulic roughness. They concluded that, for two channels with the same τ_b, the rougher channel is expected to have finer particle sizes at the surface. In a channel with significant hydraulic

roughness, the observed D_{50} was up to 90% smaller than D_{50} predicted from total boundary shear stress (Buffington and Montgomery, 1999).

As explained by Buffington and Montgomery (1999), the reduced particle size given greater hydraulic roughness may be attributed to a reduction in bed shear stress, resulting in lower channel competence and diminished bedload transport capacity in the rougher channel. Lower competence and capacity will both promote textural fining.

4.1.2. Roughness due to particles on the bed and to channel form

The particulate roughness, including roughness due to grains and to cobbles and boulders, is controlled by the same factors that control particle interactions, i.e., by the size and position of particles in any given local configuration. Roughness due to larger scale undulations in the sediment surface, including undulations of the bed and banks, is termed 'form roughness.' Characterizations of grain and form roughness are then used to evaluate the resistance to flow, which includes resistance generated by features of all sizes on the bed. Another partitioning, that identifies both 'skin friction' due to grains and larger particles separately from the form drag component contributed by the larger particles would provide additional insight, because cobbles and boulders may generate form drag. However, it is more complex to partition resistance to flow in this way.

The effect of particle-scale roughness is identified as the roughness observed when particles alone contribute resistance to flow, i.e., for a channel surface without large-scale variations in form, such as those inherent in the presence of channel bars or undulations of the channel bed and banks. Then, the total observed resistance to flow is partitioned into resistance due to the sediment grains and larger particles on the bed, plus an additional component due to the presence of larger scale undulations. Thus, the grain resistance identified in most studies of gravel and coarser streams typically includes both skin friction and some component of drag.

The effect of particle roughness is typically evaluated based on particle size. The size used is typically the median size, D_{50}, although D_{84} is also used. Gessler (1990) suggested that particle size does not adequately parameterize roughness of the sediment surface, and that shear stress provides a better parameter for predicting roughness (Ahmed, 1989).

However, where there are patch scale variations in particle size, shear stress may also not adequately parameterize sediment transport. Paola (1996) presented a conceptual model and accompanying analysis of the effect of spatial variations in particle size, consisting of textural patches on the channel bed, as well as undulations that result in local variations in depth of the flow. Most importantly, local particle transport responds to variations in both local particle size and local shear stress. Ferguson (2003) evaluated effects of such spatial variation in the channel, including variations in channel width, depth, cross-sectional profile and median particle size. Where patch scale variations in particle size and local boundary shear stress both occur, they will modify fractional transport values for each of the particle sizes, as size and shear stress vary from patch to patch, and in particular between pool and riffle sections.

4.1.3. Approaches to characterizing and estimating roughness

Rosport (1997) summarized evaluations of roughness in hydraulics. He distinguished between the equivalent sand roughness, k_s and the geometric roughness, k, with k_s defined in terms of its effects on flow, and k in terms of particle size. These parameters distinguish between roughness as resistance to flow, and roughness characterized in terms of a length scale characterizing the sediment forming the bed. The equivalent sand roughness, k_s has been described as linearly related to the geometric roughness height k, and is dependent on the arrangement and density of roughness elements (Rosport, 1997). Rosport (1997) noted that Rouse (1965) quantified the effect of different roughness structures on flow resistance, and found that the resistance to flow evaluated as the Darcy-Weisbach friction factor, f, varied by a factor of 10

with different roughness structure, for comparable water depth, h_w and geometric roughness height, k.

Resistance to flow is commonly represented in a logarithmic form, as a function of the relative submergence, h/k or R/k, where h is depth and R is the hydraulic radius. The resistance factor k can be evaluated as

$$k = \sqrt{\frac{8}{f}} = A \ln\left(\frac{R}{d_c}\right) + B_r$$

where A and B_r are empirical constants (Rosport, referencing Bathurst 1985, Bray 1979). For the resistance parameter based on the Keulegan version of this law, Br is 6.25.

The surface roughness is often evaluated by relating a single characteristic particle size to the resistance to flow, also known as a 'friction factor.' The three resistance variables commonly used are the Darcy-Weisbach friction factor, f, Manning's n, and the Chezy coefficient, C. To separate grain resistance from form resistance, grain resistance is often evaluated from a characteristic particle size, using either the Keulegan relation or empirical correlations from field or flume studies. The remaining resistance to flow is attributed to form resistance.

Gessler (1990) evaluated the effective, or 'controlling,' roughness of a particulate surface as the roughness height, k, which would produce the observed energy slope, S_e, based on flume studies with steady, uniform flow and a plane bed. The calculated effective roughness height corresponds to a constant Shields criterion. The effective roughness height was found to range from somewhat less than, up to 4 times the maximum particle size (Gessler, 1990). Gessler noted that roughness heights exceeding the maximum particle size imply that a characteristic particle spacing influences the flow resistance.

Ahmed (1989) conducted a series of flume runs with increasing discharge, flow depth, and grain Reynolds number. Slope generally decreased and controlling roughness generally increased

with these factors. Discharge ranged from 0.023 to 0.057 m^3s^{-1} and shear stress from 2 to 3.5 Pascals. A characteristic spacing of coarse particles was observed and evaluated. The most well-developed characteristic spacing occurred at intermediate flow intensities, although the small number of runs (six) means that the drop observed at the highest discharge is not well-established. The controlling roughness ranged from 0.008 to 0.012 meters (8 to 12 millimeters). From modeling, Gessler (1990) estimated that particles at the size of the controlling roughness have a low, but non-zero (six percent) chance of entrainment. This study identifies a partial mobility effect that forms particle patterns. Many factors influence roughness of the channel surface (Table 4.1). Some roughness methods incorporate estimates of the effect of particulate structure (Dittrich and others, 1996). Rosport (1997) notes that in steep channels, flow is not unstable, but large clasts cause hydraulic jumps in the wake area of obstacles, dissipating energy. Bathurst and others

Table 4.1. Influences on roughness as resistance to flow

Flow variables
- Froude number (Bathurst and other, 1981; Dittrich 1996)

Channel dimensions
- channel width (Bathurst and other, 1981, evaluating obstacle clasts)
- width or width-to-depth ratio (i.e., channel shape factor)
- cross-sectional area (Dittrich and others, 1996)

Relationship of channel to sediment dimensions
- relative submergence: Dittrich and others, (1996) suggested that k_s/D is a function of h/D

Sediment characteristics
- clast width (Bathurst and other, 1981, evaluating obstacle clasts)
- sediment gradation (as standard deviation defined there as log (D_{84}/D_{50}) (Bathurst and other, 1981, evaluating obstacle clasts)
- effective roughness concentration (density or spacing) (Bathurst and other, 1981, evaluating obstacle clasts; Dittrich, 1996)

after Rosport, 1997; Dittrich and others, 1996; Bathurst and others, 1981

(1981) indicate that the additional resistance from this energy dissipation can be characterized as a function of Froude number, channel width, clast width, sediment gradation (as standard deviation, defined there as log[D84/D50]) and an effective roughness concentration. A third approach is to measure surface elevation on a fine-scale, as was done by Furbish (1987) and Robert (1988), as well as others.

4.1.4. A field evaluation of roughness in steep, gravel-to-cobble streams

An overview of roughness variation in steep streams is provided by an integrated analysis by Bathurst (2002). Bathurst analyzed field data relevant to roughness in steep streams, based on 27 data sets for mountain rivers. Bathurst found that resistance from bed surface particles appeared to be controlled by (a) a characteristic particle size, D_r, (b) the width of the size distribution, w_p, (c) the channel slope, S and (d) relative submergence h/D_{84} (or inverse of the fractional height at D_{84}; where h is flow depth and D_{84} is the bed particle size at the 84th percentile accumulating from fine to coarse).

Bathurst notes that a dependence on channel slope is expected given the physics of grain entrainment, and that a slope effect on roughness had not previously been identified empirically. Which mechanisms contribute to the identified slope effect in the data is not known (Bathurst 2002).

Bathurst (2002) notes that a semi-logarithmic relationship is generally used to relate resistance to relative submergence, but suggests that a power law may more accurately describe the relationship, especially at high flow. Bathurst derives two empirical relationships for resistance to flow from these field data. The relationships are for slopes, S, above and below a transitional range from 0.80 and 0.96 %. The relationships relate an apparent minimum flow resistance, f_{min}, to relative submergence, h/D_{84}. The minimum resistance is evaluated as $(8/f_{min})(1/2)$, where f_{min} is a minimum Darcy-Weisbach resistance coefficient. For $S < 0.8\%$, the

equation fitted to the data is $(8/f_{min})(1/2) = 3.84(h/D_{84})^{0.547}$, and for $S > 0.8\%$ the fitted equation is $(8/f_{min})(1/2) = 3.10(h/D_{84})^{0.93}$ (correlation coefficients, r^2, are 0.986 and 0.959, respectively). Bathurst (2002) notes that these high correlation coefficients suggest an improved accuracy compared with other field-based relationships. A dependence of resistance to flow on particle size distribution characteristics may also be expected, but Bathurst identified no dependency on bed material size distribution in the data. Bathurst (2002) suggests this lack of correlation with particle size implies that the distinction between the two empirical relationships accounts in part for differences in bedform development in the two groups of data. Note that the transition between these two identified relationships is near the 1% slope at which the transition from pool-riffle to plane-bed forms is expected to occur.

4.1.5. Other influences on roughness in steep, gravel-to-cobble streams

Ahmed (1989) conducted a flume study and documented non-random arrangements of the coarsest particles. These arrangements consisted of a bias toward linear arrangements of gravel particles. The arrangements varied from lateral lines to longitudinal lines on the bed. The strength of the pattern was greatest at an intermediate shear stress.

Wohl and Ikeda (1998) studied the effect of spacing on resistance to flow. Flume results for resistance with varied spacing of obstacles on the bed showed that resistance to flow peaked when the obstacles were at an intermediate spacing. In a flume study, the coarse obstacle particles were found to cover about 7.3 percent of the bed area at the highest shear stress, and under conditions where particles were preferentially aligned across the flow (Ahmed, 1989).

Similarly, Church and others (1998) documented the spacing of obstacles in a pool-riffle stream by identifying boulders in an aerial photograph of the channel. The boulders in the resulting map appear as rough transverse alignments of the boulders. Hassan and Church (2000) documented non-random particle arrangements in flume runs. The large particles they

documented showed a roughly hexagonal form, in which individual coarse particles were stabilized by the presence of adjacent coarse particles.

In pool-riffle streams, it appears that the roughness of the sediment surface increases with slope (Bathurst, 2002). Surface roughness was parameterized as resistance to flow, specifically the Darcy-Weisbach friction factor. For a given grain size, Bathurst and others (1981) found that the dimensionless critical shear for the D_{50} particle size, τ^*_{c50}, systematically increased with relative roughness, D/h. (Relative roughness is the inverse of relative submergence.) Buffington and Montgomery (1997) indicated that increasing roughness with increasing slope is indirectly related to slope. Where relative submergence is small, the particles that rise higher into the flow may inhibit oscillatory flow and associated flow convergence and divergence. Smaller relative submergence also means greater form drag and less energy available for scour and transport (Buffington and others, 2002)

Bathurst identified a distinct difference in resistance to flow (presented as the Darcy-Weisbach friction factor) as slope increased from less than to greater than about 0.01. Because particle size tends to increase as slope increases, increased particle size may tend to inhibit transport at steeper slopes. However, Bathurst did not find a statistically significant relationship between roughness and particle size. One may infer that particle size does not have a simple relationship to roughness. The effects of these relationships between slope, particle size and bed form characteristics remain only approximately understood.

4.1.6. Roughness and bed width

Wider channels have been shown to develop more lateral variability in depth in flume studies (Toro-Escobar and others, 2000). Thus, greater form roughness is expected in wider channels.

Stream studies indicate that channel width, and the length of pools and riffles, scale in different proportions, as the channel width increases (see Chapter 3). The lengths of pools, riffles

and the width of the channel scale at different rates, giving rise to trends in pool and riffle lengths as channel width varies. Several existing data sets were evaluated in Chapter 3, and the results indicate that both riffle lengths and pool lengths increase as channel width increases. However, the rate of increase is highly variable, and includes cases where riffles increase faster than pools, and the reverse, so that the relative length of riffles and pools is variable. This means that the channel roughness, as resistance to flow, should not be expected to have a simple relationship with channel width. Instead, it would be expected to vary depending on which of these bedform characteristics, generally controlled by variation in other variables, is most adjustable.

4.1.7. Roughness and slope

Steep streams are generally expected to be rougher than streams with lower slope, because larger sediment particles are characteristic at steeper slopes. In steep streams, the high proportion of the sediment that is coarse may be in part a characteristic of the sediment supply, with larger sediment being delivered to steeper streams. However, particle size and slope appear to be closely related, suggesting that the channel slope and sizes of sediment at the surface are mutually adjusted. The lengths of pools and riffles also vary with slope, but in such a way that, in a given study area, pool lengths increase and riffle lengths decrease with slope. These opposing trends between riffles and pool lengths, and between particle size and riffle length, suggest that the roughness of pool-riffle streams may either increase or decrease with slope. Bathurst and others (1981) observed that roughness of the sediment surface increased with slope.

4.1.8. Roughness and width of the particle size distribution

Einstein (1950) noted that the dimensionless mobility of sediments in flume runs varied widely for poorly-sorted sediments, but was relatively well-constrained for uniform sediments. Einstein (1950) recommended that at least three particle size classes be used in evaluating sediment transport to address the effect of the width of the particle size distribution.

Bathurst considered the effect of sediment gradation in an evaluation of roughness in streams, relating it to the graphic standard deviation, defined as log (D_{84}/D_{50}) (Bathurst and others, 1981). Variations in the quantity of sediment supply may also modify channel roughness (Einstein, 1950; Kirchner and others, 1990; Buffington and others, 2002).

The distribution of the exposed height of particles is related to, but different than, the particle size distribution. The distribution of height differences between pairs of nearby particles depends directly on particle exposure, which is only indirectly related to the median particle size.

For instance, if a sediment mixture consists of primarily gravel, it may have a void volume of perhaps 20 to 25 percent or even up to 30 percent (Pizzuto, 1990). If the sediment size distribution is strongly bimodal, consisting for example of medium sand and medium gravel, a fraction of sand approaching the void volume would probably be required to generate a relatively smooth surface between the larger particles. Then, the difference in height of nearby particles may be quite small, i.e. the surface may be relatively smooth with, in many places, only the top of larger particles rising above the local level of the bed. If there is a relative lack of finer particles, the larger particles will tend to rise relatively high above their surroundings, especially the recently deposited particles.

The maximum height difference between nearby particles can also be greater than the particle size. For example, in a pebble cluster where several large particles are piled on top of each other, perhaps buttressed by other large particles, the width of the cluster may be similar to typical particle sizes, but the height difference between the top of the cluster and adjacent particles is much greater than the typical particle size. Thus, fine grains may fill the interstices between larger particles, resulting in a relatively smooth surface, but, with fewer fines, the larger particles may rise well above their surroundings (e.g., Kirchner and others, 1990).

The experiments of Iseya and Ikeda (1987) suggest that an increasing content of fines enhances mobility, thus resulting in a lower channel slope at equilibrium. Assuming that greater

fines are associated with lower roughness, these experiments suggest that particulate roughness decreases as the fines content increases, and there are associated reductions in slope and increases in particle mobility. Buffington and others (2002) note that laboratory experiments demonstrate that scour at obstructions decreases as the width of the particle distribution increases, and also with an increase in the median particle size. Because the relationship appears to depend more on size than on width of the distribution, it is not clear whether this case is analogous to the case in the model, where fines increase as the width of the particle size distribution increases. Thus, these observations suggest that particulate roughness increases and the trend in form roughness is unclear.

4.1.9. Roughness and shear stress

Gessler (1990) argued that a characteristic particle size was not adequate to predict resistance to flow, given the variability in transport and the development of particle patterns on gravel bed surfaces under water-flows. The associated flume studies of Ahmed (1989) suggested that roughness due to particle arrangements peaked at about the critical shear stress for the mixture. Bathurst and others (1981) noted that critical shear stress and roughness of the sediment surface both increase with slope, suggesting an increase in roughness with shear stress.

4.1.10. Roughness and particle protrusion

Variations in the distribution of particle sizes in sediment allow variations in the extent to which fines allow development of a relatively smooth surface. An additional factor is the distribution of relative particle exposure for the particles, i.e., what fraction of an individual particle typically protrudes above its surroundings. Individual particles may rise high above their surroundings, may all be centered at about the same level, or the larger particles may be generally surrounded and set well below the level of the largest particles, corresponding to the variations of the surface from rough to smooth. A simple thought experiment suggests a general criterion for characterizing the distribution of relative particle protrusion on a sediment surface. A recently

deposited particle is most likely to have a high relative particle protrusion, not yet being surrounded by many subsequently deposited particles. The particles of a particle size class that occupies a disproportionate fraction of the surface will then tend to also have a disproportionate fraction of particles with high relative particle exposure.

Parker and Klingeman (1982) concluded on theoretical grounds that an increased protrusion of coarse particles conferred a relatively minor increase in mobility of the coarse particles. They identified the primary element that tended to enhance mobility of large particles, expected as a mechanism necessary to offset the greater mobility of fine particles, as increased areal exposure of the larger particles as a result of surface coarsening process.

4.1.11. Surface roughening evaluations in physics

Work in physics on roughness of particulate surfaces has found that the surface evolves to a stable roughness, and the stable state is rougher for surfaces with a larger area. This trend in the surface roughness is characterized as a finite size effect. Essentially, direct interactions between particles are short-range, but where each small area of the bed is somewhat correlated with nearby areas, the effective correlation length increases.

One of the particle dynamics models reported in the physics literature includes an analysis of the 'tilt-dependence' of roughening. The existence of tilt dependence, i.e., a variation of roughness with slope of the particulate surface, provides evidence for the presence of a non-linear response in the system evaluated (Krug, 1989, Barabási, 1992). An analysis by Barabási documented the degree of roughness associated with varying tilt (varying slope) and differing degree of coupling between the particle layer and a fluid layer. The result is a convoluted pattern of variation in roughness as the slope varies.

4.2. Methods: summary of the model

The model results presented here are derived from a particle interactions cellular automata model, or PICA model, which uses simple parameterizations of sediment and water flows in a channel, moves all sediment particles that are deemed mobile in a given time step, and thus evolves the channel form. The model is described in detail in Chapter 1.

Mechanisms in the model are kept to a minimum. Simulations reflect particle interactions as the fundamental control on which particle configurations persist and which configurations are unstable, so that they are 'dissembled' during sediment transport. In the PICA model, the transport direction of a mobile particle or group of particles is always toward the lowest adjacent cell (cells connected only along the diagonal are not considered to be adjacent). No other controls are reflected in the model design. In particular, no influence that arises with spatial variations in flow is included. A diagrammatic sketch of the model surface is shown in Figure 4.1

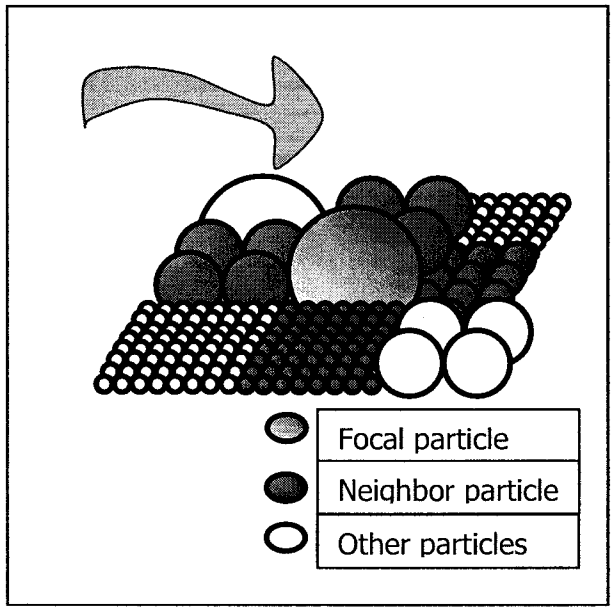

Figure 4.1. Sketch showing the relationship of a focal particle and its surrounding neighbor particles. The above sketch shows a view of the model grid, with particles of different sizes assigned to model cells. A given particle, termed the focal particle, is determined to be mobile only if the four surrounding particles leave the focal particle sufficiently exposed.

The flow complexities are strongly simplified in the model, such that all flow effects are based on a mean value, and subsumed in the criterion for motion. Conversely, although sediment is also simplified, it is less simplified than in the typical approach that replaces spatial variation in particle size with a mean size throughout the area of the channel, or perhaps an average across a cross-section.

The threshold for motion of the particles in the model is defined in terms of the relative particle exposure. The sketches in Figure 4.2 show the relationship between *e*, the average exposed height, and the particle diameter, *D*. The runs described here generally have a constant relative particle exposure threshold near 1/8th, for which 0.13 of the height of the particle is exposed. A particle with a relative particle exposure at about 1/8 is shown in Figure 4.2b. In one series of model runs, the threshold was not constant, but was varied from 0.23 up to 0.48.

Channel roughness was evaluated in several sets of runs in which only one variable was incremented between each run in a given set. The variation series includes five sets of runs, with variation in bed width, slope, fines fraction, mobility threshold value and channel length. Variation in the mobility threshold may be considered as either reflecting a variation in flow intensity (parameterized by discharge, shear stress, etc.), or a range of uncertainty in the mobility threshold for a given particle size in a given configuration of particles on the channel bed.

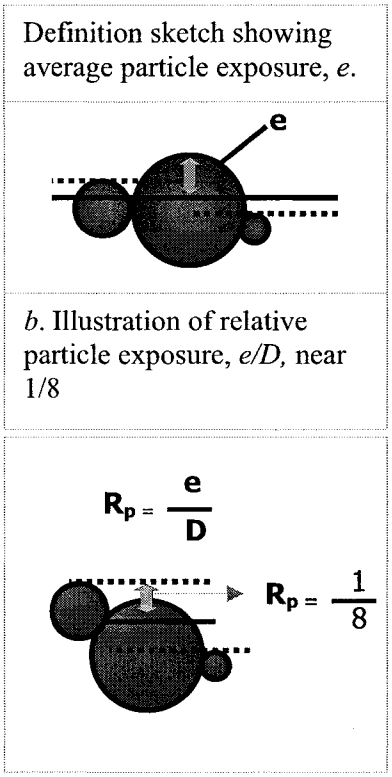

Figure 4.2. Definition sketch for relative particle exposure. The average of the height that particles in one cell rise above (or are inset below) the average height of particles in the four neighbor cells is defined as the exposure, *e*. The relative exposure is defined as the ratio of *e* to particle size, *D*.

In the runs with increasing channel width, the width was modified by expanding the width of the channel bed only. The length scale in both plots is defined as the square root of the channel area, so the rates of change with increasing length scale are comparable in the two plots.

4.3. Methods: scaling relation for roughness.

4.3.1. Evaluating roughness of the modeled channel surfaces

The roughness of the model surface is characterized using the interface width. The interface width is defined as the root mean square of the height deviations, normalized by the square root of system size. This definition is currently used in physics to evaluate the roughness of surfaces resulting from the deposition and subsequent movement of particles. The method is also closely related to the zero-crossing method used in some evaluations of pool-riffle channels.

The height deviations are the set of measurements of how high surface particles rise above (or are inset below) their surroundings. The height deviation for an individual cell is simply defined as the difference between the tops of the particles in that cell, and the local height of a sloping plane fitted through the whole undulating surface being evaluated. A schematic illustrating height deviations is shown in Figure 4.3 and the height deviations in individual cells are denoted by the vertical arrows (up and down) in the figure. The height deviations for several adjacent cells are illustrated in Figure 4.3.

The height deviations, h_d, are defined as

$$h_d = [\, h - h_{mn} \,]^2 \qquad (4.1)$$

where h_d is the height deviation for an individual cell, h is the height of the tops of the particles in the cell, and h_{mn} is the local height of a sloping plane fitted through the surface forming the bed. The interface width, w_r, is defined based on the root mean square of the height deviations. The interface width is given, for cells, i, as

$$w = \frac{1}{L_s}\sqrt{\sum h_d^2(i)} \qquad (4.2)$$

where L_s is the system size (Barabási and Stanley, 1995), defined as a length scale. The system size was defined for this study as the square root of the area of the channel domain evaluated.

Roughness data were obtained for two different areas, for the channel as a whole and for the channel bed. In both cases, the system size was based on the area evaluated.

$$L_s = (W L)^{1/2} \qquad (4.3)$$

Roughness in the sense defined above may reflect the combination of all roughness elements, including particles, bedforms, form of the banks, etc., not only particle (i.e., grain) roughness.

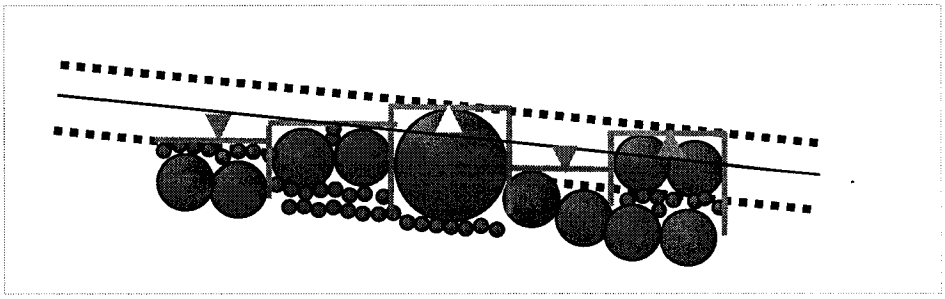

Figure 4.3. Sketch showing a vertical profile through particles at the interface. The cell boundaries and elevation of the particles in each cell are indicated by the thick gray lines. The dashed lines bracket the highest and lowest level of the tops of the particles, indicating the top and bottom levels of the interface. The thin black line shows the average level of the interface. The vertical arrows pointing up and down show the particle exposure, i.e., the height of the particles in each cell relative to the average level in the interface.

The detailed form of the banks is included in the channel roughness. Bank forms are largely excluded from the evaluations of bed roughness. The primary reason is that conditions at the banks control input of sediment from the bank area to the bed area. Thus conditions in the bank areas may affect the observed roughness.

4.3.2. Roughness scaling of the relative particle exposure model.

The full scaling relation, for both the dynamic phase (increasing roughness) and stable state (constant roughness on average), can be written as follows (Amar and Family, 1990):

$w_r(t) \sim L^{\alpha}\, \mathbf{f}(t/L^{\alpha/\beta})$

where the scaling function, **f** is given by

$\mathbf{f}(u) \sim u^{\beta}$, for $u << 1$,

and

$\mathbf{f}(u) \rightarrow$ constant, for $u >> 1$.

The variables of interest in the interface dynamics are the roughness exponent, α and the growth exponent, β. These characterize the scaling of the interface width; $w_r(t)$ with system size, L, and time, t, respectively (Amar and Family, 1990; Barabási and Stanley, 1995). The exponent $z = \alpha / \beta$, is referred to as the dynamic exponent.

4.3.3. Roughness scaling of the relative particle exposure model.

In surface growth models in physics, the temporal pattern of surface roughening has been characterized as follows (Barabási and Stanley, 1995). The earliest evolution is characterized by initial transients in the roughness, w_r. Next, the roughness begins to adjust, increasing or decreasing with time, and showing a trend over time, although the roughness at any timestep is quite variable. Finally, the roughness 'saturates,' reaching a value that is steady on average, although with continuing fluctuations that vary from small to large. The characteristic of being steady on average is referred to here as a quasi-stable roughness, and often shortened to a 'stable roughness.' The time at which the surface roughness transitions to a stable roughness value is referred to as the time at saturation, or the time at crossover, t_x. The roughness and length of time to saturation together characterize the rate of roughness change.

The relationships between roughness, time to saturation and rate of roughening are diagramed in Figure 4.4. In the first sketch, at the lower left, the evolution of roughness is plotted for three simple examples of a time series. All the variables are log-transformed; $\log_{10}$ is used in this study. All three plots start at the origin and the roughness, shown on the y-axis, initially increases over time. Each curve (line trace) in the plot reaches its maximum roughness at a different time, giving three different cross-over times. In the saturated phase after cross-over, the three curves each become horizontal, but each at a different level of saturated roughness.

The relationships can be simplified by rescaling the plots. The x-axis, showing the roughness, is rescaled as log (w/L^{a}), as shown in the upper sketch. The y-axis, showing time, is rescaled to log (L^{z}). The rescaled plot, shown in the lower right, shows that all the plots are identical in a rescaled plot.

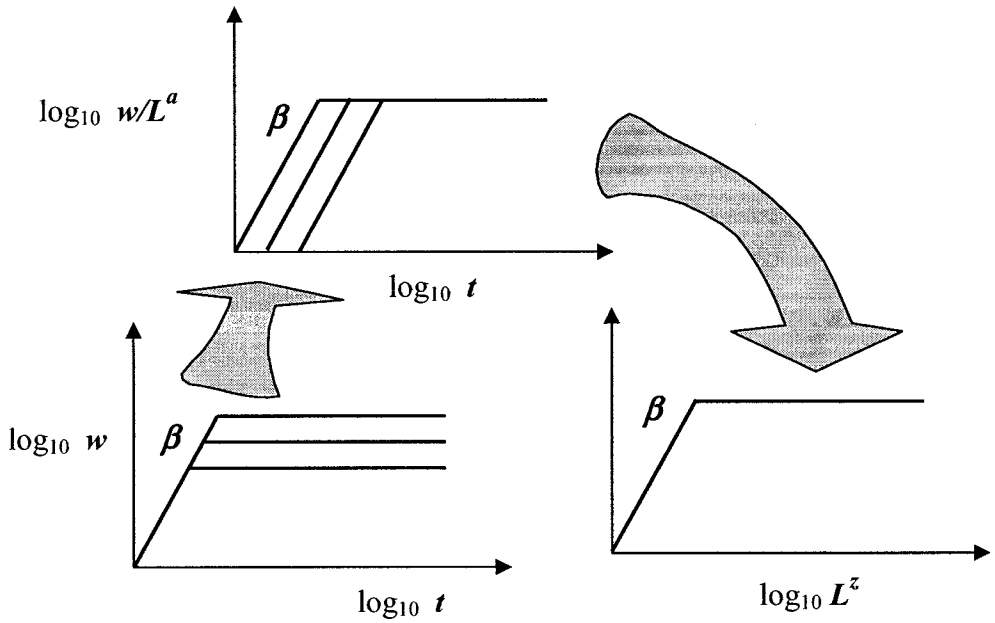

Figure 4.4. Scaling form. Sketch illustrating the process of scaling the roughness for individual systems by a power of system size, L and by a power of time, t (in model timesteps) to reach a stable roughness state. The roughness rescaled by w/L^{α} is represented in the lower left sketch; α is a scaling exponent, referred to as the roughness exponent. The roughness is also rescaled by L^{β}. The final rescaling, shown in the lower right, is by L^{z}, where z is referred to as the dynamic exponent, and is given by $z = \alpha/\beta$ (*after* Barabási and Stanley, Figure 2.5, p. 24).

The mechanism that generates the scaling relationship has been interpreted as a result of short range correlations that effectively expand over wider areas as particle transport (deposition and erosion) proceeds. The correlations have an effective length, and that length may increase until it spans the entire system. In the absence of any characteristic length scale, the interface width is expected to grow with some power of time. After a characteristic time, the length over

which the fluctuations in interface width are correlated becomes comparable to the length, L. At longer times, the surface correlations stop growing and the surface reaches a steady state characterized by a constant width (Family, 1990, p. 563). In the steady state, "the surface is a scale-invariant self-affine fractal" (Family, 1990, p. 565)." A self-affine fractal is a fractal that does not have exactly the same shape as it occurs over a wide range of scales, but rescaling different dimensions by different factors makes the rescaled feature exactly the same at all spatial scales.

The interface width $w_I(L,t)$ is a measure of the roughness of the interface. It may be regarded as a measure of the correlation length perpendicular to the surface, symbolized ($\xi_\perp$). There is an analogous parallel correlation length, $\xi_\parallel$, which is proportional to t^z for small time, and to L for time beyond the characteristic time (Family, 1990, p. 565 - 566).

Family (1990) considered that the best available technique to evaluate non-equilibrium surface growth was a general scaling approach and this is the approach outlined above. It has become the standard approach to surface roughening analysis in physics (Family, 1990, p. 562; Barabási and Stanley, 1995). Based on the model results, the general pattern of roughness evolution in the PICA model is the same as the pattern found for similar models of particle deposition and erosion in physics. The PICA model is, however, more complicated to evaluate because it has a wider range of adjustable characteristics than most such models. Rather than simply including deposition, erosion and transport, this model also features multiple particle sizes, banks which influence both sediment supply and size of the domain, and variable slope and mobility of particles.

The beginning of the stable state duration was identified as the time when the difference between a linear trend through the previous generally increasing series of roughness values and the subsequent series of values that is near constant on average, reached a maximum. This method has the effect of incorporating any transition between the two in the dynamic phase. The

results of applying this method do not always select what visually looks like the break point (see Figure 4.5).

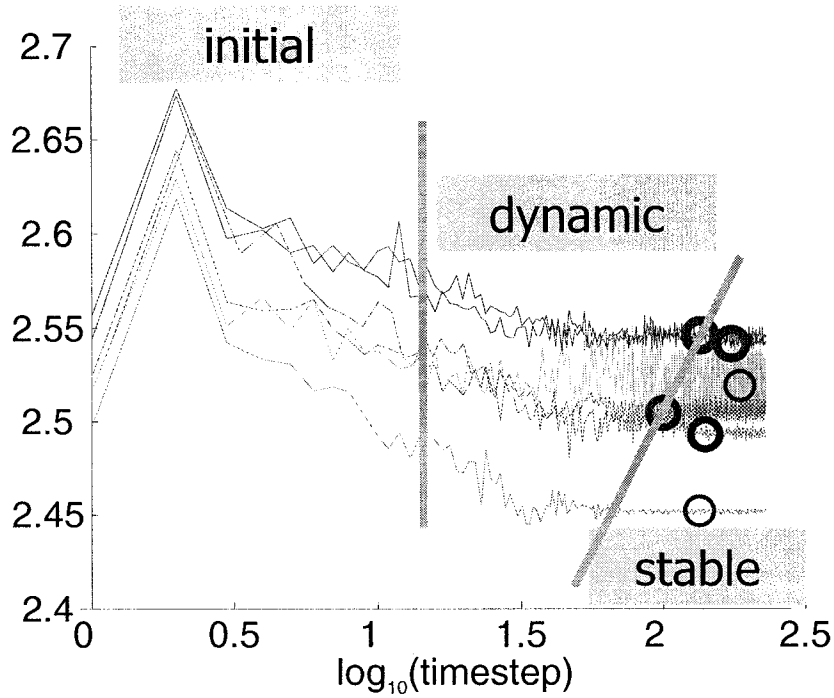

Figure 4.5. Roughness evolution in the model. Example illustrating the initial transients, the dynamic adjustment phase, and the following stable state in the roughness of the model channel boundary. The evolution of the surface roughness shown in the plot represents larger areas in the upper two plots shown in dark gray, the plots with patterned gray lines show the intermediate size domains, and the plots with light gray lines represent the smallest domains. The saturated roughness tends to be greater in larger domains. The wide gray lines show the transitions between initial transients, dynamic phase and stable roughness. The large circles show the time at which an automated routine identified the maximum difference between correlations of the roughness trend for earlier and later time. The most heavily drawn circles represent the cross-over picks for the two runs with the largest domains, the most finely drawn circles represent the cross-over picks for the smallest domains.

In the model, system size is parameterized as the square root of the area of the channel bed. The time evolution of the roughness for channels of three different sizes is illustrated in Figure 4.5, which shows the initial transients, the dynamic phase during which the surface roughness adjusts, and the quasi-steady state in which roughness has a stable value on average.

In summary, the basic relationships are as follows. In the absence of any characteristic length scale, the width is expected to grow with some power of time, i.e.,

$$w_r(L,t) \sim t^{\beta}. \qquad (2.3)$$

The saturated width, w_r is expected to have a power law dependence on L, with an exponent termed the growth exponent, α

$$w(l,t \rightarrow \infty) = L^{\alpha} \qquad (2.4)$$

4.3.4. Evaluating the time to saturation

The extracted time series of roughness values can be viewed as two time periods, an early time with increasing roughness over time, and a later time with a stable mean value of roughness. The transition point between the time period when roughness adjusts and the time with steady-state roughness was evaluated by finding the intermediate time step that maximized the difference between the slope of the correlation lines through roughness values for later and earlier time.

4.3.5. Controls on roughness as system size varies

The influence of the model initial conditions and mobility rules was evaluated for conditions at values spanning the range most relevant to the development of pool-riffle and steeper channels (Table 4.2). Because roughness has been shown to vary with system size, runs were also conducted with varying values of reach length. The bed widths range from 1.25 to 3 nominal meters. Reach lengths vary from 20 to 42 nominal meters. The values for initial slope range from 0.005 to about 0.11, channel width from about 4.6 m to 6.9 (18 to 27), and particle size distribution widths of 3 to 9 ϕ-size classes. The threshold for mobility varies from 0.13 to about 0.48. The range was chosen because particles that have a threshold near 0.5, i.e., half exposed, are expected to still be mobile in many cases. Even lower thresholds are used in some runs, representing increasing partial mobility of the particles. Although these relative particle exposure values may seem high for the degree of particle exposure at which entrainment occurs, the values

reflect the average of the 4 neighbor cell height, rather than an actual height which the particle has to surmount at initial motion.

The threshold for mobility in the model has more than one possible analogue in streams. It may be viewed as reflecting different levels of mean flow velocity, boundary shear stress, or related threshold criteria. Alternatively, different values of the threshold may be viewed as reflecting the uncertainty in the threshold criterion, the relative particle exposure, of motion for individual particles.

Table 4.2. Range of variation variable values in model runs

Reach length	80 to 165 cells (nominally 20 to 42 m)
Bed width	5 to 12 cells (nominally 1.25 to 3 m)
Channel slope	0.005 to 0.095
Particle size distribution width	3 to 9 phi size classes
Threshold relative particle exposure	0.18 to 0.48

The data are summarized below in the following form:

1. *Base roughness*. Define a base value of roughness for a surface with a slope that is common for pool-riffle channels (0.02), a moderate width (4.5 m), a reach somewhat longer (22.5 m) than it is wide, moderate bankfull depth (0.23 m), wide particle size distribution (8 phi sizes), and intermediate relative particle exposure threshold (e/D = 0.13). These runs have a channel length of 90 cells, giving a reach length 5 times as long as the channel width (Table 4.1).
2. *Effect of varying initial channel characteristics.* The roughness will be presented as variations in roughness as each channel variable is varied. Variation in roughness with system

size will also be presented as an exponent in the Family-Viscek scaling relationship. Variation in the rate of roughness adjustment will also be presented for each variable.

Roughness relationships were summarized for two cases; roughness within the area of the channel and within the area of the active (wetted) bed in the runs. However, the channel and the bed presented relatively similar relationships to roughness, and only the roughness of the bed is presented.

The variation series are presented as follows (see also Table 4.2).

1. *Reach length variation series.* A series of runs with reach length increasing from 23 to 42 m. The range of lengths is 90 to 165 cells.
2. *Channel width variation series.* Using the series with increasing width, define the variation of roughness with increasing channel area.
3. *Slope variation series.* A series of runs with slope increasing from 0.01 to 0.107.
4. *Particle size distribution variation series.* A series of runs with increasing width of the particle size distribution from 3 to 9 phi size classes.
5. *Mobility threshold variation series.* Variations in the relative particle size threshold from about 0.18 to 0.48.

The data obtained from the variation series can be used to define the following relationships:

1. A power law relationship for the saturated roughness for a given reach length and bed width as the size of the channel increases.

The direction and relative magnitudes of changes in roughness as initial channel characteristics of slope, particle size distribution and threshold value vary.

4.4. Results: preliminary experiments and roughness variation with system size.

4.4.1. Preliminary experiments

Two forms of the mobility threshold were considered. Bak (1996) describes 'extremal' rules, in which the model processes are limited to one or a few processes that are expected to control

long-term evolution, whereas processes that are expected to modify form and decay on rapid time-scales are not modeled. Early model runs included experiments with an extremal model, in which only the least stable particle moved in each time step – i.e., a single patch of sediment that was least stable. That model developed patches much more quickly and the patches were more distinct. However, I chose to use a deterministic rather than an extremal model for which the fundamental model process selection was based on an assumption that I felt would be more difficult to support.

4.4.2. System size: effect of channel width and reach length on roughness

The roughness evolution in the model runs varies as system size increases. As size increases, the surface roughness evolution includes (a) a longer dynamic phase and (b) greater roughness at the stable state. This is in accord with the results obtained in physics (compare Figures 4.4 and 4.5).

Roughness values for the model runs with varying channel width and length are shown in Figure 4.6. Figure 4.6a shows the modeled increase in roughness with increase in channel width; Figure 4.6b shows variation with reach length. The paired dot and triangle symbols represent two different methods for calculating roughness. The dot symbol represents the roughness evaluated by averaging over the duration when the channel bed had a stable average value for roughness. The transition times identified by the method are indicated by large circles on the time series plots. There is a general pattern to these selected points, but they only roughly follow a pattern. An approximate trend in the time to cross-over is indicated by the slanting, thick, gray line.

The triangle symbol shows the steady state roughness obtained by extending a correlation line through the steady state roughness time series, and identifying its intercept. If the identified steady state time is not nearly constant on average, the roughness intercept differs from the estimate obtained by averaging. Where the estimates are not the same, there is some residual trend of changing roughness over time. Note that there is one plotted roughness where the triangle

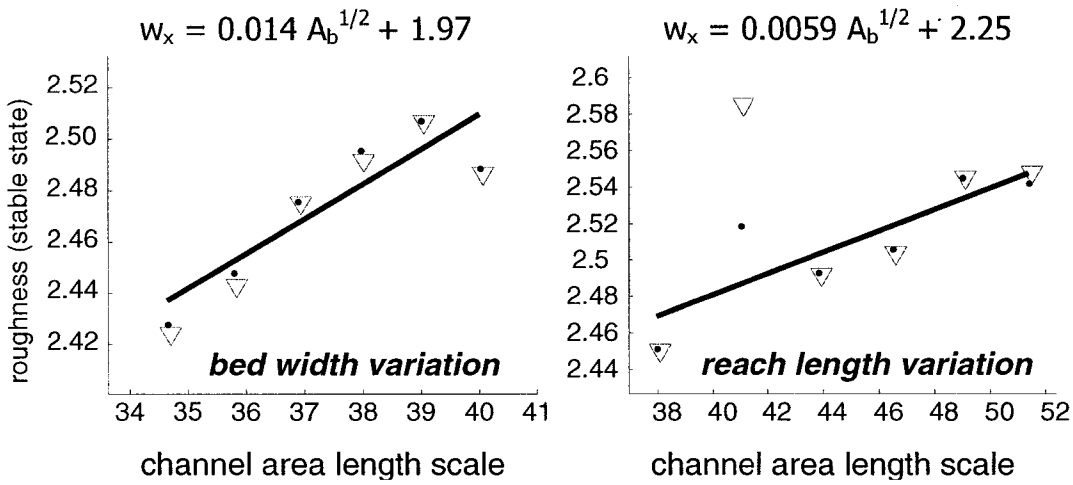

Figure 4.6. Roughness variation with width and length. Surface roughness scales with the size of the domain in which particle interactions occur, i.e., roughness increases as the width of the bed increases, and as the length of the reach increases.

and dot symbols for a run plot at distinctly different roughness. Aside from that anomalous point, the plotted data in Figure 4.6 span about the same range for increasing width and increasing length. For both variations, the roughness spans a range from about 2.4 to 2.5. Given the difficulty in determining the cross-over time, there may be no more than one significant digit in these correlations. Even with only two digits, the intercept values in the correlations are similar, whereas the slopes are quite different. The correlation for bed width shows an order of magnitude greater response than the correlation for increasing reach length. Roughness increases more rapidly with reach length than with bed width, at least for relatively narrow channel beds such as used in these runs.

In the runs with increasing channel width, the width was modified by expanding the width of the channel bed only. The length scale in both plots is defined as the square root of the channel area, so the rates of change with increasing length scale are comparable in the two plots. In both plots, roughness is plotted against the square root of the evaluation area (an approximation of the area of the bed).

Roughness increases more rapidly with reach length than with bed width, at least given the narrower channel bed used in these runs. The concept that roughness is expected to vary with domain size is well-established in the evaluations of surface roughness in physics. In terms of streams, the size of the domain should be defined as in the technical meaning of a reach; i.e., a length of stream where processes and forms are essentially constant, without distinct variations in discharge, sediment input, or externally imposed form characteristics.

In this study, early work with a model version with wrapped boundaries rather than channel banks indicated that width and length of the reach had equal effect on roughness. That is, the roughness varied with the area of the reach. However, when the model channel is confined by banks, roughness responds differently to an increase in channel width and an increase in reach length (Figure 4.6a, 4.6b). It is expected that the effect of channel width and reach length on roughness will also vary for streams. The relationship with domain size must consider variation of roughness with channel length and with channel width as independent variables.

In the model runs presented here, width of the channel bed has a much greater effect on roughness than does reach length. Wider channels have been shown to develop more lateral variability in depth in flume studies (Toro-Escobar and others, 2000), and this may explain the greater responsiveness of roughness to changes in width. The effect of changes in width may also vary as other parameters vary.

4.5. Results: roughness as slope, width of the particle size distribution and the threshold for motion vary

4.5.1. Effect of slope on roughness

The model results show no trend in the roughness of the channel as a whole as channel slope is varied (Figure 4.7, left panel). The slope of the bed may be more relevant than surface roughness. Roughness of the bed is shown relative to bed slope in the Figure 4.7 central panel. The roughness is much less for the bed (near 0.52 rather than near 2.45). The lower roughness is

present because the channel banks constitute large roughness elements. There is variability in roughness as the final slope varies, but no clear trend. The area included in evaluating bed slope is based on the form of the channel bed.

The right-hand panel presents a comparison of the roughness in the active bed area and in the channel as a whole, relative to the active bed slope. The plotted estimate of roughness is the estimate obtained from averaging the stable state roughness values. The data show that the roughness of the channel (diamond symbol) exceeds the roughness of the active area. Also, the steeper the slope, the greater the difference, with decreasing roughness of the active area.

4.5.2. Discussion of variations with slope

Thus, the roughness of the channel shows no trend as slope increases, but is highly variable for the bed, and is similarly variable but increasingly less rough in the active area. The high variability in the bed area may reflect varying erosion along the bed, and a greater particle size in the outer margins of the bed. The greater smoothness in the active area may be attributed to the larger fraction of fines in the central portion of the channel.

The lack of variation in roughness with slope seems surprising because common experience is that steeper streams are coarser. However, this is not a necessary association, only a common one, because coarser sediment is more likely to be available and move from hillslopes into the channel in steeper terrain. The variability of roughness in the channel area suggests that the processes that develop roughness are more variable with slope than with the other variables considered here. There are three distinct types of possibilities. The first type of possibility is that evaluation of a single surface from the run results in anomalies because of short-term fluctuations. However, that did not appear to be an issue in the other variation series. Because the variability in the relationship between roughness and an influencing variable is most significant for the slope variation series, it may be related to within-channel variations in slope, i.e., with

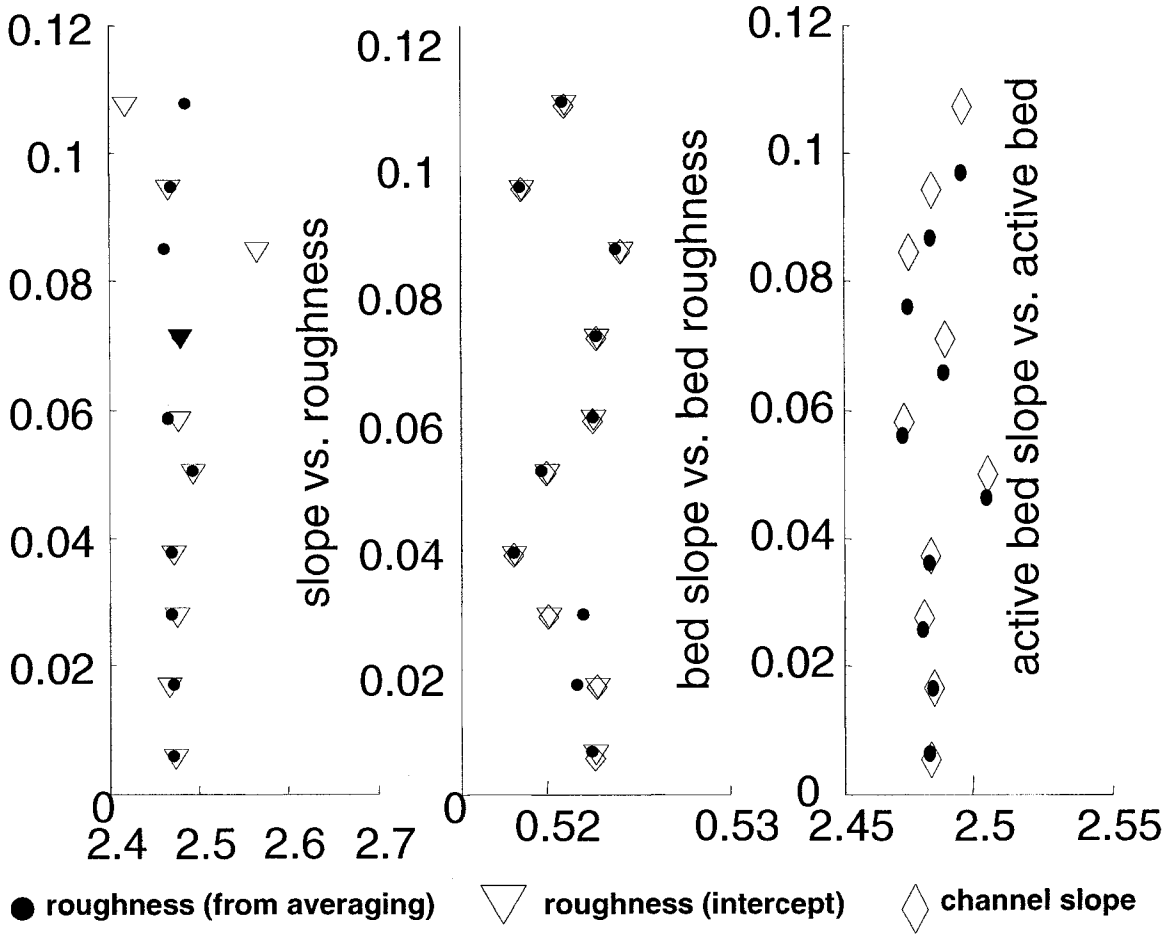

Figure 4.7. Variation in surface roughness with channel slope. The three plots show roughness, from left to right, for the channel as a whole, for the bed, and for the active bed. The two plots on the left show the intercept and averaging estimates of roughness for the channel and for the bed (symbols as usual). The plot on the far right shows the averaging estimates of roughness for the channel (diamond symbol), and for the active bed (dot symbol). Roughness does not appear to vary systematically with slope in any of these channel domains. However, the third plot shows that the active bed slope systematically deviates farther below the channel slope, as the channel and active bed slopes increase. Last panel shows bed roughness decreases relative to channel roughness as slope increases.

curvature along the channel length, which was apparent in some runs. A second category of influences is that the process that controls roughness must be the selection and direction of motion of the particles that are transported, and this is inherently a noisy process. The third possibility is that there is an interaction between slope and transport that inherently results in a pattern of roughness variation with slope that is complex. A complex pattern of variation was predicted by a study of tilt-dependent roughening (Barabási, 1992). That result suggests that the observed pattern of variation between roughness and slope may depend more on an interaction between the two, via the transport process, than on random influences. Such a pattern of variability is likely to involve interaction between slope, particle mobility, and the relative magnitudes of lateral and downstream transport, which are expected to change as slope increases. The following summary documents the effect of increasing channel slope on the distribution of transport directions, modifying the balance between upstream, downstream and lateral motion of particles.

The number of moves during steady-state time (4.8a) and the number of all moves during the run, in both dynamic and steady-state time (Figure 4.8b), are poorly correlated with slope. They show a tendency of fewer moves as slope increases, but with wide variability about the trend. The decrease in particle motion as slope decreases is surprising, but may represent a net increase in the fraction of particles that are stable, associated with the greater height difference between adjacent cells as slope increases. Moves in the downstream direction are constant, on average, and unrelated to slope (4.8c). Effective transport is defined as the difference between moves in the downstream direction and moves in the upstream direction. The net downstream transport is well-correlated with slope, and increases as slope increases (Figure 4.8d), as generally expected, absent the type of interaction effects documented by Iseya and Ikeda (1987).

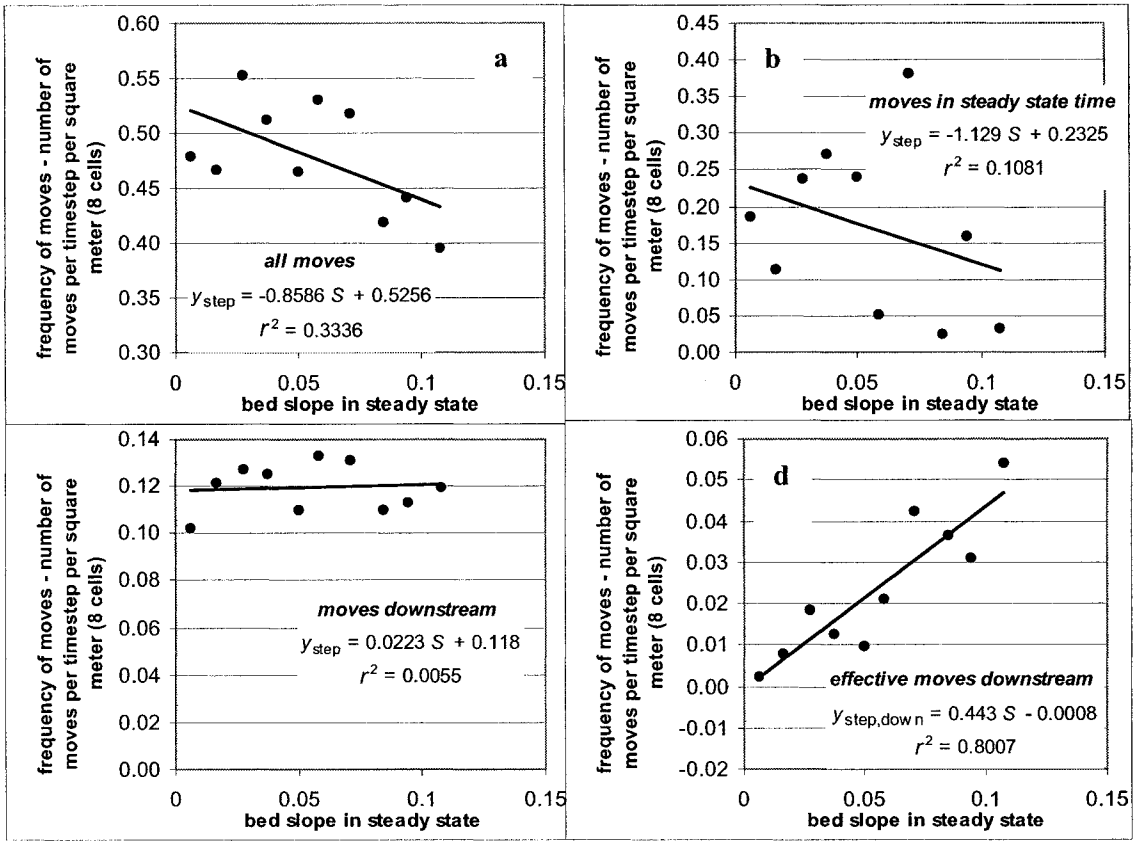

Figure 4.8. Relationships between the number of sediment 'parcels' that move, and the steady state slope of the bed. Increasing channel slope modifies transport direction such that net downstream transport increases as slope increases. Panels *a* and *b* show the all moves during steady-state time and all moves, respectively. These are poorly correlated with slope, but show a tendency to decreasing numbers of moves as slope increases (see text for discussion of this effect). Panel *c* shows the total number of moves in the downstream direction, and the number is constant on average and unrelated to slope. Panel *d* shows effective transport, which is the difference between the number of moves in the downstream direction, and the number of moves in the upstream direction. The net number of downstream transport steps is well-correlated with slope, so that downstream transport increases as slope increases.

4.5.3 Effect of particle size distribution width on slope.

The particle size distribution also affects the stable state slope, with decreasing slope as the width of the particle size distribution increases (Figure 4.9). The effect of particle size distribution was suggested as a significant control on transport by Einstein (1950), and this effect of the

particle size distribution appears to be one of the interacting factors to consider in evaluating slope evolution.

The effect of the width of the particle size distribution was investigated by documenting roughness in two series of runs with varying slope and with two different widths of the particle size distribution (Figure 4.10). The particle size distributions contain two and eight particle size classes, respectively. Roughness is greater when there are fewer size classes, but the trends with slope are parallel. These relationships indicate that roughness with eight particle size classes is less, at 2.47, whereas roughness is greater for the runs with two particle size classes, 2.59 (for the reaches at a standard length of 90 cells).

Finally, the roughness increases as the width of the particle size distribution increases, with the increase consisting entirely of finer particles a as shown in Figure 4.11. Roughness decreases as the width of the particle size distribution increases.

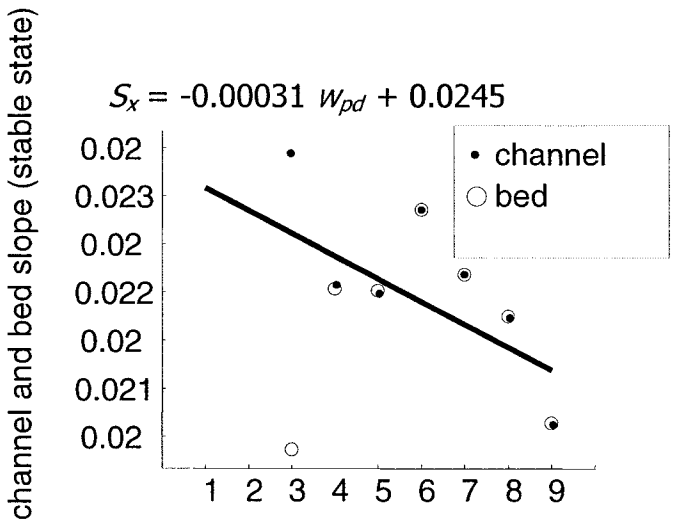

Figure 4.9. Variation in slope as the width of the particle size distribution varies. The slopes of the channel and of the bed are typically the same for the poorly sorted sediments. The difference between the channel and bed slopes is greater for the better sorted sediments, indicating greater adjustment when the width of the size distribution is narrower. Note that maximum size of sediment is the same in all of these runs, whereas the minimum size in the sediment increases to the right. Thus, the points on the left represent channels without fines, and the channels that plot on the right have more fines. Two to nine particle size classes were used in the runs.

4.5.4. Effect of threshold for mobility on roughness

The threshold for mobility varies from 0.13 to about 0.48, representing an increase in the fraction of the particles that are mobile. In the model runs, roughness increases as the threshold increases, i.e., channels are

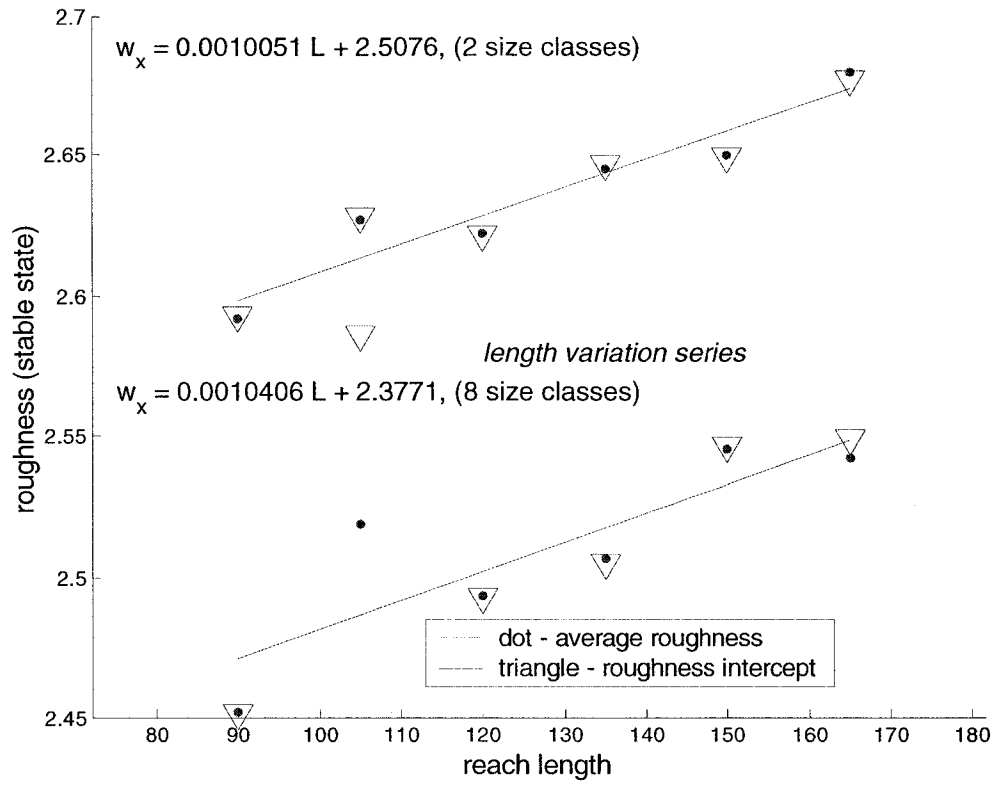

Figure 4.10. Roughness variation with reach length for different particle size distributions. The roughness intercepts differ for the two series, but the slope of the correlation is similar for the two studies. Thus width of the particle size distribution sets the magnitude of roughness, but does modify its pattern of variation with channel length. Reach length is given in cells; each cell is nominally 0.256 m in length and width.

rougher when sediment is less mobile (Figure 4.12). This variation in roughness is greater than the variation with any other of the controls considered, with roughness values from about 2.49 to 2.52.

4.5.5. Effect of transport on relative particle exposure

The minimum, mean and maximum values of relative particle exposure at the surface of the channel bed also vary with transport (Figure 4.12). For the threshold variation series, the maximum value increases slightly, and the minimum value increases considerably. The variation in the minimum value is observed for the relative particle exposure in a series in which the threshold is used as the criterion for motion. Thus, as

the mobility of the sediment decreases through the series (as a result of the increasing threshold for motion), the minimum values of relative particle exposure range from -176 to -56 mm as the relative particle exposure threshold increases from 0.018 to 0.048 (mobility decreases).

4.6. Rates of channel adjustment

The model also provides information on variation over time, presented here as the rate of roughness adjustment. A series of five plots are presented in Figures 4.13 and 4.14. The first two graphs show the rate of change of roughness as channel width and length increase (Figure 4.13). The rate of roughening increases as reach length increases. This effect is dependent on the limited length of the model domain, but may have an analogue in streams. For example, where stream characteristics are homogenous, on average, for a

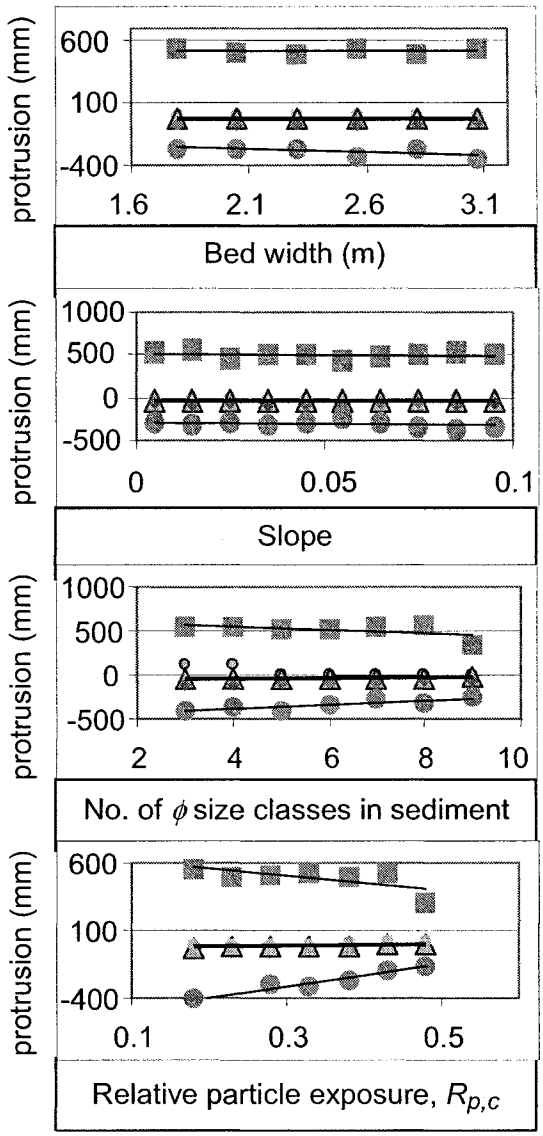

Figure 4.11. Variation in the distribution of the height of protrusion in the variation series. The minimum, 25th, 50th and 75th percentiles, as well as the maximum values of the height that particles on the bed rise above their neighbors (the shelter margin) are shown for the four variation series. The threshold variation series shows a decrease in the range of particle exposure. The series with varying width of the particle size distribution also shows a similar but lesser degree of adjustment.

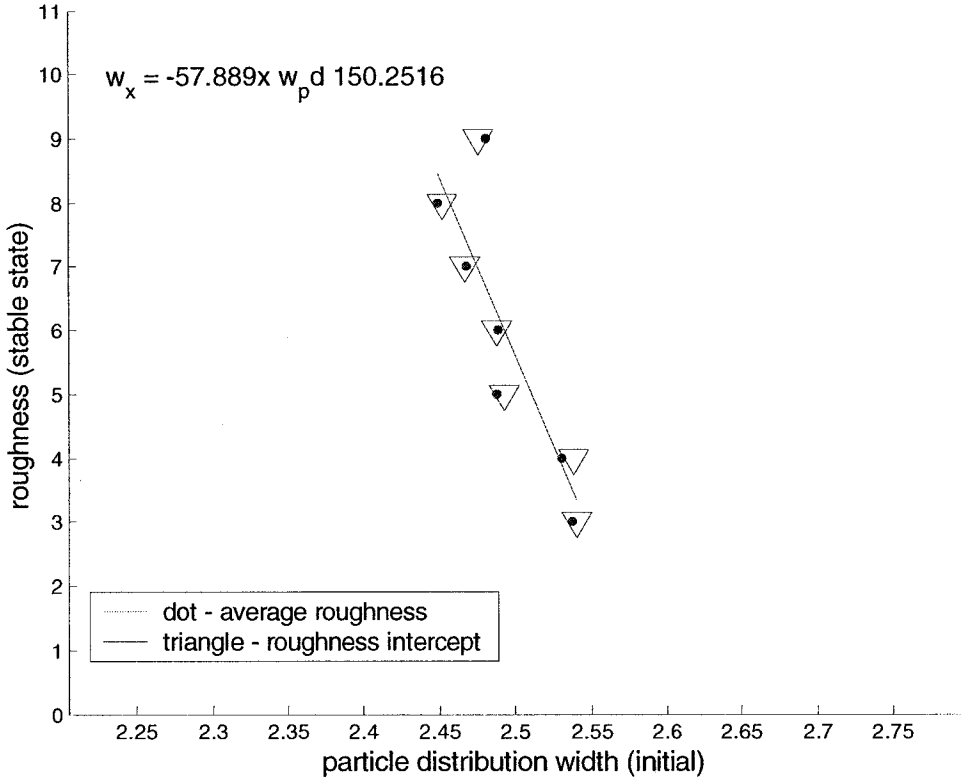

Figure 4.12. Roughness variation as the width of the particle size distribution varies. Roughness decreases as the width of the particle size distribution increases.

considerable length , followed by a reach with different channel form or transport conditions (as at a channel construction or at a confluence), each reach may adjust toward a different stable roughness condition, and thus the break in channel characteristics acts as an effective length of the domain within which roughness has a constant, on average, roughness. The rate of roughening decreases as bed width increases.

The last two graphs (Figure 4.15) show that the rate of roughening decreases when the sediment has an increasing component of finer particles, and the roughening rate increases as the mobility threshold increases

Table 4.3. Correlation equations for steady state roughness, w_x for various channel conditions

standard configuration	$w_x \sim 2.45$	
reach length	$w_x = 0.0059\ A_b^{1/2} + 2.25$	$n = 6$
initial channel width	$w_x = 0.014\ A_b^{1/2} + 1.97$	$n = 6$
initial slope	*constant*	$n = 10$
initial particle distribution width	$w_x = -57.9\ w_p + 150$	$n = 7$
threshold	$w_x = 0.078\ e/D + 2.48$	$n = 7$

Table 4.4. Correlation equations for roughening rate for various channel conditions

reach length	$dw_x = -0.00028\ L^{-017}$	$n = 6$
initial channel width	$dw_x = -0.025\ W^{0.083}$	$n = 6$
initial slope	$dw_x = 0.058\ S^{-0.031}$	$n = 10$
initial particle distribution width	$dw_x = -0.0039\ w_p^{-0.011}$	$n = 7$
threshold	$dw_x = 0.108\ e/D^{-0.04}$	$n = 7$

The third plot shows rates of roughness adjustment for systems with a range of slope. There may be a tendency to increase, but, as with the stable state data, there may also be a more complex variation, with the rate of roughening rising and falling.

4.7. Summary of roughness variations

In summary, the data presented illustrate features of channel roughness that arise in a model in which particle interactions are the primary control on particle mobility. Given that particle interactions control channel adjustment, the model suggests, first, that roughness increases with the mobility threshold, and that channel adjustment is faster when the exposure threshold is lower (higher mobility). This corresponds to faster roughening and faster evolution to a stable state when sediment is more mobile.

Larger systems evolve more slowly and for a longer time than smaller systems. However, this is balanced by the fact that larger systems continue to evolve until they are rougher than smaller systems. This increased roughening is stronger for longer reaches (at least reaches up to 20 m) and weaker for wider channels (at least channels up to 3 to 4 meters wide). Note that the effect of reach length probably contains at least two components; one is an effect of the limited length of the model domain, and the other is the greater likelihood of unstable sites where local change can be initiated. The latter may mean that narrower streams are more likely to be limited in their ability to adjust by the finite width of the system.

Roughness changes with varying slope appear to interact with multiple channel characteristics. These include, at minimum, interactions with sediment mobility and particle size distributions. The dependence of roughness on transport characteristics is expected to reflect interaction among at least: (1) transport thresholds, (2) width of the particle size distribution and its influence on slope, and (3) interactions with slope, including (a) enhanced downstream transport relative to mobilization when slopes are high, and (b) adjustment of active bed slope as a result of transport-driven adjustments in particle size. Roughness also increases as the threshold for motion increases, which decreases the mobility of the sediment, thus decreasing its ability to modify the channel roughness.

4.8. Rate of roughening

The results of the variation series, with variations in width, slope, particle size distribution and sediment mobility, were used to document the rate of change in roughness with time prior to reaching the steady state roughness (quasi-steady state condition). The rate of roughening of the channel bed surface shows little variation with reach length, decreases with bed width, and shows

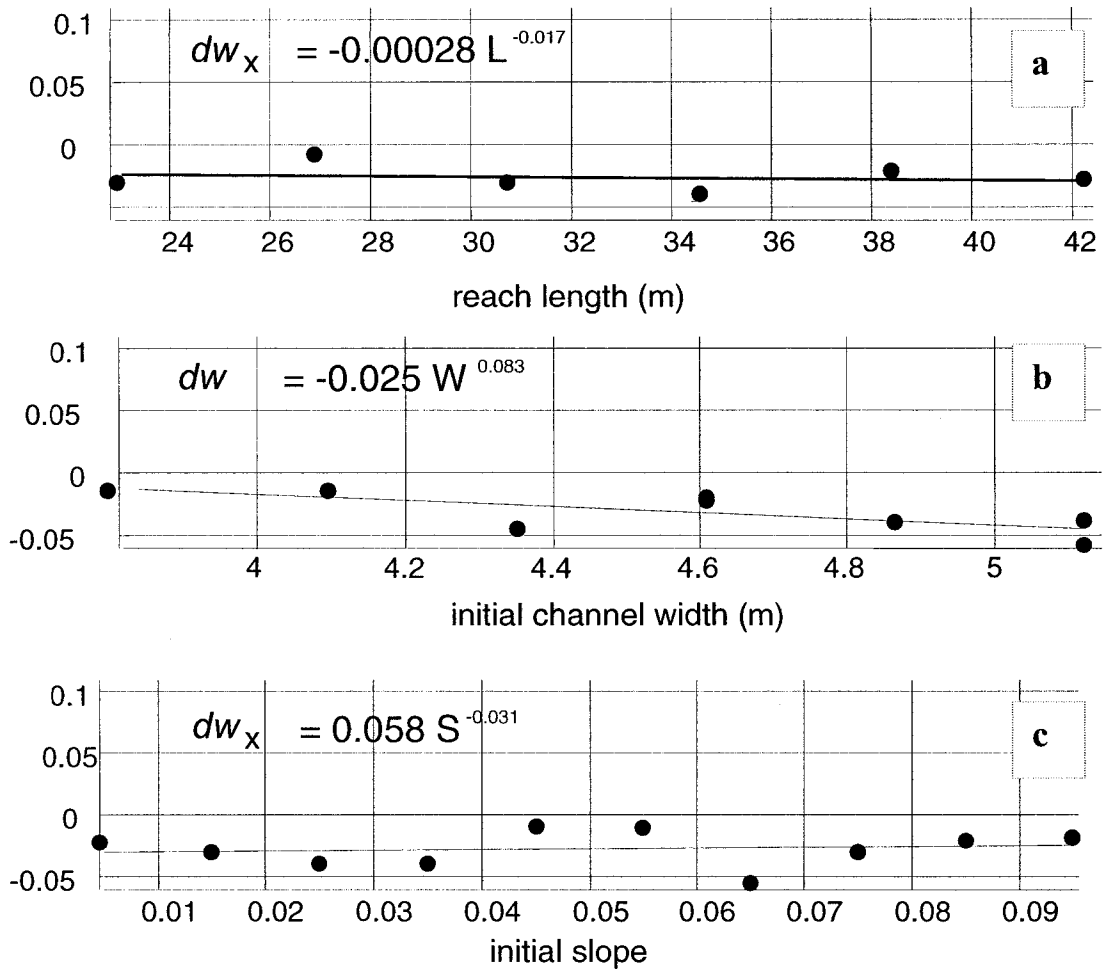

Figure 4.13. Rate of roughening as reach length, bed width and slope increase. The rate of roughening varies little with channel length, and decreases as the channel width increases. The rate of roughening has no distinct trend with slope.

no clear trend with slope. The rate of roughening varies with both the particle size distribution of the sediment and the threshold for motion. Roughening of the bed surface in the model runs was less rapid as more, finer particle size fractions were added to the sediment. The rate of roughening increased as the relative particle exposure threshold for motion increased, i.e., for less mobile beds. It is counterintuitive that roughness would increase as the mobility goes down, but this is likely to reflect the effects of scattered and sporadic motion, in contrast to smoothing of the

interface that occurs when many particles move until the surface becomes smooth enough that most particles are sheltered by their surroundings.

4.9. Particle exposure

4.9.1. Particle arrangements and distributions of particle exposure

Particle arrangements include formation of textural patches, described above, and variation in the exposure of particles, described in this section. Particle exposure varies as channel form changes, and may include patches where particles are more well-exposed or less well-exposed. The relative particle exposure generally does not exhibit distinct, statistically significant patchy or regular patterns at the channel bed surface. However, several distinct patches are visible in the low mobility runs of the threshold variation series.

In addition, both the range of particle exposure values, and the height of exposure varies within the runs, as shown in Figure 4.13. The minimum, 25th, 50th and 75th percentiles and the

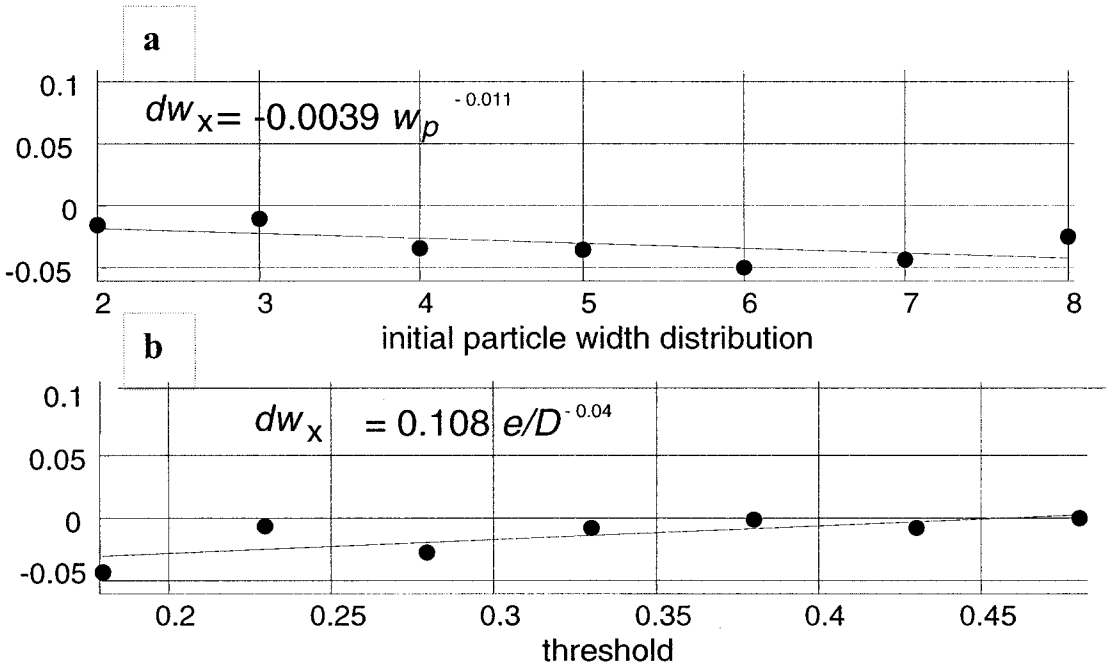

Figure 4.14. Rate of roughening as width of the particle size distribution and the mobility threshold increase. The rate of roughening decreases with the width of the particle size.

maximum values of the height that particles on the bed rise above their neighbors (the shelter margin) are shown for the four variation series. The threshold variation series shows a decrease in the range of particle exposure. The series with varying width of the particle size distribution also shows a similar but lesser degree of adjustment. A minor adjustment is also shown by the minimum height of protrusion in the bed width and slope variation series.

4.10. Fluctuations in particle transport over time

4.10.1. Fluctuations and self-organized criticality.

Large fluctuations in the quantity of sediment in transport occur during early phases of the model adjustment. These fluctuations tend to die out with time. Others have described such intermittency of events as a characteristic of self-organized critical systems (Bak, 1996; Hergarten, 2002). Such fluctuations are a result of variations in the relative particle exposure, which determines particle mobility in the model, as shown in Figure 4.14. The upper panel in the figure shows the time sequences and sorted threshold values (log10-log10) for at transport events, for a run with a relative particle exposure threshold of 0.13. The second panel shows the relative particle exposure value sorted to present the distribution of the threshold values for transport events. Panels three and four show the same data, but with relative particle exposure in millimeters.

4.10.2. Relationship between transport and steady state slope.

Relationships between the number of sediment 'parcels' that move and the steady state slope of the bed are shown in Figure 4.8. Increasing channel slope modifies transport direction such that net downstream transport increases as slope increases. Panels *a* and *b* show the total number of moves during steady-state time and all moves, respectively. These are poorly correlated with slope, but show a tendency to decreasing numbers of moves as slope increases. Panel *c* shows the moves in the downstream direction, and the number is constant on average and unrelated to slope. Panel *d* shows effective transport, which is the difference between the number

of moves in the downstream direction, and the number of moves in the upstream direction. The net number of downstream transport steps is well-correlated with slope, so that downstream transport increases as slope increases.

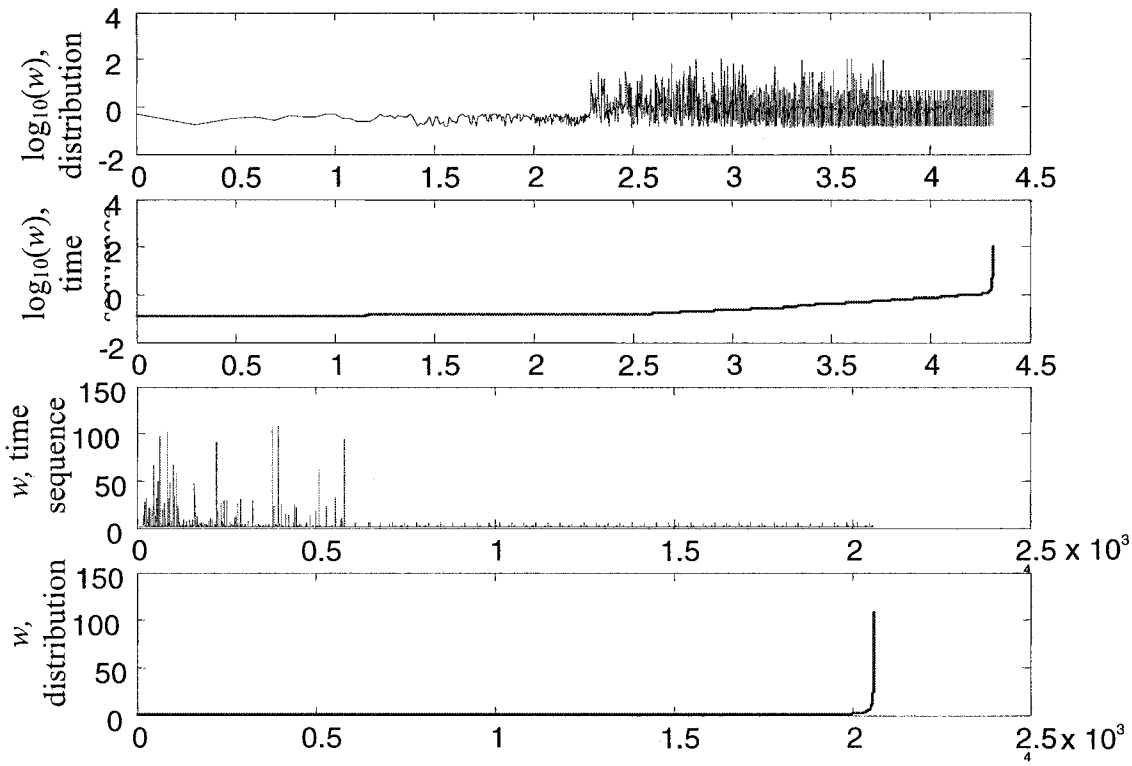

Figure 4.15. Time sequence of the relative particle exposure value at mobilization. a. The upper panel shows the time sequences and sorted threshold values (log10-log10) for a run with a relative particle exposure threshold of 0.13. *b.* The second panel shows the distribution of the relative particle exposure values. *c, d.* The same data, but with relative particle exposure in mm.

4.11. Summary and discussion

The PICA model provides an overview of interactions between channel, sediment and transport characteristics and the geometric roughness of the sediment surface when particle interactions are the dominant control on transport. The results indicate that roughness varies most strongly with the threshold for motion. Roughness increases as the threshold increases, corresponding to a decrease in mobility. Roughness decreases with an increase in the component of finer particles in the distribution. The roughness shows no trend with channel slope. Focusing

on the channel bed, the roughness of the bed is characterized by relatively high variability in roughness as slope increases. This may reflect interactions between slope and transport, but additional study is needed to evaluate which influences lead to this variability. Roughness also increases as the width and length of the bed increase. This phenomenon has been evaluated in studies in physics, and roughness has been related to the area of the domain in which transport occurs. Here, the model has different boundary conditions at the up- and downstream ends than along the sides, which may shed sediment toward the center of the model, but tends to prevent motion toward the banks. With these boundary conditions, roughness is not directly related to area, but varies by different factors with increase in width and length of the domain evaluated. In terms of reach length, the results indicate that detailed measurements will tend to document greater roughness if a longer domain is evaluated.

The model results also show that trends in the distribution of particle protrusion occur most strongly as particle mobility varies, somewhat less so for variations in the width of the particle size distribution (which may be measured, for example, by the standard deviation of the particle size distribution). Variations in particle protrusion appear to be insignificant with variations in slope and bed width.

Finally, the model provides a detailed record of particle motions, and the temporal sequence of particle motions indicates that significant transport events are both intermittent and highly variable in size during the adjustment phase. Such intermittency may indicate that the system evolves to a self-organized critical state, as described by Bak (1996).

4.12. References

Ahmed, M.M.E. 1989. *Rearrangement of coarse grains and patterns in armor coats*. PhD dissertation. Colorado State University, CO. 186 pp.

Amar, J.G. and F. Family. 1990. Phase transition in a restricted solid-on-solid surface-growth model in 2+1 dimensions. *Physical Review Letters* 64 543 - 547.

Bak, P. 1996. *how nature works: the science of self-organized criticality*. Copernicus, New York, NY, 212 pp.

Barabási, A.-L. 1992. Dynamic scaling of coupled nonequilibrium interfaces. *Physical Review A* 46(6): R2977 – R2980.

Barabási, A.-L. and H.E. Stanley. 1995. *Fractal concepts in surface growth*. Cambridge University Press, Cambridge, England, 366 pp.

Bathurst, J.C. 1985. Flow Resistance Estimation in Mountain Rivers. *Journal of Hydraulic Engineering* 111 (4): 625-643.

Bathurst, J.C. 2002. At-a-site variation and minimum flow resistance for mountain rivers. *Journal of Hydrology* 269(1-2): 11 – 26.

Bathurst, J.C., R.-M. Li and D.B. Simons, 1981. Resistance equation for large-scale roughness. *Journal of the Hydraulics Division*, ASCE 107(HY12): 1593-1613.

Billi, P., V. D'Agostino, M.A. Lenzi and L. Marchi, 1998. Bedload, slope and channel processes in a high altitude Alpine torrent. *Gravel-Bed Rivers in the Environment*. P.C. Klingeman, R.L. Beschta, P.D. Komar, and J.B. Bradley eds., 15-38, Water Resources Publications LLC, Highlands Ranch, Colorado.

Bray, D.I., 1979. Estimating average velocity in gravel-bed rivers. *Journal of the Hydraulics Division, ASCE* 105(HY9): 1103-1122.

Buffington, J.M., and D.R. Montgomery. 1999: A procedure for classifying textural facies in gravel-bed rivers. *Water Resources Research* 35(6):1903-1914.

Buffington, J.M., T.E. Lisle, R.D. Woodsmith, S. Hilton, 2002. Controls on the size and occurrence of pools in coarse-grained forest rivers. *River Research and Applications* 18(6):507-531.

Church, M., M.A. Hassan and J.F. Wolcott, 1998. Stabilizing self-organized structures in gravel-bed stream channels: field and experimental observations. *Water Resources Research* 34: 3169-3179.

Dittrich A., F. Nestmann, and P. Ergenzinger. 1996. Ratio of lift and shear forces over rough surfaces. in: *Coherent Flow Structures in Open Channels*. Ashworth, P., Best, J., Bennett, S. and McLelland, S. (eds.). Wiley, New York. (p. 125 to 135).

Einstein, H.A., 1950. *The bed-load function for sediment transportation in open channel flows.* U.S. Dept. of Agriculture, Soil Conservation Service, Technical Bulletin 1026, 71 pp.

Family, F. 1990. Dynamic scaling and phase transitions in interface growth. *Physica A* 168:561-580.

Ferguson, R.I. 2003. The missing dimension: effects of lateral variation on 1-D calculations of fluvial bedload transport.

Furbish, D.J., 1987. Conditions for geometric similarity of coarse stream-bed roughness. *Mathematical Geology* 19 (4): 291-307.

Gessler, J., 1990. Friction factor of armored river beds. *Journal of Hydraulic Engineering* 116 (4): 531-543.

Hassan, M.A., and M. Church. 2000. Experiments on surface structure and particle sediment transport on a gravel bed. *Water Resources Research* 36(7):1885-1895.

Hergarten, S. 2002: *Self-organized criticality in earth systems.* Springer-Verlag, New York, NY, 272 pp.

Iseya, F. and H. Ikeda. 1987. Pulsations in bedload transport rates induced by a longitudinal sediment sorting: a flume study using sand and gravel mixtures. *Geografiska Annaler* 69A:15 – 27.

Kirchner, J.W., W.E. Dietrich, F. Iseya and H. Ikeda, 1990. The variability of critical shear stress, friction angle, and grain protrusion in water-worked sediments. *Sedimentology* 37: 647-672.

Krug, J. 1989. Classification of some deposition and growth processes. *Journal of Physics A-General* 22:L769-L773.

Paola C., 1996, Incoherent structure: Turbulence as a metaphor for stream braiding, In: *Coherent Flow Structures in Open Channels* (Eds P.J. Ashworth, S.J. Bennett, J.L. Best and S.J. McLelland): John Willy & Sons, p. 706-723.

Parker, G. and P.C. Klingeman, 1982. On why gravel bed streams are paved. *Water Resources Research* 18(5): 1409-1423.

Pizzuto, 1990. Numerical simulation of gravel river widening. *Water Resources Research* 26(9), 1971-1980.

Robert, A. 1988. Statistical properties of sediment bed profiles in alluvial channels, *Mathematical Geology*, 20(3): 205-225.

Rosport, M., 1997. Hydraulics of steep mountain streams. *International Journal of Sediment Research* 12 (3): 99-108.

Rouse, H., 1965. Critical analysis of open-channel resistance. *Journal of the Hydraulics Division, ASCE*, 91(HY4): 1-23.

Talbot, T., and M. Lapointe, 2002. Numerical modelling of gravel bed river response to large-scale meander rectification: the coupling between the evolution of bed pavement and long profile. *Water Resources Research* 38 (6):Article no. 1074.

Toro-Escobar, C.M. Paola, G. Parker, P.R. Wilcock, J.B. Southard. 2000. Experiments on downstream fining of gravel. II: Wide and sandy runs. *Journal of Hydraulic Engineering, ASCE*, 126(3): 185-197.

Wohl, E.E. and H. Ikeda, 1998. The effects of roughness configuration on velocity profiles in an artificial channel. *Earth Surface Processes and Landforms* 23: 159-169.

CHAPTER 5

PARTICLE PATTERNS AND THEIR RELATIONSHIP TO POOLS RIFFLES AND ROUGHNESS

in a particle interactions model of steep gravel-to-cobble streams

5.1. The PICA Model

The model presented in this study provides an opportunity to investigate the multiple factors that are modified as a channel adjusts from an arbitrary initial condition to a stable state. The resulting integrated data set on channel adjustment allows a relatively rapid review of influences and interactions that affect channel form. The model results presented here are derived from a particle interactions cellular automata, or *PICA,* model which uses simple parameterizations of sediment and water flows in a channel, moves the sediment particles that are deemed mobile in a given time step, and thus evolves the channel form. Mechanisms in the model are kept to a minimum. Simulations are controlled by particle interactions as the fundamental control on which of the particle configurations persist and which configurations are unstable, so that they are 'dissembled' during sediment transport. In the *PICA* model, the transport direction of a mobile particle or group of particles is always toward the lowest adjacent cell (cells connected only along the diagonal are not considered to be adjacent). The particle interaction control is applied to individual small groups of particles, or single particles, which occupy a given cell. No other

controls are included in the model process. In particular, no influence that arises with spatial variations in flow, at a scale larger than the scale of a few particles, is included.

The PICA model presented here falls in the generic category of cellular automata, because (a) the model is cell-based, (b) contains only a minimal number of crucial processes, (c) all model controls are local, depending only on interactions with nearby cells, and (d) all controls are homogenous, defined such that a single mobility criterion and a single criterion determining the direction of motion are applied throughout the channel.

In the model, time is implicit rather than explicit. No controls depend on time. The duration of 'real' time in a given model time step may vary within and between runs, and has no necessary relation to time as observed for a particular stream process. The model is 'scale-free' in that the cell dimensions and the diameter of the maximum particle size are a multiple of the cell dimension, and all dimensions in the model can be related to the cell dimension. The actual relationship of the model dimensions to any given stream dimension is undetermined, but the relative model dimensions may be adjusted to match the relative dimensions in any given stream. The basic interpretation of the model results is that they to reflect the results when particle interactions are the dominant control on transport.

The model required a control on particle motion that reflects the effects of particle interactions. Such a model control must depend on both the degree of particle exposure and on particle weight. To achieve this, a characteristic threshold that can be applied to any given combination of particle size and particle exposure was defined. This is the relative particle exposure, $R_{p,c}$, defined as the ratio of the height that a particle rises above its surrounding to the diameter of the particle. This relative particle exposure is related to the dimensionless critical shear stress for an individual particle, and is based on an analysis of experimental data by Fenton and Abbot (1977).

The model is based on the following conceptual view of the water-sediment controls: (a) particle size and interactions within the local particle configurations are the dominant controls on particle motion, (b) flow velocity is an important control, and average streamwise velocity is an adequate parameterization of flow effects for evaluating particle motion in steep, gravel-to-cobble-dominated streams; and this control is adequately represented by a threshold criterion, (c) local conditions in terms of the continuum from very high particle stability through very high particle mobility can be modeled via locally-averaged particle sizes, using a threshold criterion and an evaluation of particle mobility dependent on the local particle sizes, which are viewed as forming 'characteristic' local particle configurations, and (d) the range of velocities that controls channel roughness, including particle arrangements and topographic 'form' roughness, is more dependent on relatively large flows characterized as bankfull flows, rather than lower flows. The last criterion is important in that the model transports sediment, and thus evolves the channel, at a constant threshold criterion, analogous to a constant local shear stress. In the model, it is effectively assumed that the work accomplished (i.e., sediment transport) at this discharge determines the resulting channel form; that smaller flows have no lasting effect on the form, whereas larger flows are too rare to have a significant control on the form.

The flow complexities are strongly simplified in the model, such that all flow effects are based on a mean value, and subsumed in the criterion for motion. Conversely, although sediment is also simplified, it is less simplified than in the approach that assumes random spatial distribution of particle characteristics.

The sketches in Figure 4.1 show the relationship between e, the average exposed height, and the particle diameter, D used in determining the relative particle exposure. The runs described here generally have a relative particle exposure threshold near 1/8th, for which 0.13 of the height of the particle is exposed. A particle with a relative particle exposure at the standard value is

shown in Figure 4.1b. In one series of model runs, the threshold was not constant, but was varied from 0.23 up to 0.48.

Channel roughness was evaluated in several sets of runs in which only one variable was incremented between each run in a given set. The variations consist of five series of runs, in which bed width, slope, particle sorting, mobility threshold value, and channel length are varied. Variation in the mobility threshold may be considered as reflecting a combination of variations in overall flow intensity. It may also reflect a range of uncertainty in the mobility threshold for a given particle size in a given configuration of particles on the channel bed. Roughness increases more rapidly with reach length than with bed width, at least given the narrow channel bed used in these runs. Based on theoretical models developed in physics, the area of the channel bed, rather than just the channel width may influence surface roughness. The model data indicate that roughness of the model domain increases both the width and the length of the domain, and more increases more strongly with the length. A simple, basic explanation of this is that short range correlations between particle characteristics develop as a result of particle interactions, and the full range of variation is greater when larger areas are evaluated, up to some maximum size. In terms of evaluating stream characteristics in the field, this simply means, as is known, that long reaches may need to be evaluated to correctly characterize roughness.

The study was designed based on the hypothesis that longitudinally-differentiated streams, such as pool-riffle, step-pool and cascade-pool streams may be strongly influenced by particle interactions, based known results in which particle interactions were observed to result in longitudinally differentiated beds in a flume study (Iseya and Ikeda, 1987).

The model results provide a useful, integrated dataset for evaluating the effects of particle interactions in steep, gravel to cobble stream channels. The model mimics a number of the features found in pool-riffle channels. This appears surprising because local variations in shear stress are typically viewed as necessary for developing pool-riffle channels. However, the model

results suggest that, in steep, rough streams, pool-riffle and related forms such as step-pool and cascade-pool sets may reflect responses to particle interactions. This is not to suggest that flow turbulence and spatial patterns in shear stress are unimportant, but to suggest that particle interactions also contribute strongly to the observed characteristics of at least longitudinally-differentiated streams such as pool-riffle channels. However, in the model presented here, only particle interactions are included, as a means to evaluate the effects of particle interactions alone.

5.2. The length of pools and riffles

The spacing of pools in the PICA model was derived by identifying connected areas in the model that are deep, and designating pools as deeps areas that have a length scale (defined as the square root of the deep area) that is, at minimum, one-half the channel width. The spacing of the model pools increases with bed width, and is nearly constant with slope and the threshold for motion. The spacing of model pools decreases strongly and non-linearly with width of the particle size distribution. The model data were compared to data on pool spacing from a set of mountain rivers (Wohl and Merritt, 2005), referred to here as the Mountain Rivers dataset. The data analyzed were selected to reflect channel width, slope, particle size and shear stress comparable to steep, gravel-to-cobble streams, with pool-riffle or other longitudinally-differentiated channel form. These field data indicate spacing increases with all of the factors varied in the model, with width, slope, particle size and threshold for motion. The model pools and their spacing may be characterized as generally showing a trend similar to trends in mountain rivers, with some uncertainty about what the relationship between spacing and width of the particle size distribution actually is in streams. A wider subset of the Mountain Rivers data was analyzed in hopes of clarifying the relationship of width of the particle size distribution on pool-riffle spacing. However, the additional data, spanning a wider range of channel conditions, suggest a wider range of variation without indicating a clear pattern of variation.

The length of the model pools was also summarized. In the model data, pool size decreases as the channel width, slope, and the threshold for mobility increase (the last corresponding to a decrease in mobility). The length of the model pools is effectively constant with width of the particle size distribution.

Large, coarse patches were also identified in the model bed surfaces. The length and spacing of these patches were compared to field data in five studies of pool-riffle channels that reported lengths of riffle subunits, or of coarse textural patches.

The field data indicate that riffles tend to occupy less than half of the pool-riffle cycle, particularly when the cycle is long, but range from longer to shorter than pools. In some cases riffles are considerably longer than pools. The field data are intriguing in that the length of riffles within and between study areas varies in opposite directions in several comparisons: in the relationship of the ratio of riffle length to channel width versus either the ratio of pool length to channel width, or the ratio of pool-riffle spacing to channel width. Study of these contrasts within and between studies should provide insight into the mechanisms that control riffle form. In the field data, riffle length tends to increase as channel width, width of the particle size distribution and the threshold for motion increase. The data show an inverse relationship for a correlation of riffle length versus slope.

When normalized by channel width, average normalized riffle lengths are constant in some study areas but increase with channel width in other studies. Within study areas, normalized riffle lengths are constant with slope, although the constant value differs for different study areas.

When not normalized by channel width, riffle lengths in the field data increase with channel width, and generally decrease with slope. Riffle lengths increase as the width of the particle size distribution increases, although this is based on only three data points from one study. Riffle lengths are directly proportional to discharge and increase with shear stress.

Data in two studies (Buffington and Montgomery, 1999b; Lisle and others, 2002) indicate that patch length increases with channel width, as do riffles, but the length of large coarse patches in the model decrease with bed width. Patch lengths decrease with slope in the two field studies, as well as in the model. The direction of increase in textural patch length with the width of the particle size distribution is unclear in the field data, having different trends in the two studies, and again, the effect of the width of the particle size distribution is not clear. Because patch lengths are constant with width of the particle size distribution in the model, these field data suggest that these patch length variations in rivers reflect variation in factors other than the particle size distribution.

The variable relationships between the patterns of variation of riffle and textural patch length in streams mean that their relationship to the model patches is unclear. In addition, the variability suggests that factors other than the particle interactions incorporated in the model are likely to be important in the development of riffles, patches or both. The interpretation is further complicated by the complex variations in riffle length apparent in the field data, and the limited data for some variables, making it difficult to know what the field relationship is between riffle length and other channel characteristics.

The field and model data together suggest that the size of pools in streams varies in the directions observed in the model, as channel width, slope, particle size distribution and shear stress vary. The model data also indicate that for extremely wide particle size distributions, there is a nonlinear decrease in the size of pools. The field data indicate that riffle lengths vary independently of pool lengths. Both the riffle data and additional field data on the length of patches show quite variable patterns in the relationship between riffle length and the model variables, in the different field studies. This suggests that factors other than particle interactions affect the length of riffles. A likely means of understanding the variability in the length of riffles is the minimum energy dissipation criterion, as outlined in Yang's (1971) hypothesis, which

suggests that streams have a fundamental tendency to maintain alternating steep and less steep channel segments, such as those characteristic of pool-riffle channels. Yang's hypothesis indicates that this is an inherent tendency because this minimizes the time rate of energy dissipation per unit volume of water. The relative length of riffles and pools will then reflect the adjustability of the channel, and the relative lengths will vary depending on what constraints limit the channel's ability to adjust its form.

5.3. Spatial patterns in bed surface characteristics

A statistical analysis of the spatial pattern of bed characteristics, including cell-scale highs and low, coarse and fine particles, high and low values of both particle exposure and relative particle exposure. These data indicate that the only common pattern is a non-random spacing of the high points on the surface, where high points were identified as areas at or above the 66^{th} percentile in terms of elevation relative to a sloping plane at the lowest elevation of the bed. There is a significant lack of high points at a spacing corresponding to 10 particle diameters of the largest particle size in the model, or nominally 2.5 meters. The two lowest mobility runs were also characterized by an excess of high points spaced about 5 cells apart, corresponding to 1.25 coarse particle diameters, indicating small-scale clustering becomes statistically significant when the sediment is weakly mobile.

5.4. Particle size distributions and armoring.

Coarsening of the channel bed surface is a common characteristic of pool-riffle channels and mountain rivers in general. Coarsening of the surface occurs in all runs in the model, as may be expected given that the model is constructed with cyclic boundaries, making it analogous to a recirculating flume (Parker and Wilcock, 1995). The particle size distributions on the model bed surface adjust over time and as the beds coarsen, resulting in a decrease in fines and an increase in coarse sediment at the surface. The depletion of fines in this model occurs entirely as a result of the mixing process inherent in sediment transport, and includes no other processes such as

fines slipping downward through the interstices between static coarse particles. The sediment size distributions in the model also adjust differently between areas that are pools and areas that are large coarse patches. Although all areas exhibit coarsening, particle size distributions in deep areas are little modified from the initial size distribution. Particle size distributions in areas that are not deep are more modified; these distributions tend to show a distinct break in the slope of the distribution between the coarser sizes which form the armor, and the finer sizes that are depleted. Particle size distributions in areas that are identified as pools adjust in the same direction as the non-pool areas, but are even more modified than the other areas. Two anomalous runs, consisting of the two runs with the highest mobility threshold (lowest particle mobility), show a very strong depletion of the coarsest two size fractions, adjustment in the intermediate fractions, and essentially no reduction in the frequency of the finest sizes.

The surface of the channel bed indicates an increase in the spatial segregation of areas that are coarse and areas that are pools as bed width and the threshold for motion increase. The degree of differentiation shows no trend with slope. The degree of differentiation decreases as the model particles include an increasing number of fine particle size classes in the particle size distribution. The particle size distributions in pools and coarse areas in the model, combined with spatial segregation between pools and deeps indicates that the model results simulate the basic characteristics of pool-riffle channels. Since the model process depends entirely on particle interactions, this suggests that particle interactions alone are sufficient to generate at least an approximation of the most fundament characteristic of pool-riffle channels.

Two other notable observations on the model data are included here. The initial stages of channel adjustment show highly intermittent variations in the number of cells where particles move in a given time step. The pattern of variation suggests that the transport process is characterized by self-organized criticality. Second, a limited investigation of the characteristics of transport, as opposed the sediment surface, indicates that increasing channel slope modifies

transport direction such that net downstream transport increases as slope increases. This is in spite of the fact that the total number of transport steps does not increase as slope increases.

A great deal of additional information provided by the model was not analyzed in this study. In particular, the relationships between the model results discussed here, and sediment transport characteristics, have only been touched on.

5.5. Future directions

The model constructed and presented in this study provides an integrated data set on channel adjustment, relevant to channels where the particle interactions control channel evolution. The summary here presents an overview of how particle interactions may contribute to the formation of pools and riffles in streams. The model results suggest that particle interactions alone are sufficient to generate at least an approximation of the most fundament characteristic of pool-riffle channels. The model results indicate patterns of variation in pool length that are similar to those found in streams. The results from the patterns of variation in the lengths of riffles and textural patches indicate that the controls on these features are more complicated. The data on roughness provide insight into how the mutual adjustment between channel form and particle size distributions that result from mobility constraints are derived from particle interactions. The model surfaces also show that large coarse patches and large deeps have a tendency to occupy different areas of the bed, although with considerable overlap.

The model surfaces are not significantly different from being spatially random in particle size and particle exposure. The sediment surfaces are however characterized by significantly non-random spacing of high points on the bed, reflecting a regularity in the spacing of high points, at a spacing of about two meters, and, when the sediment is weakly mobile, the regularly spaced high points are accompanied by clustering of high points on the bed at a smaller scale.

The results of the model presented here provide considerable insight into the interrelationships between local channel deeps and locally coarse areas of the channel bed. These

features can be defined for a sediment surface in which the distribution of particles by size is essentially random, although the surface elevations are not. Yet the adjustments of particle size and particle position that result from transport of these randomly-distributed particle sizes result in systematic variation in the average spacing and length of coarse patches and of local deeps. These observations also indicate that the process in the model is fundamentally different than the sorting processes identified in flume runs by Iseya and Ikeda, in which different rates of transport result in significant sorting into longitudinal zones of differing particle size. Because both results are clearly a result of particle interactions, it is worth considering, in future, whether the difference is related to a difference between the behavior of bimodal sediment and the very poorly sorted sediment included in this model.

The model results presented here are less similar to the patterns of variation in riffle length observed in the field, and the pattern of variation of riffle length also appears to be more complex than that of pools, in the sense that field results also present more complicated trends. In particular, the lengths of riffles and textural patches appear to vary in the different directions as the variables of channel width, slope, particle size distribution and shear stress vary. However, additional data on both riffle length and patch length are necessary to provide a better characterization of the trend in riffle length with other channel variables. Additional work to identify the controls on riffle lengths, the relationship of riffle length to pool length, and how they adjust within other constraints on the channel, should be a fruitful area of research.

The method applied here to evaluate roughness of the channel bed has considerable promise for clarifying controls on roughness and ultimately predicting roughness. The multiple influences on roughness in streams means that this is complicated, and will require a number of different studies, including studies of roughness in streams, in flumes and in models. Methods of analysis used in physics will also be helpful in mapping out the complex variations that may result from the motion of particles, under the flow of water, and with considerable random variability

inherent in the effectively random or near-random positioning of particles on the channel bed. A great deal of theory has been established by these studies, and may be directly applied to studies of sediment transport in which particle interactions are important.

5.5. Reference: Chapter 5

Buffington, J.M., T.E. Lisle, R.D. Woodsmith, S. Hilton, 2002. Controls on the size and occurrence of pools in coarse-grained forest rivers. *River Research and Applications* 18(6):507-531.

Buffington, J. M., and D.R. Montgomery. 1999b. Effects of hydraulic roughness on surface textures of gravel-bed rivers. *Water Resources Research* 33(11):3507-3521.

Fenton, J.D and J.E. Abbott, 1977. Initial movement of grains on a stream bed: the effects of relative protrusion. *Proceedings of the Royal Society of London* A 352:523-537.

Iseya, F. and H. Ikeda. 1987. Pulsations in bedload transport rates induced by a longitudinal sediment sorting: a flume study using sand and gravel mixtures. *Geografiska Annaler* 69A:15-17.

Lisle, T.E., J.M Nelson, J. Pitlick, M.A. Madej, B. L. Barkett. 2000. Bed mobility variability in natural gravel-bed channels and adjustments to sediment load at local and reach scale. *Water Resources Research* 36(12):3743-3755.

Parker, G. and P. Wilcock. 1995. Sediment feed and recirculating flumes - fundamental difference. Journal of hydraulic engineering - ASCE 121(3)L293-294.

Wohl, E.E. and D. Merritt. 2005. Prediction of mountain stream morphology. *Water Resources Research* 41(Article W08419):1-10.

Yang, C.T. 1971. Formation of riffles and pools. *Water Resources Research* 7(6): 1567-1574.